National Research
Council Canada

Conseil national
de recherches Canada

NRC · CNRC

Canadian Journal of Fisheries and Aquatic Sciences

Journal canadien des sciences halieutiques et aquatiques

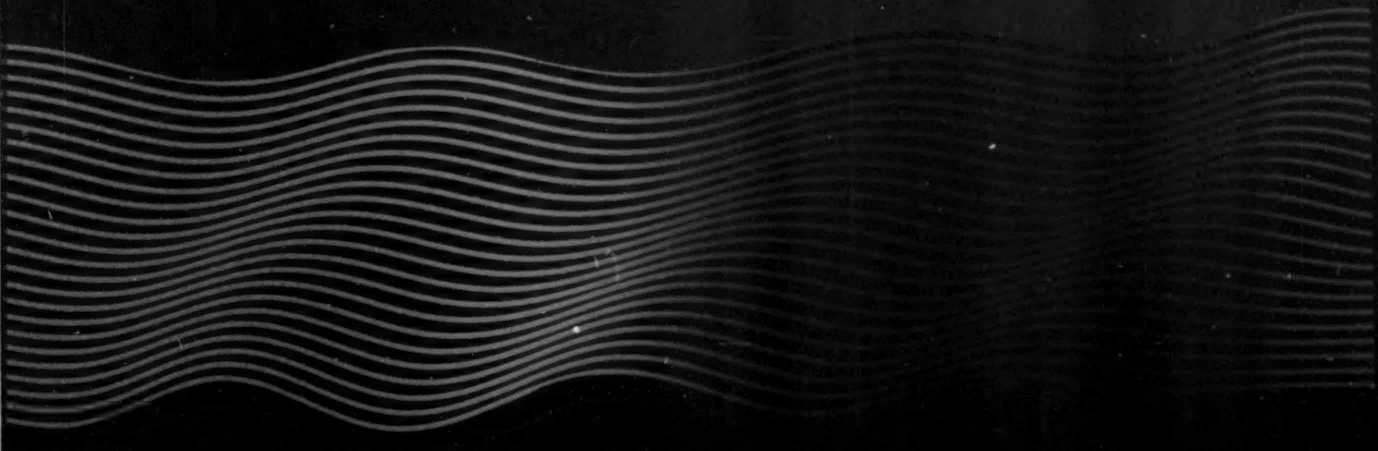

http://cjfas.nrc.ca

http://jcsha.cnrc.ca

ISSN 0706-652X / CJFSDX 60(11) 1307–1432 (2003)

The *Canadian Journal of Fisheries and Aquatic Sciences*, previously published as *Contributions to Canadian Biology* 1901–1925, *Contributions to Canadian Biology and Fisheries* 1926–1934, *Journal of the Biological Board of Canada* 1934–1937, and *Journal of the Fisheries Research Board of Canada* 1938–1979, is issued monthly to form annual volumes of 12 numbers plus supplements.

Editorial policy. The Journal publishes original research articles, perspectives (syntheses, critiques, re-evaluations), discussions (comment and reply), and rapid communications. Manuscripts may concern cells, organisms, populations, communities, ecosystems, or processes that affect aquatic systems. They may cover a range of disciplines including biology and ecology of marine and freshwater organisms, limnology, oceanography, physiology, toxicology, genetics, economics, disease, and management. Preference will be given to manuscripts that emphasize understanding of observed phenomena and interpretation of experimental results. The Journal encourages papers that lead from clearly stated purpose or rationale and from testable hypotheses, concepts, or questions to identifiable conclusions or syntheses. Such papers may amplify, modify, question, or redirect accumulated knowledge embodied in contemporary perceptions of a particular state of aquatic sciences. The Journal discourages papers that are essentially descriptive, except in emerging disciplines; have only site-specific or local applications (a certain year, place, taxon, chemical compound, etc.); only confirm previously established principles; or apply standard techniques without breaking new methodological ground.

Manuscripts for publication should be submitted to the Senior Editor, *Canadian Journal of Fisheries and Aquatic Sciences*, Department of Zoology, University of Guelph, Guelph, ON N1G 2W1, Canada (519-824-4120 ext. 52646; fax: 519-767-9798; e-mail: cjfas@uoguelph.ca).

Submissions in either English or French are acceptable. The information must be original, that is, not copyrighted, published, or submitted elsewhere except in abstract form or unless by written consent of the Editor.

Correspondence concerning accepted manuscripts and corrected proofs should be sent to NRC Research Press, National Research Council of Canada, Ottawa, ON K1A 0R6, Canada (fax: 613-952-7656; e-mail: pubs@nrc-cnrc.gc.ca).

Instructions to Authors are published once a year in the first issue of each volume. Copies are available from NRC Research Press or at http://cjfas.nrc.ca. The **Publication Policy** of NRC Research Press is available at http://pubs.nrc-cnrc.gc.ca.

Microfilm. Issues from 1934 through the current volume can be purchased on 16- or 35-mm microfilm. Photocopies of individual articles or issues can be purchased from University Microfilms International, 330 North Zeeb Road, Ann Arbor, MI 48106, U.S.A.

U.S. periodical postage paid at Champlain, N.Y., and at additional mailing offices. Attention U.S. POSTMASTER: Send address changes to **Canadian Journal of Fisheries and Aquatic Sciences**, c/o USACAN Media Distribution Center, P.O. Box 2888, Plattsburg, NY 12901, U.S.A.

Publié sans interruption depuis 1901, le *Journal canadien des sciences halieutiques et aquatiques* a paru sous plusieurs titres : *Contributions to Canadian Biology* 1901–1925, *Contributions to Canadian Biology and Fisheries* 1926–1934, *Journal of the Biological Board of Canada* 1934–1937, et *Journal of the Fisheries Research Board of Canada* 1938–1979. Le Journal paraît tous les mois, formant ainsi un volume de 12 numéros, et offre en plus jusqu'à deux suppléments par année.

Politique éditoriale. On publie, dans le Journal, des articles rendant compte de recherche originale, des perspectives (synthèses, critiques et réévaluations), des discussions (commentaires et réponses) et des communications rapides. Les documents peuvent porter sur les cellules, organismes, populations, communautés, écosystèmes ou processus qui affectent les systèmes aquatiques. Ils peuvent relever de divers domaines y compris la biologie et l'écologie des organismes marins et d'eau douce, la limnologie, l'océanographie, la physiologie, la toxicologie, la génétique, l'économie, la pathologie et la gestion. On accorde la préséance aux articles qui contribuent à la compréhension de phénomènes observés et à l'interprétation de résultats expérimentaux. On invite les auteurs à soumettre des articles ayant des objectifs précis ou relevant d'hypothèses, de concepts ou de questions vérifiables et se terminant par de solides conclusions ou d'utiles synthèses. Ces articles enrichissent, changent, mettent en question ou réorientent les connaissances acquises sur divers aspects des sciences aquatiques. On décourage toutefois la soumission d'articles simplement descriptifs (à moins qu'il ne s'agisse de nouvelles disciplines), d'application très limitée (applicables à une seule année, une seule région ou un seul taxon, portant sur un unique composé chimique, etc.); d'articles qui ne font que reprendre les principes énoncés dans des articles précédents; et d'articles rendant compte de l'application de normes sans gain de méthodologie.

Les auteurs voudront adresser leurs **manuscrits** à la directrice scientifique principale, *Journal canadien des sciences halieutiques et aquatiques*, Department of Zoology, University of Guelph, Guelph, ON N1G 2W1, Canada (519-824-4120 poste 52646; télécopieur : 519-767-9798; courriel : cjfas@uoguelph.ca).

Les contributions peuvent être en anglais ou en français. Elles doivent être originales, c.-à.-d. qu'elles ne doivent pas avoir fait l'objet d'un copyright, avoir été publiées ou soumises ailleurs, sauf sous forme abrégée ou avec le consentement du rédacteur. Le CNRC ne se tient en aucune façon responsable des opinions exprimées par un collaborateur ou des déclarations qui pourrait faire ce dernier.

La correspondance ayant trait aux manuscrits acceptés et les **épreuves corrigés** doivent être envoyées aux Presses scientifiques du CNRC, Conseil national de recherches du Canada, Ottawa, ON K1A 0R6, Canada (télécopieur : 613-952-7656; courriel : pubs@nrc-cnrc.gc.ca).

Les Recommandations aux auteurs sont publiées une fois par année dans le premier numéro de chaque volume. Des copies sont disponibles auprès du Bureau de la rédaction aux Presses scientifiques du CNRC ou au http://jcsha.cnrc.ca. **La Politique de publication** est disponible auprès des Presses scientifiques du CNRC ou au http://pubs.nrc-cnrc.gc.ca.

Microfilms. On peut acheter sur microfilms de 16 ou 35 mm tous les numéros depuis 1934. Des photocopies d'articles ou de numéros individuels sont aussi en vente auprès de University Microfilms International, 330 North Zeeb Road, Ann Arbor, MI 48106, É.-U.

This Journal is indexed or abstracted in / Cette revue est signalée ou résumée dans
ABSEARCH, Aquatic Sciences and Fisheries Abstracts, Biological Abstracts, Biological & Agricultural Index, CAB Abstracts, Chemical Abstracts, Current Contents, Elsevier BIOBASE, Environmental Abstracts, Environmental Periodicals Bibliography, GEOBASE, GeoRef, Internationale Bibliographie der Zeitschriftenliteratur, Life Sciences Collection, Meteorological and Geoastrophysical Abstracts, Oceanic Abstracts, PASCAL Database, and Science Citation Index.

Volume 60, Number 11, November 2003

Canadian Journal of Fisheries and Aquatic Sciences

Published by the National Research Council of Canada

Volume 60, numéro 11, novembre 2003

Journal canadien des sciences halieutiques et aquatiques

Publié par le Conseil national de recherches du Canada

Senior Editor / Directrice scientifique principale Moira M. Ferguson

Editors / Directeurs

Jeffrey A. Hutchings, *Dalhousie University, Halifax*
Pierre Pepin, *Northwest Atlantic Fisheries Centre, DFO/MPO, St. John's, Newfoundland*
W. Gary Sprules, *University of Toronto at Mississauga*
Assistant to the Editors / Adjointe aux directeurs scientifiques **Holly Foster**

Associate Editors / Directeurs scientifiques associés

M.T. Arts, *Environment Canada, Burlington*
D. Boisclair, *Université de Montréal*
U. Borgmann, *Environment Canada, Burlington*
S.E. Campana, *DFO/MPO, Dartmouth*
R. Carignan, *Université de Montréal*
J.J. Dodson, *Université Laval*
G.T. Evans, *DFO/MPO, St. John's, Newfoundland*
K.T. Frank, *DFO/MPO, Dartmouth*
M.M. Hansen, *Danish Institute for Fisheries Research, Silkeborg, Denmark*
R. Hilborn, *University of Washington*
A. Hontela, *Université du Québec à Montréal*
D.F. Houlihan, *University of Aberdeen*
F.A. Huntingford, *University of Glasgow*
G.S. Jamieson, *DFO/MPO, Nanaimo*
B. Jonsson, *Norwegian Institute for Nature Research, Oslo, Norway*
P. Magnan, *Université du Québec à Trois Rivières*
C.T. Marshall, *University of Aberdeen*
R.B. Millar, *University of Auckland, New Zealand*
Y.T. Prairie, *Université du Québec à Montréal*
T.J. Quinn II, *University of Alaska–Fairbanks, Juneau, Alaska*
T.P. Quinn, *University of Washington*
R.D. Robarts, *Environment Canada, Saskatoon*
B. Sainte-Marie, *DFO/MPO, Mont-Joli*
D.W. Schindler, *University of Alberta*
R.E.H. Smith, *University of Waterloo*
S.J. Smith, *DFO/MPO, Dartmouth*
W.F. Vincent, *Université Laval*
R.D. Vinebrooke, *University of Regina*
C.J. Walters, *University of British Columbia*
R.D. Ward, *CSIRO Marine Research, Australia*
B. de Young, *Memorial University of Newfoundland*

NRC Research Press / Presses scientifiques du CNRC

Editor-in-Chief / Directeur général **Bruce P. Dancik**
Assistant Editor-in-Chief / Directeur général adjoint **Iain E.P. Taylor**

Journals Program / Programme des revues

(Fax / Télécopieur : 613-952-7656; e-mail / courriel : pubs@nrc-cnrc.gc.ca;
URL / URL : http://pubs.nrc-cnrc.gc.ca)
Director / Directrice **Aldyth Holmes**
Business Manager / Gestionnaire des affaires **Paul McClymont**
Manager, Journals Program / Gestionnaire, Programme des revues **Carolyn Brown**
Managing Editor / Rédactrice administrative **Cecily M. Pearson** (613-993-9099)
Publication Officers / Agentes de publication **Jennifer McColl**
Advertising / Annonces publicitaires **Judy Gorman** (613-993-0151)
Reprints / Tirés à part **Roxanne Landriault** (613-990-2254)
Subscriptions / Abonnements **Eileen Evans-Nantais** (613-990-7873)

The National Research Council of Canada accepts no responsibility for statements or opinions expressed by a contributor. Acceptance of an advertisement, announcement, or other material does not imply endorsement by either the Journal's Senior Editor or the National Research Council.

© National Research Council of Canada 2003. All rights reserved.

No part of this publication may be reproduced, stored, or transmitted in any form or by any means, without the written permission of the publisher, except as stated below.

The National Research Council of Canada grants **permission*** to individuals to make single copies of articles for personal use. Any person may reproduce short excerpts from articles in the journal for any purpose that respects the moral rights of authors, provided that the source is fully acknowledged. As a courtesy, the consent of authors of such material should be obtained directly from the author.

Authorization to reproduce items for other than personal use, as stated above, is granted by the National Research Council of Canada provided that the copyright fee of $7.00 per copy is paid directly to CANCOPY, One Yonge Street, Suite 1900, Toronto, ON M5E 1E5, Canada.

*The above permission does not extend to other kinds of copying, such as copying for general distribution, for advertising, or promotional purposes, for creating new collective works, or for resale. For such copying, arrangements must be made with the publisher, National Research Council of Canada, Ottawa, ON K1A 0R6, Canada.

Subscription information

The *Canadian Journal of Fisheries and Aquatic Sciences* (ISSN 0706-652X) is published monthly by the National Research Council of Canada. The 2003 annual subscription rates (second class postage) for Canada are $830CAN institutional and $257CAN personal, for US & foreign $830US institutional and $257US personal. For air mail add $175US to foreign rate. Canadian customers please include 7% GST (business no. 12149 1807 RT 0275). Subscriptions are entered for the calendar year. Remittances should be made payable to the Receiver General for Canada credit NRC. Price for regular single issues: institutional, $105.00; personal, $35.00. Supplements will be priced separately. Special rates apply to members of Canadian scientific and engineering societies if they subscribe through their respective societies.

There are no refunds on cancelled subscriptions once delivery has begun. Claims for missing issues should be made within four months (N. America) or six months (outside N. America) following the date of publication. The publisher expects to supply missing issues only when losses have occurred in transit and when the reserve stock will permit. For change of address and subscription enquiries: Subscription Office, NRC Research Press, National Research Council of Canada, Ottawa, ON K1A 0R6, Canada; tel.: 613-993-9084; fax: 613-952-7656; e-mail: pubs@nrc-cnrc.gc.ca.

Microform backfiles are available from UMI, P.O. Box 1346, Ann Arbor, MI 48106-1346, U.S.A., and Micromedia Ltd., 20 Victoria St., Toronto, ON M5C 2N8, Canada.

All issues of the *Canadian Journal of Fisheries and Aquatic Sciences* since 1996 are available on the Web. Pricing information can be found at http://pubs.nrc-cnrc.gc.ca.

Le Conseil national de recherches du Canada ne se tient en aucune façon responsable des opinions exprimées par un collaborateur ou des déclarations que pourrait faire ce dernier. La publication d'annonces publicitaires, d'avis et autres n'implique pas l'endossement de leur contenu par la directrice principale de la Revue ou le CNRC.

© Conseil national de recherches du Canada 2003. Tous droits réservés.

Il est interdit de reproduire, de sauvegarder ou de transmettre quelque partie de la présente publication dans quelque format ou de quelque façon sans le consentement écrit de l'éditeur, à l'exception des conditions suivantes.

Le Conseil national de recherches du Canada accorde aux particuliers le droit de faire des copies individuelles pour leur usage personnel. Toute personne peut reproduire de courts extraits des articles de la Revue pour autant que les droits moraux de l'auteur soient respectés et que la mention de provenance soit clairement indiquée. Il est de convenance de demander le consentement de l'auteur avant de faire mention de son travail.

On obtiendra l'autorisation de reproduire des articles à d'autres fins que l'usage personnel (tel qu'on l'a décrit ci-dessus) auprès du Conseil national de recherches du Canada pour autant que des redevances de droits d'auteurs de 7,00 $/copie soient versées au CANCOPY, 1, rue Yonge, bureau 1900, Toronto, ON M5E 1E5, Canada.

*La permission ci-dessus ne s'applique pas à la reproduction à grande échelle, telle que la reproduction aux fins de distribution générale, publicitaire ou promotionnelle, de compilation de nouveaux ouvrages collectifs ou de revente. Dans de tels cas, il faudra ratifier une entente particulière avec l'éditeur, le Conseil national de recherches du Canada, Ottawa, ON K1A 0R6, Canada.

Renseignements sur l'abonnement

Journal canadien des sciences halieutiques et aquatiques (ISSN 0706-652X) est une publication mensuelle du Conseil national de recherches du Canada. Le prix de l'abonnement annuel au Canada (courrier de deuxième classe) est de 830 $CAN pour les organismes et de 257 $CAN pour les particuliers. À l'étranger (y compris les É.-U.), le prix de l'abonnement est de 830 $US pour les organismes et de 257 $US pour les particuliers. L'expédition par avion exige des frais de 175 $US en sus du prix d'abonnement à l'étranger. Les clients du Canada doivent ajouter la TPS de 7% (numéro d'entreprise 12149 1807 RT 0275). Les abonnements sont pour l'année civile. Tout paiement doit être adressé au Receveur général du Canada, crédit du CNRC. Le prix par numéro est de 105 $ pour les organismes et de 35 $ pour les particuliers. Le prix des hors-série varie. Les membres des sociétés canadiennes de sciences et de génie bénéficient de taux préférentiels en s'abonnant via leurs sociétés respectives.

Aucun remboursement ne sera accordé ni aucune annulation acceptée une fois que les livraisons auront commencé. Les réclamations de numéros manquants devront être soumises dans les quatre mois (Amérique du Nord) ou dans les six mois (à l'extérieur de l'Amérique du Nord) suivant la date de publication. L'éditeur ne fournira de numéros manquants que si le document a été perdu pendant l'expédition et que si le stock le permet. Adressez tout changement d'adresse ou toute question quant à l'abonnement au : Bureau des abonnements, Presses scientifiques du CNRC, Conseil national de recherches Canada, Ottawa, ON K1A 0R6, Canada; téléphone : 613-993-9084; télécopieur : 613-952-7656; courriel : pubs@nrc-cnrc.gc.ca.

On peut obtenir les fichiers rétrospectifs sur **microforme** auprès de UMI, P.O. Box 1346, Ann Arbor, MI 48106-1346, É.-U., et auprès de Micromedia Ltée, 20, rue Victoria, Toronto, ON M5C 2N8, Canada.

À partir de 1996, tous les numéros de *Journal canadien des sciences halieutiques et aquatiques* sont accessibles sur le Web. On trouvera des renseignements sur les tarifs à http://pubs.nrc-cnrc.gc.ca.

The differing crustacean zooplankton communities of Canadian Shield lakes with and without the nonindigenous zooplanktivore *Bythotrephes longimanus*

Stephanie A. Boudreau and Norman D. Yan

Abstract: The nonindigenous predatory cladoceran *Bythotrephes longimanus* is spreading rapidly among Canadian Shield lakes, but only one case study of its impacts exists. In Harp Lake, the abundances of several cladoceran and one cyclopoid species fell after the invasion, and far fewer species benefited. To determine if Harp Lake provides typical results, we compared the summer crustacean zooplankton communities of 17 invaded and 13 noninvaded (reference) lakes in Ontario. The communities of the two lake groups differed. Average species richness was 30% higher in the reference (15.3 species) vs. the invaded lakes (11.8 species). Total zooplankton biomass was significantly lower in the invaded lakes, mainly because of lower abundances of all common epilimnetic cladoceran species. As these results were quite similar to those of Harp Lake, it is apparent that current summer zooplankton communities of Canadian Shield lakes with *Bythotrephes* differ substantially from noninvaded lakes.

Résumé : Bien que le cladocère prédateur non indigène *Bythotrephes longimanus* se répande rapidement dans les lacs du Bouclier canadien, il n'existe qu'une seule évaluation de son impact. Dans le lac Harp, les abondances de plusieurs espèces de cladocères et d'une espèce de cyclopoïdes ont décliné depuis l'invasion, alors qu'un petit nombre d'espèces en a tiré bénéfice. Pour voir si la situation au lac Harp est caractéristique, nous avons comparé les communautés de crustacés zooplanctoniques d'été dans 17 lacs colonisés et 13 lacs non colonisés (témoins) de l'Ontario. Les communautés des deux groupes de lacs sont différentes. La richesse moyenne en espèces est de 30 % plus élevée dans les lacs témoins (15,3 espèces) que dans les lacs affectés (11,8 espèces). La biomasse totale du zooplancton est significativement plus basse dans les lacs envahis, principalement à cause des densités réduites de toutes les espèces communes de cladocères épilimnétiques. Ces résultats sont très semblables à ceux obtenus au lac Harp et il est donc clair que les communautés actuelles de zooplancton en été des lacs envahis par *Bythotrephes* diffèrent considérablement de celles des lacs non affectés.

[Traduit par la Rédaction]

Introduction

Bythotrephes longimanus Leydig (Crustacea, Branchiopoda, Onychopoda), hereafter simply called *Bythotrephes*, is a large, predatory cladoceran species native to much of Eurasia (Grigorovich et al. 1998; Therriault et al. 2002). First discovered in the Laurentian Great Lakes in the early 1980s, *Bythotrephes* almost certainly arrived in the ballast water of transoceanic ships (Mills et al. 1993). It was first reported in inland lakes in Ontario in 1989 (Yan et al. 1992), and since then it has spread to close to 50 Canadian Shield lakes in Ontario (MacIsaac et al. 2000; Therriault et al. 2002). We have only one thorough case study of the impacts of the invader on zooplankton of Shield lakes. In 1993, *Bythotrephes* was recorded in Harp Lake, a lake with a long record of preinvasion monitoring. Following the invasion, zooplankton species richness declined significantly, as did average abundances of many small-bodied cladoceran species and *Mesocylops edax*. A smaller number of larger species (*Daphnia mendotae*, *Holopedium glacialis*) became more abundant (Yan and Pawson 1997; Yan et al. 2001, 2002). Although there are no other Shield lake case studies, *Bythotrephes* has also been implicated in zooplankton community changes in Lake Michigan (Lehman and Cácares 1993; Makarewicz et al. 1995) and in Long Lake, Mich., U.S.A. (Hoffman et al. 2001).

Bythotrephes is found in a wide range of lakes in Europe (Grigorovich et al. 1998; Therriault et al. 2002); however, it most commonly occurs in large, deep, oligotrophic lakes (MacIsaac et al. 2000). There are many such lakes in temperate North America, particularly on the Canadian Shield. Thus, if the Harp Lake results prove to be typical, there may

Received 1 January 2003. Accepted 31 August 2003. Published on the NRC Research Press Web site at http://cjfas.nrc.ca on 17 November 2003.
J17259

S.A. Boudreau[1] and N.D. Yan.[2] Department of Biology, York University, 4700 Keele Street, Toronto, ON M3J 1P3, Canada.

[1] Present address: 55 Brittany Avenue, Kingston, NS B0P 1R0, Canada.

[2] Corresponding author (e-mail: nyan@yorku.ca).

doi: 10.1139/F03-111

be widespread changes in zooplankton populations on the Shield in response to *Bythotrephes* introductions. The best test of this prediction would be a comparison of pre- and post-invasion zooplankton assemblages in several lakes, but pre-invasion data sets are not commonly available. An alternative is to compare the zooplankton communities from carefully selected invaded and noninvaded Shield lakes. We do such a comparison herein. Our objective is to compare the crustacean zooplankton communities of Shield lakes that have and have not been invaded by *Bythotrephes*. As we see no reason for the Harp Lake results to be particularly atypical (Yan et al. 2002), we hypothesize that there will be large differences in the zooplankton communities of these two groups of lakes, differences similar to those that followed the introduction of *Bythotrephes* into Harp Lake.

Methods

We selected the two sets of lakes (with and without *Bythotrephes*) ensuring that means of several variables known to influence Shield lake zooplankton communities did not differ (see Boudreau (2002) for details). The 30 lakes were located in the Muskoka, Parry Sound, and Haliburton regions of south-central Ontario, Canada, the area on the Shield with the highest *Bythotrephes* incidence. Lakes with *Bythotrephes* were identified from previous sightings (Yan et al. 1992; Borbely 2001; Therriault et al. 2002). In two cases, lakes that were initially chosen as reference lakes (Kennisis and Three-Mile) unexpectedly supported *Bythotrephes* populations. Thus, although we had aimed for an equal number of invaded and reference lakes, our final data set had 17 invaded lakes and 13 reference lakes. Lake names, locations, and basic limnological characteristics are described in Boudreau (2002).

In selecting lakes, we ensured that averages of lake area ($t = 0.6$, $p = 0.56$), maximum depth ($t = -0.08$, $p = 0.94$), total phosphorus concentrations ($t = -1.6$, $p = 0.1$), pH ($t = 0.42$, $p = 0.68$), and lake alkalinity ($t = 0.037$, $p = 0.97$) did not differ between reference and invaded lakes. Of 14 total chemical and morphometric variables examined (Boudreau 2002), only sodium concentrations differed between the two groups of lakes. Sodium levels averaged 3.02 $\text{mg}\cdot\text{L}^{-1}$ in the invaded lakes, significantly higher (independent samples t test, $p = 0.011$) than the 1.57 $\text{mg}\cdot\text{L}^{-1}$ in the reference lakes. The primary source of elevated Na in continental temperate lakes in North America is salt applied to roads in winter as a de-icer (Rosenberry et al. 1999; Mayer et al. 1999). Differences in Na of the magnitude detected in the two groups are not known to have any impacts on zooplankton composition.

We assessed *Bythotrephes* abundance in each lake, reasoning that any impacts on zooplankton would covary with *Bythotrephes* abundance. To assess *Bythotrephes* abundance, we employed Yan and Pawson's (1998) protocol, sampling *Bythotrephes* in vertical hauls from 3 m above bottom to the surface, using a 0.75 m diameter, 2.5 m long, 285 μm mesh, Rigosha meter-equipped net at each of 10 randomly located stations in each lake. All samples were fixed and preserved in a 4% buffered sucrose–formalin solution in the field and were subsequently examined in their entirety for *Bythotrephes*. *Bythotrephes* abundances were calculated from sample volumes corrected for the measured haul filtration efficiency.

Crustacean zooplankton were sampled using a Dorset Research Centre (DRC) net (McQueen and Yan 1993), an 80 μm mesh, 0.12 m diameter, 0.75 m long, conical, metered tow net. One vertical haul was taken to the surface from 2 m off bottom at the deepest spot in the lake. Sample volumes were calculated correcting for haul filtration efficiency, which averaged 77%. Animals were counted and their video images were measured with electronic calipers using a semi-automated zooplankton counting system (Allen et al. 1994) on a Nikon SMZ-10 dissecting scope (Nikon Canada Instruments, Cooksville, Ont.). Animals were identified using 20 standard and modern taxonomic references (listed in Boudreau 2002). The counting protocol was designed to identify, count, and measure the body lengths of a minimum of 300 individuals in subsamples generated with a Folsom plankton splitter (Wildco Wildlife Supply Co., Saginaw, Mich.). Splits were designed to ensure that adequate numbers of rarer taxa were enumerated. Indeed, the entire sample was usually counted to ensure identification of these rare taxa. Where length–weight regressions employed had been developed from formalin-preserved animals, weights were increased by 37% to correct for weight loss in formalin (Giguère et al. 1989). The original Ahmic Lake sample (a 23-m haul) was lost before processing. In this one case, a vertical sample through the epilimnnion and metalimnion (13-m haul) was counted in place of the lost sample. We had taken these samples as backups in every case.

To reduce any confounding influence of seasonal changes in composition (lakes were sampled between July and September of 2001), the order of sampling lakes was randomized. To ensure that we did not ourselves become *Bythotrephes* transit vectors, all nets were sterilized with a 10% bleach solution between lakes, and the boat and trailer were washed with a high-pressure washer (Canadian Tire Corp. Ltd., Toronto, Ont.) then dried in the sun between sampling trips.

We were interested in testing for differences in species richness between the two groups of lakes, and it is widely recognized that richness increases with sample size. On average, significantly more animals (t test, $p = 0.004$) were counted in the reference lakes (mean of 294) than in the invaded lakes (mean of 243). However, there was no correlation between numbers counted and species richness ($r^2 = 0.01$, $p = 0.64$); therefore, no correction of richness for sample size was needed.

We summarized the counting data as the density ($\text{animals}\cdot\text{L}^{-1}$ or $\text{animals}\cdot\text{m}^{-3}$), biomass ($\mu\text{g}\cdot\text{L}^{-1}$ dry weight (dw)), richness ($\text{species}\cdot\text{sample}^{-1}$), mean body length (mm), and average body weight (μg dw) of each species. To test for differences between the zooplankton assemblages in the two sets of lakes, the data were first normalized using $\log(x + 1)$ transformation. At a community level of data integration, an independent-samples t test was used to determine if the total zooplankton density, richness, biomass, or mean animal size differed between the two sets of lakes. The more conservative, unequal variance assumption was used in the test if a Levene's test detected unequal variances. The test was repeated for total density and richness of Cladocera, Calanoida, and Cyclopoida. To detect changes in species composition between the two lake sets, multiple analysis of

Fig. 1. Scattergram of the frequency of occurrence of crustacean zooplankton species in the lakes with vs. without (i.e., reference lakes) *Bythotrephes*. Unidentified immatures are excluded. Species are numbered for their ranked frequency of occurrence in the reference lakes: 1, *Diacyclops bicuspidatus thomasi*; 2, *Mesocyclops edax*; 3, *Daphnia mendotae*; 4, *Holopedium glacialis* (commonly called *H. gibberum*); 5, *Bosmina freyi*; 6, *Leptodiaptomus minutus*; 7, *Skistodiaptomus oregonensis*; 8, *Diaphanosoma birgei*; 9, *Epischura lacustris*; 10, *Tropocyclops extensus* (commonly called *Tropocyclops prasinus mexicanus*); 11, *Daphnia dubia*; 12, *Daphnia longiremis*; 13, *Bosmina longispina*; 14, *Cyclops scutifer*; 15, *Chydorus sphaericus*; 16, *Daphnia catawba*; 17, *Bosmina tubicen*; 18, *Acanthocyclops vernalis* complex; 19, *Polyphemus pediculus*; 20, *Sida crystallina*; 21, *Ceriodaphnia lacustris*; 22, *Daphnia pulicaria*; 23, *Daphnia retrocurva*; 24, *Daphnia ambigua*; 25, *Latona setifera*; 26, *Bosmina liederi*; 27, *Limnocalanus macrurus*; 28, *Senecella calanoides*; 29, *Orthocyclops modestus*; 30, *Bosmina coregoni*; 31, *Leptodiaptomus ashlandi*; 32, *Leptodiaptomus sicilis*.

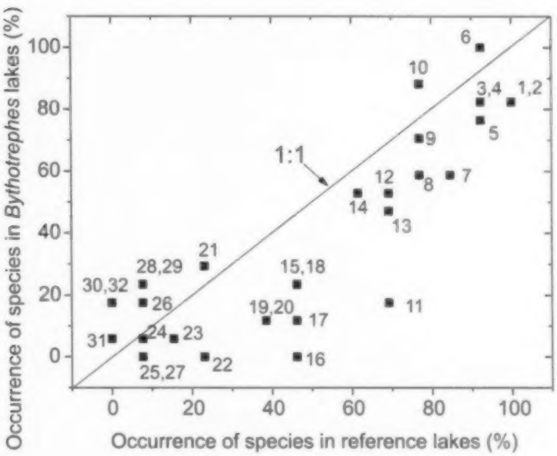

Fig. 2. Box-and-whisker plots of total crustacean zooplankton density (animals·L^{-1}), biomass (μg dry weight·L^{-1}), and species richness (species·sample^{-1}) in lakes with (w) and without (w/o) *Bythotrephes*. The box boundaries and mid-rib represent the quartiles and median. The mean (■) is within the box. Whiskers represent 99% confidence limits.

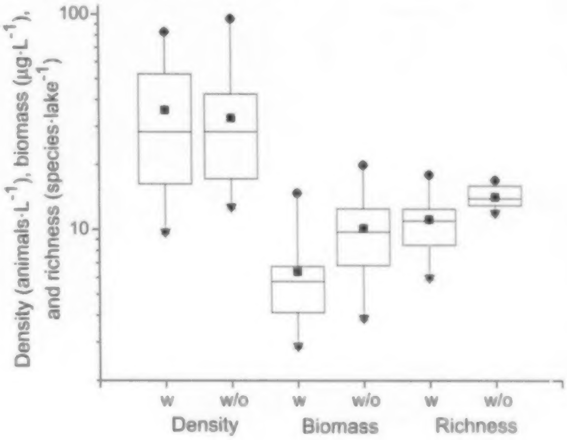

variance (MANOVA) was used on the abundances of individual species. Species found in less than 10% of the lakes (*Daphnia ambigua*, *Latona setifera*, *Leptodiaptomus ashlandi*, *Limnocalanus macrurus*, and an unidentified Harpacticoida species) were excluded from the MANOVAs, but immature copepods were included. *Polyphemus pediculus* was also excluded, as it is notoriously patchy and its abundances are not presumed to be well estimated at a single mid-lake station.

The well-known problem of increased probability of type 1 error (incorrect declaration of a significant difference) arises with the use of multiple tests. This probability is calculated as $1 - (1 - \alpha)^n$, where n is the number of tests. The standard solution, the Bonferroni adjustment of α, may create its own problems (Perneger 1998), potentially overprotecting for type 1 error rates at the expense of creating type 2 errors (failing to declare a difference that is real). In our study, we erected null hypotheses at three different hierarchical levels: the entire crustacean zooplankton community, the ordinal or subordinal taxonomic level (Cladocera, Calanoida, Cyclopoida), and the species level. Community-level differences were assessed with total abundance, biomass, richness, and mean animal body size, whereas differences at the species level were assessed by MANOVAs on species within Cladocera, Calanoida, and Cyclopoida. As we planned on rejecting the nulls of no difference between the two lake groups at a prespecified hierarchical level if any component test at that level was significant, adjustments for multiple tests were appropriate. Because of the overly conservative nature of Bonferroni adjustments, we adopted the Legendre and Legendre (1998) alternative. We computed adjusted p values (p') for each test where $p' = p(k - i + 1)$, with k being the number of p values and i being the rank of the particular p value from lowest to highest. No corrections for tied p values were necessary.

We tested three principal null hypotheses, i.e., that there were no differences in zooplankton assemblages between the two groups of lakes at the community level ($k = 4$ for richness, biomass, abundance, and body size), at the ordinal or subordinal levels ($k = 6$ for richness and abundance of Cladocera, Calanoida, and Cyclopoida), and at the species level ($k = 3$ for the MANOVA on cladoceran, cyclopoid, and calanoid species). We rejected these nulls when any one component $p' < 0.05$. We recognize that adjustments for multiple tests are contentious in ecology, and many ecologists wish to preserve the option of evaluating each test. For this reason, we report both p and p' values.

Results

We observed 32 crustacean zooplankton species in the 30 lakes, and there were clear and significant differences in the communities of the two groups of lakes. These differences were not evident in overall species rankings, as frequencies of occurrence of species were highly correlated ($r = 0.86$, $n = 32$; Fig. 1) in the two lake groups. However, the frequencies of occurrence of all but two of the 20 species found in >35% of the reference lakes were reduced in the lakes with *Bythotrephes* (Fig. 1). As a result, species richness was 30% higher ($t = 3.380$, $p = 0.003$, $p' = 0.012$; Fig. 2) in the refer-

Table 1. Summary of the *t* tests used to determine if cladoceran, calanoid, and cyclopoid density (animals·m^{-3}) and richness (species·lake^{-1}) differed between lakes with (Y) and without (N) *Bythotrephes*.

Metric	Invaded status	Mean	*t*	df	*p*	*p′*
Density						
Cladocera	N	6 616	2.98	28	**0.006**	**0.03**
	Y	3 181				
Calanoida	N	7 086	−0.43	28	0.77	1.0
	Y	7 089				
Cyclopoida	N	19 712	−0.96	28	0.24	0.72
	Y	25 571				
Richness						
Cladocera	N	9.55	3.83	22.3*	**0.001**	**0.006**
	Y	5.89				
Calanoida	N	3.55	−0.22	28	0.825	0.825
	Y	3.63				
Cyclopoida	N	4.90	1.36	28	0.184	0.736
	Y	4.47				

Note: *t* tests were run on log-transformed data, but arithmetic means are provided. Values in bold type indicate $p < 0.05$, and the asterisk (*) indicates degrees of freedom (df) adjusted for unequal variances. See Methods section for p' calculation method.

Fig. 3. Scatterplot of the invaded vs. reference lake mean abundances of the 19 species (all but *Polyphemus*) most commonly occurring in the reference lakes. Species are coded as in Fig. 1. Open symbols are copepods, i.e., Calanoida (○) and Cyclopoida (◇). Solid squares (■) are Cladocera. 1:1 and 10:1 (reference–invaded ratio) lines are provided for reference.

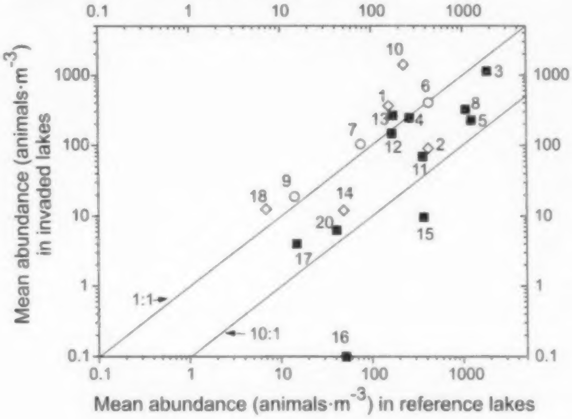

ence lakes (mean of 15.3 species·sample^{-1}) than in the invaded lakes (mean of 11.8 species·sample^{-1}). Total zooplankton density did not differ between the two groups of lakes ($t = 0.251$, $p = 0.8$, $p' = 0.8$; Fig. 2), with arithmetic means of 35.8 animals·L^{-1} in invaded lakes and a similar 32.9 animals·L^{-1} in reference lakes. In contrast, total zooplankton biomass averaged 5.41 µg dw·L^{-1} in the invaded lakes, significantly lower after log transformation ($t = 2.753$, $p = 0.01$, $p' = 0.03$) than the mean of 9.17 µg·L^{-1} recorded in the reference lakes (Fig. 2). This difference in biomass, without a corresponding difference in abundance, suggested that mean animal weight was larger in the reference lakes than in the invaded lakes; however, mean animal weight did not differ between the two groups of lakes after *p* values were adjusted for the four tests run at the community level ($t = 2.17$, $p = 0.039$, $p' = 0.078$). In the reference lakes, the mean animal weight was 0.35 µg dw in comparison with 0.21 µg in the lakes with *Bythotrephes*.

The communities of the two groups of lakes also differed significantly at the ordinal or subordinal levels. Total calanoid and cyclopoid density and richness did not differ, after log transformation, between the two groups of lakes, but the differences were significant for the Cladocera (Table 1). Cladoceran density and richness were, respectively, 50% and 36% lower in the invaded lakes.

The differences in total cladoceran standing stocks between the two groups of lakes could have been produced by many different changes in underlying cladoceran species composition. Further, the lack of differences in the copepod summary metrics could have masked significant, but counterbalanced, changes in copepod species composition. Hence, MANOVAs were performed to detect any differences in species composition between the two groups of lakes, and once again, the predominant differences detected were for Cladocera. The MANOVA on the calanoid and cyclopoid species abundances indicated no difference between invaded and reference lakes ($p = 0.77$ and $p' = 0.77$ and $p = 0.24$ and $p' = 0.48$, respectively). In contrast, the MANOVA on the cladoceran species ($p = 0.006$, $p' = 0.018$) detected a difference between the two groups of lakes. An examination of the mean abundances of common species in the two groups of lakes accounts for the MANOVA results. Excluding *Polyphemus*, which was assumed to be poorly sampled, 19 species (Fig. 1) were found in more than two-thirds of the reference lakes. Of these 19, the mean abundances of the adults of the three common calanoid species (*Leptodiaptomus minutus*, *Skistodiaptomus oregonensis*, and *Epischura lacustris*) were almost identical in the two groups of lakes (Fig. 3). Of the five commonly occurring cyclopoid species, *Tropocyclops extensus* was more abundant on average in the invaded lakes, whereas *Mesocyclops edax*, in particular, was much less abundant in invaded lakes. A more consistent pattern emerged for the Cladocera, especially among the epilimnetic taxa. Of 11 common species, mean abundances of the hypolimnetic *Daphnia longiremis* and *Bosmina longispina* (numbers 12 and 13 in Fig. 3) were quite similar in the invaded and reference lakes, as were abundances of the gelatin-encapsulated *Holopedium* (number 4 in Fig. 3). Mean abundances of the other cladoceran taxa were lower in the invaded lakes. *Daphnia catawba* and *Chydorus sphaericus* were more than 10 times lower in the invaded lakes, whereas mean abundances of *Bosmina tubicen*, *Sida crystallina*, *Daphnia dubia*, *Bosmina freyi*, and *Diaphanosoma birgei* were, respectively, 4, 7, 5, 5, and 3 times lower in the invaded lakes (Fig. 3). This consistent pattern among the epilimnetic and unprotected cladoceran species, large helmets or body size do not protect Cladocera from *Bythotrepehes* (Schulz and Yurista, 1999), accounts for the MANOVA results.

Discussion

There have been many mid-summer surveys of zooplankton in Canadian Shield lakes (e.g., Sprules 1975; Keller and

Yan 1991; Yan et al. 1996), and our results from the noninvaded lakes differ from several of these past studies in two important ways. The zooplankton biomasses that we observed are, in general, lower than other published data for Canadian Shield lakes (e.g., Yan and Strus 1980) and the species richness is higher than what has been previously recorded in nonacidic lakes (Keller and Yan 1991; Yan et al. 1996, 2002). In both cases, methodological differences between studies are the cause. The low biomass is attributable to differences between studies in sampling methods. We collected zooplankton in a single, vertical haul, whereas Yan et al. (1996) and Yan and Pawson (1997) collected volume-weighted composite samples, which inevitably yielded higher biomass estimates because they included a greater representation of surface waters, with their higher zooplankton densities. These differences in biomass estimation methods do not interfere with our ability to detect differences in relative biomass between invaded and reference lakes. Several previous studies have detected an average of 10 species of crustacean zooplankton per count in nonacidic lakes in Ontario (Sprules 1975; Keller and Yan 1991; Yan et al. 1996), somewhat lower than our richness estimates from noninvaded lakes. Again, our higher species richness is due to differences in counting protocol. Unlike previous studies, most of our samples were examined in their entirety for rare species. Such rigour is not characteristic of the literature. Again, these differences from the literature do not obscure our ability to detect differences between the invaded and reference lakes.

There were large differences in the crustacean zooplankton communities in the two sets of lakes. There are two possible explanations: a *Bythotrephes* effect or some other uncontrolled factor or factors. To be confident that a *Bythotrephes* effect was detected, we must first consider other possibilities. Factors known to influence the species richness and composition of zooplankton communities in Shield lakes include lake acidity (Havens et al. 1993), size (Yan et al. 1996; Keller and Conlon 1994), productivity (Dodson et al. 2000) or its covariate total phosphorus (Yan 1986), elevation and location (Keller and Pitblado 1989; Patalas 1990), water hardness (Keller and Pitblado 1989), fish predation (Magnan 1988; Yan et al. 2001), time of sampling, and annual climatic differences (Rusak et al. 2002). We can eliminate most of these alternative possibilities, all but differences in fish communities.

By design, there was no difference in when the two groups of lakes were sampled. The mean day of year at sampling did not differ between the two groups ($t = 0.278$, $p = 0.78$, df = 28), and all lakes were sampled in the same year. By design, there were no differences in the mean pH, total phosphorus concentration, or size of the study lakes (see Methods for details). As was previously mentioned, samples were collected in the summer at a single deep spot in each lake as is the conventional norm in synoptic zooplankton surveys (e.g., Sprules 1975; Patalas 1990; Keller and Conlon 1994). Hence, the differences in zooplankton communities that we observed between the two groups of lakes were not an artifact of differences in times of sampling or of water quality and lake size. We have very little fisheries data for the study lakes; however, the changes in cladoceran densities, i.e., the reductions in abundance of many small species, are not indicative of direct fisheries effects. Although our lack of good fish survey data prevents our testing of alternative fish-related hypotheses, it would appear that the differences detected between the two groups of lakes are not attributable to most logical uncontrolled factors in the study design.

Fig. 4. Scatterplot of cladoceran density (animals·m^{-3}) vs. *Bythotrephes* density (animals·m^{-3}) in the lakes with *Bythotrephes*.

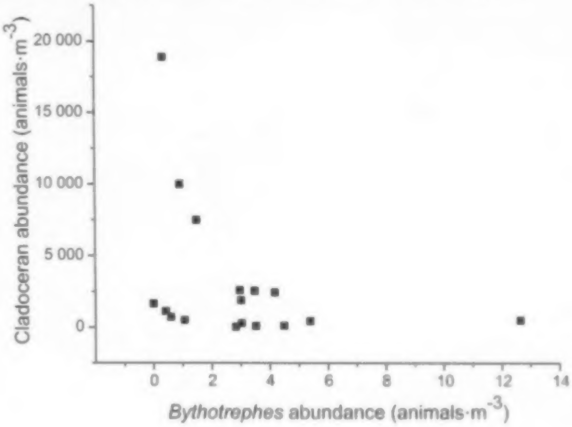

The differences that we detected between the lakes with and without *Bythotrephes* in our survey largely concur with temporal trends observed in the small number of previous studies on lakes invaded by *Bythotrephes*. Cladoceran species appear to be the most vulnerable to the invasion, as they are a suspected preferred food item (Grigorovich et al. 1998; Schulz and Yurista 1999). Consistent with our results, cladoceran biomass declined in Lake Michigan (Lehman and Cáceres 1993) and in Harp Lake (Yan et al. 2001) after the introduction of *Bythotrephes*. Also consistent with our results, cladoceran species richness declined in Harp Lake (Yan et al. 2002) and probably in Lake Michigan (Makarewicz et al. 1995) after invasion. Further, the epilimnetic cladoceran species apparently least impacted in our survey, *Holopedium* and *Daphnia mendotae*, are also the least-impacted Cladocera in Harp Lake (Yan et al. 2001). *Mesocyclops edax* was the cyclopoid taxon with largest intergroup difference in density in our study, and it is the only copepod for which density declined significantly in Harp Lake (Yan et al. 2001). Reasons for the apparent particular sensitivity of *M. edax* among Cyclopoida to *Bythotrephes* clearly warrant study.

Of course, it is not possible to use our data to prove that *Bythotrephes* was responsible for the differences in zooplankton communities observed between the two groups of lakes. Pre-invasion data from these lakes do not exist, nor can we model the actual impacts of *Bythotrephes* predation on zooplankton without far more than single mid-summer samples. What we do know is that the results are very consistent with the one, long-term, intensive study that is available, i.e., the study of Harp Lake (Yan and Pawson 1997; Yan et al. 2001; Dumitru et al. 2001). In addition, correlations between cladoceran abundance and *Bythotrephes* abundance are consistent with a causal *Bythotrephes* link (Fig. 4). A nonlinear, but negative, relationship between cladoceran density and *Bythotrephes* abundance in the invaded lakes is consistent with the hypothesized *Bythotrephes* effect and suggests an effect threshold of about 3–5 *Bythotrephes*·m^{-3}. A regression of log cladoceran species richness vs. *B. longimanus* abundance is also consistent with the *Bythotrephes* effect, i.e., it is negative and marginally significant (r^2 = 0.22, p = 0.056). Against expectation (Yan 1986), cladoceran density (log-transformed) was not correlated with total phosphorus ($r^2 = 0.01$, $p = 0.66$) in this data set. Similarly, cladoceran richness was not related to lake area (r^2 = 0.07, $p = 0.30$). Hence, there was no need to build multiple regression models to predict cladoceran abundance or richness from lakewater phosphorus and lake area in addition to *Bythotrephes* abundance.

The evidence is building that *Bythotrephes* is having an effect on the zooplankton communities of inland Ontario lakes, particularly on the cladoceran fauna. Although ours was a small synoptic study, it certainly suggests that the Harp Lake results are not unique. We may be at the early stages of broad-scale reductions in zooplankton biodiversity and cladoceran abundances in small and mid-size Canadian Shield lakes, i.e., lakes similar to those that we sampled, in response to the introduction and spread of *Bythotrephes*, although only additional monitoring will tell the tale. This could have impacts on both the predators and prey of zooplankton. Water clarity may change in response to changes in cladoceran herbivory should such changes occur (Carpenter et al. 1985), and small zooplanktivorous fish may be forced to compete more heavily for their prey with the invertebrate predator, *Bythotrephes* (Lehman and Branstrator 1995). Coupled with the Harp Lake trends, the results of our survey indicate that it is time to look for any such broader food-web impacts of *Bythotrephes* introductions into Shield lakes.

Acknowledgements

Support for this research was provided by the EJLB Foundation, the Canada Trust Friends of the Environment Foundation, and a Natural Sciences and Engineering Research Council of Canada (NSERC) research grant to N.D.Y. We thank staff of the Dorset Environmental Science Centre, Dorset, Ont., particularly R. Girard, for technical support and for water quality data. We also thank J. Cullen for constructing the "Woody Winder", used to haul the *Bythotrephes* net, and A. Boudreau and L. Whitty for technical support.

References

Allen, G., Yan, N.D., and Geiling, W.T. 1994. ZEBRA2 — Zooplankton Enumeration and Biomass Routines for APIOS: a semiautomated sample processing system for zooplankton ecologists. Ontario Ministry of Environment and Energy.

Borbely, J. 2001. Modelling the spread of the spiny waterflea (*Bythotrephes longimanus*) in inland lakes in Ontario using gravity models and GIS. M.Sc. thesis, University of Windsor, Windsor, Ont. Natl. Libr. Can., Can. Theses Amicus No. 25968094.

Boudreau, S. 2002. *Bythotrephes longimanus*, tracking the spread of a nonindigenous species and evaluating its impact on the crustacean zooplankton communities of Ontario inland lakes. M.Sc. thesis, York University, Toronto, Ont.

Carpenter, S.R., Kitchell, J.F., and Hodgson, J.R. 1985. Cascading trophic interactions and lake productivity. BioScience, **35**: 634–639.

Dodson, S.I., Arnott, S.E., and Cottingham, K. 2000. The relationship in lake communities between primary productivity and species richness. Ecology, **81**: 2662–2679.

Dumitru, C., Sprules, W.G., and Yan, N.D. 2001. Impact of *Bythotrephes longimanus* on zooplankton assemblages of Harp Lake, Canada: an assessment based on predator consumption and prey production. Freshw. Biol. **46**: 241–251.

Giguère, L.A., St. Pierre, J.F., Bernier, B., Vezina, A., and Rondeau, J.G. 1989. Can we estimate the true weight of zooplankton samples after chemical preservation? Can. J. Fish. Aquat. Sci. **46**: 522–527.

Grigorovich, I.A., Pashkova, O.V., Gromova, Y.F., and van Overdijk, C.D.A. 1998. *Bythotrephes longimanus* in the Commonwealth of Independent States: variability, distribution and ecology. Hydrobiologia, **379**: 183–198.

Havens, K.E., Yan, N.D., and Keller, W. 1993. Lake acidification: effects on crustacean zooplankton populations. Environ. Sci. Technol. **27**: 1621–1624.

Hoffman, J.C., Smith, M.E., and Lehman, J.T. 2001. Perch or plankton: top-down control of *Daphnia* by yellow perch (*Perca flavescens*) or *Bythotrephes cederstroemi* in an inland lake? Freshw. Biol. **46**: 759–775.

Keller, W., and Conlon, M. 1994. Crustacean zooplankton communities and lake morphometry in Precambrian Shield lakes. Can. J. Fish. Aquat. Sci. **51**: 2424–2434.

Keller, W., and Pitblado, R. 1989. The distribution of crustacean zooplankton in Northern Ontario, Canada. J. Biogeogr. **16**: 249–259.

Keller, W., and Yan, N.D. 1991. Recovery of crustacean zooplankton species richness in Sudbury area lakes following water quality improvements. Can. J. Fish. Aquat. Sci. **48**: 1635–1644.

Legendre, P., and Legendre, L. 1998. Numerical ecology. 2nd ed. Developments in environmental modelling 20. Elsevier Science Ltd., Amsterdam.

Lehman, J.T., and Branstrator, D.K. 1995. A model for growth, development, and diet selection by the invertebrate predator *Bythotrephes cederstroemi*. J. Great Lakes Res. **21**: 610–619.

Lehman, J.T., and Cáceres, C.E. 1993. Food-web responses to species invasion by a predatory invertebrate: *Bythotrephes* in Lake Michigan. Limnol. Oceanogr. **38**: 879–891.

MacIsaac, H.J., Ketelaars, H.A.M., Grigorovich, I.A., Ramcharan, C.W., and Yan, N.D. 2000. Modeling *Bythotrephes longimanus* invasions in the Great Lakes basin based on its European distribution. Arch. Hydrobiol. **149**: 1–21.

MacIsaac, H.J., Grigorovich, I.A., and Ricciardi, A. 2002. Reassessment of species invasions concepts: the Great Lakes basin as a model. Biol. Invasions, **3**: 405–416.

Magnan, P. 1988. Interactions between brook charr, *Salvelinus fontinalis*, and nonsalmonid species: ecological shift, morphological shift, and their impact on zooplankton communities. Can. J. Fish. Aquat. Sci. **45**: 999–1009.

Makarewicz, J.C., Bertram, P., Lewis, T., and Brown, E.H., Jr. 1995. A decade of predatory control of zooplankton species composition of Lake Michigan. J. Great Lakes Res. **21**: 620–640.

Mayer, T., Snodgrass, W.J., and Morin, D. 1999. Spatial characterization of the occurrence of road salt and their environmental correlations as chlorides in Canadian surface waters and benthic sediments. Water Qual. Res. J. Can. **34**: 545–574.

McQueen, D.J., and Yan, N.D. 1993. Metering filtration efficiency of fresh water zooplankton hauls: reminders from the past. J. Plankton Res. **15**: 57–65.

Mills, E.L., Leach, J.H., Carlton, J.T., and Secor, C.L. 1993. Exotic species in the Great Lakes: a history of biotic crises and anthropogenic introductions. J. Great Lakes Res. **19**: 1–54.

Patalas, K. 1990. Diversity of the zooplankton communities in Canadian lakes as a function of climate. Verh. Int. Verein. Limnol. **24**: 360–368.

Perneger, T.V. 1998. What is wrong with Bonferroni adjustments. Br. Med. J. **136**: 1236–1238.

Rosenberry, D.O., Buckaveckas, P.A., Buso, D.C., Likens, G.E., Shapiro, N.M., and Winter, T.C. 1999. Movement of road salt to a small New Hampshire lake. Water Air Soil Pollut. **109**: 179–206.

Rusak, J.A., Yan, N.D., Somers, K.M., Cottingham, K.L., Micheli, F., Carpenter, S.R., Frost, T.M., Paterson, M.J., and McQueen, D.J. 2002. Temporal, spatial, and taxonomic patterns of crustacean zooplankton variability in unmanipulated north-temperate lakes. Limnol. Oceanogr. **47**: 613–625.

Schulz, K.L., and Yurista, P.M. 1999. Implications of an invertebrate predator's (*Bythotrephes cederstroemi*) atypical effects on a pelagic zooplankton community. Hydrobiolgia, **380**: 179–193.

Sprules, W.G. 1975. Factors affecting the structure of limentic crustacean zooplankton communities in central Ontario lakes. Verh. Int. Verein. Limnol. **19**: 535–643.

Therriault, T.W., Grigorovich, I.A., Cristescu, M.E., Ketelaars, H.A.M., Viljanen, M., Heath, D.D., and MacIsaac, H.J. 2002. Taxonomic resolution of the genus *Bythotrephes* Leydig using molecular markers and re-evaluation of its global distribution. Divers. Distrib. **8**: 67–84.

Yan, N.D. 1986. Empirical prediction of crustacean zooplankton biomass in nutrient poor Canadian Shield lakes. Can. J. Fish. Aquat. Sci. **43**: 788–796.

Yan, N.D., and Pawson, T.W. 1997. Changes in the crustacean zooplankton community of Harp Lake, Canada, following invasion by *Bythotrephes cederstroemi*. Freshw. Biol. **37**: 409–425.

Yan, N.D., and Pawson, T.W. 1998. Seasonal variation in the size and abundance of the invading *Bythotrephes* in Harp Lake, Ontario, Canada. Hydrobiologia, **361**: 157–168.

Yan, N.D., and Strus, R. 1980. Crustacean zooplankton communities of acidic, metal contaminated lakes near Sudbury, Ontario. Can. J. Fish. Aquat. Sci. **37**: 2282–2293.

Yan, N.D., Dunlop, W.I., Pawson, T.W., and MacKay, L.E. 1992. *Bythotrephes cederstoemi* (Schoedler) in Muskoka lakes: first records of the European invader in inland lakes in Canada. Can. J. Fish. Aquat. Sci. **49**: 422–426.

Yan, N.D., Keller, W., Somers, K.M., Pawson, T.W., and Girard, R.E. 1996. Recovery of crustacean zooplankton communities from acid and metal contamination: comparing manipulated and reference lakes. Can. J. Fish. Aquat. Sci. **53**: 1301–1327.

Yan, N.D., Blukacz, A., Sprules, W.G., Kindy, P.K., Hackett, D., Girard, R.E., and Clark, B.J. 2001. Changes in zooplankton and the phenology of the spiny water flea, *Bythotrephes*, following its invasion of Harp Lake, Ontario, Canada. Can. J. Fish. Aquat. Sci. **58**: 2341–2350.

Yan, N.D., Girard, R., and Boudreau, S. 2002. An introduced predator (*Bythotrephes*) reduces zooplankton species richness. Ecol. Lett. **5**: 481–485.

Zooplankton biomass enhances growth, but not survival, of first-feeding *Pomoxis* spp. larvae

David B. Bunnell, María J. González, and Roy A. Stein

Abstract: We used otoliths to estimate growth and survival of white (*Pomoxis annularis*) and black (*Pomoxis nigromaculatus*) crappie larvae in five Ohio reservoirs. Because *Pomoxis* spp. larvae are among the smallest freshwater larvae and competition with gizzard shad larvae (*Dorosoma cepedianum*) is likely, we hypothesized that first-feeding *Pomoxis* spp. larvae would be susceptible to slow growth and starvation. We estimated survival by comparing proportional weekly cohort distributions of *Pomoxis* spp. larvae and juveniles. When distributions differed, a cohort survival index was evaluated against density of appropriately sized zooplankton biomass (crustaceans and rotifers), as well as temperature, turbidity, and density of all limnetic larvae that occurred during hatch week, when exogenous feeding began. Growth of first-feeding larvae (<10 days old) increased with total zooplankton biomass ($r^2 = 0.64$); growth of larvae aged 10–16 days was unrelated to all measured variables. Survival was positively correlated with zooplankton biomass in only one of four reservoirs, and other variables did not correlate as expected. This result casts doubt on whether zooplankton contributes to survival of freshwater larvae.

Résumé : Les otolithes nous ont servi à estimer la croissance et la survie des larves de mariganes blanches (*Pomoxis annularis*) et noires (*Pomoxis nigromaculatus*) dans cinq lacs de barrage de l'Ohio. Parce que les larves de *Pomoxis* spp. sont parmi les plus petites larves de poissons en eau douce et qu'il y a vraisemblablement de la compétition entre elles et les larves de l'alose à gésier (*Dorosoma cepedianum*), nous avons émis l'hypothèse selon laquelle les larves de *Pomoxis* spp. qui se nourrissent pour la première fois sont susceptibles d'avoir une croissance lente et de souffrir de carence alimentaire. Une comparaison des distributions proportionnelles hebdomadaires des cohortes de larves et de jeunes *Pomoxis* spp. nous a permis d'estimer la survie. Lorsque les distributions étaient différentes, nous avons évalué un coefficient de survie de la cohorte en fonction de la densité de la biomasse du zooplancton de taille appropriée (crustacés et rotifères), ainsi qu'en fonction de la température, de la turbidité et de la densité de l'ensemble des larves limnétiques présentes durant la semaine de l'éclosion, au moment où l'alimentation exogène a débuté. La croissance des larves qui se nourrissent pour la première fois (âgées de <10 jours) augmente en fonction de la biomasse totale du zooplancton ($r^2 = 0{,}64$), mais celle des larves âgées de 10–16 jours est indépendante de toutes les variables mesurées. La survie est en corrélation positive avec la biomasse du zooplancton dans seulement un de quatre lacs de barrage et les autres variables ne présentent pas les corrélations prévues. Ces résultats font douter de l'importance du rôle du zooplancton dans la survie des larves des poissons d'eau douce.

[Traduit par la Rédaction]

Introduction

Variable survival of young fish can drive population fluctuations (Houde 1987). To explain variable offspring survival of fishes, early marine studies focused on the role of starvation during the period when larvae shift from feeding endogenously on yolk sacs to exogenously on zooplankton (Hjort 1914). This hypothesis later was extended to freshwater environments. In experiments, survival of freshwater larvae generally increases with zooplankton density (e.g., Hart and Werner 1987; Welker et al. 1994). Despite experimental support for this hypothesis, zooplankton prey densities are generally unrelated to survival in freshwater field studies (e.g., Welker et al. 1994; Betsill and Van Den Avyle 1997; Garvey et al. 2002). The positive relationship between fish size and resistance to starvation (Hunter 1981; Miller et al. 1988) may help explain these conflicting results. Larvae hatching at larger sizes have the advantage of potentially higher energy reserves, as well as larger gapes, which permit access to more (i.e., larger) zooplankton, than those hatching at smaller sizes (Hunter 1981). Because freshwater larvae are generally larger at hatch than marine larvae, Houde (1994)

Received 2 June 2003. Accepted 12 August 2003. Published on the NRC Research Press Web site at http://cjfas.nrc.ca on 17 November 2003.
J17563

D.B. Bunnell[1,2] and R.A. Stein. Aquatic Ecology Laboratory, Department of Evolution, Ecology, and Organismal Biology, The Ohio State University, 1314 Kinnear Road, Columbus, OH 43212-1156, U.S.A.
M.J. González. Department of Zoology, Miami University, Oxford, OH 45056, U.S.A.

[1] Corresponding author (e-mail: bunnell@cbl.umces.edu).

[2] Present address: University of Maryland Center for Environmental Science, Chesapeake Biological Laboratory, P.O. Box 38, Solomons, MD 20688, U.S.A.

doi: 10.1139/F03-112

predicted that larval starvation would be less likely to occur in freshwater larvae. Thus, starvation during the larval stage may be rare for freshwater fishes.

Beyond the direct effects of starvation, low zooplankton densities also can influence larval survival via indirect effects. First, starved larvae swim more slowly than better-fed conspecifics, which may increase their vulnerability to predators (Rice et al. 1987). Second, low zooplankton densities and resultant slow growth increase the length of vulnerability to gape-limited predators (Crowder et al. 1987). Finally, small size resulting from slow growth will continue to limit the sizes of available zooplankton prey. Thus, faster growth and resultant larger size likely confers a suite of survival advantages to age-0 fishes (Miller et al. 1988).

Growth and survival of larvae can be influenced by factors other than density of prey. Temperature can modify egg development (Siefert 1968) and influence larval growth (Houde 1997). Turbidity can alter the visual environment for larvae, which in turn can mediate growth rates (Miner and Stein 1993). Density of co-occurring larval competitors also may reduce growth and survival of larvae by reducing densities of zooplankton prey (DeVries and Stein 1992). Herein, we sought to evaluate an extension of Hjort's (1914) critical period hypothesis with white (*Pomoxis annularis*) and black (*Pomoxis nigromaculatus*) crappie, popular freshwater sport fishes that frequently exhibit variable recruitment. Specifically, we evaluated how density of appropriately sized zooplankton biomass, water temperature, turbidity, and density of fish larvae occurring during the week that larvae hatch and become exogenous feeders influences their growth and survival to the juvenile stage.

We hypothesized that first-feeding *Pomoxis* spp. larvae may be vulnerable to low zooplankton densities because of their small size and potential vulnerability to competitors in Ohio reservoirs. In a compilation by Auer (1982) of 99 freshwater species (including 22 families) native to the Great Lakes basin, mean length at hatch was 6.24 mm; white crappie was the smallest species and black crappie was the third smallest (Auer 1982). Owing to the positive relationship between larval size at hatch and resistance to starvation (Miller et al. 1988), *Pomoxis* spp. are likely more vulnerable to starvation than most freshwater larvae. Second, interspecific competition with gizzard shad (*Dorosoma cepedianum*) larvae may reduce available zooplankton densities for crappie larvae. Previous research in hypereutrophic Ohio reservoirs has documented bluegill (*Lepomis macrochirus*) survival to be compromised by competitive interactions with gizzard shad (reviewed by Stein et al. 1995). High densities of age-0 gizzard shad deplete crustacean zooplankton (DeVries and Stein 1992), which in turn reduces survival of bluegill larvae (DeVries and Stein 1992; Garvey et al. 1998). Timing of larval hatch is critical: larvae hatching after the peak density of larval gizzard shad survive poorly (DeVries and Stein 1992; Garvey and Stein 1998). In 24 reservoir and year combinations in Ohio, the peak of bluegill larval density occurs at the same time as (36%) or after (40%) the peak of gizzard shad (Garvey and Stein 1998). Similarly, peak density of *Pomoxis* spp. larvae occurs at the same time as (21%) or after (41%) the peak density of gizzard shad larvae across 21 Ohio reservoir and year combinations (D.B. Bunnell, unpublished data). Because diets of first-feeding *Pomoxis* spp. and gizzard shad larvae overlap (DeVries et al. 1998), crappie larvae also may be vulnerable to competitive interactions with gizzard shad.

We used otoliths to understand how zooplankton density, water temperature, turbidity, and density of fish larvae (i.e., mostly gizzard shad) influenced the growth and survival of *Pomoxis* spp. larvae. By providing fish age, otoliths provide estimates of both growth rate (e.g., Claramunt and Wahl 2000) and hatch date. To understand factors influencing survival, we first determined whether the proportional weekly cohort distributions of limnetic larvae and surviving juveniles were different. If so, we then related weekly cohort survival to the aforementioned abiotic and biotic factors that occurred during the week that each cohort hatched and began feeding exogenously.

Materials and methods

Species life history

As different species, white and black crappies often co-occur and can hybridize (Smith et al. 1994). Although white crappies predominate in our study reservoirs (Table 1), the two species were pooled in this study because the larvae cannot be visually distinguished. Adults of both species spawn for 6–8 weeks during late spring through early summer (Pope and Willis 1998; D.B. Bunnell, unpublished data), exhibiting similar reproductive strategies as males build nests in the littoral zone (0.2- to 0.8-m depth; Siefert 1968) and then provide nest defence to incubating eggs (2–4 days) and embryos (i.e., yolk-sac larvae, 2–6 days; Siefert 1968). Larvae depart the nest at about the time of yolk-sac absorption (Siefert 1968), migrating to the limnetic zone where exogenous feeding begins. As larvae grow to the juvenile stage, both species migrate to benthic (offshore) habitat, where zooplankton remain their primary prey (Pine and Allen 2001; D.B. Bunnell, unpublished data).

Field and laboratory

Zooplankton sampling and estimation

Zooplankton were sampled weekly during May–June from five reservoirs during 2000 (Table 1). All collections were made during the day. With a conical, 54-μm-mesh net, we sampled crustacean zooplankton and rotifers from 1 m above the reservoir bottom to its surface at fixed inflow and outflow sites. Upon collection, zooplankton were preserved in 70% ethanol. In the laboratory, cladoceran zooplankters were identified to genus (e.g., *Daphnia*, *Bosmina*, *Eubosmina*, *Ceriodaphnia*, *Chydorus*, *Diaphanosoma*, and *Moina* spp.), and copepod zooplankters were classified as calanoid, cyclopoid, or nauplii. Rotifers were counted and identified to genus using a compound microscope. Crustacean zooplankton were counted following Stahl and Stein (1994). We measured crustacean total length (excluding spines on cladocerans, but including up to the base of the caudal rami on copepods) to the nearest 0.01 mm of the first 22 individual crustaceans encountered in each taxon, using a Sigma Scan digitizing system (SPSS Inc., Chicago, Ill.). We then used taxon-specific, length – dry weight equations (Dumont et al. 1975; Rosen 1981; Culver et al. 1985) to convert length to biomass. We measured up to 25 individuals from each rotifer

Table 1. Characteristics of Ohio study reservoirs.

Reservoir	County	Code	Surface area (km^2)	Chlorophyll *a* ($\mu g \cdot L^{-1}$)	Trophic status	White crappie population (%)	Mean white and black crappie adult CPE (fish per net-night)
Acton	Butler	AT	2.44	51.68	>E	100.0	3.13
Burr Oak	Morgan	BO	2.69	7.13	M	98.2	0.97
Caesar Creek	Warren	CC	11.45	12.09	>M	84.9	1.80
LaDue	Geauga	LD	6.07	15.07	>M	88.9	2.28
Pleasant Hill	Richland	PH	3.44	25.26	>M	97.4	5.48

Note: Chlorophyll *a* ($\mu g \cdot L^{-1}$) was the grand mean of inflow- and outflow-integrated water samples collected weekly during May–June 2000. Trophic status was based on Wetzel (2001), where E represents eutrophic and M represents mesotrophic; greater or less than signs were used when concentrations fell between two trophic indicators. White crappie population was the percentage of adult white crappie (by number) of the total adult *Pomoxis* spp. populations (black crappie + white crappie) pooled over 4 years (1998–2001) of autumn trap-netting. Mean white and black crappie adult (age ≥2) catch per effort (CPE, fish per net-night) provided a relative size of the adult populations during 1998–2001.

genus to the nearest 0.1 mm using the ocular micrometer on a compound microscope. Rotifer biomass was calculated using geometric formulas that approximate the volume of individuals (Ruttner-Kolinsko 1977). Volume was converted to wet weight assuming a specific gravity of 1. Dry weight was estimated as 0.1 × wet weight (Doohan 1973).

Collection and aging of larvae

Limnetic larvae were sampled weekly during the day in the top metre of water with neuston nets (1 m × 2 m wide mouth, 0.5-mm mesh) from the same reservoirs, years, and sites in which zooplankton were collected. Each of two replicates was a 5-min tow at 1 $m \cdot s^{-1}$, except when high zooplankton densities necessitated shorter tows. A flowmeter mounted at the mouth of the net provided estimates of volume sampled. Across a productivity gradient of Ohio reservoirs, *Pomoxis* spp. larvae are evenly distributed across the top 3 m of water in the day (Arend 2002). Thus, our sampling should provide an appropriate representation of larval densities in the epilimnion. Larvae were identified as gizzard shad, *Lepomis* spp., or *Pomoxis* spp. Similar numbers of myomeres prevented us from partitioning *Pomoxis* (Siefert 1969) or *Lepomis* genera into species.

To estimate density, at least 200 individuals were counted from a known percentage of the sample and then were extrapolated to a total estimate. If fewer than 200 individuals were in a sample, all individuals were counted. In some samples, however, larvae in a taxon were extremely rare (i.e., fewer than three larvae in at least 25% of the sample). To reduce processing time, we determined how well extrapolating from 25% predicted the complete count. For 36 estimates in 1998, we found the extrapolated estimate to be a strong predictor of the complete count ($r^2 = 0.69$, $F_{[1,34]} = 77.3$, $P < 0.0001$). Hence, we used the extrapolated estimate when fewer than three larvae were counted in at least 25% of the sample for the samples processed in 1999–2000. We measured total length (nearest 0.01 mm) of up to the first 50 *Pomoxis* spp. larvae encountered in all replicate samples (if less than 50 were collected, then all larvae were measured).

The 9-week sampling period was divided into three, 3-week periods: early, middle, and late. For all reservoir-years, we quantified age of *Pomoxis* spp. larvae during 1 week in the middle period (between late May and early June) because larvae were captured at the highest density and the widest length distribution at this time. For two reservoirs, we also estimated ages of larvae sampled during the early and late periods (for more details, see Larval survival section in Analyses). Thirty fish per site were selected for age estimation such that the length distribution of those to be aged mirrored the length distribution of previously measured fish. Right and left sagittal otoliths were removed and mounted on glass slides with Canada balsam. White crappie larvae lay their first ring at hatch, and subsequent rings are formed daily (Sweatman and Kohler 1991); we assumed that black crappie larvae also lay daily rings (sensu Pine and Allen 2001). Daily rings were counted at 100–200× magnification; number of rings estimated age in days. From a subset of 100 aged otoliths, readers disagreed no more than 2 days on 97% of the otoliths with age estimates less than 11 days. Disagreements on the remaining 3% of otoliths were 3 days. Thus, all otoliths that had an initial age estimate less than 11 days were not aged by a second reader. Those initially aged to be at least 11 days were aged by a second reader. In this case, a mean of the two age estimates was used when the estimates differed by 3 or fewer days. When the age estimates differed by more than 3 days (occurred ~10% of otoliths), a third "consensus" read occurred (Welker et al. 1994). In about 3% of consensus reads, the otolith was determined to be unreadable.

Collection and aging of juveniles

Pomoxis spp. juveniles were sampled with a bottom trawl (mouth width = 3.7 m; body length = 4.6 m; bar mesh body = 8.4 mm; bar mesh bag = 6.4 mm; same as Pine and Allen 2001) during 11–14 July 2000. At each reservoir, we pulled four to seven trawls for a minimum of 3 min at depths of 3–6 m in both inflow and mid-reservoir sites. Trawls in deeper outflow sites, near the dam, yielded no juvenile crappies. Within each reservoir, *Pomoxis* spp. (N = 76–250 per reservoir) were measured (nearest mm total length (TL)) and then pooled across sites. For aging of larvae, we used the length distribution to subsample a similarly distributed length distribution of 60 juveniles to be aged. Otoliths were prepared as described for larvae, except otoliths older than 20 days were ground with 1- to 9-μm wet–dry sandpaper owing to their more convex shape and opaque color.

Analyses

Larval growth

Daily growth rate (DGR) was estimated as (TL − 3.23)/age, where TL (mm) represents total length at capture, 3.23 is TL at hatch, and age is the number of days since hatch. Length at hatch was the y intercept in the age versus length regression for all larvae aged (TL = 3.23 + 0.46(age), $F_{[1,1720]} = 10896$, $r^2 = 0.86$, $P < 0.0001$) and was more than some previous estimates (2.2 mm TL, Auer 1982; 2.56 mm TL, Siefert 1969) and less than others (4 mm TL, Chatry and Conner 1980). From the inflow site only, we evaluated how growth was influenced by abiotic and biotic factors. Because larvae captured from the outflow site could have been transported from the inflow site, we related growth only with larvae captured at the inflow site. Larvae aged younger than 17 days were grouped as a function of reservoir, week of hatch, week of collection, and age-class (age-class I, 3–9 days; age-class II, 10–16 days) to estimate a mean daily growth rate of fishes that experienced similar conditions. Groups with at least five larvae were used. Within each age-class, we pooled growth rates of groups across reservoirs to evaluate whether variability in mean DGR was explained by some measure of zooplankton biomass (see below), density of all limnetic larvae (gizzard shad + *Pomoxis* spp. + *Lepomis* spp.), turbidity, and temperature. Because these four independent variables (with interactions) could generate multiple linear regression models, we used Akaike's information criterion (AIC) to choose the suite of models that best described our data set, rather than an iterative multiple regression that selects only the "best" model. From each of 12 a priori models that we hypothesized to explain variation in daily growth rate, we estimated parameters and residual sums of squares and then used Burnham and Anderson (1998) to calculate second-order AIC (AIC_c; because our ratio of parameters to observations was <40). For each model, Δ_i was reported as $AIC_c - \min(AIC_c)$, where $\min(AIC_c)$ is the smallest AIC_c value among the models. Models for which $\Delta_i \leq 2$ provided "substantial" support in explaining variation in the data (Burnham and Anderson 1998).

For each group of larvae, the independent variables were the average value from the week of hatch until week of capture. All variables were measured weekly at each site, except temperature, which was measured by remote data loggers every 4 h at a 1-m depth. We estimated turbidity (nearest 0.01 nephelometric turbidity units (NTU)) of euphotic water with a nepholometer in Acton, Burr Oak, and Caesar Creek; in the other reservoirs, we estimated turbidity with an inverse polynomial relationship between turbidity and secchi depth ($\mathrm{NTU} = -6.3 + (3010.5 \cdot \mathrm{secchi}^{-1}) + (-236983.7 \cdot \mathrm{secchi}^{-2}) + (6572005.8 \cdot \mathrm{secchi}^{-3})$, $r^2 = 0.56$, $P < 0.0001$, $N = 266$). We hypothesized that two measures of zooplankton biomass could relate to growth: (1) total zooplankton biomass, which included all appropriately sized crustacean zooplankton and rotifers (first-feeding *Pomoxis* spp. larvae consume rotifers (Arend 2002; D.B. Bunnell, unpublished data), and (2) preferred crustacean zooplankton biomass, which included all appropriately sized calanoid and cyclopoid copepods, nauplii, and *Diaphanosoma* spp. (DeVries et al. 1998; Pope and Willis 1998; D.B. Bunnell, unpublished data). We used Pearson's correlation to determine which zooplankton measure to include in the general linear model, i.e., which was most positively correlated to growth. Because first-feeding *Pomoxis* spp. larvae are gape-limited (DeVries et al. 1998), our estimates included only the zooplankton biomass that *Pomoxis* spp. larvae were able to eat. Using mean TL of each group of larvae, we estimated *Pomoxis* spp. gape size, and the resultant maximum zooplankton size, with a TL – gape size regression (DeVries et al. 1998). We used the length measurements for each zooplankton taxon at each site per sampling week to estimate weekly biomass of appropriately sized zooplankton taxa as

$$B = \sum p_i(A_i)(B_i) \tag{1}$$

where p_i is proportion of individuals in taxon i that were smaller than or equal to the larval gape, A_i is the total zooplankton abundance (number·L^{-1}) for taxon i, and B_i is the mean calculated biomass of individuals in taxon i that were smaller than or equal to the larval gape. For all rotifer taxa, $p_i = 1.0$, except for *Asplanchna* spp., which can exceed the gape of *Pomoxis* spp. larvae smaller than 8 mm TL.

Larval survival

Collecting a sample of juvenile survivors enabled us to use otoliths to calculate hatch dates (day of capture – estimated age) and compare proportional weekly cohort distributions of juvenile survivors with proportional weekly cohort distributions of recently hatched larvae. For each juvenile aged, we calculated a hatch date and assigned it to a cohort. We then calculated a proportional cohort distribution of juvenile survivors for each reservoir.

To estimate a proportional cohort distribution of larvae, we sought to include only fish that had arrived in the limnetic zone since our previous sampling event. This approach eliminated biasing the distribution toward cohorts in which larvae were surviving well, as those cohorts could be sampled during multiple weeks. Larvae collected in the neuston net were aged as young as 4 days, corroborating when *Pomoxis* spp. larvae depart the nest and begin to feed exogenously (Siefert 1968). We assumed that all larvae recruited to the limnetic zone by age 5 days; in our weekly sampling schedule, the oldest fish that could have recruited to the limnetic zone between weekly sampling events would be age 11 days. Fish older than 11 days should have been captured in earlier sampling efforts and, thus, were not included in our later analyses. We are confident that our sample was representative of all larvae that initially recruited to the limnetic zone from the nest (i.e., that larvae did not starve before being sampled). Their size at hatch predicts that 50% of starved larvae will survive 14 days (Miller et al. 1988). With our weekly sampling schedule, starved *Pomoxis* spp. larvae would have to survive a maximum of 6 days before being collected, minimizing the likelihood that significant numbers of larvae died from starvation before being sampled.

To assign larvae to cohorts, we used reservoir-specific, length vs. age regressions, rather than reading otoliths of all larvae sampled. In each reservoir, the regression was developed using fish sampled during the middle period. In Caesar Creek and Burr Oak, insufficient sample sizes made regression estimation infeasible in early or late periods. However, early and late period regressions were developed for Pleasant Hill and LaDue to explore how potential differences in growth rates between periods could influence construction of the distribution. The regression assigned ages and weekly cohorts to all measured fish. At each site on each sampling day, we estimated the proportion represented by each cohort. We also used the ages to estimate the proportion of measured individuals that were 11 days or younger (i.e., recently hatched) and then multiplied that fraction by the total catch.

Next, we multiplied the proportion of each cohort by this estimate of recently hatched larvae to generate a cohort-specific hatch density for each site – sampling day combination. Because we could not link surviving juveniles to a specific site, we added cohort-specific densities across sites and sampling days and then determined a proportional cohort distribution of larvae for each reservoir.

In assigning cohorts to juveniles, we considered the likelihood that older juveniles were less likely to be sampled than younger juveniles, owing to higher cumulative mortality for the older ones (sensu Campana and Jones 1992). To correct for this, we used a daily juvenile mortality rate to standardize cohort distributions such that the juvenile abundance represented fish captured at similar ages. Specifically, we subtracted the median age of the youngest cohort sampled from the median age of each cohort. We then estimated the survival rate for the cohort during that period and multiplied the inverse of that survival rate by the relative abundance of each cohort (Methot 1983). Without knowing the daily mortality rate of juveniles, we expected it to be lower than that of larvae, which we estimated to be between 0.10 and 0.15 through catch curve analyses (D.B. Bunnell, unpublished data). We evaluated the effects of both a low and high juvenile mortality rate in correcting the juvenile hatch date distribution. We used 0.05 as a low daily mortality rate and 0.15 as a high one, the low rate being smaller than our larval mortality rate and the high rate being within the range measured for juvenile black crappies in Florida (0.09–0.25; Pine and Allen 2001).

With proportional cohort distributions for both larvae and juveniles, we first compared the distributions with a Kolmogorov–Smirnov (K–S) test. When the distributions differed, we calculated an index of cohort larval survival, β_i, as J_i/H_i, where i represents cohorts 1 through 9, J_i is the proportion of juvenile crappies sampled from cohort i, and H_i is the proportion of all larvae hatched from cohort i (Crecco and Savoy 1985; Garvey et al. 2002). For all scenarios of daily juvenile mortality regimes (i.e., zero (uncorrected), low (0.05), and high (0.15)), we used Pearson's correlation to relate β_i to variables measured during the week that larvae hatched and became exogenous feeders. Measured characteristics used in the analyses were the same as those used in the growth analyses: density of all fish larvae, temperature, turbidity, and two measures of appropriately sized zooplankton biomass (e.g., total zooplankton biomass or preferred crustacean biomass). We predicted survival to be negatively correlated with density of fish larvae and turbidity and positively correlated with zooplankton and temperature. If the predicted linkage was consistent for all three scenarios, then we concluded it to be insensitive to potential juvenile mortality regimes. If the predicted linkage occurred at fewer scenarios, then we concluded it to exist only under specific assumptions. Finally, if the predicted linkage was not realized under any scenario, then we concluded that it was not supported by our data.

For all measures of zooplankton biomass, we used 6.0 mm TL (i.e., predicted length at age 6 days) to determine the gape size (DeVries et al. 1998) and biomass (see eq. 1) of zooplankton sufficiently small for first-feeding larvae to consume each week. Because we could not determine whether juvenile survivors came from inflow or outflow sites and because zooplankton and temperature vary between sites, we used the proportion hatching from each site to weight the site-specific variables.

Results

Zooplankton availability

Density and composition (crustacean vs. rotifer) of zooplankton varied across weeks within reservoirs (Fig. 1). Crustacean biomass was generally always higher than rotifer biomass in all reservoirs except Acton Reservoir, the most eutrophic reservoir (see Table 1). Pleasant Hill also exhibited some weeks when rotifer biomass exceeded crustaceans, which was driven by high densities of *Asplanchna* spp. With regard to abundance, rotifers exceeded crustacean zooplankters at both sites of all reservoirs. In fact, across all reservoirs mean crustacean abundance was less than 50 L^{-1}, with the highest abundance observed equaling 78 L^{-1} and the median density equaling 13 L^{-1}. Mean total abundance (including rotifers) increased to at least 150 L^{-1} at all inflow sites and 60 L^{-1} at all outflow ones. Thus, fish larvae in each reservoir were faced with a prey environment that varied both in composition (i.e., rotifer and crustacean zooplankton) and in density (i.e., biomass and abundance) across weeks.

Larval growth

Mean growth rates of *Pomoxis* spp. larvae ranged from 0.43 to 0.57 mm·day^{-1}. For first-feeding larvae in age-class I (age 3–9 days), total zooplankton biomass was positively correlated with growth ($r = 0.80$, $N = 11$ groups, $P = 0.003$); preferred crustacean zooplankton biomass was unrelated to growth ($r = 0.002$, $N = 11$ groups, $P = 0.95$). Among a priori models, the one that included only total zooplankton biomass had the lowest AIC$_c$ value (Table 2), indicating the highest support for explaining variation in growth. As expected, growth increased with increasing total zooplankton biomass density (95% confidence limits of slope = 3.31^{-4} to 1.19^{-3}). A second model that included total zooplankton biomass and density of fish larvae also deserved consideration for explaining variation with a Δ_i value less than 2.00 (Burnham and Anderson 1998). The slope of the larval fish density parameter, however, did not differ from zero (95% confidence limits = –0.011 to 0.001). Among older larvae in age-class II (ages 10–16 days), neither total zooplankton biomass ($r = 0.20$, $N = 8$ groups, $P = 0.64$) nor preferred crustacean zooplankton biomass ($r = 0.28$, $N = 8$ groups, $P = 0.49$) was positively related to growth. Among a priori models, the four models that included only one slope parameter ranked the highest (Table 2). In each model, however, the slope did not differ from zero (95% confidence limits: turbidity = –0.01 to 0.005; preferred crustacean zooplankton biomass = -2.42^{-3} to 4.46^{-3}; temperature = –0.019 to 0.021; larval fish density = –0.008 to 0.008), indicating that our measured variables were largely unsuccessful in explaining variation in growth of larvae older than 9 days.

Larval survival in 2000

To estimate cohort survival, β, we compared proportional cohort distributions of recently hatched larvae with those of surviving juveniles. For larvae, weekly cohorts were assigned using a length versus age regression derived from

Fig. 1. Mean density of crustacean zooplankton (solid bars) and rotifer (open bars) biomass at the inflow and outflow sites of (*a*) Acton, (*b*) Burr Oak, (*c*) Caesar Creek, (*d*) LaDue, and (*e*) Pleasant Hill reservoirs as a function of week during May–June 2000.

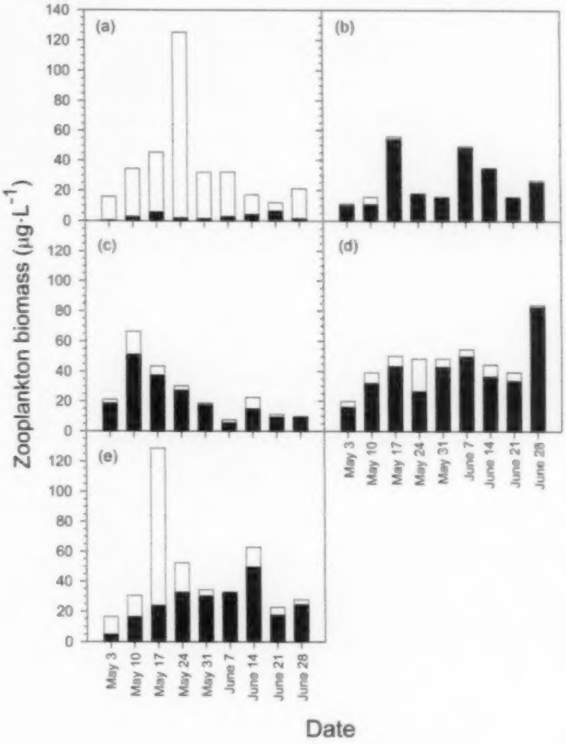

Table 2. Rankings of a priori models to explain variation in larval growth of (*a*) age-class I and (*b*) age-class II *Pomoxis* spp. larvae from five Ohio reservoirs.

Model	K	AIC$_c$	Δ_i	w_i	r^2
(a) Age-class I (3–9 days old)					
ZP	3	–75.21	0.00	0.547	0.64
ZP, L	4	–73.70	1.51	0.257	0.74
ZP, Tp	4	–70.72	4.49	0.058	0.66
ZP, Tu	4	–70.06	5.15	0.042	0.64
ZP, ZP × Tp	4	–70.04	5.16	0.041	0.64
ZP, ZP × Tu	4	–69.96	5.24	0.040	0.64
ZP, L, Tu	5	–66.55	8.66	0.007	0.75
L	3	–64.48	10.72	0.003	0.05
Tp	3	–64.14	11.07	0.002	0.02
Tu	3	–64.11	11.10	0.002	0.02
ZP, Tp, Tu	5	–63.43	11.77	0.002	0.67
ZP, Tp, Tu, L	6	–55.80	19.40	0.000	0.75
(b) Age-class II (10–16 days old)					
Tu	3	–44.89	0.00	0.323	0.12
ZP	3	–44.54	0.35	0.272	0.08
Tp	3	–43.89	1.00	0.196	0.00
L	3	–43.85	1.03	0.193	0.00
ZP, Tu	4	–36.26	8.63	0.004	0.20
ZP, ZP × Tu	4	–35.74	9.15	0.003	0.14
ZP, ZP × Tp	4	–35.55	9.34	0.003	0.12
ZP, L	4	–35.47	9.42	0.003	0.11
ZP, Tp	4	–35.28	9.60	0.003	0.09
ZP, Tp, Tu	5	–17.68	27.20	0.000	0.20
ZP, Tu, L	5	–17.67	27.22	0.000	0.20
ZP, Tp, Tu, L	6	37.67	82.55	0.000	0.27

Note: Rank was determined by AIC$_c$ values (smallest value equals highest rank). In each model, ZP represents zooplankton biomass, L represents density of all fish larvae, Tp represents water temperature, and Tu represents turbidity. Column headings include *K* (the number of slope parameters plus the error and intercept), Δ_i (difference between each model and the model with the minimum AIC$_c$ value), w_i (the relative "weight" of evidence for each model), and r^2 (the proportion of variance explained by the model).

larvae sampled during the middle period in each reservoir. Length was a strong predictor of age in all reservoirs (range of r^2 = 0.68 to 0.84, mean = 0.76). To determine whether differences in growth rates between sampling periods would change the proportional cohort distribution, we compared a distribution that used period-specific (i.e., early, middle, and late) length vs. age regressions with one that applied the middle period regression to all periods in Pleasant Hill and LaDue reservoirs. For each, no differences existed (Kolmogorov– Smirnov test: LaDue, K–S = 0.007, D = 0.01, P = 1.00; Pleasant Hill, K–S = 0.004, D = 0.008, P = 1.00), likely because the range of predicted age across periods was generally about 1 day (e.g., for an 8-mm fish, range of Pleasant Hill predicted ages = 7.9–9.1 days, range of LaDue predicted ages = 8.9–9.2 days), which would rarely affect the assignment of a fish to a weekly cohort. Thus, applying the middle-period regression to all periods provided an accurate representation of proportional cohort distribution for larvae.

Within each reservoir, juvenile survivors ranged widely in size (minimum range = 29 mm; maximum range = 42 mm) and age (minimum range = 28 days; maximum range = 42 days). Correcting for a higher cumulative juvenile mortality for earlier-hatched cohorts altered the juvenile cohort distributions: the higher the mortality rate, the higher the proportion of earlier cohorts (Fig. 2). Overall, the proportional hatch distribution of juveniles rarely matched that of larvae. Only when juvenile mortality was assumed to be high in Caesar Creek and Pleasant Hill (dotted lines in Figs. 2*c* and 2*e*, respectively) were the distributions similar between juveniles and larvae (Kolmogorov–Smirnov test: Caesar Creek, K–S = 0.06, D = 0.12, P = 0.79; Pleasant Hill, K–S = 0.06, D = 0.12, P = 0.81). Comparing distributions in Acton was inappropriate because the proportion of early-hatching larvae was underestimated owing to larvae not being sampled in the second week of May.

When the cohort distributions of larvae and juveniles differed, we used Pearson's correlation to evaluate whether the differential cohort survival was related to abiotic and biotic characteristics during the week when larvae hatched and became exogenous feeders. Because of our uncertainty regarding juvenile mortality, we ran these analyses under zero (0.0 daily mortality), low (0.05), and high (0.15) daily juvenile mortality rate scenarios. Within each reservoir, correlations between cohort survival and biotic and abiotic characteristics during hatch week revealed few correlations (Table 3). Sur-

Fig. 2. Survival of *Pomoxis* spp. larvae to the juvenile stage in (*a*) Acton, (*b*) Burr Oak, (*c*) Caesar Creek, (*d*) LaDue, and (*e*) Pleasant Hill reservoirs as a function of hatch week for each cohort. Proportion of cohorts of larvae (sampled May–June) is depicted as shaded, vertical bars on the left *y*-axis, and the proportion of cohorts of juveniles (sampled 11–14 July 2000) is depicted as lines on the right *y*-axis. Cohort distributions of juveniles were corrected for differences in cumulative mortality between the oldest and youngest cohorts (see Materials and methods). For clarity, the two extreme mortality possibilities are depicted: zero mortality (i.e., no correction) with the solid line and high mortality (daily mortality = 0.15) with the dotted line. The asterisk (*) on the proportional distribution of larvae in (*a*) indicates that the distribution likely underestimates the proportion of larvae hatched during the week of 3 May 2000 as a result of no larval samples collected during the week of 10 May 2000 in Acton.

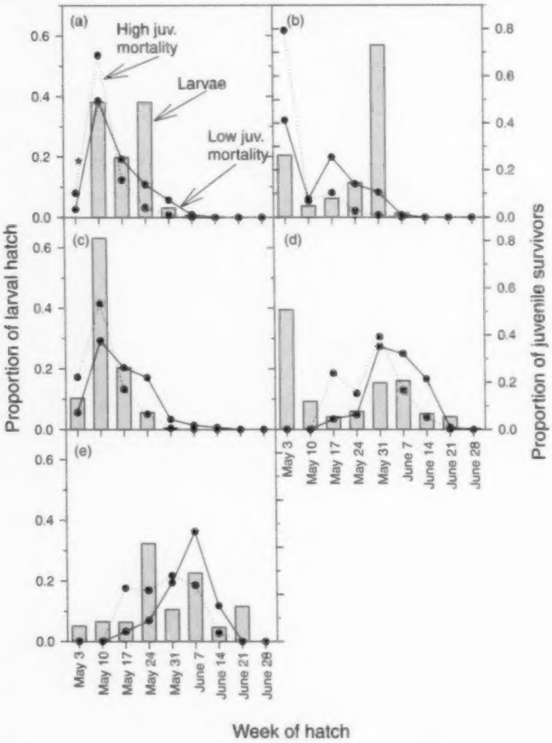

vival increased with total zooplankton biomass only in Burr Oak, when juvenile mortality was assumed to be zero or low (0.05). Preferred crustacean zooplankton biomass also failed to yield correlations with survival. In addition, neither density of fish larvae nor turbidity was ever negatively associated with survival, which was counter to our predictions. Temperature, which could have increased survival by increasing egg development or larval growth rate, was never positively associated with survival. Thus, among a range of possible juvenile mortality scenarios, we failed to document support that the abiotic and biotic environment in the first week of life was critical to survival to the juvenile stage.

Table 3. Pearson's correlation coefficient and *P* value (in parentheses) between β_i, an index of *Pomoxis* spp. larval survival during 2000, and total zooplankton biomass (crustaceans and rotifers), density of all fish larvae (i.e., gizzard shad, *Lepomis* spp., *Pomoxis* spp.), turbidity, and temperature during the week of *Pomoxis* spp. hatch in four Ohio reservoirs under three different juvenile mortality regimes: zero (0.0 daily mortality), low (0.05 daily mortality), and high (0.15 daily mortality).

		Zooplankton			Density of all fish larvae			Turbidity			Temperature		
		Juvenile mortality correction			Juvenile mortality correction			Juvenile mortality correction			Juvenile mortality correction		
Reservoir	*N*	Zero	Low	High	Zero	Low	High	Zero	Low	High	Zero	Low	High
Burr Oak	7	**0.87** **(0.01)**	**0.86** **(0.01)**	0.34 (0.45)	**0.85** **(0.02)**	0.47 (0.29)	–0.34 (0.46)	0.05 (0.92)	–0.10 (0.83)	–0.26 (0.57)	–0.36 (0.43)	–0.57 (0.18)	**–0.76** **(0.05)**
Caesar Creek	7	–0.39 (0.39)	–0.53 (0.23)		0.59 (0.16)	0.66 (0.11)		0.06 (0.90)	–0.12 (0.79)		**0.77** **(0.04)**	0.66 (0.11)	
LaDue	9	–0.02 (0.97)	0.12 (0.77)	0.42 (0.26)	0.24 (0.53)	0.13 (0.75)	–0.23 (0.55)	–0.13 (0.74)	0.02 (0.95)	**0.82** **(0.01)**	0.38 (0.31)	0.23 (0.56)	–0.42 (0.26)
Pleasant Hill	8	–0.18 (0.68)	–0.19 (0.65)		0.33 (0.43)	0.50 (0.21)		**0.73** **(0.04)**	0.61 (0.11)		0.56 (0.15)	0.44 (0.27)	

Note: Significant ($P \leq 0.05$) correlations are depicted in bold. *N* is the number of weekly cohorts for which β_i was measured in each reservoir. We did not estimate correlations in Acton Lake because no larval samples were collected in the second week of May, which underestimated the number of early-hatching larvae. We did not estimate correlations for the high juvenile mortality scenario for Caesar Creek and Pleasant Hill because those proportional distributions were similar between juveniles and larvae.

Discussion

We hypothesized that growth and survival of *Pomoxis* spp. larvae would increase with zooplankton biomass and temperature and decline with turbidity and density of larval fish competitors. As predicted, growth of first-feeding larvae (age 3–9 days) increased with biomass of crustacean zooplankton and rotifers; other variables, however, were unimportant. Growth of older larvae (age 10–16 days) was unrelated to all measured variables. With regard to survival, higher zooplankton biomass for first-feeding larvae was associated with high survival in only one of four reservoirs. None of the remaining variables revealed the hypothesized associations. Thus, despite positive effects of zooplankton biomass on growth of first-feeding *Pomoxis* spp. larvae, we found minimal evidence that survival to the juvenile stage was enhanced by higher zooplankton biomass.

For first-feeding *Pomoxis* spp. larvae (age-class I), total zooplankton biomass best explained daily growth rate, suggesting rotifers and other small nonpreferred prey (e.g., genera *Bosmina*, *Chydorus*, *Eubosmina*, *Asplanchna*, *Brachionus*, etc.) improved growth of gape-limited larvae. Such a strong relationship ($r^2 = 0.64$), however, was not documented for older, age-class II larvae. Conceivably, characterizing the growth environment is more difficult for older larvae than for younger larvae. Relative to older larvae, younger larvae may well be more closely associated with their sampling location and hence their abiotic and biotic environment. Previous work with *Pomoxis* spp. larvae provides somewhat different results. In Illinois reservoirs, growth was negatively correlated with crustacean zooplankton density and temperature but positively correlated with copepod nauplii density and percent of water volume occupied by littoral habitat (Claramunt and Wahl 2000). We did not evaluate volume of littoral habitat and we documented that temperature, as well as fish larvae and turbidity, were unrelated to growth. We are unsure why warmer temperatures did not increase growth. Growth rates in Ohio reservoirs (range = 0.43–0.57 $\text{mm}\cdot\text{day}^{-1}$, mean = 0.50 $\text{mm}\cdot\text{day}^{-1}$) were within the range of those measured in Illinois (range = 0.26–1.00 $\text{mm}\cdot\text{day}^{-1}$, mean = 0.58 $\text{mm}\cdot\text{day}^{-1}$; Claramunt and Wahl 2000) but higher than those measured in Alabama (range = 0.25–0.35 $\text{mm}\cdot\text{day}^{-1}$; Dubuc and DeVries 2002).

To evaluate factors influencing survival of *Pomoxis* spp. larvae, we first compared proportional cohort distributions of larvae and juveniles constructed from otoliths. Proportional distributions of larvae and juveniles differed in all reservoirs when corrections for juvenile mortality were not made. Proportional cohort distributions of juveniles, however, should be adjusted to account for the probability that older cohorts are less likely to be captured than younger cohorts owing to a higher cumulative mortality rate (sensu Campana and Jones 1992). Ideally, the juvenile distribution would be adjusted by a known juvenile mortality rate; in our case, however, only larval mortality estimates were available (0.10–0.15; D.B. Bunnell, unpublished data). Without this estimate, we adjusted the distribution to reflect both a relatively low (0.05) and high (0.15) daily mortality rate to cover a range of scenarios. Although black crappie juvenile mortality was estimated as high as 0.25 in Florida (Pine and Allen 2001), we used 0.15 because we would not expect mortality to increase between the larval and juvenile periods (Campana and Jones 1992). Comparison of these adjusted juvenile distributions to larval cohort distributions maintained differences in the low mortality scenario for each reservoir. In the high mortality scenario, however, the distributions of larval and juvenile cohorts were similar in two of four reservoirs. Thus, unless mortality of juveniles was high, the proportion of larvae hatched was not a good indicator of the number of juveniles that survived. We hypothesized that zooplankton biomass, temperature, turbidity, and number of larval competitors present during hatch week could explain this variable cohort survival.

Given their extremely small size at hatch among freshwater species and the potential negative impact of larval competitors, we expected survival of *Pomoxis* spp. larvae to be most influenced by low zooplankton biomass. Indeed, many experiments predict that survival of freshwater larvae should increase with zooplankton densities (Hart and Werner 1987; Welker et al. 1994), and reviews reveal that resistance to starvation increases with length at hatch (e.g., Miller et al. 1988). With regard to size at hatch, *Pomoxis* spp. are among the smallest 3% of freshwater larvae in the Great Lakes basin (Auer 1982). Previous research in hypereutrophic Ohio reservoirs also predicts that survival of *Pomoxis* spp. larvae may be compromised by high densities of gizzard shad larvae, which can deplete zooplankton densities for larvae that co-occur or hatch later (see review by Stein et al. 1995).

Despite the suggestions that zooplankton densities for first-feeding larvae should be important, supporting evidence for this hypothesis was limited at best. Without adjusting for juvenile mortality, survival increased with total zooplankton biomass only in Burr Oak. Adjusting for juvenile mortality did not reveal positive associations in the other three reservoirs, and the relationship in Burr Oak was not present if juvenile mortality was high. Thus, in our multireservoir approach, zooplankton biomass and survival were generally unrelated, even when corrections for juvenile mortality were made. It is worth exploring, however, why this relationship occurred in Burr Oak, which was the least productive reservoir in terms of chlorophyll *a* but had densities of crustacean zooplankton biomass that were similar to other systems. One unique factor was its consistently low biomass of rotifers. Given the importance of including rotifer biomass in generating a strong predictive relationship between growth of first-feeding larvae and zooplankton, rotifers also may enhance survival of first-feeding larvae.

Why were negative effects of gizzard shad on *Pomoxis* spp. survival not detected? One explanation could be that our study reservoirs included mostly mesotrophic reservoirs, whereas negative gizzard shad effects are strongest in hypereutrophic ones (sensu Stein et al. 1995). Unfortunately, we could not relate our index of survival to densities of zooplankton biomass or fish larvae in Acton, the most eutrophic reservoir with the highest densities of gizzard shad larvae ($15\ \text{m}^{-3}$ on 18 May 2000) because of failed larval sampling during 1 week in early May. If cohort survival had been calculated for Acton, might negative impacts of gizzard, through consumption of zooplankton, have been revealed? Although we cannot know, it is notable that 80% of juvenile survivors were hatched 10 May to 24 May 2000, when densities of zooplankton were dominated by rotifers (rotifers, 34–315 L^{-1}, 31.2–122.9 $\mu\mathrm{g}\cdot\mathrm{L}^{-1}$; crustaceans, 2–6 L^{-1}, 2.2–6.1 $\mu\mathrm{g}\cdot\mathrm{L}^{-1}$). We would have expected such a low density of crustaceans to result in poor survival. However, because such a high proportion of the juvenile survivors were hatched during those weeks, rotifers again appear more important to sustaining growth and survival of first-feeding larvae than previously thought, especially in highly productive reservoirs.

Our freshwater field study joins others that have failed to relate higher zooplankton densities to increased survival (e.g., Welker et al. 1994; Betsill and Van Den Avyle 1997; Garvey et al. 2002). How can these field results be reconciled with laboratory studies that reveal survival to increase with zooplankton densities? In our view, whereas the laboratory evidence does indeed demonstrate the positive effects of zooplankton, it also demonstrates the hardiness of first-feeding larvae. Although no starvation experiments have been conducted on crappie larvae, time to 50% survival was about 7 days after first-feeding had begun for pumpkinseed larvae (*Lepomis gibbosus*) (Hart and Warner 1987), which is in the same family and just slightly longer at hatch than *Pomoxis* spp. (Auer 1982). Length at hatch versus time to 50% mortality regression generated in the review paper by Miller et al. (1988) predicts that 50% of starved crappie larvae could survive 14 days. Of course, in nature, spatial patchiness of zooplankton or low visibility could lead to a short-term, zero-prey environment, i.e., approximating the laboratory starvation experiments. In our view, however, starvation for several consecutive days is unlikely. Thus, starvation alone is unlikely to regulate survival of crappies or other freshwater larvae.

Our failure to link survival of *Pomoxis* spp. larvae to gizzard shad, via low zooplankton biomass, supports previous experimental work (Pope and DeVries 1994). Complementary research in these same Ohio reservoirs reveals that densities of adults and subsequent larvae limit recruitment to age-2 (D.B. Bunnell, unpublished data). If crappie year-class strength is indeed set by larval density (Sammons and Bettoli 1998; D.B. Bunnell, unpublished data), then processes governing mortality between the larval period and age-2 should be fairly similar across Ohio reservoirs. Because factors that vary across reservoirs (e.g., zooplankton, turbidity, density of fish larvae) did not influence larval survival, our results are consistent with the hypothesis that year-class strength is set by density of hatched larvae.

If survival of *Pomoxis* spp. larvae is unrelated to zooplankton biomass, temperature, turbidity, and larval fish density, what other mechanisms could regulate larval survival? In terms of abiotic factors, the impact of wave action resulting from strong winds during late spring and early summer storms may reduce survival of limnetic larvae. However, we know of no supporting evidence for this hypothesis. Predation remains a viable hypothesis (e.g., Mason and Brandt 1996). Potential predators of larvae are numerous, including earlier-hatched larvae, such as cannibalistic *Pomoxis* spp. larvae, or limnetic walleye and yellow perch, as well as other limnetic adults such as white crappie (Kim and DeVries 2001). In our view, multiple biotic and abiotic factors likely interact to regulate survival of larvae.

In conclusion, increasing densities of zooplankton biomass increased growth rates of first-feeding *Pomoxis* spp. larvae, as expected. With this result, we expected to document higher larval survival when zooplankton biomass was high. However, survival increased with zooplankton biomass only in one of four reservoirs. Temperature, turbidity, and density of fish larvae occurring during the first week of life also were unrelated to survival to the juvenile stage, suggesting that the initiation of exogenous feeding is not critical for *Pomoxis* spp. survival. Given their small size at hatch (among the smallest 3% of freshwater larvae), we expected crappies to be quite vulnerable to starvation at first-feeding. Conversely, *Pomoxis* spp. larvae survived despite low crustacean zooplankton abundance (<50 L^{-1}) across mesotrophic and eutrophic reservoirs. In our view, these results cast doubt on whether zooplankton contributes to survival of freshwater larvae. This work joins previous studies in failing to link larval survival to zooplankton biomass (e.g., Garvey et al. 2002), despite countering experimental evidence that low zooplankton should both directly (through starvation; Hart and Werner 1987; Welker et al. 1994) and indirectly (through slow growth and small body size; Rice et al. 1987; Miller et al. 1988) compromise larval survival.

Acknowledgments

We thank B. Pine for teaching us how to effectively sample juvenile crappies. J. Fricke, J. Pyzoha, S. Thomas, J. Sieber-Denlinger, D. Glover, R. Ginsberg, D. Gloeckner, M. Haugen, C. Hutt, B. Lutmerding, H. McLean, S. Miehls, A. Peer, J. Ritchie, M. Schmidt, A. Spencer, M. Thomas, M. Tomasi, J. Williams, and S. Hale and the Ohio Department of Natural Resources, Division of Wildlife, provided valuable assistance with fieldwork and laboratory processing. M. Vanni was most helpful in estimating chlorophyll *a*. M. Allen, J. Holomuzki, E. Marschall, D. Secor, and an anonymous reviewer provided helpful and insightful suggestions. This research was funded by Federal Aid in Sport Fish Restoration Project F-69-P, administered jointly by U.S. Fish and Wildlife Service and Ohio Department of Natural Resources, Division of Wildlife, National Science Foundation grant DEB 9726877 to RAS and MJG, and the Department of Evolution, Ecology, and Organismal Biology at The Ohio State University.

References

Arend, K.K. 2002. Do vertical gradients affect larval fish depth distribution and prey electivity among reservoirs that vary in productivity? M.Sc. thesis, Ohio State University, Columbus, Ohio.

Auer, N.A. 1982. Identification of larval fishes of the Great Lakes basin with emphasis on the Lake Michigan drainage. Great Lakes Fishery Commission, Ann Arbor, Mich.

Betsill, R.K., and Van Den Avyle, M.J. 1997. Effect of temperature and zooplankton abundance on growth and survival of larval threadfin shad. Trans. Am. Fish. Soc. **126**: 999–1011.

Burnham, K.P., and Anderson, D.A. 1998. Model selection and inference. Springer-Verlag, New York.

Campana, S.E., and Jones, C.M. 1992. Analysis of otolith microstructure data. *In* Otolith microstructure examination and analysis. *Edited by* D.K. Stevenson and S.E. Campana. Can. Spec. Publ. Fish. Aquat. Sci. No. 117. pp. 73–100.

Chatry, M.F., and Conner, J.V. 1980. Comparative developmental morphology of the crappies, *Pomoxis annularis* and *P. nigromaculatus*. Biol. Serv. Program U.S. Fish Wildl. Serv. **43**: 45–57.

Claramunt, R.M., and Wahl, D.H. 2000. The effects of abiotic and biotic factors in determining larval fish growth rates: a comparison across species and reservoirs. Trans. Am. Fish. Soc. **129**: 835–851.

Crecco, V.A., and Savoy, T.F. 1985. Effects of biotic and abiotic factors on growth and relative survival of young American shad, *Alosa sapidissima*, in the Connecticut River. Can. J. Fish. Aquat. Sci. **42**: 1640–1648.

Crowder, L.B., McDonald, M.E., and Rice, J.A. 1987. Understanding recruitment of Lake Michigan fishes: the importance of size-based interactions between fish and zooplankton. Can. J. Fish. Aquat. Sci. **44**(Suppl. 2): 141–147.

Culver, D.A., Boucherle, M.M., Bean, D.J., and Fletcher, J.W. 1985. Biomass of freshwater crustacean zooplankton from length–weight regressions. Can. J. Fish. Aquat. Sci. **42**: 1380–1390.

DeVries, D.R., and Stein, R.A. 1992. Complex interactions between fish and zooplankton: quantifying the role of an open-water planktivore. Can. J. Fish. Aquat. Sci. **49**: 1216–1227.

DeVries, D.R., Bremigan, M.T., and Stein, R.A. 1998. Prey selection by larval fishes as influenced by available zooplankton and gape limitation. Trans. Am. Fish. Soc. **127**: 1040–1050.

Doohan, M. 1973. An energy budget for adult *Brachionus plicatilis* Muller (Rotatoria). Oecologia, **13**: 351–362.

Dubuc, R.A., and DeVries, D.R. 2002. An exploration of factors influencing crappie early life history in three Alabama impoundments. Trans. Am. Fish. Soc. **131**: 476–491.

Dumont, H.J., Van de Velde, I., and Dumont, S. 1975. The dry weight estimate of biomass in a selection of Cladocera, Copepoda, and Rotifera from the plankton, periphyton and benthos of continental waters. Oecologia, **19**: 75–97.

Garvey, J.E., and Stein, R.A. 1998. Competition between larval fishes in reservoirs: the role of relative timing of appearance. Trans. Am. Fish. Soc. **127**: 1021–1039.

Garvey, J.E., Dingledine, N.A., Donovan, N.S., and Stein, R.A. 1998. Exploring spatial and temporal variation within reservoir food webs: predictions for fish assemblages. Ecol. Appl. **8**: 104–120.

Garvey, J.E., Herra, T.P., and Leggett, W.C. 2002. Protracted reproduction in sunfish: the temporal dimension in fish recruitment revisited. Ecol. Appl. **12**: 194–205.

Hart, T.F., and Werner, R.G. 1987. Effects of prey density on growth and survival of white sucker, *Catostomus commersoni*, and pumpkinseed, *Lepomis gibbosus*, larvae. Environ. Biol. Fishes, **18**: 41–50.

Hjort, J. 1914. Fluctuations in the great fisheries of northern Europe. Rapp. P-v. Réun. Cons. Perm. Int. Explor. Mer, **20**: 1–228.

Houde, E.D. 1987. Fish early life dynamics and recruitment variability. Am. Fish. Soc. Symp. **2**: 17–29.

Houde, E.D. 1994. Differences between marine and freshwater fish larvae: implications for recruitment. ICES J. Mar. Sci. **51**: 91–97.

Houde, E.D. 1997. Patterns and consequences of selective processes in teleost early life histories. *In* Early life history and recruitment in fish populations. *Edited by* R.C. Chambers and E.A. Trippel. Chapman and Hall, London. pp. 173–196.

Hunter, J.R. 1981. Feeding ecology and predation of marine fish larvae. *In* Marine fish larvae: morphology, ecology and relation to fisheries. *Edited by* R. Lasker. University of Washington Press, Seattle. pp. 33–79.

Kim, G.W., and DeVries, D.R. 2001. Adult fish predation on freshwater limnetic fish larvae: a mesocosm experiment. Trans. Am. Fish. Soc. **130**: 189–203.

Mason, D.M., and Brandt, S.B. 1996. Effect of alewife predation on survival of larval yellow perch in an embayment of Lake Ontario. Can. J. Fish. Aquat. Sci. **53**: 1609–1617.

Methot, R.D. 1983. Seasonal variation in survival of larval northern anchovy, *Engraulis mordax*, estimated from the age distribution of juveniles. Fish. Bull. **81**: 741–750.

Miller, T.J., Crowder, L.B., Rice, J.A., and Marschall, E.A. 1988. Larval size and recruitment mechanisms in fishes: toward a conceptual framework. Can. J. Fish. Aquat. Sci. **45**: 1657–1670.

Miner, J.G., and Stein, R.A. 1993. Interactive influence of turbidity and light on larval bluegill (*Lepomis macrochirus*) foraging. Can. J. Fish. Aquat. Sci. **50**: 781–788.

Pine, W.E., and Allen, M.S. 2001. Differential growth and survival of weekly age-0 black crappie cohorts in a Florida lake. Trans. Am. Fish. Soc. **130**: 80–91.

Pope, K.L., and DeVries, D.R. 1994. Interactions between larval white crappie and gizzard shad: quantifying mechanisms in small ponds. Trans. Am. Fish. Soc. **123**: 975–987.

Pope, K.L., and Willis, D.W. 1998. Early life history and recruitment of black crappie (*Pomoxis nigromaculatus*) in two South Dakota waters. Ecol. Freshw. Fish, **7**: 56–68.

Rice, J.A., Crowder, L.B., and Binkowski, F.P. 1987. Evaluating potential sources of mortality for larval bloater (*Coregonus hoyi*): starvation and vulnerability to predation. Can. J. Fish. Aquat. Sci. **44**: 467–472.

Rosen, R.A. 1981. Length – dry weight relationships of some freshwater zooplankton. J. Freshw. Ecol. **1**: 225–229.

Ruttner-Kolinsko, A. 1977. Suggestions for biomass calculations of plankton rotifers. Commun. Int. Assoc. Theor. Appl. Limnol. **8**: 71–76.

Sammons, S.M., and Bettoli, P.W. 1998. Larval sampling as a fisheries management tool: early detection of year-class strength. N. Am. J. Fish. Manag. **18**: 137–143.

Siefert, R.E. 1968. Reproductive behavior, incubation, and mortality of eggs, and post-larval food selection in the white crappie. Trans. Am. Fish. Soc. **97**: 252–259.

Siefert, R.E. 1969. Characteristics for separation of white and black crappie larvae. Trans. Am. Fish. Soc. **98**: 326–328.

Smith, S.M., Maceina, M.J., and Dunham, R.A. 1994. Natural hybridization between black crappie and white crappie in Weiss Lake, Alabama. Trans. Am. Fish. Soc. **123**: 71–79.

Stahl, T.P., and Stein, R.A. 1994. Influence of larval gizzard shad (*Dorosoma cepedianum*) density on piscivory and growth of young-of-year saugeye (*Stizostedion vitreum* × *S. canadense*). Can. J. Fish. Aquat. Sci. **51**: 1993–2002.

Stein, R.A., DeVries, D.R., and Dettmers, J.M. 1995. Food-web regulation by a planktivore: exploring the generality of the trophic cascade hypothesis. Can. J. Fish. Aquat. Sci. **52**: 2518–2526.

Sweatman, J.J., and Kohler, C.C. 1991. Validation of daily otoliths increments for young-of-the-year white crappies. N. Am. J. Fish. Manag. **11**: 499–503.

Welker, M.T., Pierce, C.L., and Wahl, D.H. 1994. Growth and survival of larval fishes: roles of competition and zooplankton abundance. Trans. Am. Fish. Soc. **123**: 703–717.

Wetzel, R.G. 2001. Limnology: lake and river ecosystems. Academic Press, San Diego, Calif.

The effect of acute changes in temperature and light on the aerobic metabolism of embryos and yolk-sac larvae of turbot (*Scophthalmus maximus*)

Roderick Nigel Finn and Ivar Rønnestad

Abstract: The effect of acute changes of temperature and light on the rates of oxygen consumption and ammonia excretion of developing embryos and yolk-sac larvae of turbot (*Scophthalmus maximus*) reared at 15 °C were studied. Short-term temperature adjustments of ±2 °C gave a mean Q_{10} of 2.6 for the rate of oxygen consumption. Neither the presence nor the absence of light significantly influenced this response to acute temperature changes, despite light causing a significantly higher rate of oxygen consumption in the yolk-sac larvae between 9 and 12 days after fertilisation. This elevated metabolic rate in the presence of light occurred after pigmentation of the eyes and was probably due to activity associated with food-searching behaviour of this visual feeder. Similarly, for most development, the presence or absence of light and acute temperature adjustments did not cause any significant shift in the relative fraction of amino acids catabolised at 15 °C. However, on day 10 after fertilisation when peak rates of oxygen consumption occurred in the yolk-sac larvae exposed to light, the significantly elevated apparent nitrogen quotients indicated that greater amounts of amino acids were utilised for catabolic substrate oxidation.

Résumé : Nous avons examiné les effets de changements aigus de température et de lumière sur les taux de consommation d'oxygène et d'excrétion d'ammoniaque chez des embryons et des larves vésiculées de turbots (*Scophthalmus maximus*) au cours de leur développement à 15 °C. Les ajustements à court terme de température de ±2 °C suivent un Q_{10} moyen de 2,6 pour le taux de consommation d'oxygène. Ni la présence, ni l'absence de lumière n'influencent cette réaction aux changements aigus de température de façon significative; néanmoins, la lumière cause un accroissement significatif du taux de consommation d'oxygène chez les larves vésiculées entre les jours 9 et 12 après la fécondation. Ce taux métabolique accru en présence de lumière a lieu après la pigmentation des yeux et est sans doute causé par une activité reliée au comportement de quête de nourriture chez ce poisson qui se nourrit à vue. De même, durant presque tout le développement, ni la présence, ni l'absence de lumière, ni les variations aiguës de température ne causent de changement significatif dans la fraction relative des acides aminés catabolisés à 15 °C. Cependant, au jour 10 après la fécondation, lorsque les taux maximaux de consommation d'oxygène se produisent chez les larves vésiculées exposées à la lumière, l'accroissement significatif des quotients apparents d'azote indique que de plus grandes quantités d'acides aminés sont utilisées pour l'oxydation catabolique de substrats.

[Traduit par la Rédaction]

Introduction

Temperature and light have recently been shown to be important extrinsic factors governing the metabolic rate of the free-swimming, early life stages of Atlantic cod, *Gadus morhua* (Finn et al. 2002). Unlike free-swimming juveniles or adults, embryos of oviparous fishes, while captive inside their chorions, are unable to avoid short-term climatic changes (Russell 1976), which regularly influence the coastal waters of Western Norway (Aure and Danielssen 2003). Such embryos rely on inherent cell and intermediary metabolism to deal with rapid changes in ambient temperature or light. Regulatory mechanisms may involve adjustments in membrane integrity, catalytic efficiency, substrate transport, substrate affinity, and changes in intracellular pH (Hazel 1993; Hochachka and Somero 2002). When integrated among the various tissues and organs, these modifications combine to give the whole organism's net response to an environmental challenge. Ectothermic embryos need to cope with such challenges while undergoing profound functional changes in their cells, tissues, and organs and may therefore be particularly sensitive at different stages of development.

This influence on the metabolism of the pelagic embryos of marine teleosts has largely been overlooked. According to Rombough (1988), the effect of temperature on aerobic metabolism has only been studied in embryos and larvae of three species of teleost that spawn pelagic eggs. The Q_{10} response of metabolic rate to changes in temperature of the embryos and larvae of these species ranged from 1.8 to 4.8, with an extreme value of 6.4. Removal of the extreme value gave a mean Q_{10} of 2.7. Nevertheless, Rombough (1988) suggested that temperature changes are of greater significance during early life. To test the notion that the metabo-

Received 20 January 2003. Accepted 31 August 2003. Published on the NRC Research Press Web site at http://cjfas.nrc.ca on 19 November 2003.
J17298

R. Nigel Finn[1] and I. Rønnestad. Department of Zoology, University of Bergen, Allégaten 41, N-5020 Bergen, Norway.

[1] Corresponding author (e-mail: nigel.finn@zoo.uib.no).

doi: 10.1139/F03-113

lism of the early life stages of marine fishes is particularly sensitive to changes of temperature and light, we studied a developing series of embryos and yolk-sac larvae of turbot (*Scophthalmus maximus* L.). The rate of oxygen consumption ($\dot{V}\text{O}_2$) was used to characterise the aerobic metabolic response, whereas the ratio of the rate of ammonia excretion ($\dot{V}\text{NH}_3$) to $\dot{V}\text{O}_2$ was used to determine the effect of the acute changes on fuel preference. Embryos and yolk-sac larvae of turbot were used as models for these studies as we already have a good understanding of their metabolism and fuel preference at 15 °C (Rønnestad et al. 1992; Finn et al. 1996).

Materials and methods

In the present contribution, the binomial nomenclature recommended by Wheeler (1992) is adopted for turbot (*Scophthalmus maximus*, Linnaeaus 1758). A single series of embryos and yolk-sac larvae of turbot were studied. Eggs were stripped from a single female, fertilised with the milt from three males, and incubated in static glass aquaria in prefiltered (0.2 µm) seawater at 15.0 ± 0.02 °C, 34.5‰. Water was exchanged once or twice each day, and photoperiod was regulated at 12 h light –12 h dark. Temperature was maintained via an arrangement of antagonistic thermostats and coolers (Heto, Birkerød, Denmark) and monitored using a Squirrel (type SQ8-4U; Grant Instruments (Cambridge) Ltd., Shepreth, Cambridgeshire, U.K.) data logger.

The effect of acute temperature changes on the $\dot{V}\text{O}_2$ and $\dot{V}\text{NH}_3$ was determined following incubation (1 h before experimentation) of the 15 °C reared embryos and yolk-sac larvae to experimental temperatures of 13 °C and 17 °C. These temperatures were chosen to remain within close physiological limits of the optimal rearing temperature of embryos and yolk-sac larvae of turbot (Jones 1972). During temperature acclimation, embryos and yolk-sac larvae were illuminated with ambient light using Luma long-life standard colour fluorescent lamps (36 W/L-73 emitting 70% daylight at 3000°K), which were suspended over the aquaria. Irradiance at the water surface was determined to be 35–50 $\mu\text{E}\cdot\text{s}^{-1}\cdot\text{m}^{-2}$ using a 180° LI-192SA cosine-corrected underwater quantum sensor attached to a LI-1000 light meter (LI-COR Inc., Environmental, Lincoln, Nebr.). It has earlier been documented that the amount of photosynthetic active irradiance impinging at sea level in Western Norway varies between a daily mean of ~200 to ~800 $\mu\text{E}\cdot\text{s}^{-1}\cdot\text{m}^{-2}$ but can be as high as 1600 $\mu\text{E}\cdot\text{s}^{-1}\cdot\text{m}^{-2}$. The compensation depth at which photosynthetic active irradiance is 5 $\mu\text{E}\cdot\text{s}^{-1}\cdot\text{m}^{-2}$ varies between 10 and 25 m below sea surface (Erga 1989). The light levels used in the present study therefore reflect the natural conditions of pelagic turbot embryos and larvae in the upper euphotic zone. Because we had earlier found no significant effect of light or darkness on either the $\dot{V}\text{O}_2$ or $\dot{V}\text{NH}_3$ of turbot embryos and larvae at 15 °C (Finn et al. 1996), we only checked the effect of darkness at each temperature on early embryos and hatched larvae. Respiratory measurements were conducted at 13, 15, and 17 °C using closed respirometers (glass Quickfit FR:S vials, 10–30 mL) as described by Finn et al. (2002). Groups of 9–45 pooled embryos in 5–6 replicate respirometers or 4–12 pooled yolk-sac larvae in 5–6 replicate respirometers were compared with four blank respirometers at each experimental temperature while exposed to either light (25–30 $\mu\text{E}\cdot\text{s}^{-1}\cdot\text{m}^{-2}$ at the respirometer surface) or complete darkness. The group size varied with stage to give a significant drop in the oxygen tension (Δp_{O_2}) in the respirometers. The oxygen tension (p_{O_2}) was measured using a polarographic oxygen sensor (radiometer E5046 electrode in conjunction with a pH M73 blood gas analyser), and the $\dot{V}\text{O}_2$ was calculated from the difference between blank and test respirometers. Respirometer incubation times varied between a minimum and maximum of 12 and 28 h, respectively, yielding minimum and maximum Δp_{O_2}s of 1.33 and 5.47 kPa, respectively. The p_{O_2} of each respirometer was measured in duplicate or triplicate with a 90-s response setting on the radiometer. A total of 36 test and 24 blank respirometers were measured each day. The solubility of oxygen in seawater ($\mu\text{mol}\cdot\text{L}^{-1}\cdot\text{kPa}^{-1}$) was calculated after Green and Carrit (1967) and Forstner and Gnaiger (1983). The concentration of ammonia, [NH_3], was determined by sampling 1 mL of the respirometer water (four replicates) and analysed according to the procedure of Bower and Holm-Hansen (1980). The $\dot{V}\text{NH}_3$ was calculated from the [NH_3] difference between test and blank respirometers. Following the respiratory measurements, eggs and yolk-sac larvae were characterised for linear dimensions (egg diameter or standard length) using a binocular microscope, wet mass using a top balance (accurate to 0.1 mg), and dry mass after lyophilisation using a microbalance (accurate to 1 µg) as described by Finn et al. (1996). Gravimetric and biometric characterisation is given in Table 1.

The molar ratio of $\dot{V}\text{NH}_3$ to $\dot{V}\text{O}_2$ is the apparent nitrogen quotient (NQ), which gives an estimate of the mass fraction of amino acids used as fuel (Gnaiger 1983), depending on the co-substrate catabolised. Because Gnaiger's (1983) recommendations were based on mammalian proteins, the following nonlinear equations were derived by stoichiometry from the data of Finn et al. (1996) and used to calculate the relevant mass fractions of amino acids catabolised in turbot:

$$(1) \qquad K_{\text{AA/CHO}} = 3.221(\text{NQ}) + 2.571(\text{NQ})^2 + 4.064(\text{NQ})^3$$

$$(2) \qquad K_{\text{AA/LIPID}} = 8.069(\text{NQ}) - 25.267(\text{NQ})^2 + 36.732(\text{NQ})^3$$

where eq. 1 represents the mass fraction of amino acids (AA) catabolised when carbohydrate (CHO) is the co-substrate, and eq. 2 when lipid (neutral or polar) is the co-substrate.

The influence of temperature was assessed via the van't Hoff equation for Q_{10} (Eckert 1997) for intervals of 15–13 °C and 15–17 °C. Using SPSS 10 for Macintosh computers (SPSS Inc., Chicago, Ill.), data were statistically analysed via model III three-way analysis of variance (ANOVA) with separate analyses of $\dot{V}\text{O}_2$, $\dot{V}\text{NH}_3$, and NQ as dependent variables using age, temperature, and light as fixed variables in accordance with the principles of Sokal and Rohlf (2000) and Crawley (2002). Tukey's honestly significant difference (HSD) was used for post hoc testing of significant differences, which were acknowledged at the 5% level.

Table 1. Gravimetric and biometric characterisation of the developing embryos and yolk-sac larvae of turbot (*Scophthalmus maximus*) at 15 °C.

Stage	Egg diameter (mm)	Standard length (mm)	Wet mass (μg·ind.$^{-1}$)	Dry mass (μg·ind.$^{-1}$)
Eggs: fertilisation–hatch	1.03±0.002 (150)		623±9.7 (67)	56±1.0 (19)
Hatched larvae (DPF 5.2)		2.42±0.027 (30)	440±44.3* (5)	44±5.0 * (5)
Larvae at EoY (DPF 10.3)		3.20±0.072 (30)		33±2.8 (5)

Note: Mean values ±95% confidence intervals are given with *N* in parentheses. For wet and dry masses, the *N* refers to replicate measurements of 14–100 pooled eggs or 15–20 pooled larvae. EoY, end of yolk; DPF, days after fertilisation; ind., individual. Values with an asterisk (*) include yolk mass.

Results

The $\dot{V}\mathrm{O}_2$ of the light-exposed turbot embryos at 15 °C increased steadily from 0.44 ± 0.08 nmol·individuals^{-1}·h^{-1} at the early gastrula phase through hatch to reach peak larval rates of 5.97 ± 0.37 nmol·individual^{-1}·h^{-1} at 10 days after fertilisation (DPF; Fig. 1). Although there was a significant interaction between the presence or absence of light and age ($p < 0.001$), the lack of light did not significantly influence the metabolic rate until 9 DPF. Between 9–12 DPF, the $\dot{V}\mathrm{O}_2$s of dark-adapted larvae were significantly lower ($p < 0.05$) compared with the light-exposed larvae (Fig. 1). In contrast to the presence or absence of light, the acute increase or decrease of 2 °C significantly ($p < 0.05$) affected the $\dot{V}\mathrm{O}_2$ at all stages of development. This effect was independent of light or darkness ($p = 0.35$). Calculated Q_{10} values for embryos varied from 1.9 to 3.6, whereas those of the yolk-sac larvae varied from 1.6 to 3.3 (Table 2). Neither the stage nor the direction of temperature change was found to significantly alter the Q_{10} (ANOVA, $p > 0.05$). Thus, for light- or dark-adapted embryos and yolk-sac larvae of turbot, a general Q_{10} temperature coefficient of 2.6 ± 0.23 (95% confidence interval, $N = 28$) for the aerobic metabolic rate was derived.

Before epiboly (0.7 DPF), the $\dot{V}\mathrm{NH}_3$ of both the light- and dark-exposed embryos at 15 °C were significantly greater than zero ($p < 0.05$), with mean rates of 0.11 ± 0.06 nmol·individual^{-1}·h^{-1} (Fig. 2). At this stage, only the $\dot{V}\mathrm{NH}_3$ of embryos at 17 °C in darkness were significantly elevated compared with all other measurements. After completion of epiboly (2.7 DPF), the $\dot{V}\mathrm{NH}_3$ of the light-adapted embryos had not altered, but by 3.7 DPF, it had increased significantly ($p < 0.05$). Following hatch, the $\dot{V}\mathrm{NH}_3$ declined to low levels of 0.26 ± 0.04 on 7.8 DPF in both the light- and dark-exposed larvae but increased thereafter as the yolk was depleted. The effect of altered temperature was variable. Until 3.7 DPF, the 2 °C changes had no significant effect on the $\dot{V}\mathrm{NH}_3$, whereas thereafter, the $\dot{V}\mathrm{NH}_3$ was mostly correlated to the direction of temperature change, although the rate did not always differ significantly from that at 15 °C. With the exception of the 17 °C measurements on days 9 and 11.8 after fertilisation, exposing the embryos and yolk-sac larvae to darkness caused a significant reduction in the $\dot{V}\mathrm{NH}_3$ from day 7.8 until the end of the study (Fig. 2). The influence of temperature on the $\dot{V}\mathrm{NH}_3$ was thus generally similar to that on the $\dot{V}\mathrm{O}_2$.

Because of the high rate of $\dot{V}\mathrm{NH}_3$ compared with $\dot{V}\mathrm{O}_2$ on 0.7 DPF, the apparent NQs were also high and showed great variability at each temperature (Fig. 3). At this early stage of development, the NQs were not significantly different, and they were uncorrelated to temperature, light, or darkness. By 2.7 DPF, the NQs of the light-exposed embryos ranged from 0.07 to 0.11, but by 3.7 DPF, approximately 1 day before

Fig. 1. Rates of oxygen consumption ($\dot{V}\mathrm{O}_2$) of developing embryos and yolk-sac larvae of turbot (*Scophthalmus maximus*): (*a*) $\dot{V}\mathrm{O}_2$ of embryos and yolk-sac larvae exposed to light (25–30 μE·s^{-1}·m^{-2} at the respirometer surface) and (*b*) $\dot{V}\mathrm{O}_2$ of embryos and yolk-sac larvae in darkness. Embryos and yolk-sac larvae were reared at 15 °C (solid triangles) and acutely exposed to 13 °C (open circles) and 17 °C (shaded diamonds). Data points represent means ± standard deviations of groups of 9–45 pooled embryos in 5–6 replicate respirometers or 4–12 pooled yolk-sac larvae in 5–6 replicate respirometers. Shaded vertical bar indicates hatch, which occurred between day 4.5 and day 4.7 after fertilisation.

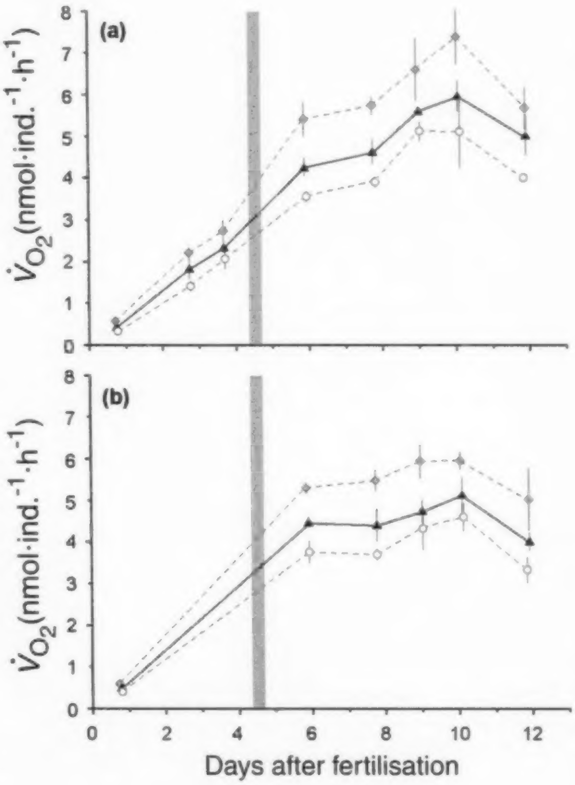

Table 2. Q_{10} temperature coefficients for the routine rates of oxygen consumption of developing embryos and yolk-sac larvae of turbot (*Scophthalmus maximus*).

	Light		Darkness	
DPF	15 → 13 °C	15 → 17 °C	15 → 13 °C	15 → 17 °C
0.7	3.5	3.6	3.4	2.1
2.7	3.7	2.5	—	—
3.7	1.9	2.2	—	—
5.9	2.5	3.3	2.4	2.3
7.8	2.4	2.9	2.4	2.9
9.0	1.6	2.2	1.6	3.1
10.1	2.2	2.9	1.7	2.1
11.8	3.1	1.8	2.5	3.1
Mean (±95% CI)	2.6 (0.64)	2.7 (0.51)	2.4 (0.68)	2.6 (0.49)

Note: Embryos and yolk-sac larvae were reared at 15 °C, 34.5‰, and short-term acclimated (1 h before measurement) to either 13 or 17 °C. Measurements at each temperature were conducted using 5–6 replicates of 9–45 pooled embryos or 5–6 replicates of 4–12 pooled larvae, which were exposed to either light (10–25 $\mu E \cdot s^{-1} \cdot m^{-2}$ at the respirometer surface) or darkness. Mean $\dot{V}O_2$ of each experiment were used to calculate the relevant Q_{10} coefficients. The Q_{10} data are summarised as means ± 95% confidence intervals (CI) of each treatment. DPF, days after fertilisation.

hatch, the NQs had risen significantly to levels of 0.2–0.3. After hatch, however, the NQs declined to levels of 0.05–0.08 between days 8 and 10 after fertilisation. On day 10 after fertilisation, the light-exposed larvae had significantly higher NQs at each experimental temperature compared with the larvae in darkness. Thereafter, as the yolks were depleted, the NQs significantly increased to levels of 0.16–0.20. With the exception of day 10 after fertilisation, when the $\dot{V}O_2$ of the light-exposed larvae was at its peak, neither short-term temperature acclimation nor the presence or absence of light had any consistently significant effect on the NQs.

Fig. 2. Rates of ammonia excretion ($\dot{V}NH_3$) of developing embryos and yolk-sac larvae of turbot (*Scophthalmus maximus*): (*a*) $\dot{V}NH_3$ of embryos and yolk-sac larvae exposed to light (25–30 $\mu E \cdot s^{-1} \cdot m^{-2}$ at the respirometer surface) and (*b*) $\dot{V}NH_3$ of embryos and yolk-sac larvae in darkness. Lines are not extrapolated between day 0.7 and day 5.9 after fertilisation for the embryos in darkness because the data for the larvae exposed to light do not indicate a linear increase with respect to development. Embryos and yolk-sac larvae were reared at 15 °C (solid triangles) and acutely exposed to 13 °C (open circles) and 17 °C (shaded diamonds). Data points represent means ± standard deviations of groups of 9–45 pooled embryos in 5–6 replicate respirometers or 4–12 pooled yolk-sac larvae in 5–6 replicate respirometers. Shaded vertical bar indicates hatch, which occurred between day 4.5 and day 4.7 after fertilisation.

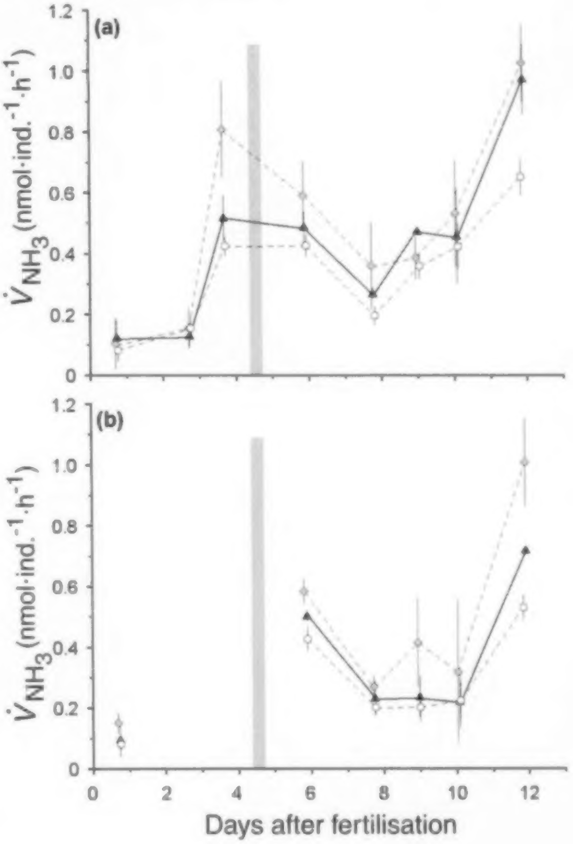

Discussion

The estimates of $\dot{V}O_2$ at 15 °C are in close agreement with the earlier measurements of the aerobic metabolic rate (Rønnestad et al. 1992; Finn et al. 1996) and provide a sound basis for evaluating the acute thermal response of developing embryos and yolk-sac larvae of turbot. Because this is the first report on the effect of acute temperature changes on the embryos and yolk-sac larvae of this species and data for the Q_{10} of other teleosts that spawn pelagic eggs are limited, we compare the current data set with those obtained from older turbot. Earlier studies of the metabolic response of turbot to altered environmental temperature have only been examined for temperature-acclimatised juveniles and adults and are conflicting. Brown et al. (1984) reported that the mass-specific metabolic rate of 4–1000 g turbot increased with increasing temperature between 7 and 16 °C, without any indication of metabolic compensation, such that a mean Q_{10} of ~3.4 can be estimated from their equations. Scherrer (1984), however, documented that both the routine and standard metabolic Q_{10} response of 5–20 g turbot that had been grown at six different temperatures decreased from 4.2–4.8 at 12–14 °C to 0.75–0.95 at 22–25 °C and argued that this was evidence of metabolic compensation. Waller (1992) found a positive relation of $\dot{V}O_2$ with temperature between 8 °C and 19 °C for 1.5–1073 g turbot and a mean Q_{10} of ~2.0 can be estimated from their data. Similarly, Imsland et al. (1995) found higher mass-specific metabolic rates at 16 °C compared with at 10 °C for long-term acclimated juvenile turbot of 5–125 g and a mean Q_{10} of ~2.6–3.0 can be estimated by normalising their data and assuming a metabolic exponent of 0.7 and 0.75 suggested by Waller (1992) and Brown et al. (1984), respectively. More recently, Burel et al.

Fig. 3. Apparent nitrogen quotient (NQ) of developing embryos and yolk-sac larvae of turbot (*Scophthalmus maximus*): (*a*) NQs of embryos and yolk-sac larvae exposed to light (25–30 $\mu E \cdot s^{-1} \cdot m^{-2}$ at the respirometer surface) and (*b*) NQs of embryos and yolk-sac larvae in darkness. Lines are not extrapolated between day 0.7 and day 5.9 after fertilisation for the embryos in darkness because the data for the larvae exposed to light do not indicate a linear change with respect to development. Embryos and yolk-sac larvae were reared at 15 °C (solid triangles) and acutely exposed to 13 °C (open circles) and 17 °C (shaded diamonds). Data points represent means ± standard deviations of groups of 9–45 pooled embryos in 5–6 replicate respirometers or 4–12 pooled yolk-sac larvae in 5–6 replicate respirometers. Shaded vertical bar indicates hatch, which occurred between day 4.5 and day 4.7 after fertilisation. The fuel axes were constructed as described in the Materials and methods and are nonlinear.

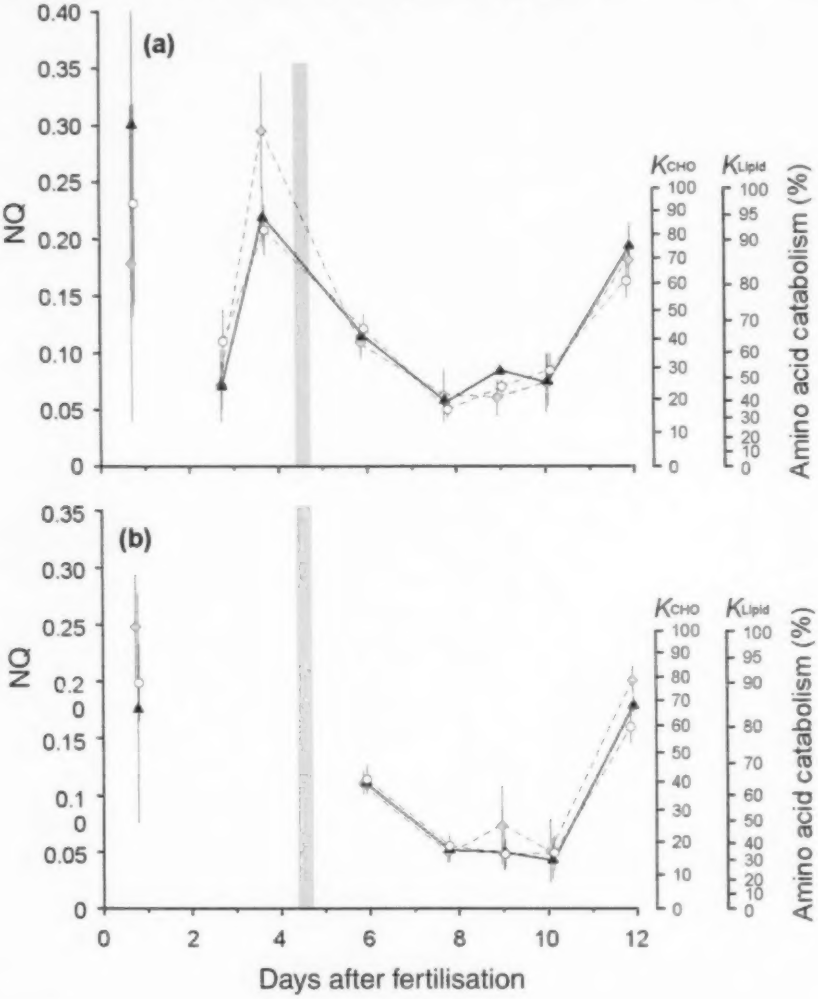

(1996) suggest that the metabolic response of turbot to long-term temperature acclimation declines from Q_{10} values of 2.3–3.0 (recalculated from their data) in small juveniles of 70–110 g to thermo-independent values of 1.0 in larger juveniles of 500–600 g. However, the most recent data for the standard metabolic rate of turbot in the same size range (400–600 g) found a Q_{10} of 2.7 between 10 and 22 °C (Mallekh and Lagardère 2002). Although embryos and yolk-sac larvae of a given species may have significantly different intermediary metabolic regulation compared with juveniles or adults (Segner et al. 1994; Goolish 1995) and acute responses to temperature adjustments may differ from that of long-term temperature acclimatisation, our finding of a mean Q_{10} of 2.6 supports the earlier studies that showed small turbot to have a general Q_{10} of between 2.3 and 3.0. Indeed, a Q_{10} of 2.6, as found in the present study, is in excellent agreement with the theoretical predictions of Weltzien et al. (1999) and also with the general thermal response of other species of embryonic teleost (Rombough 1988). These comparisons are in part validated by the studies of Overnell and Batty (2000), who did not find evidence that temperature affected the scaling of citrate synthtase activity, a key aerobic enzyme, in either herring (*Clupea harengus*) or another flatfish, plaice (*Pleuronectes platessa*).

The current data for the aerobic metabolic rates of the embryos and yolk-sac larvae further reveal that the presence or absence of light did not significantly influence the temperature effect, an observation also noted for the rate of development of embryonic turbot (Iglesias et al. 1995).

Quantification of the $\dot{V}_{\mathrm{NH}_3}$ is important for establishing the fraction of amino acids used as catabolic fuel. To accurately determine the mass fraction of amino acids catabolised, all forms of nitrogen excretion should be measured and any accumulated nitrogen recorded. In the present study, the rate of NH_4^+ accumulation was not measured, but in two previous studies, Rønnestad et al. (1992) and Finn et al. (1996) found similar levels of NH_4^+ accumulation during the embryonic stage, which was rapidly lost when the larvae hatched. If these levels of NH_4^+ accumulation and release are respectively added and subtracted from the pre- and post-hatch $\dot{V}_{\mathrm{NH}_3}$ data at 15 °C in the present study, then the NQs just before hatch would increase slightly while the NQs of the hatched larvae between 5.5 and 8 DPF would fall. Such adjusted NQs would virtually mimic the earlier findings of Finn et al. (1996). As discussed by Wood (2001), any ammonia production due to adenylate deamination resulting from burst swimming events would not affect the apparent NQs because the ammonia is retained intracellularly. However, it is also important to know that the released nitrogen measured in the respirometer is of metabolic origin. This can best be determined by comparing stoichiometrically the amount of ammonia (primarily as NH_4^+ (Walsh 1998)) excreted with the amount of substrate decline in the organism. Such an approach has been conducted for several pelagic embryos of marine fish (reviewed by Wright and Fyhn 2001). As in several of these earlier studies, the earliest rates of $\dot{V}_{\mathrm{NH}_3}$ determined for the embryos at all temperatures in the present study gave NQs that were far in excess of any physiologically relevant value. Because no nitrogenous substrate was found to be depleted before gastrulation (Rønnestad et al. 1992; Finn et al. 1996), the released ammonia may be associated with the restructuring of the chorion after fertilisation and water activation (Oppen-Bernsten et al. 1990). Before gastrulation of turbot, it has been suggested that intracellular glycogen fuels metabolism (Finn et al. 1995).

In addition to ammonia, urea has been found to be a significant form of excretory nitrogen (up to 20% of total nitrogen excreted) both in juvenile and adult turbot as a result of a delayed postprandial degradation of dietary arginine (Burel et al. 1996; Gouillou-Coustans et al. 2002). Urea excretion has also been documented in embryos and yolk-sac larvae of Atlantic cod, *Gadus morhua*, and Atlantic halibut, *Hippoglossus hippoglossus* (Chadwick and Wright 1999; Terjesen et al. 2002). If urea is a significant form of excretory nitrogen in embryos and yolk-sac larvae of turbot, then the present NQs represent minimum levels for interpreting the mass fraction of amino acids used as fuel.

The data at 15 °C support the earlier studies in which free amino acid catabolism peaks just before hatch, is followed by an intense lipid mobilisation after hatch, and re-enters a phase of amino acid catabolism from proteins as the yolk is depleted (Rønnestad et al. 1992; Finn et al. 1996). The increased $\dot{V}_{\mathrm{O}_2}$ in the presence of light between 9 and 12 DPF is most likely to be due to activity associated with food-searching behaviour of this visual feeder (Skiftesvik 1992; Champalbert and Le Direach-Boursier 1998). On day 10 after fertilisation, however, the significantly higher NQs of the light-exposed larvae indicate that they had begun to burn greater amounts of amino acids compared with the dark-exposed larvae. According to Van den Thillart and Van Raaij (1995), lipids and proteins are the preferred fuels of sustainable exercise in fishes, with proteins actually being preferred to lipids. Wood (2001), however, argues that the contribution of protein oxidation to overall fuel use remains unchanged during sustained exercise. If the peak $\dot{V}_{\mathrm{O}_2}$ of the light-exposed turbot larvae in the present study is due to swimming activity, then the higher NQs of the light-exposed larvae on day 10 after fertilisation support the notion that amino acids are the preferred fuel during exercise in this species.

Unlike the presence or absence of light, the acute adjustment of temperature of 2 °C had no significant effect of the fuel preference at any stage of development. Although 2 °C seems a moderate adjustment, several studies have demonstrated that such an increase causes a significant elevation of protein turnover rate in rainbow trout, *Oncorhynchus mykiss* (Reid et al. 1995, 1997, 1998; Morgan et al. 1998). The temperatures used are well within the physiological range of this species and support the study of Egginton (1996), who did not find any evidence of thermal acclimation affecting substrate preference for β-oxidation in five species of teleost. Our study indicates that if molecular adjustments in membrane, enzyme, or substrate transporters occur in response to moderate temperature perturbation, they do so in a manner that conserves fuel preference.

Acknowledgements

This study is Contribution No. 137 of the Marine Larvae Locus at the University of Bergen. Support was provided by the School of Mathematics and Natural Sciences at the University of Bergen to R.N.F. and the Norwegian Research Council (projects HB 26605 and V110.011).

References

Aure, J., and Danielssen, D. 2003. Kystklima. *In* Havets miljø 2003. Chap. 4. Økosystemene på kystene og på fjordane. *Edited by* L. Asplin and E. Dahl. Fisken Havet. Spec. Publ. 2. Havforskningsinstituttet, Bergen, Norway. pp. 48–52.

Bower, C.E., and Holm-Hansen, T. 1980. A salicylate–hypochlorite method for determining ammonia in seawater. Can. J. Fish. Aquat. Sci. **37**: 794–798.

Brown, J.A.G., Jones, A., and Matty, A.J. 1984. Oxygen metabolism of farmed turbot (*Scophthalmus maximus*). I. The influence of fish size and water temperature on metabolic rate. Aquaculture, **36**: 273–281.

Burel, C., Person-Le Ruyet, J., Gaumet, F., Le Roux, A., Sévère, A., and Boeuf, G. 1996. Effects of temperature on growth and metabolism in juvenile turbot. J. Fish Biol. **49**: 678–692.

Chadwick, T.D., and Wright, P.A. 1999. Nitrogen excretion and expression of urea cycle enzymes in the Atlantic cod: a comparison of early life stages with adults. J. Exp. Biol. **202**: 2653–2662.

Champalbert, G., and Le Direach-Boursier, L. 1998. Influence of light and feeding conditions on swimming activity rhythms of larval and juvenile turbot *Scophthalmus maximus* L.: an experimental study. J. Sea Res. **40**: 333–345.

Crawley, M.J. 2002. Statistical computing. An introduction to data analysis using S-Plus. John Wiley & Sons, Chichester, U.K.

Eckert, R. 1997. Animal physiology. Mechanisms and adaptation. W.H. Freeman & Co., New York.

Egginton, S. 1996. Effect of temperature on the optimal substrate for β-oxidation. J. Fish Biol. **49**: 753–758.

Erga, S.R. 1989. Ecological studies on the phytoplankton of Boknafjorden, Western Norway. 1. The effect of water exchange processes and environmental factors on temporal and vertical variability of biomass. Sarsia, **74**: 161–176.

Finn, R.N., Widdows, J., and Fyhn, H.J. 1995. Calorespirometry of developing embryos and yolk-sac larvae of turbot (*Scophthalmus maximus*). Mar. Biol. **122**: 157–163.

Finn, R.N., Fyhn, H.J., Henderson, R.J., and Evjen, M.S. 1996. The sequence of catabolic substrate oxidation and enthalpy balance of developing embryos and yolk-sac larvae of turbot (*Scophthalmus maximus* L.). Comp. Biochem. Physiol. A, **115**: 133–151.

Finn R.N., Rønnestad, I., van der Meeren, T., and Fyhn, H.J. 2002. Fuel and metabolic scaling during the early life stages of Atlantic cod (*Gadus morhua*). Mar. Ecol. Prog. Ser. **243**: 217–234.

Forstner, H., and Gnaiger, E. 1983. Calculation of equilibrium oxygen concentration. *In* Polarographic oxygen sensors. Aquatic and physiological applications. *Edited by* E. Gnaiger and H. Forstner. Springer-Verlag, New York. pp. 321–333.

Gnaiger, E. 1983. Calculation of energetic and biochemical equivalents of respiratory oxygen consumption. *In* Polarographic oxygen sensors. *Edited by* E. Gnaiger and H. Forstner. Springer-Verlag, Berlin, Heidelberg. pp. 337–345.

Goolish, E.M. 1995. The metabolic implications of body size. *In* Biochemistry and molecular biology of fishes. Vol. 4. Metabolic biochemistry. *Edited by* P.W. Hochachka and T.P. Mommsen. Elsevier Science, Amsterdam. pp. 335–366.

Gouillou-Coustans, M.F., Fournier, V., Métailler, R., Vachot, C., Desbruyères, E., Huelvan, C., Moriceau, J., Le Delliou, H., and Kaushik, S.J. 2002. Dietary arginine degradation is a major pathway in ureagenesis in juvenile turbot (*Psetta maxima*). Comp. Biochem. Physiol. A, **132**: 305–319.

Green, E.J., and Carritt, D.E. 1967. New tables for oxygen saturation of seawater. J. Mar. Res. **25**: 140–147.

Hazel, J.R. 1993. Thermal biology. *In* The physiology of fishes. *Edited by* D.H. Evans. CRC Press, Boca Raton, Fla. pp. 427–467.

Hochachka, P.W., and Somero, G.N. 2002. Biochemical adaptation: mechanism and process in physiological evolution. Oxford University Press Inc., New York.

Iglesias, J., Rodríguez-Ojea, G., and Peleteiro, J.B. 1995. Effect of light and temperature on the development of turbot eggs (*Scophthalmus maximus* L.). ICES Mar. Sci. Symp. **201**: 40–44.

Imsland, A.K., Folkvord, A., and Stefansson, S.O. 1995. Growth, oxygen consumption and activity of juvenile turbot (*Scophthalmus maximus* L.) reared under different temperatures and photoperiods. Neth. J. Sea Res. **34**: 149–159.

Jones, A. 1972. Studies on egg development and larval rearing of turbot, *Scophthalmus maximus* L., and brill, *Scophthalmus rhombus* L., in the laboratory. J. Mar. Biol. Assoc. U.K. **52**: 965–986.

Mallekh, R., and Lagardère, J.P. 2002. Effect of temperature and dissolved oxygen concentration on the metabolic rate of the turbot and the relationship between metabolic scope and feeding demand. J. Fish Biol. **60**: 1105–1115.

Morgan, I.J., D'Cruz, L.M., Dockray, J.J., Linton, T.K., McDonald, D.G., and Wood, C.M. 1998. The effects of elevated winter temperature and sub-lethal pollutants (low pH, elevated ammonia) on protein turnover in the gill and liver of rainbow trout (*Oncorhynchus mykiss*). Fish Physiol. Biochem. **19**: 377–389.

Oppen-Berntsen, D.O., Helvik, J.V., and Walther, B.T. 1990. The major structural proteins of cod (*Gadus morhua*) eggshells and protein cross-linking during teleost egg hardening. Dev. Biol. **137**: 258–265.

Overnell, J., and Batty, R.S. 2000. Scaling of enzyme activity in larval herring and plaice: effects of temperature and individual growth rate on aerobic and anaerobic capacity. J. Fish Biol. **56**: 577–589.

Reid, S.D., Dockray, J.J., Linton, T.K., Mcdonald, D.G., and Wood, C.M. 1995. Effects of a summer temperature regime representative of a global warming scenario on growth and protein-synthesis in hardwater-acclimated and softwater-acclimated juvenile rainbow-trout (*Oncorhynchus mykiss*). J. Therm. Biol. **20**: 231–244.

Reid, S.D., Dockray, J.J., Linton, T.K., McDonald, D.G., and Wood, C.M. 1997. Effects of chronic environmental acidification and a summer global warming scenario: protein synthesis in juvenile rainbow trout (*Oncorhynchus mykiss*). Can. J. Fish. Aquat. Sci. **54**: 2014–2024.

Reid, S.D., Linton, T.K., Dockray, J.J., McDonald, D.G., and Wood, C.M. 1998. Effects of chronic sublethal ammonia and a simulated summer global warming scenario: protein synthesis in juvenile rainbow trout (*Oncorhynchus mykiss*). Can. J. Fish. Aquat. Sci. **55**: 1534–1544.

Rombough, P.J. 1988. Respiratory gas exchange, aerobic metabolism, and effects of hypoxia during early life. *In* Fish physiology. Vol XI. The physiology of developing fish. Part A. Eggs and larvae. *Edited by* W.S. Hoar and D.J. Randall. Academic Press, London. pp. 59–161.

Rønnestad, I., Fyhn, H.J., and Gravningen, K. 1992. The importance of free amino acids to the energy metabolism of eggs and larvae of turbot (*Scophthalmus maximus*). Mar. Biol. **114**: 517–525.

Russel, F.S. 1976. The eggs and planktonic stages of British marine fishes. Academic Press, London.

Scherrer, P. 1984. Influence de la température et de la salinité sur la croissance et la consommation d'oxygène du juvénile de turbot *Scophthalmus maximus* L. (phase nurserie). Thesis, Univesité de Bretagne Occidentale, 29285 Brest CEDEX, France.

Segner, H., Storch, V., Reinecke, M., Klaos, W., and Hanke, W. 1994. The development of functional digestive and metabolic organs in turbot, *Scophthalmus maximus*. Mar. Biol. **119**: 471–486.

Skiftesvik, A.B. 1992. Changes in behaviour at onset of exogenous feeding in marine fish larvae. Can. J. Fish. Aquat. Sci. **49**: 1570–1572.

Sokal, R.R., and Rohlf, F.J. 2000. Biometry. W.H. Freeman and Co., New York.

Terjesen, B.F., Finn, R.N., Norberg, B., and Rønnestad, I. 2002. Kinetics and fates of ammonia, urea, and uric acid during oocyte maturation and ontogeny of the Atlantic halibut (*Hippoglossus hippoglossus* L.). Comp. Biochem. Physiol. A, **131**: 443–455.

Van den Thillart, G., and Raaij, M. 1995. Endogenous fuels: noninvasive versus invasive approaches. *In* Biochemistry and molecular biology of fishes. Vol. 4. Metabolic biochemistry. *Edited by* P.W. Hochachka and T.P. Mommsen. Elsevier Science Ltd., Amsterdam. pp. 33–63.

Waller, U. 1992. Factors influencing routine oxygen consumption in turbot, *Scophthalmus maximus*. J. Appl. Ichthyol. **8**: 62–71.

Walsh, P.J. 1998. Nitrogen excretion and metabolism. *In* The physiology of fishes. *Edited by* D.H. Evans. CRC Press, Boca Raton, Fla. pp. 199–214.

Weltzien, F.A., Planas, M., and Fyhn, H.J. 1999. Temperature dependency of early growth of turbot (*Scophthalmus maximus* L.) and its implications for developmental progress. J. Exp. Mar. Biol. Ecol. **242**: 201–210.

Wheeler, A. 1992. A list of the common and scientific name of the fishes of the British Isles. J. Fish Biol. **41**(Suppl. B): 1–37.

Wood, C.M. 2001. Influence of feeding, exercise, and temperature on nitrogen metabolism and excretion. *In* Nitrogen excretion. *Edited by* P.A. Wright and P.M. Anderson. Academic Press, London, New York. pp. 201–238.

Wright, P.A., and Fyhn, H.J. 2001. Ontogeny of nitrogen metabolism and excretion. *In* Nitrogen excretion. *Edited by* P.A. Wright and P.M. Anderson. Academic Press, London, New York. pp. 149–200.

The role of sewage in a large river food web

Adrian M.H. deBruyn, David J. Marcogliese, and Joseph B. Rasmussen

Abstract: We evaluated the role of sewage as a resource for the littoral food web of the fluvial St. Lawrence River near Montreal, Quebec. Stable isotope analysis indicated that macroinvertebrate primary consumers were feeding on local epiphytic production at sites outside the sewage plume, but shifts in $\delta^{15}N$ of primary and secondary consumers revealed a substantial uptake of sewage-derived resources within the plume, up to 10 km from the outfall. Daily secondary production of macroinvertebrates was 1.8- to 4.1-fold higher at sewage-enriched sites, and the fraction of this production attributable to larval Chironomidae increased from 46% (outside the plume) to 85% (at sewage-enriched sites). Sewage enrichment also stimulated increases in daily fish production based on algivory–detritivory (1.3- to 4.4-fold), invertivory (1.7- to 10-fold), and piscivory (11- to 73-fold). We estimate a daily flux of 13 tonnes of sewage-derived particulate matter, 184 kg of total nitrogen, and 13 kg of total phosphorus into the food web over 1.2 km^2 of the littoral zone within 10 km of the outfall. These values represent no more than a few percent of the total daily discharge of sewage-derived resources but were sufficient to support an overall fivefold increase in secondary production relative to sites outside the plume.

Résumé : Nous avons évalué le rôle des égouts comme ressource dans le réseau alimentaire littoral du tronçon fluvial du Saint-Laurent, près de Montréal, Québec. Une analyse des isotopes stables révèle que les consommateurs primaires parmi les macroinvertébrés se nourrissent de la production locale des épiphytes aux sites en dehors du panache des égouts; toutefois, dans le panache, des changements de $\delta^{15}N$ chez les consommateurs primaires et secondaires indiquent qu'il y a une ingestion importante de ressources provenant des égouts, jusqu'à 10 km en aval du déchargement. La production secondaire journalière des macroinvertébrés est de 1,8 à 4,1 fois plus élevée aux sites enrichis par les égouts et la proportion de la production attribuable aux larves de chironomidés augmente de 46 % (hors du panache) à 85 % (aux sites enrichis par les égouts). L'enrichissement par les égouts entraîne aussi une augmentation de la production journalière de poissons en conséquence de la consommation d'algues et de détritus (augmentation de 1,3 à 4,4 fois) d'invertébrés (1,7 à 10 fois) et de poissons (11 à 73 fois). Nous estimons à 13 tonnes le flux quotidien de matière particulaire provenant des égouts qui entre dans le réseau alimentaire dans les 1,2 km^2 de la zone littorale qui s'étend sur les 10 km en aval de la décharge; l'azote total représente 184 kg et le phosphore total 13 kg. Ces valeurs ne représentent qu'un faible pourcentage du déversement quotidien total de ressources provenant des égouts, mais elles sont suffisamment élevées pour expliquer un accroissement général de l'ordre de 500 % de la production secondaire, par comparaison aux sites situés hors du panache de déversement.

[Traduit par la Rédaction]

Introduction

River ecologists have developed a small but powerful body of general theory, central to which is the overriding importance of longitudinal (upstream–downstream) and lateral (watershed–river) connections. These connections interact with physical forces that change along the course of a river, producing a continuum of morphological and hydrological features. The result is a shift in the relative importance of basal resources, from allochthonous litterfall in headwater streams to autochthonous producers in midsized rivers (Vannote et al. 1980). The metabolism of larger rivers is dominated by fine particulates transported in the main channel, although autochthonous production in the littoral zone and allochthonous inputs from riparian vegetation and floodplains are energetically more important to higher trophic levels (Thorp and Delong 1994, 2002).

Most of the world's large rivers are influenced to some extent by human activities and this often includes substantial pollution with sewage (Meybeck and Helmer 1989), but the role of sewage as a resource in river food webs is frequently overlooked. Previous work on sewage in rivers has tended to focus on nuisance blooms of algae or on systems so heavily enriched that hypoxia is a dominant environmental factor. In

Received 17 January 2003. Accepted 30 July 2003. Published on the NRC Research Press Web site at http://cjfas.nrc.ca on 21 November 2003.
J17294

A.M.H. deBruyn[1,2] and J.B. Rasmussen. Department of Biology, McGill University, 1205 Docteur Penfield Ave., Montreal, QC H3A 1B1, Canada.
D.J. Marcogliese. St. Lawrence Centre, Environment Canada, 105 McGill St., Montreal, QC H2Y 2E7, Canada.

[1] Corresponding author (e-mail: adebruyn@sfu.ca).

[2] Present address: School of Resource and Environmental Management, Simon Fraser University, 8888 University Drive, Burnaby, BC V5A 1S6, Canada.

Can. J. Fish. Aquat. Sci. **60**: 1332–1344 (2003)   doi: 10.1139/F03-114

most cases, however, the rate of sewage loading does not exceed the capacity of the river to maintain sufficient dissolved oxygen for metazoan life. Adequate dilution (high river discharge relative to sewage loading) and strong vertical mixing protect large rivers from these negative effects and permit the biota to exploit sewage nutrients and organic matter. Even in rivers that do experience severe oxygen depletion, biochemical oxygen demand is eventually satisfied, and the response of downstream biota to sewage enrichment is not constrained by hypoxia.

We studied the role of sewage in the littoral food web of a large, temperate river. The municipal wastewater treatment plant of Montreal, Canada, has been discharging >450 tonnes (t) of phosphorus, >8000 t of nitrogen, and >90 000 t (wet weight) of particulate organic matter (POM) annually into the St. Lawrence River since 1988 (Purenne 2001). High current speeds and strong vertical mixing prevent deoxygenation and net sedimentation in this reach of the river, so the primary effect is sustained enrichment with dissolved nutrients and POM. We used stable isotope analysis to identify sites enriched by sewage, and we evaluated the degree to which sewage-derived resources are assimilated by the biota of the river, increasing production of fish and macroinvertebrates.

Materials and methods

Study system

The St. Lawrence River is a large, fast-flowing, temperate river with a constrained channel. At the Island of Montreal, the river has two distinct, adjacent water masses: the clear, hard, "green water" of the Great Lakes (80% of the total discharge) and the humic, soft, "brown water" of the Ottawa River (St. Lawrence Centre 1996). Neither water mass has high nutrient levels (dissolved $P < 30\ \mu g \cdot L^{-1}$; dissolved $N < 0.5\ mg \cdot L^{-1}$), and neither is very productive (median summer chlorophyll $a < 2.5\ \mu g \cdot L^{-1}$) (Hudon and Sylvestre 1998). Flow rates are typically $1–2\ m \cdot s^{-1}$ in the main channel, and net sedimentation of suspended material is restricted to the deepest areas outside the main channel. Permanent deposition is a small component of the suspended solids budget of this river (Carignan and Lorrain 2000).

The Montreal Urban Community (MUC) wastewater treatment plant is a primary treatment facility serving 1.8 million people and 8000 commercial establishments on the Island of Montreal (Pham et al. 1999; Purenne 2001). Wastewater is treated to promote coagulation, passed through settling ponds (2–3 h, reducing suspended solids by 85%), and discharged directly into the St. Lawrence River via an underwater pipe at a depth of 7 m. Effluent is discharged at an average rate of $2 \times 10^6\ m^3 \cdot day^{-1}$ and contains approximately $100\ mg \cdot L^{-1}$ POM (wet mass, WM), $0.5\ mg \cdot L^{-1}$ total phosphorus, and $9\ mg \cdot L^{-1}$ total nitrogen (Purenne 2001). This discharge contributes $450\ t \cdot year^{-1}$ total phosphorus, $8000\ t \cdot year^{-1}$ total nitrogen, and $90\,000\ t \cdot year^{-1}$ (WM) sewage-derived particulate organic matter (SDPOM) to the waters of the St. Lawrence River (Purenne 2001).

Lateral mixing in this reach of the St. Lawrence is minimal. The MUC wastewater is discharged into the middle of a narrow mixing zone between the two water masses and seems to widen very gradually downstream (Boulanger 1984). However, the discharge rate of wastewater has increased from $5\ m^3 \cdot s^{-1}$ to $30\ m^3 \cdot s^{-1}$ since Boulanger's study was conducted, and the current extent of the plume is not well known.

Sample sites

We studied 12 sites in the fluvial St. Lawrence River downstream of the Island of Montreal, Quebec, Canada (Fig. 1). All sites were shallow (<2.5 m) and had sand–clay sediment. Three sites were known to be in the discharge plume of the municipal wastewater treatment plant, within 10 km of the outfall. Four were clearly reference sites, hydrodynamically isolated from the plume. The rest were downstream of the outfall and of unknown exposure, but stable isotope analysis (described below) indicated that there was no sewage influence at these downstream sites, and they are hereafter referred to as "reference" sites. It is important to note that all of these reference sites serve as a reference only with respect to Montreal's sewage. Most probably receive other sources of anthropogenic nutrients (e.g., sewage from local communities or far upstream, agricultural runoff); we consider this to be background noise against which we attempt to detect the influence of Montreal's sewage.

The sewage effluent has a higher conductivity than the receiving water, permitting a rough estimation of effluent concentration in this area (see also Pham et al. 1999). Effluent ($723\ \mu S \cdot cm^{-1}$ in June–August 2000; Purenne 2001) is discharged into the mixing zone between the green ($280 \pm 6.1\ \mu S \cdot cm^{-1}$, $n = 17$) and brown ($134 \pm 20.1\ \mu S \cdot cm^{-1}$, $n = 14$) water masses. Upstream of the outfall, this mixed water has a conductivity of $265 \pm 2.7\ \mu S \cdot cm^{-1}$ ($n = 7$). The sewage-exposed sites all have higher conductivity than this (Île Ste-Thérèse, $278 \pm 13.7\ \mu S \cdot cm^{-1}$ ($n = 3$); Îles Robinet, $277 \pm 1.9\ \mu S \cdot cm^{-1}$ ($n = 4$); Îlet Vert, $276 \pm 1.2\ \mu S \cdot cm^{-1}$ ($n = 3$)), and conductivity declines to the north and south of all three sites, so this higher conductivity does not simply reflect a greater influence of Great Lakes (green) water. These conductivity values indicate a consistent contribution of about 3% sewage by volume at these sites.

The three sewage-exposed sites varied in abundance of submerged macrophytes from about 10% to about 60% cover. We therefore selected reference sites to represent a gradient of submerged macrophyte cover that encompassed the variation among sewage-exposed sites, from about 5% to over 80% cover. Thus, our sites represent a wide gradient of physical structure and surface area for epiphytic primary production. Submerged vegetative cover was quantified on each visit after seining was completed: the entire seined area (to a depth of about 2.5 m) was inspected both by wading and from the boat, the area was mapped out and divided into zones with similar cover (e.g., dense weedbeds, scattered bunches of tall plants), and the percent cover of each zone was estimated visually. Vegetative cover changed little over the months between sampling dates, and we use the mean value in all analyses.

Sampling

We collected fish and invertebrates on two visits to each site between 17 July and 7 September 2000. Fish were captured with a 40 m × 2 m seine (0.5-cm mesh) deployed from the boat in a semicircle (open side facing land), which was then closed and drawn in to shore. At least three seine hauls

Fig. 1. Location of study sites on the St. Lawrence River (R, reference; S, sewage-exposed) near Montreal, Quebec, Canada. Shaded area in lower inset is approximate location of Montreal's sewage plume.

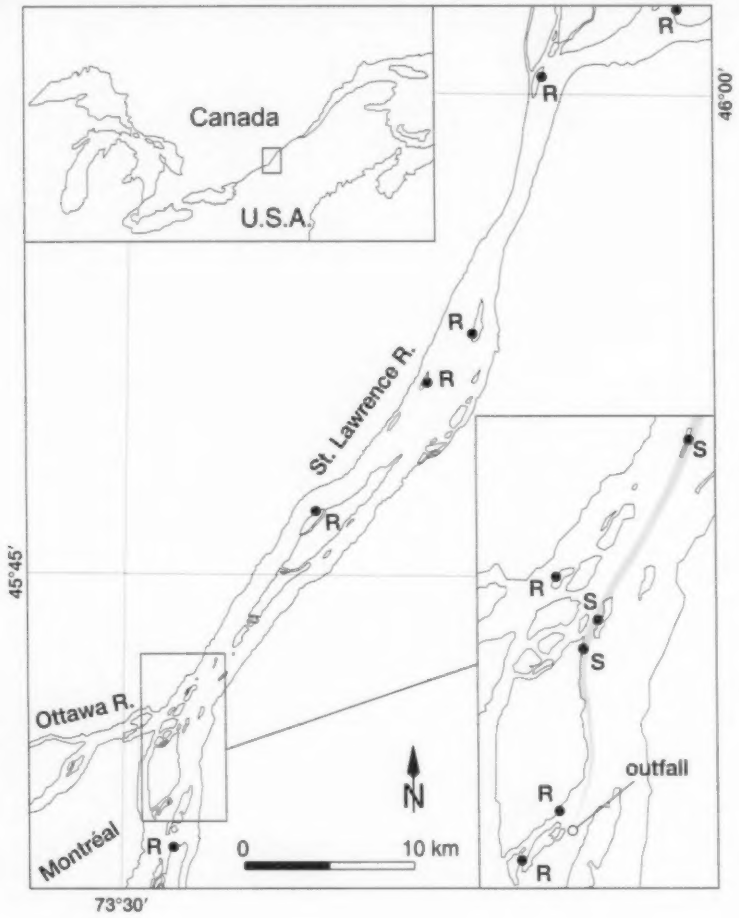

were taken on each visit, 50–100 m apart and successively upstream. One or two additional hauls were taken if low numbers of fish were obtained. The seined area was calculated from the shape of the deployed net (mean area per haul = 320 m^2). Five to 10 individuals of each species per visit (or as many as were available) were sacrificed and frozen for gut content and stable isotope analysis. All other fish were measured before release, and their wet weights were calculated using length–mass relationships derived from sacrificed fish. Gut contents (total $n = 622$) were quantified as percent volume.

Benthic invertebrates were collected on the same two visits to nine of these sites (all three sewage-exposed sites and six reference sites), using a D-frame net (0.5-mm mesh) to scoop up 0.25-m^2 grab samples of surface sediment and overlying vegetation. Replicate samples were taken in dense weedbeds (two samples, typically ~1 m deep) and in relatively bare areas (two samples each at 0.5-m and 1-m depths). Invertebrates were removed from each sample under a dissecting microscope, sorted into three size classes within each taxon, dried in preweighed tin capsules, and weighed. Invertebrates for stable isotope analysis were sorted from grab samples within a few hours of collection.

Sewage-derived particulate matter was collected at the wastewater treatment plant on 27 June, 21 July, and 11 August 2000. Suspended particulate matter was collected in the two water masses adjacent to the plume eight times between 24 July and 7 September 2000. Particulate matter was collected on precombusted Whatman GF/C filters and stored at –20 °C until processing. Epiphytes were collected by shaking several macrophytes in a plastic bottle with a small amount of river water. The resulting suspension was filtered through a 0.5-mm screen, inspected carefully for invertebrates and plant fragments, and stored at –20 °C until processing.

Stable isotope analysis

Invertebrates for stable isotope analysis were held alive for a few hours to allow gut clearance, stored at –20 °C, and subsequently dried for 48 h at 70 °C. Whole invertebrates (5–10 per taxon) were pulverized and subsampled for analysis. Frozen fish were dissected to obtain a piece of dorsolateral muscle tissue. Particulate matter was recovered by scraping the surface of the glass-fibre filter after drying. $\delta^{13}C$ and $\delta^{15}N$ were determined on a mass spectrometer at the G.G. Hatch Isotope Laboratory, University of Ottawa.

Secondary production

We estimated secondary production (P_{MD}) of each size class of each invertebrate taxon using the growth equations of Morin and Dumont (1994) and the measured mean body mass of each size class. Total production was then calculated for macroinvertebrate carnivores (Odonata, Hydracarina, and Notonectidae) and macroinvertebrate primary consumers (all other taxa). We assumed that dry mass is 20% of wet mass.

We estimated secondary production for each fish species at each site using growth increment summation (P_{GIS}) and instantaneous growth rate (P_{IGR}) methods (Rigler and Downing 1984). All fish masses were first corrected to a standard date by the following method to account for differences in sampling date among sites. Each fish was assigned to an age class based on inspection of size–frequency distributions of pooled data for each species. Linear regression was used to describe the relationship between log mass and date for each age class of each species. The slope of this line was then used to project the mass of each individual fish in that age class backward or forward to 1 August, removing any bias toward larger fish at sites that were sampled later in the season.

Growth increment summation estimates the total biomass added to each age class over the previous year by linear interpolation of numerical density between adjacent age classes. When no members of an age class were captured at a site, the mean age-class mass was replaced with the mean for that species at all other sites. The instantaneous growth rate method estimates the biomass added to each age class on a single day (1 August). These two production-estimation methods ultimately rely on the same biomass data but estimate the rate at which that biomass is elaborated in different ways. Thus, each method includes a unique component of information from the data, and each speaks to a different aspect of fish production: total annual P_{GIS}, or (approximately) maximum, midsummer P_{IGR}.

Total production based on piscivory was calculated by multiplying the production of each age class of each species by the proportion of its diet consisting of fish, then summing these products over all age classes of all species. Diet composition was considered separately for sewage-exposed and reference sites. Total production based on invertivory and on algivory–detritivory was calculated in a similar manner. Consumption rates for each trophic level were estimated by assuming conversion efficiencies (CE) of 45% for macroinvertebrate carnivores (Benke 1996), 15% for macroinvertebrate primary consumers (assuming that basal resources are a mixture of algae (CE = 25–30%; Elser et al. 2000) and detritus (CE = 2%; Benke 1996)), 5% for algivorous–detritivorous fish, 10% for invertivorous fish, and 15% for piscivorous fish (Trudel et al. 2001; Pazzia et al. 2002).

Fluxes of sewage-derived resources

The areal flux of basal resources into the littoral food web at each site (g WM·m^{-2}·year^{-1}) was back-calculated from areal production at each trophic level (Ney 1990). The areal flux of sewage-derived resources was then calculated for the three sewage-exposed sites. It was assumed that sewage-derived resources supported all secondary production in excess of that observed at reference sites of comparable vegetative cover (interpolated from a regression of secondary production versus vegetative cover for reference sites only). The areal fluxes of sewage-derived nutrients (g N or P·m^{-2}·year^{-1}) were then calculated from the estimated percent nitrogen and percent phosphorus in these basal resources (estimates described below).

The total mass flux of sewage nutrients into the littoral food web in our study reach (g N or P·year^{-1}) was calculated as the product of area of littoral zone in the sewage plume (within 10 km of the outfall) and the areal flux of sewage-derived nutrients, weighted for the distribution of macrophyte cover in this area. The area of littoral zone in this section of the plume was estimated using the 2.5-m depth contour on hydrographic charts.

Statistical analysis

All means are reported ±1 standard deviation. Where values were estimated from regression equations fit to our data, we used the model standard error of estimate to calculate the standard deviation of each estimated value. Analysis of covariance (ANCOVA) was used to test for effects of vegetative cover (continuous), sewage exposure (categorical), and their interaction on secondary production of each trophic group. We used $\alpha = 0.05$ for all ANCOVA and regression analyses, but because our sample size was limited, and thus our power to detect weak patterns was likely low, we report and discuss a few trends in the data that exceeded this value. Spatial correlograms with Moran's I statistic were used to test for spatial autocorrelation among our study sites (Legendre and Legendre 1998). We tested for spatial autocorrelation of vegetative cover among all 12 sites, but for other variables (stable isotope signatures and production estimates), we separated sewage-enriched from reference sites to meet the intrinsic assumption (Legendre and Legendre 1998, p. 718). We used six distance categories for each variable and, therefore, six significance tests against a Bonferroni-corrected alpha. All production estimates were log-transformed to stabilize residual variance.

Results

Stable isotope analysis

$\delta^{13}C$ of macroinvertebrate primary consumers was highly variable within and among reference sites (−17.6 ± 2.6‰; Fig. 2), whereas $\delta^{15}N$ was much more consistent (+8.6 ± 0.7‰; Fig. 2). The isotopic signatures of all three taxa spanned a similar range at these sites indicating an overall dietary $\delta^{13}C$ that varied among sites but a relatively constant dietary $\delta^{15}N$ (assuming a similar trophic fractionation shift among taxa). Potential resources at reference sites include seston from the Ottawa River ($\delta^{13}C$ = −25.9 ± 1.6‰, $\delta^{15}N$ = +4.9 ± 0.2‰, atomic C:N = 8.6 ± 1.0; n = 7) and Great Lakes ($\delta^{13}C$ = −20.1 ± 0.7‰, $\delta^{15}N$ = +4.5 ± 0.2‰, atomic C:N = 8.1 ± 0.7, n = 8) water masses and epiphytic biofilm ($\delta^{13}C$ = −15.8 ± 3.8‰, $\delta^{15}N$ = +6.6 ± 0.9‰, atomic C:N = 8.5 ± 0.8, n = 9). These materials have similar C–N ratios

Fig. 2. $\delta^{15}N$ versus $\delta^{13}C$ of macroinvertebrate primary consumers at sewage-exposed (solid symbols) and reference (open symbols) sites on the St. Lawrence River. Taxa are Amphipoda (circles), Chironomidae (triangles), and Trichoptera (squares). Potential epiphytic resources at sewage-exposed (×) and reference (+) sites are also shown. Potential sestonic resources (boxes, ±1 standard deviation) are particulate organic matter (POM) from the Montreal Urban Community wastewater treatment plant (SDPOM, sewage-derived particulate organic matter) and upstream of the outfall in the Great Lakes and Ottawa River water masses.

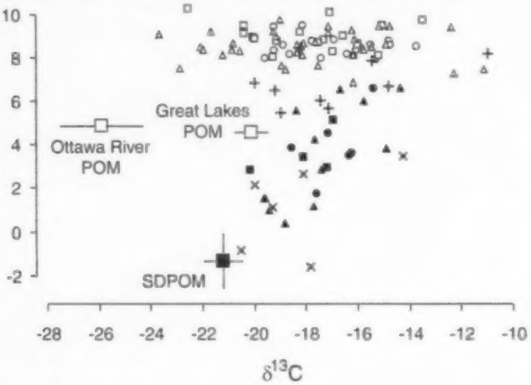

and thus are all likely to have trophic fractionation shifts of about +2‰ (Adams and Sterner 2000). The overall diet of macroinvertebrate primary consumers at the reference sites therefore has a $\delta^{13}C$ between –24‰ and –11‰ and a $\delta^{15}N$ of about +6.6‰ (approximately the isotopic signature of epiphytic biofilm).

Sewage-derived POM (SDPOM; $\delta^{13}C$ = –21.2 ± 0.7‰, $\delta^{15}N$ = –1.3 ± 1.3‰, atomic C:N = 7.4 ± 0.8, n = 6) was within the range of the non-sewage resources in $\delta^{13}C$ but was substantially lighter in $\delta^{15}N$ (a 7.9‰ difference) than the inferred diet of primary consumers at reference sites. Epiphytic resources at the sewage-exposed sites ($\delta^{13}C$ = –18.8 ± 2.5‰, $\delta^{15}N$ = +0.8 ± 2.0‰, atomic C:N = 7.0 ± 1.6, n = 5) were also shifted to lighter values of $\delta^{15}N$, but this was at least partly due to a visible accumulation of attached SDPOM.

Isotopic signatures of macroinvertebrate primary consumers at the three sewage-exposed sites were shifted toward that of SDPOM. Regression of $\delta^{15}N$ versus $\delta^{13}C$ of sewage-exposed primary consumers was highly significant (r^2 = 0.45, $F_{[1,20]}$ = 16.6, p = 0.0006), suggesting that these invertebrates are assimilating sewage-derived carbon and nitrogen in similar proportions (i.e., as SDPOM). The regression equation ($\delta^{15}N = 0.82 \cdot \delta^{13}C + 17.8‰$), solved for the $\delta^{13}C$ of SDPOM, indicated a trophic fractionation value of +1.8‰ for invertebrates consuming a diet of 100% SDPOM, consistent with the predictions of Adams and Sterner (2000) for such an N-rich resource. The observed shifts in $\delta^{15}N$ of macroinvertebrate primary consumers at the enriched sites ($\Delta\delta^{15}N$ versus the mean $\delta^{15}N$ at reference sites) did not vary monotonically downstream but decreased linearly with increasing submerged vegetative cover (VC) at the site (r^2 = 0.62, $F_{[1,24]}$ = 39, p = 0.000002; mean $\Delta\delta^{15}N$ = 6.6‰ at 15% VC, 4.9‰ at 30% VC, and 2.9‰ at 60% VC). No shift in $\delta^{15}N$ was observed at any other site.

Fig. 3. $\delta^{15}N$ versus $\delta^{13}C$ of (*a*) piscivorous fishes, (*b*) nonpiscivorous fishes, and (*c*) macroinvertebrate carnivores at sewage-exposed (solid symbols) and reference (open symbols) sites on the St. Lawrence River. YOY denotes young-of-the-year.

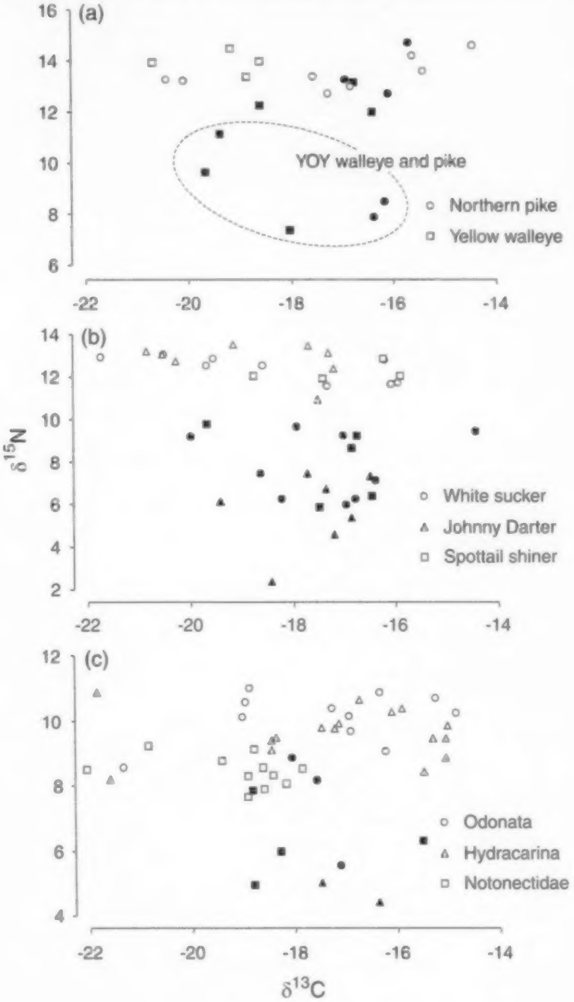

$\delta^{15}N$ of higher consumers at the three sewage-exposed sites was also shifted toward that of SDPOM (Fig. 3). Macroinvertebrate carnivores (odonates, notonectids, and mites) were 3.2‰ lighter in $\delta^{15}N$ (t_{48} = 7.62, $p < 0.00001$) at sewage-exposed ($\delta^{13}C$ = –17.5 ± 1.1‰, $\delta^{15}N$ = +6.3 ± 1.6‰, n = 9) versus reference ($\delta^{13}C$ = –18.2 ± 2.3‰, $\delta^{15}N$ = +9.5 ± 1.0‰, n = 41) sites. Benthivorous fish (white sucker, johnny darter, and spottail shiner) were 5.4‰ lighter in $\delta^{15}N$ (t_{40} = 12.1, $p < 0.00001$) at sewage-exposed ($\delta^{13}C$ = –17.5 ± 1.3‰, $\delta^{15}N$ = +7.1 ± 1.9‰, n = 21) versus reference ($\delta^{13}C$ = –18.3 ± 1.8‰, $\delta^{15}N$ = +12.5 ± 0.7‰, n = 21) sites. Age-1+ and older piscivorous fish (northern pike and yellow walleye) showed no significant shift in $\delta^{15}N$ at sewage-exposed ($\delta^{13}C$ = –16.7 ± 1.0‰, $\delta^{15}N$ = +13.0 ± 1.0‰, n = 6) versus reference ($\delta^{13}C$ = –17.9 ± 2.1‰, $\delta^{15}N$ = +13.6 ± 0.6‰, n = 12) sites, but young-of-the-year piscivores at the sewage-exposed sites were, on average,

Table 1. Taxa dominating daily production (estimated from instantaneous growth rates, P_{IGR}, or from the empirical relationships of Morin and Dumont (1994), P_{MD}) of trophic groups at reference (mean of $n = 9$ for fish, $n = 6$ for invertebrates) and sewage-exposed (mean of $n = 3$) littoral sites in the St. Lawrence River.

Reference sites		Sewage-exposed sites	
Taxon (age class)	%[a]	Taxon (age class)	%[a]
Piscivorous fish			
Northern pike (0+)	21	Smallmouth bass (2+)	74
Northern pike (1+)	19	Northern pike (1+)	18
Yellow perch (2+)	18		
Smallmouth bass (1+)	17		
Smallmouth bass (0+)	12		
Yellow perch (1+)	9		
Invertivorous fish			
Yellow perch (1+)	20	White sucker (2+)	53
White sucker (2+)	16	White sucker (0+)	24
White sucker (0+)	12	Brown bullhead (0+)	7
Golden shiner (1+)	7		
Pumpkinseed (1+)	6		
Emerald shiner (2+)	6		
Alewife (1+)	5		
Macroinvertebrate carnivores			
Hydracarina	63	Hydracarina	66
Notonectidae	28	Notonectidae	27
Odonata	10	Odonata	8
Algivorous–detritivorous fish[b]			
Emerald shiner (1+)	26	White sucker (2+)	61
Emerald shiner (2+)	16	White sucker (0+)	26
Spottail shiner (1+)	14	Emerald shiner (1+)	6
Blacknose shiner (1+)	13		
Golden shiner (1+)	10		
Golden shiner (0+)	9		
Macroinvertebrate primary consumers			
Chironomidae	46	Chironomidae	85
Gastropoda	26	Amphipoda	9
Amphipoda	21		

Note: Latin names are given in Table 4. Only taxa contributing ≥5% of total production of each trophic group are shown. Other piscivores were muskellunge and walleye; other invertivores were smallmouth bass, johnny darter, logperch, rock bass, troutperch, banded killifish, spottail shiner, blacknose shiner, and silver redhorse; other algivores–detritivores were silver redhorse; other macroinvertebrate primary consumers were Trichoptera, Ephemeroptera, Lepidoptera, Sphaeriidae, Cladocera, and Nematoda.

[a] Percent of total daily production of trophic group.

[b] These taxa are all primarily invertivorous but are nevertheless responsible for the majority of fish algivory–detritivory.

4.7‰ lighter in $\delta^{15}N$ ($\delta^{13}C = -17.9 \pm 1.6‰$, $\delta^{15}N = +8.9 \pm 1.5‰$, $n = 5$) than piscivores (all ages) at reference sites ($t_{15} = 9.46$, $p < 0.00001$).

Secondary production

Larval Chironomidae contributed 46% of the total production of benthic macroinvertebrates (P_{MD}) at reference sites and 85% at sewage-exposed sites. Amphipods (*Gammarus fasciatus*) and snails (of the genera *Amnicola*, *Bithynia*, *Ferrissia*, *Gyraulus*, *Helisoma*, *Physa*, *Pseudosuccinia*, *Stagnicola*, and *Valvata*) were also abundant, and these three taxa accounted for >80% of P_{MD} at both reference and sewage-exposed sites. The taxa dominating production in each trophic group are listed in Table 1.

Total P_{MD} of macroinvertebrates was 169 ± 58 mg $WM \cdot m^{-2} \cdot day^{-1}$ (range 76 to 237) at reference sites and 457 ± 133 mg $WM \cdot m^{-2} \cdot day^{-1}$ (range 318 to 583) at sewage-exposed sites. ANCOVA revealed a significant main effect of sewage exposure on P_{MD} of macroinvertebrate primary consumers ($F_{[1,6]} = 13.5$, $p = 0.010$; Fig. 4) but no main effect of vegetative cover nor an interaction effect. Macroinvertebrate carnivores accounted for 1.6% of total P_{MD} at reference sites and 0.25% of total P_{MD} at sewage-exposed sites. ANCOVA revealed no effect of sewage exposure or vegetative cover on carnivore production (Fig. 4).

For all invertebrate taxa combined, log P_{MD} was strongly correlated with log biomass (B) among sites ($F_{[1,14]} = 100$, $p < 0.00001$). Because of the method that we used to calculate production (Morin and Dumont 1994), the specific rate of community production (P_{MD}/B) could vary with the taxonomic composition of the fauna (chironomids have very high growth rates) or with the mean body mass of individuals.

Fig. 4. Log of daily secondary production at sewage-exposed (solid circles, solid line) and reference (open circles, broken line) sites on the St. Lawrence River as a function of submerged vegetative cover. Taxa are (*a*) piscivorous fish, (*b*) invertivorous fish, (*c*) macroinvertebrate carnivores, (*d*) algivorous–detritivorous fish, and (*e*) macroinvertebrate primary consumers. WM, wet mass.

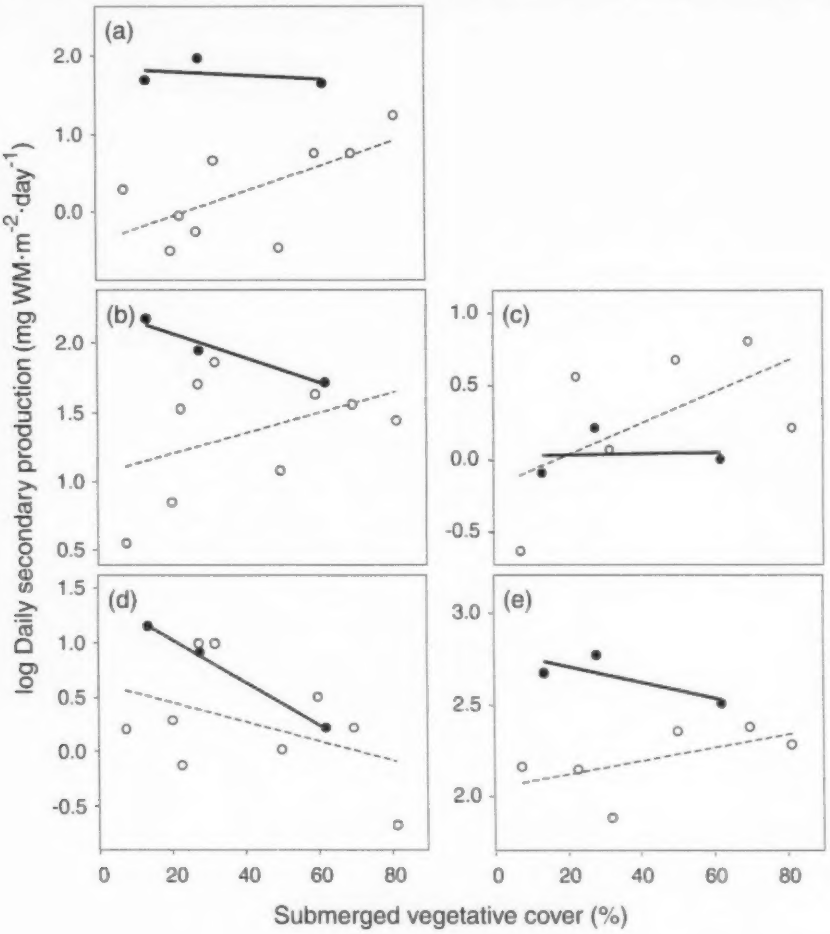

Table 2. Intercepts (*a*) and slopes (*b*) of taxon-specific relationships between log production (*P*) and log biomass (*B*) among littoral sites in the St. Lawrence River.

		log P_{MD} (daily)		
Taxon	*n*	*a*	*b*	*P*/*B*
Chironomidae	18	–0.75	0.996	0.178
Amphipoda	18	–1.40	0.937	0.042
Gastropoda	18	–1.44	0.955	0.039
Trichoptera	17	–1.48	0.956	0.038
Sphaeriidae	18	–1.23	0.950	0.071
Total invertebrates	18	–1.09	0.916	0.084

Note: Daily production (P_{MD}) was estimated from the growth equations of Morin and Dumont (1994).

ANCOVA revealed a significant interaction between sewage exposure and log *B* ($F_{[1,14]} = 6.5$, $p = 0.023$), but no main effect of sewage and, therefore, no effect of sewage on mean P_{MD}/B. None of the taxon-specific log *P* versus log *B* relationships had slopes significantly different from unity (Table 2). The mean value of P_{MD} /*B* among all sites was 0.084.

A total of 19 404 fish were captured. Most species age classes were primarily invertivorous (Table 1). White sucker and silver redhorse also consumed ≤10% detritus by volume. The four shiner species consumed invertebrates and about 30% filamentous algae by volume. Yellow perch and smallmouth bass were primarily invertivorous in younger age classes but had an increasing contribution of piscivory in older fish.

Similar patterns of fish production were obtained using the two estimation methods (correlation between P_{GIS} and P_{IGR} for all species at all sites: $r^2 = 0.89$, $F_{[1,159]} = 1332$, $p < 0.00001$). The daily estimate (P_{IGR}) is shown in Fig. 4 for comparison with daily production of invertebrates (note log scale). Invertivorous fish accounted for most daily fish production at reference sites, with similar contributions of

Table 3. Contribution of trophic groups to daily fish production (estimated from instantaneous growth rates, P_{IGR}) and annual fish production (estimated from growth increment summation, P_{GIS}) at reference (Ref., mean of $n = 9$) and sewage-exposed (Sewage, mean of $n = 3$) littoral sites in the St. Lawrence River.

	Daily fish production (P_{IGR}), %		Annual fish production (P_{GIS}), %	
Trophic group	Ref.	Sewage	Ref.	Sewage
Piscivorous fish	12.2	39.9	22.0	31.3
Invertivorous fish	77.2	55.8	74.7	63.3
Algivorous–detritivorous fish	10.6	4.31	3.35	5.36

Note: Latin names are given in Table 4.

Table 4. Intercepts (*a*) and slopes (*b*) of taxon-specific relationships between log production (*P*) and log biomass (*B*) among littoral sites in the St. Lawrence River.

		log P_{GIS} (annual)			log P_{IGR} (daily)		
Species	*n*	*a*	*b*	*P*/*B*	*a*	*b*	*P*/*B*
Alewife (*Alosa pseudoharengus*)	8	–0.341	1.06	0.52	–1.306	1.06	0.056
Bass[a]	12	–0.480	1.15	0.59	–1.962	1.22	0.025
Blacknose shiner (*Notropis heterolepis*)	10	–0.578	1.05	0.26	–1.893	1.09	0.014
Johnny darter (*Etheostoma nigrum*)	12	–0.015	1.13	1.30	–1.901	1.00	0.012
Emerald shiner (*Notropis atherinoides*)	12	–0.450	1.04	0.41	–1.829	0.98	0.014
Golden shiner (*Notemigonus crysoleucas*)	8	–0.388	1.19	0.82	–1.756	1.00	0.018
Banded killifish (*Fundulus diaphanus*)	8	–0.214	0.98	0.59	–2.053	0.97	0.008
Logperch (*Percina caprodes*)	11	–0.161	1.16	1.11	–1.651	0.91	0.017
Yellow perch (*Perca flavescens*)	12	–0.531	1.20	1.02	–2.019	0.95	0.007
Pikes[a]	10	–0.259	1.11	0.95	–1.514	0.81	0.012
Pumpkinseed (*Lepomis gibbosus*)	8	–0.615	1.24	0.57	–1.789	1.00	0.016
Rock bass (*Ambloplites rupestris*)	11	–0.140	1.24	1.42	–1.584	0.89	0.019
Spottail shiner (*Notropis hudsonius*)	12	–0.320	1.07	0.60	–1.800	1.04	0.018
Suckers[a]	12	0.229	0.94	1.15	–1.923	1.00	0.012
Troutperch (*Percopsis omiscomaycus*)	9	–0.286	1.18	0.74	–1.842	1.03	0.015
Walleye (*Stizostedeon vitreum*)	6	0.197	0.82	0.93	–1.060	0.72	0.038

[a] Species observed at fewer than six sites were combined with similar species: basses are largemouth (*Micropterus salmoides*) and smallmouth bass (*M. dolomieui*); pikes are northern pike (*Esox lucius*) and muskellunge (*E. masquinongy*); suckers are white sucker (*Catastomus commersoni*) and silver redhorse (*Moxostoma anisurum*).

piscivorous and algivorous fish production making up the rest (Table 3). Invertivorous fish also dominated daily production at sewage-exposed sites, but there was a greater contribution of piscivorous fish. Production based on primary consumption was proportionally less important and was primarily attributable to detritivores rather than algivores (Table 1). Total annual production of fish (P_{GIS}) was 4.85 ± 4.50 g $WM{\cdot}m^{-2}{\cdot}year^{-1}$ (range 0.25 to 13.6) at reference sites and 7.60 ± 1.46 g $WM{\cdot}m^{-2}{\cdot}year^{-1}$ (range 6.07 to 8.98) at sewage-exposed sites. The distribution of annual production among trophic groups was similar to that for daily production (Table 3).

ANCOVA revealed an increase in piscivore production with sewage subsidy (log P_{GIS}, $F_{[1,9]} = 8.58$, $p = 0.017$; log P_{IGR}, $F_{[1,9]} = 22.0$, $p = 0.0011$) and a positive correlation of annual piscivore production with vegetative cover (log P_{GIS}, $F_{[1,9]} = 15.6$, $p = 0.0033$). Daily estimates of invertivore production also tended to be highest at sewage-exposed sites (Fig. 4), but this trend was not significant (log P_{IGR}, ANCOVA $F_{[1,9]} = 5.00$, $p = 0.05$), and there was no main effect of vegetative cover using either production-estimation method. Annual estimates of algivorous–detritivorous production were similarly highest at sewage-exposed sites, but this trend was also nonsignificant (log P_{GIS}, ANCOVA $F_{[1,9]} = 4.70$, $p = 0.058$), and ANCOVA detected no main effect of vegetative cover using either production-estimation method. In no case was there a significant interaction between the independent variables.

ANCOVA revealed no effect of sewage exposure on the log *P* versus log *B* relationship for fish. For all fish species combined, log *P* was strongly correlated with log *B* among sites ($F_{[1,303]} = 3670$, $p < 0.00001$), although this relationship differed between methods (GIS and IGR) in both slope ($F_{[1,303]} = 31.7$, $p < 0.00001$) and intercept ($F_{[1,303]} = 117$, $p < 0.00001$). There was also a main effect of species ($F_{[15,303]} = 5.0$, $p < 0.00001$), but post-hoc multiple comparisons revealed that this was restricted to a difference between the three species with highest intercepts (alewife, rock bass, walleye) and the two with lowest intercepts (emerald and blacknose shiners). None of the species-specific log *P* versus log *B* relationships had slopes significantly different from unity (Table 4). Annual P_{GIS}/B ranged from 0.26 to 1.4

Fig. 5. Ratio of secondary production at three sewage-exposed sites to that observed at reference sites of similar submerged vegetative cover. Secondary production estimates are for piscivorous fish (Pis), invertivorous fish (Inv), algivorous fish (Alg), macroinvertebrate carnivores (MC), and macroinvertebrate primary consumers (M1°). Fish production was estimated by instantaneous growth rate (IGR) and growth increment summation (GIS) methods, and invertebrate production was estimated from the equations of Morin and Dumont (1994) (MD). Asterisks denote the significance (**, $p < 0.05$; *, $p < 0.10$) of the main effect of sewage exposure in analysis of covariance.

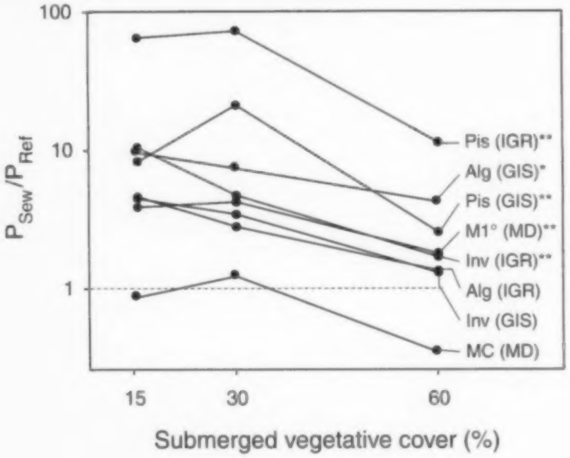

(mean 0.81), and daily P_{IGR}/B ranged from 0.001 to 0.056 (mean 0.019).

Trophic dynamics

All trophic groups except macroinvertebrate carnivores had higher mean biomass densities, greater production, and consequently greater consumption at sewage-exposed sites than at reference sites (Fig. 5; Table 5). On average (geometric mean of all trophic groups, estimation methods, and exposed sites; Fig. 5), secondary production was 5.0-fold greater at sewage-exposed than at reference sites. At reference sites, prey production exceeded (C_{Pred}:P_{Prey} = 0.54 for piscivores) or approximately met (C_{Pred}:P_{Prey} = 1.3 for invertivores) predator consumption, but at sewage-exposed sites, predator consumption exceeded prey production by a factor of 1.9 to 4.3.

Fluxes of sewage-derived resources

Estimates of the areal flux of sewage-derived resources into the benthic food web ranged from 2.4 to 19.0 g WM·m^{-2}·day^{-1} at 15% vegetative cover and from 0.82 to 9.6 g WM·m^{-2}·day^{-1} at 60% vegetative cover, depending on the trophic level used to make the estimate (Table 6). Averaged across trophic levels and scaled up to 1.2 km^2 of littoral zone in the 10-km reach downstream of the wastewater outfall, this represents a flux of 13.1 t (WM) of sewage-derived resources per day to macroinvertebrate primary consumers. At most (i.e., if enrichment of the food web is entirely via consumption of SDPOM), this flux can account for 4.7% of the daily discharge of SDPOM in summer.

Table 5. Biomass density (B, wet mass), daily production (P), and daily consumption (C) of consumers at reference (geometric mean of n = 9 for fish, n = 6 for invertebrates) and sewage-exposed (geometric mean of n = 3) sites in the St. Lawrence River.

		Reference sites				Sewage-exposed sites			
Trophic species	CE	B (mg·m^{-2})	P (mg·m^{-2}·day^{-1})	C (mg·m^{-2}·day^{-1})	C_{Pred}:P_{Prey}[a]	B (mg·m^{-2})	P (mg·m^{-2}·day^{-1})	C (mg·m^{-2}·day^{-1})	C_{Pred}:P_{Prey}
Piscivorous fish	0.15	345 (33–4490)	1.86 (0.32–17.2)	12.4 (2.16–115)	0.54	1850 (630–2630)	57.4 (43.5–92.4)	383 (314–616)	4.3
Invertivorous fish	0.10	1920 (199–13 000)	21.1 (3.36–68.4)	211 (33.6–469)	1.3	4640 (3250–6500)	83.4 (48.9–143)	834 (489–1420)	1.9
Macroinvertebrate carnivores	0.50	34.1 (3.7–153)	1.89 (0.23–6.31)	3.77 (0.45–12.6)	0.02	20.3 (14.0–29.4)	1.08 (0.79–1.62)	2.16 (1.58–3.25)	0.01
Algivorous–detritivorous fish	0.05	52.9 (10–402)	1.85 (0.21–9.69)	37.1 (4.27–194)		370 (180–644)	5.67 (1.64–13.9)	113 (32.9–279)	
Macroinvertebrate primary consumers	0.15	2320 (888–5900)	159 (76–237)	1060 (938–1580)		3870 (3130–4810)	443 (318–583)	2960 (2120–3890)	

Note: The range of values observed among sites (across a wide range of vegetative cover) is shown in parentheses. Consumption was estimated by assuming the indicated conversion efficiency (CE) for each predator's resource ($C_{Pred} = P_{Pred}$/CE).

[a] Piscivores consume both invertivorous and algivorous–detritivorous fish, invertivorous fish consume both macroinvertebrate carnivores and primary consumers.

Table 6. Consumption of sewage-derived basal resources by primary consumers at three sewage-exposed sites in the St. Lawrence River.

	Areal consumption (g WM·m^{-2}·day^{-1})		
SVC	Piscivory	Invertivory	Primary consumption
0.15	19.0±8.10	8.48±2.97	2.35±0.41
0.30	37.8±16.1	4.24±1.49	2.83±0.49
0.60	9.61±4.09	1.06±0.37	0.82±0.14
Total (t·day^{-1})[a]	29.4±12.5	7.17±2.51	2.79±0.48

Note: Consumption was back-calculated from the observed increase in secondary production of three trophic groups relative to reference sites of similar submerged vegetative cover (SVC). Estimates are shown for production based on piscivory (fish), invertivory (fish and carnivorous macroinvertebrates), and primary consumption (algivorous–detritivorous fish and noncarnivorous macroinvertebrates). WM, wet mass.

[a] Total flux over 10-km study reach, weighted by spatial distribution of vegetative cover; mean is 13.1 t·day^{-1}, equivalent to 4.7% of the total daily discharge of SDPOM.

The mean C:N of all measured resources is 7 (by mass). Assuming that carbon represents 50% of dry mass and given a mean N:P of 13.6 by mass for freshwater autotrophs (Elser et al. 2000), these resources contain approximately 7% nitrogen and 0.5% phosphorus. A primary consumption flux of 13.1 t·day^{-1} (WM) over our study reach thus represents an uptake of 13.1 kg of P and 184 kg of N per day. This flux accounts for only 1.1% of the total daily discharge of total phosphorus and 0.87% of the total daily discharge of total nitrogen in summer.

Spatial autocorrelation

Moran's I indicated a significant spatial autocorrelation in vegetative cover among all sites for the 20- to 30-km distance category only ($I = 0.47$, $p = 0.007$). There was no spatial autocorrelation at shorter or longer distances and no apparent downstream trend in vegetative cover ($r^2 = 0.06$, $F_{[1,10]} = 0.60$, $p = 0.46$). We found no significant spatial autocorrelation at any scale among reference sites in epiphyte or invertebrate stable isotope signatures, daily invertebrate production, annual fish production, or daily fish production, with the single exception of daily piscivore production in the 0- to 10-km distance category ($I = 0.62$, $p = 0.005$).

Discussion

Spatial extent and pathways of sewage enrichment

Stable isotope analysis enabled us to identify three sites that were consistently exposed to Montreal's sewage plume, where previous studies have had to rely on instantaneous measurements of exposure. δ^{13}C is the isotopic ratio most commonly used in dietary studies, but we found stronger (almost 8‰) and more consistent effects of sewage exposure on δ^{15}N of macroinvertebrate primary consumers (see also deBruyn and Rasmussen 2002). Also, δ^{13}C showed wide variation among reference sites, whereas δ^{15}N did not. This was partly due to differences in water chemistry among sites (the dissolved inorganic carbon (DIC) pool of Great Lakes water is about 10‰ enriched in ^{13}C over other large rivers like the Ottawa (Yang et al. 1996; Leggett et al. 1999)) but may also reflect local flow regimes: low current can reduce photosynthetic discrimination against ^{13}C by permitting the formation of a CO_2-depleted boundary layer at the surface of algal cells (Finlay et al. 1999). Algal δ^{15}N is influenced by human population density (Cabana and Rasmussen 1996) but varies little with local flow regime (MacLeod and Barton 1998).

Stable isotope ratios of primary consumers at the reference sites indicated that the dominant taxa were feeding primarily on local epiphytic production throughout this reach. The inferred diet of these consumers was too heavy in both isotopes to include much POM from either water mass, but it was nearly identical to the measured isotopic signature of epiphytes. Epiphytes at our reference sites were, on average, 7.2‰ enriched in ^{13}C over the mean of Great Lakes and Ottawa River seston. Attached primary producers are typically enriched about 7‰ in ^{13}C over pelagic producers (Hecky and Hesslein 1995; Vander Zanden and Rasmussen 1999).

We were unable to quantify the diet composition of primary consumers at the sewage-exposed sites because we could not physically separate SDPOM from autochthonous production in the epiphytic film (possibly because of residual coagulant in the effluent). It appears, however, that there was an important contribution of SDPOM to the observed increase in secondary production, especially at the relatively bare sites. The observed shift in δ^{15}N of macroinvertebrate primary consumers was greatest at the least-vegetated site (15% VC), where epiphytic production is probably least. This suggests that the isotopic shift was primarily due to consumption of SDPOM, rather than a shift in the δ^{15}N of epiphytic producers. The observed shift in δ^{15}N of the entire epiphytic film at sewage-exposed sites was likely due to attached SDPOM. Macroinvertebrate primary consumers showed a much smaller shift in δ^{15}N at the most vegetated site, despite a similar concentration of effluent, and thus similar levels of sewage-derived dissolved nitrogen, at all three exposed sites. This is consistent with a smaller relative contribution of the isotopically light SDPOM at a site with abundant epiphytic producers. The importance of SDPOM is also supported by the observation that algivorous minnows dominated fish primary consumers at reference sites, whereas detritivorous suckers dominated production at sewage-exposed sites.

Secondary production and sewage enrichment

Secondary production and $P{:}B$ estimates at our reference sites were similar to values reported from other systems. Our estimates of total annual fish production at reference sites (0.25–13.6 g WM·m^{-2}·year^{-1}) are similar to those measured in the Great Lakes connecting channels (5–25 g WM·m^{-2}·year^{-1}; Edwards et al. 1989). The lower estimates, from sites with low vegetative cover, are similar to values reported for lakes of similar nutrient concentrations (1.2 g WM·m^{-2}·year^{-1} at 25 μg·L^{-1} total phosphorus (TP); Downing et al. 1990). Downing et al. (1990) also report a mean annual fish community P/B of 0.76, similar to our mean P_{GIS}/B of 0.81.

Mean annual invertivorous fish production (P_{GIS}) at the reference sites was 3.7 g WM·m^{-2}·year^{-1}; assuming 10% conversion efficiency, this would require invertebrate production to be 37 g WM·m^{-2} ·year^{-1}. Back-calculating in a similar way from piscivorous fish production gives an invertebrate production estimate of 68 g WM·m^{-2}·year^{-1}. Previous work in the Great Lakes connecting channels (St. Mary's, St. Clair, Detroit, and upper St. Lawrence rivers; Edwards et al. 1989) reported macrozoobenthic production between 27 and 77 g WM·m^{-2}·year^{-1} (assuming AFDM is 20% of WM). Studies in warmer regions report comparable or higher annual macroinvertebrate production (65–400 g WM·m^{-2}·year^{-1} in a subtropical blackwater river (Benke et al. 1984) and 140 g WM·m^{-2}·year^{-1} on the Orinoco floodplain (Lewis et al. 2001), assuming C is 10% of WM). Biomass densities of invertebrates >0.5 mm at our reference sites ranged from about 1 g·m^{-2} on bare sediment to about 6 g·m^{-2} in dense weedbeds. Annual *P*/*B* estimates were therefore on the order of 5 to 15, similar to the 5 to 10 range reported by Benke et al. (1984) for univoltine insects and the mean annual *P*/*B* of 5.3 for 164 populations of lake invertebrates (Plante and Downing 1989).

Secondary production at the sewage-exposed sites was high relative to the mean at our reference sites and values reported for other unpolluted systems but not unreasonable given the high nutrient and SDPOM content of this sewage effluent. Our observation of a mean 5-fold increase in production with sewage exposure is only slightly higher than values reported in previous studies. Benthic invertebrate densities were 2- to 4-fold higher in a sewage-exposed reach of a Michigan stream (Ellis and Gowing 1957), and experimental additions of grain or soybean have produced 1.5- to 2.9-fold increases in total invertebrate biomass in midsized rivers (Mundie et al. 1983; Johnston et al. 1990). These studies only reported increases in standing stock of invertebrates; if growth rates also increase, the enhancement of secondary production may be much higher. King and Ball (1967) reported higher densities and faster growth of primary consumers downstream of a sewage outfall and could attribute less than 10% of secondary production to autochthonous production.

In fact, the methods that we used to estimate secondary production may have led us to underestimate the increase in production with sewage exposure. Our estimate of the specific rate of macroinvertebrate production (P_{MD}/B) could vary only with the taxonomic composition of the fauna (chironomids have very high growth rates) or with the mean body mass of individuals. We saw higher proportions of chironomids and higher biomass densities at sewage-exposed sites, but chironomids at sewage-exposed sites (mean of all sampled individuals = 0.32 mg WM) were actually larger than those at reference sites (0.20 mg WM), and thus the method used here would assign them lower specific growth rates. The methods that we used to estimate fish production were also poorly suited to detecting differences in growth rates. Previous work has reported increases in gut fullness, condition (Ellis and Gowing 1957), and growth rate (Katz and Howard 1955; Eggers et al. 1978; Johnston et al. 1990) of fishes in sewage-exposed streams. Unfortunately, we had to pool all 12 sites to estimate instantaneous growth rates (IGR), and this had the effect of averaging growth across sites. Thus, P_{IGR} only reflected differences among sites in total biomass and the distribution of that biomass among age classes. Growth increment summation (GIS) would only reveal differences in growth rate among sites if individuals returned to the same site each year. Otherwise, P_{GIS} would tend to underestimate any site-specific increase in growth rate, as overall faster growth would tend to reduce the observed increment between older (slower-growing) and younger (faster-growing) age classes. We found no effect of sewage exposure on the *P*/*B* relationship for any species using either production estimate. Either fish growth rates are independent of basal productivity or these species do not display interannual site fidelity. The observation that older piscivores (the biomass of which was mostly accrued in previous years) showed no shift in δ^{15}N at sewage-exposed sites tends to support the latter explanation.

It is also important to note that back calculations based on carnivorous trophic levels provide a minimum estimate of basal resource flux. In fact, this calculation estimates basal resource consumption as long as the fraction of invertebrate production that escapes predation is small (Strayer and Likens 1986). In addition, this calculation assumes a constant ratio of fish production to invertebrate production. The production ratio P_{fish}:$P_{\mathrm{invertebrates}}$ could vary because invertebrates in more densely vegetated sites may have more abundant resources and a greater fraction may escape predation. The observed relationship between invertebrate production and vegetative cover was positive despite this confounding factor, so ultimately this potential bias only strengthens our conclusions.

Trophic dynamics of sewage enrichment

We observed the greatest proportional increases in secondary production for piscivorous fish, and the ratio of daily piscivore consumption to prey fish production consequently increased from 0.54 at reference sites to 4.3 at sewage-exposed sites. This is not unreasonable, considering that this system is open and certainly not at steady state; piscivores may be depleting prey fish biomass or prey fish may be continually immigrating over the course of the summer. It is also possible that we have overestimated piscivore consumption (e.g., by underestimating conversion efficiency), but this would not explain the difference between reference and sewage-exposed sites. It is more likely that we underestimated prey fish production at the sewage-exposed sites (as discussed above).

The ratio of daily invertivore consumption to macroinvertebrate production also increased, from 1.3 at reference sites to 1.9 at sewage-exposed sites. Again, we likely underestimated macroinvertebrate production at the sewage-exposed sites, both for the methodological reasons discussed above and because we only sampled invertebrates >0.5 mm. Predator consumption at both reference and sewage-exposed sites may have included some prey smaller than this.

Vegetative cover and sewage enrichment

We found higher production of almost all trophic groups at the more-vegetated reference sites, irrespective of location along the river (i.e., no spatial autocorrelation). The apparent spatial autocorrelation in daily piscivore production may have been driven by the fact that the most densely vegetated sites, with highest piscivore production, were all in the relatively dense cluster of islands near Montreal. Macrophytes provide abundant surface area for attached algae and heterotrophic bacteria and increase the residence time of dissolved nutrients (i.e., produce "tight spirals" sensu Webster 1975). As well, these habitats support abundant grazers and their predators (Thorp and Delong 1994), so production can be effectively transferred to higher trophic levels. Macrophytes in littoral areas also enhance particle trapping (Vermaat et al. 2000), increasing nutrient concentrations in the sediment (Chambers and Prepas 1994).

It is striking, however, that we observed the reverse trend at sewage-exposed sites: production of some trophic groups decreased with vegetative cover, and the increase in production with sewage exposure was always least at the most-vegetated sites. This may reflect a shift across the gradient of vegetative cover in the relative availability of SDPOM and dissolved nutrients to biota. $\delta^{15}N$ evidence (discussed above) suggests that primary consumer production is based more heavily on SDPOM at the relatively bare sites. A greater effect of sewage exposure at bare sites therefore suggests that SDPOM represents a greater potential resource than sewage-derived nutrients. The concentration of SDPOM in the sewage effluent is about 15 times greater than that of seston in the upstream water, and the concentrations of total and dissolved nutrients are 20 times greater. At 3% effluent, then, concentrations of these resources are only elevated by 30–40% over background. A 5-fold increase in POM or nutrient concentrations (commensurate with a 5-fold increase in secondary production) would require 20–30% effluent, concentrations that we never observed even directly below the outfall. For 3% effluent to produce a 5-fold increase in suspended resource concentrations, the secondary production per unit SDPOM would have to be 10 times that for seston. Sewage-derived POM is certainly more labile than seston in the St. Lawrence (deBruyn and Rasmussen 2002). It is also possible that residual coagulant in the effluent enhances retention and makes SDPOM more available than upstream seston to benthic biota.

It is not surprising that sewage represents a resource subsidy to the food web of this river, but the magnitude of this subsidy is impressive. We observed a 5-fold increase in secondary production in our study reach and estimate that this was supported by only one or a few percent of the daily discharge of sewage nutrients and SDPOM. Previous work on sewage in rivers has tended to focus on nuisance blooms of algae or on systems so heavily enriched that hypoxia is a dominant environmental factor. The St. Lawrence River is able to accommodate Montreal's enormous discharge of SDPOM and dissolved nutrients, however, because it is protected from the negative effects of sewage exposure by hydrodynamic forces (rapid flushing, strong vertical mixing). In large river systems like this, which receive the majority of the world's sewage discharges, the importance of sewage as a resource may be substantial.

Acknowledgements

We thank Kelly W. Armstrong, Veronique Bussiers, Levi Cammack, Suresh Job, Jen Kövecses, Kristin Lunn, Andrea MacLeod, Keith Martin-Smith, Kevin McCann, Liz Moseman, Amy Nelson, Graham Peers, and Ciara Raudsepp-Hearne for help with field work. We also thank Patricia Chambers, Christiane Hudon, François Gagné, Jessica Meeuwig, Neil Price, Neil Rooney, and Yvonne Vadeboncoeur for discussions, advice, and logistical support. Pierre Purenne, Paul Leduc, and Yves Lafleur at the Montreal wastewater treatment plant were generous with their time and expertise. Financial support was provided by a Natural Sciences and Engineering Research Council (NSERC) operating grant to J.B. Rasmussen and a Vineberg Family Fellowship to A.M.H. deBruyn.

References

Adams, T.S., and Sterner, R.W. 2000. The effect of dietary nitrogen content on trophic level ^{15}N enrichment. Limnol. Oceanogr. **45**: 601–607.

Benke, A.C. 1996. Secondary production of macroinvertebrates. *In* Methods in stream ecology. *Edited by* F.R. Hauer and G.A. Lamberti. Academic Press, San Diego, Calif. pp. 557–578.

Benke, A.C., Van Arsdall, T.C., and Gillespie, D.M. 1984. Invertebrate productivity in a subtropical blackwater river: the importance of habitat and life history. Ecol. Monogr. **54**: 25–63.

Boulanger, F. 1984. Station d'épuration de la CUM. Répurcussions environmentales d'un déversement d'eaux usées prétraitées à l'émissaire de l'Ile-aux-Vaches. Montreal Urban Community, Water Treatment Service, Montreal, Quebec.

Cabana, G., and Rasmussen, J.B. 1996. Comparison of aquatic food chains using nitrogen isotopes. Proc. Natl Acad. Sci. U.S.A. **93**: 10 844 – 10 847.

Carignan, R., and Lorrain, S. 2000. Sediment dynamics in the fluvial lakes of the St. Lawrence River: accumulation rates and characterization of the mixed sediment layer. Can. J. Fish. Aquat. Sci. **57**(Suppl. 1): 63–77.

Chambers, P.A., and Prepas, E.E. 1994. Nutrient dynamics in riverbeds: the impact of sewage effluent and aquatic macrophytes. Water Res. **28**: 453–464.

deBruyn, A.M.H., and Rasmussen, J.B. 2002. Quantifying assimilation of sewage organic matter by riverine benthos. Ecol. Appl. **12**: 511–520.

Downing, J.A., Plante, C., and Lalonde, S. 1990. Fish production correlated with primary productivity, not the morphoedaphic index. Can. J. Fish. Aquat. Sci. **47**: 1929–1936.

Edwards, C.J., Hudson, P.L., Duffy, W.G., Nepszy, S.J., McNabb, C.D., Hass, R.C., Liston, C.R., Manny, B.A., and Busch, W.N. 1989. Hydrological, morphometrical, and biological characteristics of the connecting rivers of the International Great Lakes: a review. Can. Spec. Publ. Fish. Aquat. Sci. No. 106. pp. 240–254.

Eggers, D.M., Bartoo, N.W., Richard, N.A., Nelson, R.E., Wissmar, R.C., Burgner, R.L., and Devol, A.H. 1978. The Lake Washington ecosystem: the perspective from the fish community production and forage base. J. Fish. Res. Board Can. **35**: 1553–1571.

Ellis, R.J., and Gowing, H. 1957. Relationship between food supply and condition of wild brown trout, *Salmo trutta* Linnaeus, in a Michigan Stream. Limnol. Oceanogr. **2**: 299–308.

Elser, J.J., Fagan, W.F., Denno, R.F., Dobberfuhl, D.R., Folarin, A., Huberty, A., Interlandi, S., Kilham, S.S., McCauley, E., Schulz, K.L., Siemann, E.H., and Sterner, R.W. 2000. Nutritional constraints in terrestrial and freshwater food webs. Nature (Lond.), **408**: 578–580.

Finlay, J.C., Power, M.E., and Cabana, G. 1999. Effects of water velocity on algal carbon isotope ratios: implications for river food web studies. Limnol. Oceanogr. **44**: 1198–1203.

Hecky, R.E., and Hesslein, R.H. 1995. Contributions of benthic algae to lake food webs as revealed by stable isotope analysis. J. N. Am. Benthol. Sci. **14**: 631–653.

Hudon, C., and Sylvestre, A. 1998. Qualité de l'eau en aval de l'archipel de Montréal — 1994–1996. Environment Canada – Quebec Region, Environmental Conservation, St. Lawrence Center, Montreal, Quebec.

Johnston, N.T., Perrin, C.J., Slaney, P.A., and Ward, B.R. 1990. Increased juvenile salmonid growth by whole-river fertilization. Can. J. Fish. Aquat. Sci. **47**: 862–872.

Katz, M., and Howard, W.C. 1955. The length and growth of 0-year class creek chubs in relation to domestic pollution. Trans. Am. Fish. Soc. **84**: 228–238.

King, D.L., and Ball, R.C. 1967. Comparative energetics of a polluted stream. Limnol. Oceanogr. **12**: 27–33.

Legendre, P., and Legendre, L. 1998. Numerical ecology. Elsevier, Amsterdam.

Leggett, M.F., Servos, M.R., Hesslein, R., Johannsson, O., Millard, E.S., and Dixon, D.G. 1999. Biogeochemical influences on the carbon isotope signatures of Lake Ontario biota. Can. J. Fish. Aquat. Sci. **56**: 2211–2218.

Lewis, W.M., Hamilton, S.K., Rodriguez, M.A., Saunders, J.F., and Lasi, M.A. 2001. Food web analysis of the Orinoco floodplain based on production estimates and stable isotope data. J. N. Am. Benthol. Soc. **20**: 241–254.

MacLeod, N.A., and Barton, D.R. 1998. Effects of light intensity, water velocity, and species composition on carbon and nitrogen stable isotope ratios in periphyton. Can. J. Fish. Aquat. Sci. **55**: 1919–1925.

Meybeck, M., and Helmer, R. 1989. The quality of rivers: from pristine stage to global pollution. Paleogeogr. Paleoclimatol. Paleoecol. (Global and Planetary Change Section), **75**: 283–309.

Morin, A., and Dumont, P. 1994. A simple model to estimate growth rate of lotic insect larvae and its value for estimating population and community production. J. N. Am. Benthol. Sci. **13**: 357–367.

Mundie, J.H., McKinnell, S.M., and Traber, R.E. 1983. Responses of stream zoobenthos to enrichment of gravel substrates with cereal grain and soybean. Can. J. Fish. Aquat. Sci. **40**: 1702–1712.

Ney, J.J. 1990. Trophic economics in fisheries — assessment of demand–supply relationships between predators and prey. Rev. Aquat. Sci. **2**: 55–81.

Pazzia, I., Trudel, M., Ridgway, M., and Rasmussen, J.B. 2002. Influence of food web structure on the growth and bioenergetics of lake trout (*Salvelinus namaycush*). Can. J. Fish. Aquat. Sci. **59**: 1593–1605.

Pham, T-T., Proulx, S., Brochu, C., and Moore, S. 1999. Composition of PCBs and PAHs in the Montreal Urban Community wastewater and in the surface water of the St. Lawrence river (Canada). Water Air Soil Pollut. **111**: 251–270.

Plante, C., and Downing, J.A. 1989. Production of freshwater invertebrate populations in lakes. Can. J. Fish. Aquat. Sci. **46**: 1489–1498.

Purenne, P. 2001. Annual report 2000. Process Engineering Division, Wastewater Treatment Plant, Montreal Urban Community, Quebec.

Rigler, F.H., and Downing, J.A. 1984. The calculation of secondary productivity. *In* A manual on methods for the assessment of secondary productivity in fresh waters. *Edited by* J.A. Downing and F.H. Rigler. Blackwell Scientific, Oxford, U.K. pp. 19–58.

St. Lawrence Centre. 1996. State of the Environment Report on the St. Lawrence River. Vol. 1. The St. Lawrence Ecosystem. Environment Canada – Quebec Region, Environmental Conservation, and Éditions MultiMondes, Montreal, Quebec.

Strayer, D., and Likens, G.E. 1986. An energy budget for the zoobenthos of Mirror Lake, New Hampshire. Ecology, **67**: 303–313.

Thorp, J.H., and Delong, M.D. 1994. The riverine productivity model: an heuristic view of carbon sources and organic processing in large river ecosystems. Oikos, **70**: 305–308.

Thorp, J.H., and Delong, M.D. 2002. Dominance of autochthonous autotrophic carbon in food webs of heterotrophic rivers. Oikos, **96**: 543–550.

Trudel M., Tremblay, A., Schetagne, R., and Rasmussen, J.B. 2001. Why are dwarf fish so small? An energetic analysis of polymorphism in lake whitefish (*Coregonus clupeaformis*). Can. J. Fish. Aquat. Sci. **58**: 394–405.

Vander Zanden, M.J., and Rasmussen, J.B. 1999. Primary consumer $\delta^{13}C$ and $\delta^{15}N$ and the trophic position of aquatic consumers. Ecology, **80**: 1395–1404.

Vannote, R.L., Minshall, G.W., Cummins, K.W., Sedell, J.R., and Cushing, C.E. 1980. The river continuum concept. Can. J. Fish. Aquat. Sci. **37**: 130–137.

Vermaat, J.E., Santamaria, L., and Roos, P.J. 2000. Water flow across and sediment trapping in submerged macrophyte beds of contrasting growth form. Arch. Hydrobiol. **148**: 549–562.

Webster, J.R. 1975. Analysis of potassium and calcium dynamics in stream ecosystems on three Southern Appalachian watersheds of contrasting vegetation. Ph.D. dissertation, University of Georgia, Athens, Georgia.

Yang, C., Telmer, K., and Veizer, J. 1996. Chemical dynamics of the "St. Lawrence" riverine system: delta D-H2O, delta O-18(H_2O), delta C-13(DIC), delta S-34(sulfate), and dissolved Sr-87/Sr-86. Geochim. Cosmochim. Acta, **60**: 851–866.

Sexual size dimorphism of walleye (*Stizostedion vitreum vitreum*)

Bryan A. Henderson, Nicholas Collins, George E. Morgan, and Andre Vaillancourt

Abstract: Sexual size dimorphism of walleye (*Stizostedion vitreum vitreum*) is achieved by females having higher growth rates than males before and after maturation, resulting in females with greater asymptotic sizes. Mercury (Hg) concentrations in epaxial muscle by age and weight for 31 populations of walleye were used to evaluate the relative importance of differences in consumption and activity in generating sexual size dimorphism. Growth efficiency by sex, age, and maturity is estimated by a ratio of annual increments in weight (g) to annual increments of Hg (mg), using the pooled changes in weight and Hg loadings of males and females from all lakes. The higher growth rates of females arise from greater consumption and higher growth efficiency. Growth efficiency of both sexes is similar before maturity, but the growth efficiency of mature males is substantially lower than that of either immature males or mature females. We propose that the inferior growth efficiency of males is a function of the greater activity of males, particularly during the spawning season when scramble competition for fertilization is likely to produce substantial increases in male fitness as a result of increased efforts to find and spawn with females.

Résumé : Le dimorphisme sexuel de la taille chez le doré jaune (*Stizostedion vitreum vitreum*) résulte des taux de croissance plus élevés chez les femelles que chez les mâles avant et après la maturation; les femelles atteignent donc une taille asymptotique plus élevée. Les concentrations de mercure (Hg) dans le muscle épaxial en fonction de l'âge et de la masse chez 31 populations de dorés nous ont servi à évaluer l'importance relative des différences de consommation et d'activité dans l'élaboration du dimorphisme sexuel de la taille. L'efficacité de la croissance en fonction du sexe, de l'âge et de la maturité a été estimée par le rapport de l'accroissement annuel de masse (g) sur l'accroissement annuel de Hg (mg) en utilisant l'ensemble des changements de masse et d'accumulation de Hg des mâles et des femelles de tous les lacs. Les taux de croissance plus élevés des femelles résultent d'une consommation plus grande et d'une meilleure efficacité de la croissance. L'efficacité de la croissance est semblable chez les deux sexes avant la maturité, mais l'efficacité de la croissance des mâles matures est considérablement plus faible que celle des mâles immatures et des femelles matures. Nous croyons que l'efficacité de la croissance plus faible des mâles est reliée à leur plus grande activité, particulièrement durant la période de fraye, lorsque dans la compétition d'exploitation lors de la fertilisation, leurs efforts accrus pour trouver des femelles et frayer avec elles sont susceptibles d'accroître considérablement leur fitness.

[Traduit par la Rédaction]

Introduction

Darwin (1871) first suggested that sexual selection, differences in reproductive roles, and independent adaptations to the environment explained sexual size dimorphism (SSD). This hypothesis allows that SSD could be driven by primary selection for size attributes or, alternatively, by selection for sex-specific behaviours that secondarily affect growth. The rarity of behavioural and energy budgets and the ubiquity of body size data have led researchers to treat size attributes as the primary objects of selection. In mammalian (Ruckstuhl and Neuhaus 2002) and avian SSD (Shaffer et al. 2001), males are usually, but not always, larger than females, presumably as a result of the selection of larger males by females. In reptiles (Bonnet et al. 2000; Butler et al. 2000) and fish (Henderson and Nepzsy 1994; Quinn et al. 2001), there seems to be more variation in the bias of SSD. The degree of SSD is associated with variations in mating systems (Henson and Warner 1997; Dunn et al. 2001) and availability of prey (Madsen and Shine 1993). Female-biased SSD is often attributed to natural selection for large size and fecundity in species with indeterminate growth (Legrand and

Received 11 October 2002. Accepted 7 June 2003. Published on the NRC Research Press Web site at http://cjfas.nrc.ca on 21 November 2003.
J17141

B.A. Henderson[1] and N. Collins. University of Toronto at Mississauga, Biology Department, 3359 Mississauga Road North, Mississauga, ON L5L 1C6, Canada.
G.E. Morgan. Co-operative Freshwater Ecology Unit, Department of Biology, Laurentian University, Sudbury, ON P3E 2C6, Canada.
A. Vaillancourt. Ontario Ministry of the Environment, Biomonitoring Section, 125 Resources Road, Etobicoke, ON M9P 3V6, Canada.

[1] Corresponding author (e-mail: bryan.henderson@mnr.gov.on.ca).

doi: 10.1139/F03-115

Morse 2000). Small males could result from sexual selection or scramble competition favouring males with increased speed and agility (Sandercock 2001). Among freshwater fish species, SSD occurs most obviously in Centrarchidae, Percidae, and Esocidae families. In fish, males are larger than females (Quinn et al. 2001) if sperm competition and combat between males are the most important factors affecting reproductive success (Parker 1992). Males are often much smaller than females (Parker 1992), particularly when scramble competition is present (Roff 1992). In extreme cases, high adult mortality and weak male–male competition can result in populations with dwarf males. Roff (1983) proposed that males are smaller than females because the males eat less to avoid predation. The consequences of SSD can be resource partitioning by sex (Butler et al. 2000; McDonald 2002), increased mortality (Henderson and Nepszy 1994), and differences in activity of males and females (Ruckstuhl and Neuhaus 2002). Often the consequences of SSD are taken as explanations for SSD. Sexual differences in diet could reduce competition between males and females, but it is more likely a consequence of SSD rather than a cause.

Female yellow perch (*Perca flavescens*; Henderson et al. 2000) and walleye (*Stizostedion vitreum vitreum*) reach larger asymptotic sizes and mature at a larger size and older age than males (Lester et al. 2000). A general model of growth in walleye assumes that early growth of males and females is the same until maturation, when energy is allocated more to reproduction than somatic growth (Lester et al. 2000). Thus, because males mature earlier than females, males do not achieve the larger sizes of females. By inference, gross growth efficiency should be similar for males and females before maturation and then decrease markedly as maturation occurs, corresponding to the increased allocation of energy to reproduction. A reduction of growth efficiency in females can be easily explained by the allocation of energy to ovarian growth because the ovary accounts for 15% of the total weight of the females before spawning (Henderson et al. 1996). In contrast, males only allocate about 4% of their mass to the testes, so their reduction in growth cannot be easily explained by diversion of energy for testes development. We hypothesize that the bulk of the males' energy is consumed by elevated activity during spawning, leading to a decrease in energy conversion efficiency that is more marked than in females. The walleye spawning period can last for up to a month, and males seem to remain on the spawning shoals for the duration (Colby et al. 1979). Activity costs of mating in females are likely low because the females come in briefly to deposit eggs and then disperse. If a male's reproductive potential is determined more by the number of matings rather than by the amount of tissue allocated to the testes, then there may be strong selection for males with very high activity during the scramble for matings on the spawning grounds.

In this study of walleye, we argue that SSD may be driven by selection for high levels of mating activity that reduce the growth potential of males. The SSD of male walleye is likely a secondary result of the cost of reproductive behaviour rather than a genetically based difference in growth potential. Thus, the small size of males is a function of sexual behaviour, but the large size of females is a product of natural selection for fecundity. We predict that the growth efficiencies of mature males are lower than those for females, and activity costs of males are higher.

Methods

Walleye were sampled in the autumn from 31 inland lakes in Ontario in 1998–1999 using Ontario's fall walleye index netting standard (Morgan 2002). Multimesh monofilament gillnets were set on the lake bottom overnight at randomly selected locations stratified into two depth zones (2–5 m and 5–15 m). Gangs ($N = 5$–12 per lake) were set perpendicular to shore with the inshore end alternating daily between small and large meshes. Each gang of gillnets was comprised of eight sequential panels (7.6 m long × 1.8 m deep) with mesh sizes of 25, 38, 51, 64, 76, 102, 127, and 152 mm stretched measure. Fork length (FL, mm), round weight (RW, g, total wet weight), sex, maturity, and age from otoliths (Christensen 1964) were recorded for all walleye. In the analyses, it was assumed that most of the yearly growth had occurred by the autumn, so that in terms of growing seasons, the age equaled the number of annuli plus one.

Total mercury concentrations ($[\mathrm{Hg}]_{\mathrm{total}}$, $\mathrm{mg \cdot kg^{-1}}$ wet mass) were assayed from a 100-g fillet of epaxial muscle from a maximum of 20 walleye per lake, stratified by size, and estimated by atomic absorption spectrophotometry (Uthe et al. 1970). $[\mathrm{Hg}]_{\mathrm{total}}$ was also obtained for yellow perch and lake herring (*Coregonus artedii*). Mercury in fish muscle is mainly methyl mercury (MeHg), which is the form of Hg absorbed from the diet (Scheuhammer and Graham 1999). $[\mathrm{Hg}]_{\mathrm{total}}$ is therefore a good approximation of dietary MeHg accumulation. Bioaccumulations of Hg were described by a $\log_e$–$\log_e$ linear regression of $[\mathrm{Hg}]_{\mathrm{total}}$ on age. The total body concentration of Hg was corrected for the proportion of muscle mass, where most of the Hg is located (Harris and Bodaly 1998). The proportion of muscle mass was estimated from an analysis of body composition of Lake Erie walleye (Henderson et al. 1996), assuming all body proteins reside in the muscle. The curvilinear relationship between muscle mass and round weight was determined for each sex. All information was pooled across the 31 lakes because there was insufficient information on $[\mathrm{Hg}]_{\mathrm{total}}$ by lake.

Growth of immature walleye was estimated from a linear regression of FL on age by sex of immature walleye; in contrast, mature growth was described by a nonlinear fit of FL on age by sex of mature walleye, providing estimates of the von Bertalanffy parameters of k and t_0. Asymptotic sizes were estimated as the average FL from the 20 largest mature males and females. Maturity was assessed by a visual inspection of the gonads, using criteria of size and colour to distinguish immature from mature walleye (Duffy et al. 2000). There was a clear dimorphism of gonadal somatic indices (gonad weight$\cdot$RW^{-1}) between mature and immature walleye. RW was estimated from FL by linear regression (natural logarithm transformation of RW and FL). Mercury concentrations were estimated by a regression of $\log_e([\mathrm{Hg}]_{\mathrm{total}})$ on $\log_e$(age) by sex and maturity. Gross growth efficiency was estimated as the annual increment in RW divided by the increment in weight of prey consumed and was calculated separately for mature and immature males and females. Mercury concentrations in the prey were estimated from the relation between Hg concentration in their main prey and prey

Fig. 1. Mercury concentration of epaxial muscle (mg·kg^{-1}) in relation to round weight for male (●, dotted line) and female (○, solid line) walleye (*Stizostedion vitreum vitreum*) sampled from 31 inland lakes in Ontario (1998–1999).

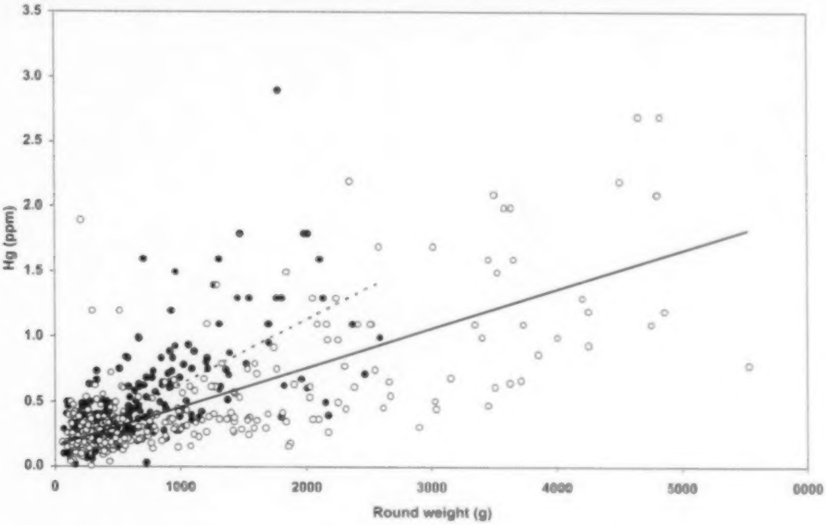

Fig. 2. Mercury concentrations of epaxial muscle (mg·kg^{-1}) in relation to age for male (●, dotted line) and female (○, solid line) walleye (*Stizostedion vitreum vitreum*) sampled from 31 inland lakes in Ontario (1998–1999).

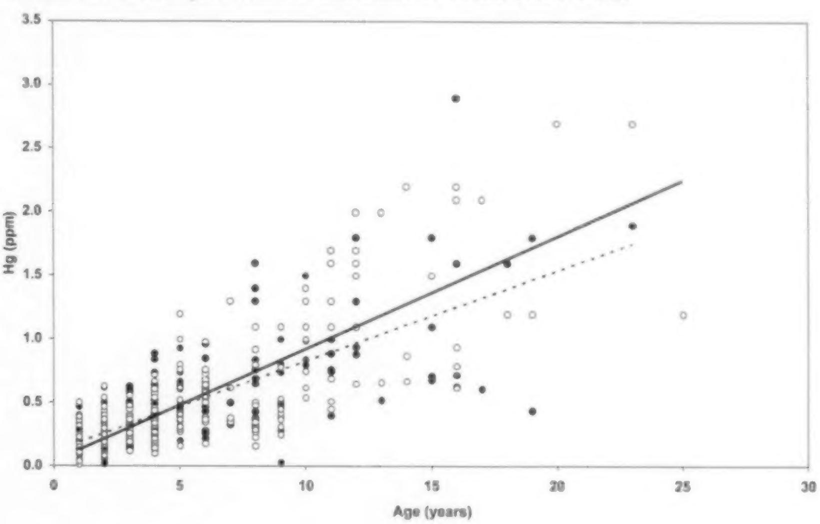

weights, assuming that the ratio of prey to predator length was 0.2 (Pierce et al. 2001). The annual weight of prey consumed was estimated as the increment in Hg of the walleye divided by the $[\mathrm{Hg}]_{\mathrm{total}}$ in prey. Increments in annual weight are adjusted for the allocation to ovaries (15%) and testes (4%) (Henderson et al. 1996) and the higher energy content of ovaries compared with somatic tissue (Henderson and Nepszy 1994).

Results

Males had significantly greater $[\mathrm{Hg}]_{\mathrm{total}}$ than females of the same weight (analysis of covariance (ANCOVA), df = 567, $P < 0.001$, Fig. 1; female $[\mathrm{Hg}]_{\mathrm{total}} = 0.128 + 0.00032\mathrm{RW}$, $r^2 = 0.60$, $N = 297$; male $[\mathrm{Hg}]_{\mathrm{total}} = 0.138 + 0.0005\mathrm{RW}$, $r^2 = 0.49$, $N = 270$). There was no significant difference in $[\mathrm{Hg}]_{\mathrm{total}}$ between males and females of the same age (ANCOVA, df = 1683, $P = 0.73$ (Fig. 2); female $[\mathrm{Hg}]_{\mathrm{total}} = 0.079\mathrm{age}^{0.933}$, $r^2 = 0.58$, $N = 297$; male $[\mathrm{Hg}]_{\mathrm{total}} = 0.088\mathrm{age}^{0.869}$, $r^2 = 0.46$, $N = 270$). Annual increments in Hg were determined separately for immature and mature walleye of each sex (mature male $[\mathrm{Hg}]_{\mathrm{total}} = 0.096\mathrm{age}^{0.8218}$, $N = 253$, $P < 0.001$; immature male $[\mathrm{Hg}]_{\mathrm{total}} = 0.112\mathrm{age}^{0.5911}$, $N = 83$, $P < 0.001$; mature female $[\mathrm{Hg}]_{\mathrm{total}} = 0.0819\mathrm{age}^{0.8967}$, $N = 130$, $P < 0.001$; immature female $[\mathrm{Hg}]_{\mathrm{total}} = 0.1047\mathrm{age}^{0.6781}$, $N = 214$, $P < 0.001$). The $[\mathrm{Hg}]_{\mathrm{total}}$ of the two main prey species was used to estimate

Fig. 3. (*a*) Fork length (mm) of mature (▲) and immature male (●) walleye (*Stizostedion vitreum vitreum*) for which there were at least five walleye by age and maturity. The fitted lines are derived from the equations described in the results. (*b*) Fork length (mm) of mature (□) and immature (○) female walleye (*Stizostedion vitreum vitreum*) for which there was at least five walleye by age and maturity. The fitted lines are derived from the equations described in the results.

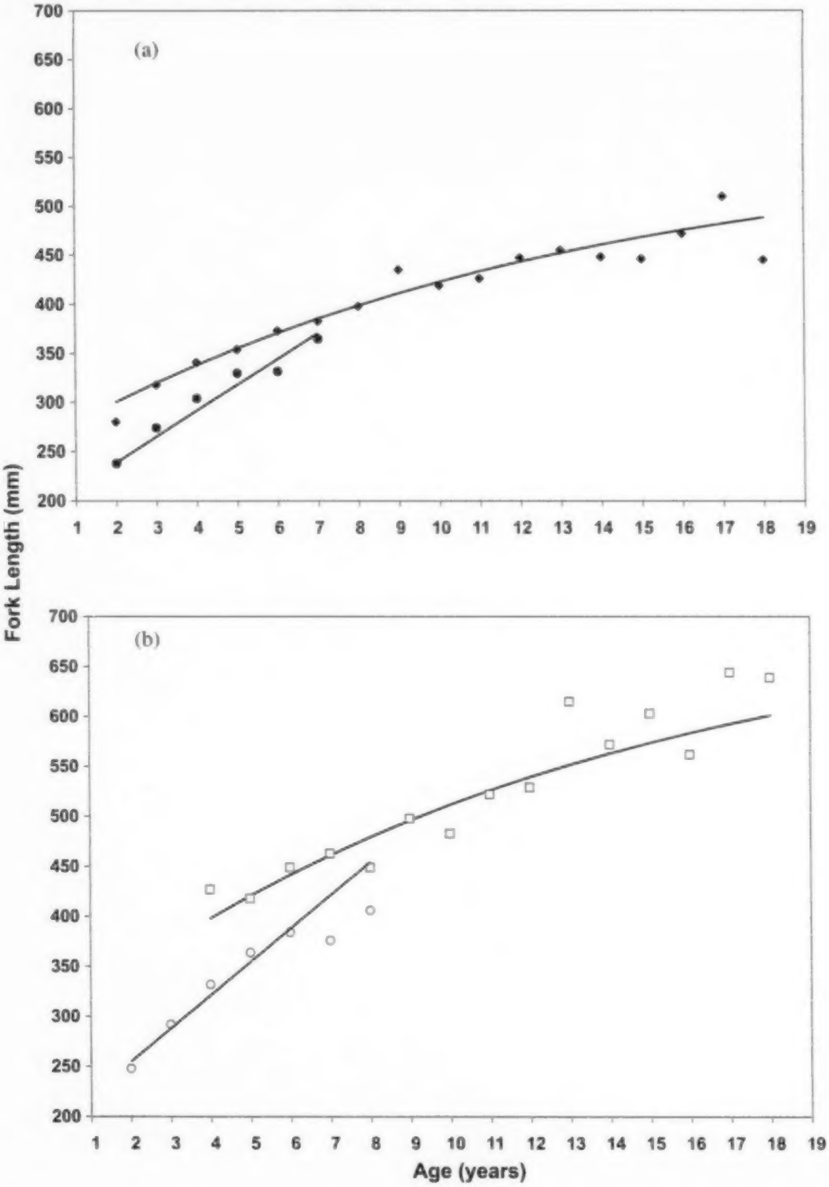

consumption (yellow perch $[Hg]_{total} = 0.0007RW + 0.0725$, $r^2 = 0.21$, $N = 124$; lake herring $[Hg]_{total} = 0.0004RW + 0.1205$, $r^2 = 0.20$, $N = 475$).

Total body Hg concentrations are about 67% of Hg concentrations in epaxial muscle (Harris and Bodaly 1998). We used the proportion of muscle (P_{mass} = protein) by RW to estimate total body burdens of Hg (male $P_{mass} = 1.125RW^{0.941}$, $N = 150$, $r^2 = 0.98$; female $P_{mass} = 0.821\ RW^{0.983}$, $N = 208$, $r^2 = 0.99$; Henderson et al. 1996). We assumed that all Hg is mainly located in the muscle. Males contained proportionally more protein (muscle) than females.

The growth of immature walleye is linearly related to age, but mature growth is curvilinearly related to age (Fig. 3). The average FL of the 20 largest males (564 ± 4.7) and females (708 ± 6.3) was used as an estimate of asymptotic size. Using these asymptotic sizes, von Bertalanffy parameters were estimated for mature males and females less than 21 years old (male $k = 0.076$, $t_0 = -6.84$, $r^2 = 0.67$, $N = 614$;

Fig. 4. Growth efficiency of immature and mature male (●) and female (○) walleye (*Stizostedion vitreum vitreum*) sampled from 31 inland lakes in Ontario (1998–1999). Growth efficiency was estimated by dividing the annual increment in round weight by the total weight of prey eaten, determined from Hg concentrations in walleye and their prey.

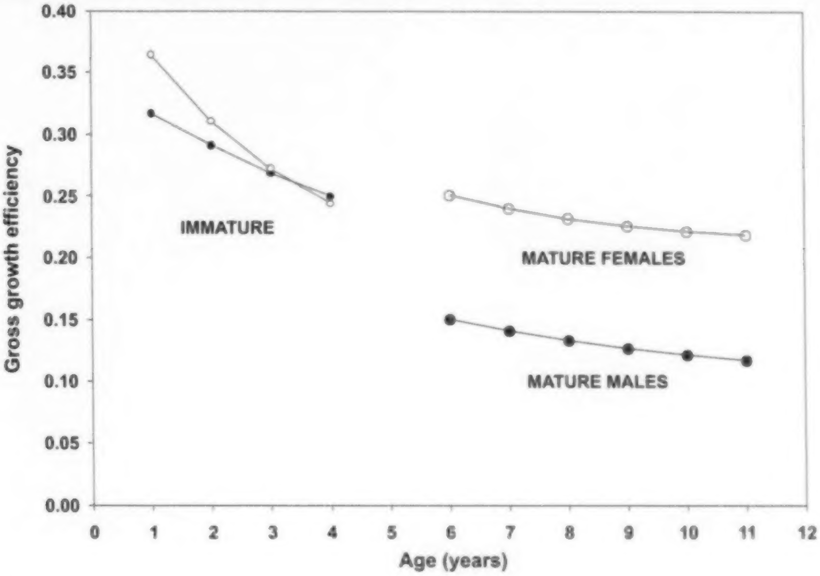

Fig. 5. Rations (g·g^{-1}·day^{-1}) of immature and mature male (●) and female (○) walleye (*Stizostedion vitreum vitreum*) sampled from 31 inland lakes in Ontario (1998–1999).

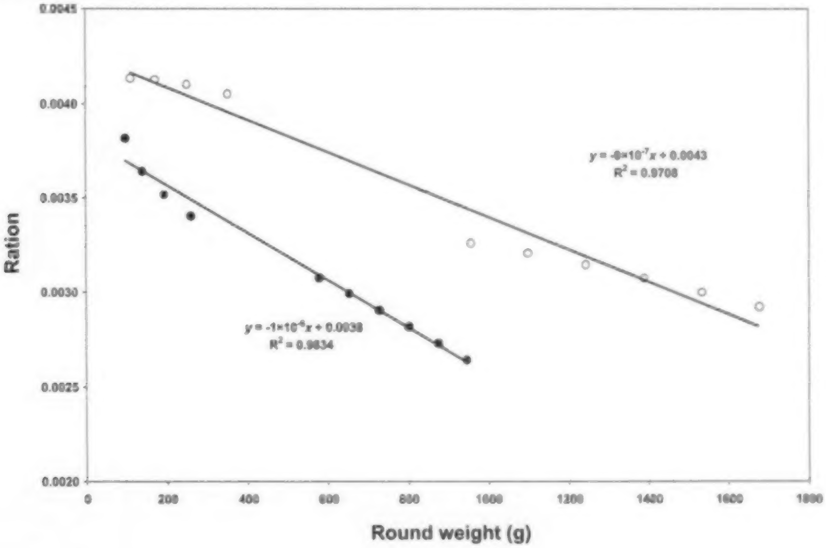

female $k = 0.078$, $t_0 = -7.75$, $r^2 = 0.78$, $N = 1861$). Immature growth for males and females was estimated from regressions of FL on age (immature male FL = 186.8 + 26.4age, $N = 1014$, $r^2 = 0.49$, $P < 0.001$; immature female FL = 188.3 + 33.3age, $N = 1780$, $r^2 = 0.55$, $P < 0.001$). Weight at age of mature and immature walleye of each sex was estimated from FL (mature male RW = 4.15208×10^{-6} FL$^{3.169}$, $N = 1486$; immature male RW = 4.751×10^{-6} FL$^{3.138}$, $N = 901$; mature female RW = 3.328×10^{-6} FL$^{3.208}$, $N = 459$; immature female RW = 4.728×10^{-6} FL$^{3.139}$, $N = 901$). Growth efficiency declined with increasing age in both males and females (Fig. 4). Growth efficiencies were similar for immature males and females but markedly lower for mature males than for mature females (Fig. 4). Rations (g·g^{-1}·day^{-1}) were greater for females than for males (Fig. 5).

Data in the present study were compiled from 31 inland lakes in northeastern Ontario so that the background Hg levels were likely similar. There was considerable variation in

$[\mathrm{Hg}]_{\mathrm{total}}$ with age, fork length, and sex, but importantly, there were internal consistencies in the relationships of $[\mathrm{Hg}]_{\mathrm{total}}$ by size and age for males and females. Males accumulate Hg faster than females of similar size, but at about the same annual rate as females. This was expected because it takes more time for males to reach a comparable size (Henderson et al. 1996), and therefore more Hg would be consumed. The estimate of prey consumption is very sensitive to estimates of $[\mathrm{Hg}]_{\mathrm{total}}$ in the prey. In this study, this would only be qualitatively important if males consumed prey with different $[\mathrm{Hg}]_{\mathrm{total}}$. Males and females eat similar prey, but at older ages, females will probably eat larger prey. The small change in $[\mathrm{Hg}]_{\mathrm{total}}$ of both yellow perch and lake herring with size was accounted for in the analysis but had little effect on the estimates of consumption. We distinguished between immature and mature walleye; some of the immature fish could have spawned before, and similarly, some mature fish could be maturing for the first time. The main consequence of this would be to decrease the difference between mature male and female growth efficiencies. Thus, the effect of these variations and errors would be to obscure any differences in growth efficiencies.

Discussion

Sexual size dimorphism is usually explained as a consequence of interplay of sexual selection (Legrand and Morse 2000) and natural selection (Szekely et al. 2000). Which sex is larger depends largely on mating systems (Henson and Warner 1997). Larger males have evolved when mating success depends on male–male conflict, sperm competition (Parker 1992), and parental care by males (Henson and Warner 1997). When large male size is not necessary to secure matings or to guard young, male size is usually smaller than that of females. This size reduction may be driven by selection to reduce risks associated with foraging (Lankford et al. 2001) and by circumstances that select directly for small size and agility (Sandercock 2001). Because small male size does not usually limit the supply of sperm, male rewards for larger size are less likely to offset the fitness costs of foraging than is the case for females. Direct selection for small size or agility of males in some mating systems (Bisazza and Pilastro 1997; Pilastro 1997) could reinforce selection for reduced foraging risk and generate even smaller male size. An alternative is that small male size is a secondary effect of selection for high levels of male activity that consequently reduce growth rates. Such activity might result in increased male fecundity in scramble competition for fertilizations. This explanation is seldom considered because it requires estimates of both consumption rates and activity costs in the field, which are rare, especially for taxa that do not build nests or defend their young. Our study represents an unusual opportunity to evaluate this alternative for males. Large females will have greater fitness, if fitness and fecundity are correlated.

In contrast with males, even in scramble mating systems, large females are likely to have greater fitness than small ones because fecundity is often proportional to body size. Natural selection would, therefore, favour larger females, and sexual selection of large females by males would enhance the evolution of large females. It is somewhat surprising that scale of SSD can be as great as it is considering the effect of genetic covariance of traits (Fairbairn 1997). Selection for large females could also result in the evolution of larger males. The alternative hypothesis that SSD evolved as an adaptation to different ecological niches (Shine 1989) would seem to be more an effect of SSD rather than a cause of SSD. However, differences in SSD could be increased if the smaller sex cannot utilize the range of prey sizes available to the larger sex (Shine et al. 1998) or was less effective in competition for resources (Oddie 2000).

There are several studies explaining the decline in growth with age as a function of the differential allocation of energy to reproduction rather than growth (Roff 1992; Day and Taylor 1997; Glazier 1999). Growth rates of immature male and female fish are similar and linear; at maturation, growth rates are curvilinear (Day and Taylor 1997). The theory is most applicable to females that allocate a substantial amount of energy to ovaries. In contrast, the reason for curvilinear growth of mature males is less easily explained because the allocation of energy to testes development is relatively small (Roff 1983). We propose that the decline in growth efficiency in males is likely explained by increased energetic costs associated with reproductive activity. In the case of walleye, SSD is a marked expression of the cost of reproductive activity of males. Sandercock (2001) proposed that females prefer small acrobatic males. Alternatively, small agile males may just have a greater chance of mating.

Several lines of evidence suggest that for walleye, energy allocations have been selected to maximize swimming power instead of body size in the competition for fertilizations. First, walleye males predominate on the spawning shoals, seemingly remaining on the shoals for the duration of the spawning season, whereas the females remain only long enough to deposit their fertilized eggs (Colby et al. 1979). Males may maximize fertilizations by sustained searches for ripe females in these circumstances. Second, males have a larger portion of muscle per unit of mass than females. Females allocate more energy as lipids for gonadal development (Henderson and Nepszy 1994). Third, mature males have lower growth efficiencies than mature females. We have inferred that the lower growth efficiency of mature males is caused by elevated activity. There is no reason to believe that mature males have higher routine metabolism unless metabolism is more related to protein mass than total mass. Fourth, the abrupt drop in growth efficiency associated with the maturation of males suggests a marked increase in activity costs associated with mating. Routine metabolism would not be expected to change suddenly during development. A decline in growth efficiency, mediated by an increase in activity costs, could also result from increasing difficulty in obtaining prey of the appropriate size (Paloheimo and Dickie 1966; Colby et al. 1987), exacerbated by the effects of high activity levels during spawning. Fifth, the natural mortality of mature male walleye calculated from catch curves indicates that males have higher annual mortality rates than females (Kushneriuk et al. 1996; Morgan et al. 2003), despite the fact that the males invest less than one-third as much in reproductive tissues and should, therefore, be energetically less stressed by reproduction. Together, this evidence suggests that at least for fishes in which scramble competition plays a significant role in mating success, the resulting selection for metabolic power and large investments in activity can produce substantial sexual dimorphisms in allocation to muscle tissue, post-maturity growth rates, and mortality rates. Roff (1983) proposed that female-biased SSD could result from males eating less to avoid predation. Similarly, Holtby and Healey (1990) concluded that female chinook salmon (*Oncorhynchus kisutch*) eat more and are more vulnerable to predation, as evidenced by the positive correlation between the ratio of female to male size and the male to female sex ratio. In our study, the growth of mature males was more easily explained by lower growth efficiencies resulting from higher activity levels. Males did, however, eat relatively less than females. Female sex ratios increased with age (Henderson and Nepszy 1994), indicating a higher mortality rate of males.

Sexual size dimorphism of walleye is in part consistent with the theoretical predictions for a shoal-spawning species with females broadcasting eggs to a queue of males externally fertilizing eggs. Male mating success does not depend on male conflict and sperm competition dependent on size. Rather, male success is more dependent on fertilizing eggs from the greatest number of females that appear briefly on the spawning shoals. Active and agile males are more likely to encounter the relatively low density of females that appear briefly on the shoals (Legrand and Morse 2000). There may be a minimum size of mature males associated with migrations to the spawning shoals, particularly for river spawners. The cost of reproduction by females is mainly reduced mature growth rates caused by the trade-off between somatic and gonadal growth (Roff 1983). The trade-off for males is between somatic growth and the energy costs of reproductive behaviour; in addition, males experience elevated mortality rates, possibly as a result of the stress of spawning behaviour. This elevated mortality of males may be compensated for, in part, by the earlier maturation of males. Our interpretation of the SSD differs from others, only because we propose that there has been selection for behaviour rather than growth characteristics of males. The observed growth of males is a consequence of their reproductive behaviour.

Acknowledgements

We thank the biologists who conscientiously sampled walleye from isolated lakes, often in inclement weather. Susan Mann determined all ages from otoliths. The co-operation of the Ontario Ministries of Natural Resources and Environment is appreciated.

References

Bisazza, A., and Pilastro, A. 1997. Small male mating advantage and reversed size dimorphism in Poecilid fishes. J. Fish Biol. **50**: 397–406.

Bonnet, X., Naulleau, G., Shine, R., and Lourdais, O. 2000. Reproductive versus ecological advantages to larger body size in female snakes, *Vipera aspis*. Oikos, **89**: 509–518.

Butler, M.A., Schoener, T.W., and Losos, J.B. 2000. The relationship between sexual size dimorphism and habitat use in Greater Antillean *Anolis* lizards. Evolution, **54**: 259–272.

Christensen, J.M. 1964. Burning of otoliths, a technique for age determination of soles and other fish. J. Cons. Int. Explor. Mer, **29**: 73–81.

Colby, P.J., McNicol, R.E., and Ryer, R.A. 1979. Synopsis of biological data on walleye (*Stizostedion v. vitreum*, Mitchell 1818). Food and Agricultural Organization of the United Nations, Rome.

Colby, P.J., Ryan, P.A., Schupp, D.H., and Serns, S.L. 1987. Interactions in north-temperate lake fish communities. Can. J. Fish. Aquat. Sci. **44**(Suppl. 2): 104–128.

Darwin, C. 1871. The descent of man and selection in relation to sex. John Murray, London.

Day, T., and Taylor, P.D. 1997. Von Bertalanffy's growth equation should not be used to model age and size at maturity. Am. Nat. **149**: 381–393.

Duffy, M.J., McNulty, J.L., and Mosindy, T.E. 2000. Identification of sex, maturity, and gonad condition of walleye (*Stizostedion vitreum vitreum*). Northwest Science and Technology Field Guide No. FG-05, Ontario Ministry of Natural Resources, Northwest Region Science and Technology Unit, Thunder Bay, Ont.

Dunn, P.O., Whittingham, L.A., and Pitcher, T.E. 2001. Mating systems, sperm competition, and the evolution of sexual dimorphism in birds. Evolution, **55**: 161–175.

Fairbairn, D.J. 1997. Allometry for sexual size dimorphism: pattern and process in the coevolution of body size in males and females. Annu. Rev. Ecol. Syst. **28**: 659–687.

Glazier, D.S. 1999. Trade-offs between reproductive and somatic (storage) investments in animals: a comparative test of the Van Noordwijk and De Jong model. Evol. Ecol. **13**: 539–555.

Harris, R.C., and Bodaly, R.A. 1998. Temperature, growth and dietary effects on fish mercury dynamics in two Ontario lakes. Biogeochemistry, **40**: 175–187.

Henderson, B.A., and Nepszy, S.J. 1994. Reproductive tactics of walleye (*Stizostedion vitreum*) in Lake Erie. Can. J. Fish. Aquat. Sci. **51**: 986–997.

Henderson, B.A., Wong, J.L., and Nepszy, S.J. 1996. Reproduction of walleye in Lake Erie: allocation of energy. Can. J. Fish. Aquat. Sci. **53**: 127–133.

Henderson, B.A., Trivedi, T., and Collins, N. 2000. Annual cycle of energy allocation to growth and reproduction of yellow perch. J. Fish Biol. **57**: 122–133.

Henson, S.A., and Warner, R.R. 1997. Male and female alternative reproductive behaviors in fishes: a new approach using intersexual dynamics. Annu. Rev. Ecol. Syst. **28**: 571–592.

Holtby, L.B., and Healey, M.C. 1990. Sex-specific life history tactics and risk-taking in coho salmon. Ecology, **7**: 678–690.

Kushneriuk, R.S., Lester, N.P., and Korver, R.M. 1996. A compendium of life history characteristics of walleye in Ontario waters. Ontario Ministry of Natural Resources, Toronto.

Lankford, T.E., Billerbeck, J.M., and Conover, D.O. 2001. Evolution of intrinsic growth and energy acquisition rates. II. Trade-offs with vulnerability to predation in *Menidia menidia*. Evolution, **55**: 1873–1881.

Legrand, R.S., and Morse, D.H. 2000. Factors driving extreme sexual size dimorphism of a sit-and-wait predator under low density. Biol. J. Linn. Soc. **71**: 643–664.

Lester, N.P., Shuter, B.J., Kushneriuk, R.S., and Marshall, T.R. 2000. Life history variation in Ontario walleye populations: implications for safe rates of fishing. Percid Community Synthesis, Population and Yield Characteristics Working Group, Ontario Ministry of Natural Resources, Toronto.

Madsen, T., and Shine, R. 1993. Phenotypic plasticity in body sizes and sexual size dimorphism in European grass snakes. Evolution, **47**: 1–4.

McDonald, R.A. 2002. Resource partitioning among British and Irish mustelids. J. Anim. Ecol. **71**: 185–200.

Morgan, G.E. 2002. Manual of instructions — fall walleye index netting (FWIN). Percid Community Synthesis, Diagnostics and

Sampling Standards Working Group, Ontario Ministry of Natural Resources, Toronto.

Morgan, G.E., Malette, M.D., Kushneriuk, R.S., and Mann, S.E. 2003. Regional summaries of walleye life history characteristics based on Ontario's fall walleye index netting (FWIN) program 1993 to 2001. Percid Community Synthesis, Diagnostics and Sampling Standards Working Group, Ontario Ministry of Natural Resources, Toronto.

Oddie, K.R. 2000. Size matters: competition between male female great tit offspring. J. Anim. Ecol. **69**: 903–912.

Paloheimo, J.E., and Dickie, L.M. 1966. Food and growth of fishes. III. Relations among food, body size, and growth efficiency. J. Fish. Res. Board Can. **23**: 1209–1248.

Parker, G.A. 1992. The evolution of sexual size dimorphism in fish. J. Fish Biol. **41**(Suppl. B): 1–20.

Pierce, C.L., Sexton, M.D., Pelham, M.E., Liao, H., and Larscheid, J.G. 2001. Dynamics of the littorial fish assemblages in Spirit Lake, Iowa, and implications for prey availability for piscivores. N. Am. J. Fish. Manag. **21**: 884–896.

Pilastro, A. 1997. Sexual selection for small size in male mosquitofish (*Gambusia holbrooki*). Proc. R. Soc. Lond. Ser. B Biol. Sci. **264**: 1125–1129.

Quinn, T.P., Hendry, A.P., and Buck, G.B. 2001. Balancing natural and sexual selection in sockeye salmon: interactions between body size, reproductive opportunity and vulnerability to predation by bears. Evol. Ecol. Res. **3**: 917–937.

Roff, D. 1983. An allocation model of growth and reproduction in fish. Can. J. Fish. Aquat. Sci. **40**: 1395–1404.

Roff, D. 1992. The evolution of life histories: theory and analysis. Chapman and Hall, New York.

Ruckstuhl, K.E., and Neuhaus, P. 2002. Sexual segregation in ungulates: a comparative test of three hypotheses. Biol. Rev. **77**: 77–96.

Sandercock, B.K. 2001. What is the relative importance of sexual selection and ecological processes in the evolution of sexual size dimorphism in monogamous shorebirds. Wader Study Group Bull. **96**: 64–70.

Scheuhammer, A.M., and Graham, J.E. 1999. The bioaccumulation of mercury in aquatic organisms from two similar lakes with differing pH. Ecotoxicology, **8**: 49–56.

Shaffer, S.A., Weimerskirch, H., and Costa, D.P. 2001. Functional significance of sexual dimorphism in Wandering albatross, *Diomedia exulans*. Funct. Ecol. **15**: 203–210.

Shine, R. 1989. Ecological causes for the evolution of sexual size dimorphism: a review of the evidence. Q. Rev. Biol. **64**: 419–461.

Shine, R., Harlow, P.S., Keogh, J.S., and Boeadi. 1998. The influence of sex and body size on food habits of a giant tropical snake, *Python reticulates*. Funct. Ecol. **12**: 248–258.

Szekely, T., Reynolds, J.D., and Figuerola, J. 2000. Sexual size dimorphism in shorebirds, gulls, and alcids: the influence of sexual and natural selection. Evolution, **54**: 1404–1413.

Uthe, J.F., Armstrong, F.A.J., and Bergman, H.L. 1970. Mercury determination in fish samples by wet digestion and flameless atomic absorption spectrophotometry. J. Fish. Res. Board Can. **27**: 805–811.

Indirect effects of zebra mussels (*Dreissena polymorpha*) on the planktonic food web

Erik G. Noonburg, Brian J. Shuter, and Peter A. Abrams

Abstract: The exotic zebra mussel (*Dreissena polymorpha*) has caused dramatic reductions in phytoplankton density in lakes with dense mussel populations. However, the indirect effects of this invader on other trophic groups have been inconsistent and difficult to interpret. In some lakes, zebra mussels appear to have had little effect on zooplankton density, despite decreasing the abundance of their phytoplankton prey. We analyze food web models to test hypothesized mechanisms for the absence of a strong effect of dreissenids on zooplankton. Our results suggest that neither reduced inedible algal interference with zooplankton filtering nor reduced phytoplankton self-shading is sufficient to explain the insensitivity of zooplankton populations to dreissenid competition. Instead, we show how the impact of benthic filter feeders can be influenced by the rate of mixing within a basin, which limits phytoplankton delivery to the benthos. We explore the predictions of a simple spatially structured model and demonstrate that differences in abiotic factors that control mixing can result in large differences in direct and indirect effects of zebra mussel filtering.

Résumé : Les lacs qui possèdent de grandes densités de moules zébrées (*Dreissena polymorpha*), une espèce exotique, subissent de fortes réductions de la densité du phytoplancton. Cependant, les effets indirects de cette espèce envahissante sur les autres groupes trophiques sont variables et difficiles à interpréter. Dans certains lacs, les moules zébrées semblent avoir peu d'effet sur la densité du zooplancton, malgré le déclin de l'abondance du phytoplancton qui leur sert de nourriture. Des modèles de réseaux alimentaires nous permettent de vérifier les mécanismes suggérés pour expliquer l'absence d'effets significatifs des dreissénidés sur le zooplancton. Nos résultats montrent que ni la réduction de l'interférence des algues non comestibles sur la filtration du zooplancton, ni la diminution de l'auto-ombrage par le phytoplancton ne sont assez importantes pour expliquer que les populations de zooplancton ne soient pas affectées par la compétition des dreissenidés. Plutôt, l'impact des filtreurs benthiques est influencé par le degré de brassage dans le bassin, ce qui limite l'apport de phytoplancton au benthos. L'examen des prédictions d'un modèle simple à structure spatiale nous permet de démontrer que des différences dans les facteurs abiotiques qui contrôlent le brassage peuvent amener des différences importantes dans les effets directs et indirects de la filtration des moules zébrées.

[Traduit par la Rédaction]

Introduction

Biological invasions pose a serious threat to native biodiversity as well as humans' ability to manage ecosystems for recreation and resource exploitation, yet managers are often unable to prevent the arrival of new species (Czech and Krausman 1997; Mack et al. 2000; Pimentel et al. 2000). Understanding and predicting the effects of exotic species are therefore crucial research goals (Parker et al. 1999). The direct effects of exotic species are often obvious, e.g., the replacement of competitors or the extirpation of prey. However, the indirect effects of exotics can be unexpected and the causal links may be difficult to demonstrate.

The introduction of dreissenid mussels to North America is an excellent example of an invasion with dramatic direct effects and multiple hypothesized indirect effects (Nalepa and Schloesser 1993; Strayer et al. 1999). Zebra mussels (*Dreissena polymorpha*) were first reported in Lake St. Clair in 1989 (Hebert et al. 1989) and have since established populations in several drainages of eastern North America (Johnson and Carlton 1996). In shallow bays and lake basins with dense mussel populations, estimates of total filtering rate are extremely high. For instance, Bailey et al. (1999) estimated the time to filter the entire water column in part of the Bay of Quinte, Lake Ontario, to be as short as 0.05 days. Not surprisingly, in areas with sufficient suitable benthic habitat to support dense mussel populations, dreissenid filtering is generally associated with declines in phytoplankton abundance (e.g., Leach 1993; Nalepa et al. 1999; Idrisi et al. 2001). In contrast, despite potentially strong competition be-

---

Received 8 October 2002. Accepted 31 August 2003. Published on the NRC Research Press Web site at http://cjfas.nrc.ca on 21 November 2003.
J17135

E.G. Noonburg[1] and P.A. Abrams. Department of Zoology, University of Toronto, 25 Harbord Street, Toronto, ON M5S 3G5, Canada.
B.J. Shuter. Department of Zoology, University of Toronto, 25 Harbord Street, Toronto, ON M5S 3G5, Canada, and Aquatic Research and Development, Ontario Ministry of Natural Resources, Lake Erie Management Unit, Box 429, Port Dover, ON N0A 1N0, Canada.

[1]Corresponding author (e-mail: noonburg@zoo.utoronto.ca).

doi: 10.1139/F03-116

tween dreissenids and zooplankton for phytoplankton, impacts on zooplankton vary from site to site. In some lakes, sampling data show no significant change in zooplankton density after dreissenids invade, despite decreases in phytoplankton density over the same time period (Wu and Culver 1991; Idrisi et al. 2001). Indeed, Wu and Culver (1991) suggested that zooplankton continued to control phytoplankton dynamics in the western basin of Lake Erie even after the establishment of dense zebra mussel beds. This interpretation has been challenged (MacIsaac et al. 1992; Nicholls and Hopkins 1993), and other investigators have suggested that zooplankton declined in response to a dreissenid invasion in some systems (e.g., Bridgeman et al. 1995; Johannsson et al. 2000).

Two general types of mechanisms might explain the absence of a consistent negative effect of zebra mussel invasions on zooplankton abundance. The first type involves indirect positive effects on phytoplankton productivity that offset the increased consumption of phytoplankton by dreissenids. For instance, Padilla et al. (1996) constructed a food web model and predicted that zebra mussel filtering would disproportionately lower the density of phytoplankton taxa that are inedible to zooplankton, thereby relaxing nutrient competition and increasing zooplankton foraging efficiency, thus permitting a less abundant but more productive and edible phytoplankton community to support equal or even higher abundances of zooplankton. A second example of this sort of mechanism is provided by Idrisi et al. (2001), who suggested that the increases in water clarity that accompany mussel colonization could stimulate phytoplankton productivity, thus maintaining existing zooplankton abundances.

The second class of mechanism involves physical factors that potentially constrain the direct effects of mussel filtering on phytoplankton populations. In particular, zebra mussels attached to the benthos are isolated to some degree from their pelagic prey. Studies of vertical chlorophyll profiles and mussel ingestion rates in the field suggest that mussels refilter the lower portion of the water column more rapidly than phytoplankton are delivered by mixing, and this might play a critical role in determining the impact of mussels on phytoplankton (MacIsaac et al. 1999; Yu and Culver 1999; Ackerman et al. 2001). Furthermore, dense dreissenid populations typically occur on hard substrates, and these can be patchily distributed across the bottom of a lake. Hence, mussel consumption of phytoplankton may be limited by vertical and horizontal mixing of the water column.

We evaluate these hypotheses using two food web models. First, we derive predictions for the effects of dreissenid invasions on the equilibrium abundances of zooplankton, phytoplankton, and phosphorus in a simple, well-mixed model of the pelagic food web. We then modify the model to incorporate inedible algal interference and phytoplankton self-shading and determine the effects of these mechanisms by comparison with results from the basic model. Using the western basin of Lake Erie as a case study, we show that primary production is insufficient to support the planktonic food web in the presence of a dense population of zebra mussels filtering a well-mixed water column. Next, we address the hypothesis that isolation of mussels from their pelagic prey limits the effect of dreissenids on zooplankton. We introduce simple spatial structure to the model and explore the effects of water column mixing on the food web response to dreissenid filtering. We show that benthic–pelagic structure can explain why dreissenid invasions do not produce a strong, consistent response in the zooplankton community. We predict that the responses of phytoplankton and zooplankton to mussel filtering are sensitive to physical factors that determine the water column mixing rate.

Model 1: a single, well-mixed compartment

Structure

We model the dynamics of phytoplankton, zooplankton, and a limiting nutrient in a small lake basin or in a bay that is homogeneous but distinct from a larger lake. Water enters the system from rivers or runoff (inflow contains nutrients, but no organisms) and leaves at the same rate, resulting in constant volume. We assume that the limiting nutrient in the system is phosphorus and measure the abundance of all trophic groups in units of phosphorus concentration.

Throughout our analysis, we assume that dreissenid biomass is not dynamically linked to phytoplankton density. Instead, we treat mussel abundance as an independent variable and calculate its effect on the equilibrium concentrations of the other food web components. Our rationale is that dreissenids are limited by suitable hard benthic substrate. Dreissenid density has been observed to fluctuate within these habitats (Nalepa et al. 1995), and dreissenids have colonized some areas with soft sediment (Dermott and Munawar 1993; Coakley et al. 1997; Berkman et al. 1998); however, differences in suitable habitat appear to be the primary determinant of differences in mussel abundance among lake regions (Mellina and Rasmussen 1994).

We divide phytoplankton into two classes based on whether they are too large to be ingested by cladocerans. Characteristics of the two phytoplankton groups generate a trade-off between vulnerability to zooplankton filtering and competitive ability: small phytoplankton, which are edible to zooplankton, are superior to large phytoplankton in nutrient competition (reviewed in Andersen 1997).

We provide a brief description of the key model components here; the full equations appear in Table 1 and the parameters are defined in Table 2. The model describes the dynamics of available phosphorus (R), large (L) and small (S) phytoplankton, and zooplankton (Z) in terms of the concentration of phosphorus associated with each of these components. The rate of change in R is the sum of contributions from abiotic processes (inflow and outflow) and biotic processes (plankton growth and phosphorus recycling):

$$(1)\quad \mathrm{d}R/\mathrm{d}t = I_R + E_R - G_R - O_R$$

where I_R is inflow, O_R is outflow, E_R is the sum of excretion and other losses from all organisms, and G_R is phytoplankton population growth. Dynamics of small and large phytoplankton are determined by the difference between population growth (G_S, G_L) and losses to filtering (F_S, F_L), outflow (O_S, O_L), and sinking and other mortality (E_S, E_L):

$$(2)\quad \mathrm{d}S/\mathrm{d}t = G_S - F_S - E_S - O_S$$

$$(3)\quad \mathrm{d}L/\mathrm{d}t = G_L - F_L - E_L - O_L$$

Table 1. Dynamic equations for the four components of the food chain model: available phosphorus (R), edible phytoplankton (S), inedible phytoplankton (L), and zooplankton (Z).

Available phosphorus, *R*	
$\frac{\mathrm{d}R}{\mathrm{d}t} = I_R + E_R - G_R - O_R$	
Inflow	$I_R = QR_{\text{in}}$
Total plankton losses	$E_R = l_S S + l_L L + l_Z Z + \frac{(1-\varepsilon)a_S SZ}{1 + a_S T_S S + a_L T_L L} + fbM(S + L)$
Total phytoplankton growth	$G_R = G_S + G_L$
Outflow	$O_R = QR$
Edible phytoplankton, *S*	
$\frac{\mathrm{d}S}{\mathrm{d}t} = G_S - F_S - E_S - O_S$	
Growth	$G_S = \frac{V_S SR}{k_S + R}$
Filtering loss	$F_S = \frac{a_S SZ}{1 + a_S T_S S + a_L T_L L} + bMS$
Other losses	$E_S = l_S S$
Outflow	$O_S = QS$
Inedible phytoplankton, *L*	
$\frac{\mathrm{d}L}{\mathrm{d}t} = G_L - F_L - E_L - O_L$	
Growth	$G_L = \frac{v_L LR}{k_L + R}$
Filtering loss	$F_L = bML$
Other losses	$E_L = l_L L$
Outflow	$O_L = QL$
Zooplankton, *Z*	
$\frac{\mathrm{d}Z}{\mathrm{d}t} = G_Z - E_Z - O_Z$	
Growth	$G_Z = \frac{\varepsilon a_S SZ}{1 + a_S T_S S + a_L T_L L}$
Losses	$E_Z = l_Z Z$
Outflow	$O_Z = QZ$

Note: Each component is expressed in terms of the concentration of phosphorus associated with that component. Each process contributing to the overall dynamics of a component is separately defined. Reasonable values for the parameters that govern these processes are listed in Table 2.

Finally, zooplankton density increases with filtering (G_Z) and decreases due to outflow (O_Z) and excretion and other mortality (E_Z):

$$\mathrm{d}Z/\mathrm{d}t = G_Z - E_Z - O_Z \tag{4}$$

The functions in eqs. 1–4 are based on a set of assumptions regarding phosphorus transfer between trophic groups. First, we assume constant inflow phosphorus concentration (R_{in}) and inflow volume per day (q). If basin volume (V) is constant, inflow and outflow rates are identical. Hence, the outflow loss term for each model component is proportional to the concentration of that component in the lake (e.g., $O_S = QS$, where $Q = q/V$ is identical for all components in the model), and inflow of available phosphorus is $I_R = QR_{\text{in}}$.

Phytoplankton growth follows the Monod model; for small phytoplankton, with maximum growth rate v_S and half-saturation concentration k_S,

$$G_S = \frac{v_S RS}{R + k_S} \tag{5}$$

The expression for G_L is equivalent, with subscripts changed appropriately.

We model zooplankton filtering with a type 2 functional response. We assume that large phytoplankton can interfere with zooplankton filtering, but that zooplankton can not ingest large phytoplankton. Hence, zooplankton spend time handling large phytoplankton but do not directly affect large phytoplankton dynamics. For attack rates a_S and a_L on small

Table 2. Parameter estimates for the western basin of Lake Erie.

Parameter	Description (units)	Value
l_S	Loss rate from edible phytoplankton (day^{-1})	0.01
l_L	Loss rate from inedible phytoplankton (day^{-1})	0.01
l_Z	Loss rate from zooplankton (day^{-1})	0.31
ε	Zooplankton assimilation efficiency (unitless)	0.54
a_S	Zooplankton attack rate on edible phytoplankton (L·(μg P·day)$^{-1}$)	0.18
a_L	Zooplankton attack rate on inedible phytoplankton (L·(μg P·day)$^{-1}$)	Variable
T_S	Zooplankton handling time for edible phytoplankton (days)	0.32
T_L	Zooplankton handling time for inedible phytoplankton (days)	0.32
v_S	Edible phytoplankton maximum phosphorus uptake rate (day^{-1})	1.8
k_S	Edible phytoplankton half-saturation phosphorus concentration (μg P·L^{-1})	0.7
v_L	Inedible phytoplankton maximum phosphorus uptake rate (day^{-1})	0.8
k_L	Inedible phytoplankton half-saturation phosphorus concentration (μg P·L^{-1})	0.7
f	Fraction of phosphorus consumed by mussels that is returned to the water column (unitless)	1
R_{in}	Inflow phosphorus concentration (μg P·L^{-1})	33
Q	Water outflow rate (day^{-1})	0.02
b	Mussel filtering rate (L·day^{-1})	Variable
M	Mussel density (L^{-1})	Variable

Note: See Appendix B for sources.

and large phytoplankton, respectively, handling times T_S and T_L, and assimilation efficiency ε,

$$(6) \quad G_Z = \frac{\varepsilon a_S SZ}{1 + a_S T_S S + a_L T_L L}$$

We do not explicitly model losses to higher trophic groups (e.g., fish predation on zooplankton) to keep the model simple. However, if the population dynamics of these groups are not tightly linked over the seasonal time scale of plankton dynamics, such consumption may be treated as part of the loss terms (e.g., E_Z).

We make two simplifying assumptions regarding dreissenid filtering. First, we model dreissenid filtering with a type 1 functional response, with attack rate b. Although dreissenid filtering rate decreases when phytoplankton density exceeds a threshold value (Walz 1978; Sprung and Rose 1988; Berg et al. 1996), this threshold is typically greater than the densities in systems considered here, and explicit consideration of the threshold does not affect our results. Second, we assume dreissenids filter small and large phytoplankton groups indiscriminately. Although there is evidence of selectivity among phytoplankton species, it generally occurs at the stage of rejection in pseudofeces (Ten Winkel and Davids 1982; Horgan and Mills 1997; Bastviken et al. 1998) after cells and colonies have been removed from the water. However, Vanderploeg et al. (2001) found that toxic *Microcystis* colonies rejected by zebra mussels could return to the water column and suggested that such filtering selectivity could facilitate *Microcystis* blooms. This situation involves a radical shift in the planktonic food web not considered in this paper.

The final set of transfers involves phosphorus recycling. For simplicity, we assume that all phosphorus losses from planktonic groups (excretion, sinking, zooplankton egestion, etc.) return directly to the available phosphorus pool. In contrast, we allow a variable fraction (f) of mussel filtrate to be recycled, whereas the remainder ($1 - f$) is lost from the system via sedimentation and burial. Given these assumptions,

$$(7) \quad E_R = E_S + E_L + E_Z + \frac{1-\varepsilon}{\varepsilon}F_Z + fbM(S + L)$$

where M is mussel density. A more realistic model structure would include a detritus compartment through which dead and egested material must pass before re-entering the available phosphorus pool. However, we have found through numerical simulations that the addition of a detritus compartment has little effect on our qualitative results, although the values of the equilibria depend on the rate at which detritus is recycled.

Qualitative behaviour

Here, we derive general qualitative predictions for the initial impact of the zebra mussel invasion on equilibrium plankton densities (Table 3). These predictions are simply the signs of the derivatives of the equilibria with respect to M, calculated at $M = 0$. In Appendix A, we derive conditions under which the initial impact of dreissenid invasion on the zooplankton equilibrium (Z^*) is positive ($\mathrm{d}Z^*/\mathrm{d}M|_{M=0} > 0$). If large phytoplankton do not interfere with zooplankton filtering ($a_L T_L = 0$), then this positive effect depends on two conditions. First, the parameter combination $(k_L - k_S)(Q + l_L)$ must be small relative to the product of large phytoplankton maximum growth rate and small phytoplankton half-saturation concentration ($v_L k_S$). The sum $Q + l_L$ will typically be small in systems such as the western basin of Lake Erie (inflow is small relative to total basin volume, large phytoplankton lose little phosphorus; see Appendix B), ensuring that this condition is met. The second condition is

$$(8) \quad \frac{v_S k_L}{v_L k_S} > 1$$

If small phytoplankton are better phosphorus competitors than large phytoplankton ($v_S > v_L$, $k_L \geq k_S$), the inequality in eq. 8 must be true. If large phytoplankton interfere with zooplankton filtering ($a_L T_L > 0$), $\mathrm{d}Z^*/\mathrm{d}M$ at $M = 0$ can increase

Table 3. Equilibria for the basic model.

All present	$R^* = \dfrac{k_L(l_L + bM + Q)}{v_L - (l_L + bM + Q)}$
	$S^* = \dfrac{(l_Z + Q)(1 + a_L T_L L^*)}{\varepsilon a_S - a_S T_S(l_Z + Q)}$
	$L^* = \left(R_{in} - \dfrac{(1-f)bMS^*}{Q} - (R^* + S^* + Z^*)\right)\left(1 + \dfrac{(1-f)bM}{Q}\right)^{-1}$
	$Z^* = \left(\dfrac{v_S R^*}{R^* + k_S} - l_S - bM - Q\right)\left(\dfrac{1 + a_S T_S S^* + a_L T_L L^*}{a_S}\right)$
L extinct	$R^* = \left(QR_{in} + l_S S^* + l_Z Z^* + \dfrac{(1-\varepsilon)a_S S^* Z^*}{1 + a_S T_S S^*} + fbMS^*\right)Q^{-1}$
	$S^* = \dfrac{l_Z + Q}{\varepsilon a_S - a_S T_S(l_Z + Q)}$
	$Z^* = \left(\dfrac{v_S R^*}{R^* + k_S} - l_S - bM - Q\right)\left(\dfrac{1 + a_S T_S S^*}{a_S}\right)$
L and *Z* extinct	$R^* = \dfrac{k_S(bM + Q + l_S)}{v_S - (bM + Q + l_S)}$
	$S^* = \dfrac{Q(R_{in} - R^*)}{\dfrac{v_S R^*}{k_S + R^*} - l_S - fbM}$

Note: As dreissenid filtering impact increases, the food chain undergoes successive simplifications as first the large phytoplankton and then zooplankton are driven to extinction (see Fig. 1). Equilibrium solutions for these simplified food chains follow the solution for the complete, native food chain. Explicit solutions can be found in each case, but extremely long solutions are left in implicit form.

or decrease with $a_L T_L$ and possibly become negative if interference is strong relative to handling time for small phytoplankton.

Direct inspection of the equation for R^* (Table 3) shows that the equilibrium concentration of available phosphorus always increases with mussel density. Furthermore, we demonstrate in Appendix A that if Z^* and R^* increase with dreissenids, then S^* and L^* must decrease.

We conclude that the initial increase in equilibrium zooplankton concentration with dreissenids does not require any of the mechanisms hypothesized to offset mussel consumption of phytoplankton. Instead, dreissenid filtering alters the competitive balance between the two phytoplankton groups. The additional mortality disproportionately affects the weaker competitor, *L*, and thereby increases the productivity of edible phytoplankton. The increased productivity is transferred to zooplankton biomass. This mechanism is independent of phosphorus recycling by dreissenids: the parameter *f* does not appear in the expression for Z^* if $a_L T_L = 0$. However, increasing *f* increases the filtering impact that can be withstood by the planktonic food web (see below).

Quantitative behaviour: western basin of Lake Erie

Parameterizing the model

The general qualitative predictions of the model offer a potential explanation for the apparent absence of a strong negative effect of dreissenids on zooplankton in some systems. If mussel density (or filtering rate, *b*) is sufficiently low or the increase in Z^* is relatively small, the effect of dreissenids on zooplankton may be difficult to detect in survey data. We assess the plausibility of this explanation by first parameterizing the model. We then ask whether dreissenid density and filtering rate fall within the range over which equilibrium zooplankton density increases and whether the predicted increase is smaller than within-season fluctuations or measurement error.

We estimated parameter values for the western basin of Lake Erie from the literature (Table 2). Because this basin is shallow and does not stratify, its limnological features may more closely approximate a well-mixed compartment than most natural systems with zebra mussels. Furthermore, estimates of phosphorus loading, dreissenid abundance, and plankton density before and after the arrival of dreissenids are available in the literature.

We detail the parameterization in Appendix B. We use average phosphorus loading (R_{in}) for 1987–1990, i.e., 2 years before and 2 years after zebra mussels established dense populations in the western basin of Lake Erie. Lumping phytoplankton into two trophic groups necessitates some sacrifice of precision, and data for phosphorus uptake by phytoplankton species separated by edibility to zooplankton are difficult to obtain. Hence, we take the approach suggested by Andersen (1997): we use the upper and lower quartiles of the distribution from his survey of measured species values for high and low maximum uptake rates (v_S and v_L). Wu and Culver (1991) found that two cladocerans, *Daphnia galeata* and *Daphnia retrocurva*, were the dominant zooplankton grazers during the dreissenid invasion of the western basin of Lake Erie. Our parameter values for zooplankton are based on *D. galeata*.

In our analysis, we focus on the occurrence of large and consistent deviations between observed and predicted behaviors and examine the sensitivity of these discrepancies to differences in the structure of our models. We do not present a detailed analysis of sensitivity to parameter variation for any one model structure because the effects produced, for reasonable parameter ranges, are small relative to the size of the deviations that we are interested in accounting for.

Responses of the food chain to increased mussel filtering impact

We show the predicted effects of dreissenid filtering on the equilibria for the western basin of Lake Erie (Fig. 1). Here, we use the product of mussel density and filtering rate (*bM*) as a measure of mussel "filtering impact". This parameter combination represents the total filtering rate of the mussel population and is equivalent to empirical measurements that incorporate effects of factors such as mussel size structure (e.g., MacIsaac et al. 1992). Filtering impact is equal to the inverse of the time required by the mussel population to filter the entire water column.

The predictions of the parameterized model are consistent with the general analysis in the previous section: as *bM* increases, zooplankton and available phosphorus initially increase and total phytoplankton decreases (*L* decreases, but *S* is independent of filtering impact if large phytoplankton do not interfere with zooplankton filtering). Further increases in *bM* drive large phytoplankton and then zooplankton extinct.

To generate Fig. 1, we let $f = 1.0$, which implies that all phosphorus consumed by dreissenids is returned to the water column via excretion or decomposition of feces, pseudofeces, and mussel biomass. Although complete recycling is unrealistic, decreasing f reduces the filtering impact that can be tolerated by the planktonic food web (all lines in Fig. 1 move to the left); hence, $f = 1.0$ gives the most conservative estimate of dreissenid effects. In simulations of the model, we found that loss of even a small fraction of phosphorus consumed by dreissenids has an extremely large negative effect on plankton productivity. We return to this issue below.

Given the density of mussels and their filtering rate, we can calculate the filtering impact for the western basin of Lake Erie, i.e., the appropriate point on the horizontal axis in Fig. 1. We can then use the model to predict the effect of the dreissenid invasion on phytoplankton and zooplankton populations. Zebra mussels primarily colonize hard substrate on reefs in the western basin of Lake Erie. This habitat is patchily distributed and makes up only approximately 15% of the total surface area of the basin (MacIsaac et al. 1992). Within these patches, mussel abundance varies widely, and surveys have found densities greater than 3×10^5 mussels·m^{-2} (Leach 1993). We use population survey data from MacIsaac et al. (1992) because their density estimates are typical of samples taken during the first few years after the dreissenid invasion and they measured size structure, which has a large effect on the estimate of filtering rate (Kryger and Riisgård 1988). We calculate two estimates of filtering impact based on the local density of mussels on reefs or the average density assuming that the impact is distributed over the entire basin.

Fig. 1. Equilibria with parameters estimated for the western basin of Lake Erie and no inedible phytoplankton interference ($a_L = 0$): (*a*) solid line, available phosphorus, R^*; broken line, large phytoplankton, L^*; (*b*) solid line, small phytoplankton, S^*; broken line, zooplankton, Z^*. For high filtering impact (*bM*), $S^* \rightarrow 0$ and $R^* \rightarrow R_{in}$ (not shown). Arrows indicate low and high estimates of whole-basin filtering impact. Estimates of local filtering impact are too large to be displayed in this plot.

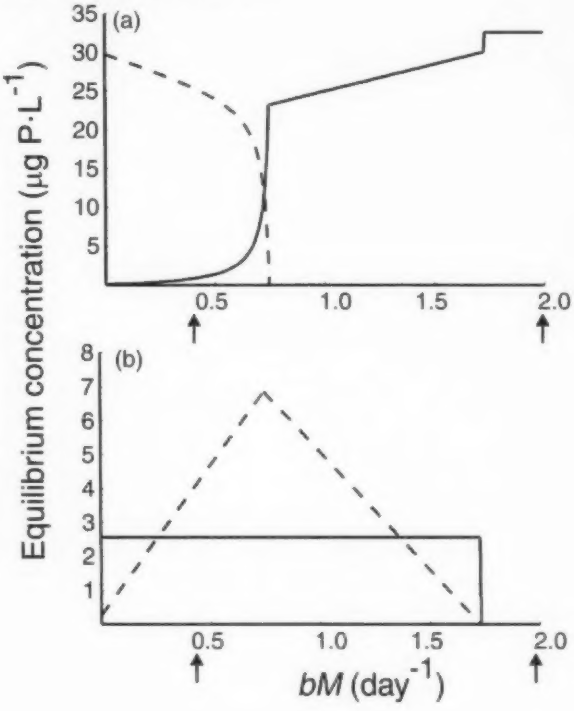

Estimates of zebra mussel filtering rate, measured in the laboratory and in the field, also vary considerably (Reeders et al. 1993). Padilla et al. (1996) used a value from Walz (1978), which is approximately in the middle of the range of 15 studies reviewed by Reeders et al. (1993, their table 1). MacIsaac et al. (1992) used the allometric scaling function for size-specific filtering rate from Kryger and Riisgård (1988). This function gives the highest value of filtering rate among the estimates compiled by Reeders et al. (1993). We compare the predictions of our model using low (Walz 1978) and high (Kryger and Riisgård 1988) estimates of filtering rate. These estimates ignore the effects of refiltration (Yu and Culver 1999); we consider the effects of incomplete mixing explicitly with the two-compartment model below.

The resulting values of local and whole-basin average filtering impact for the two filtering rate measurements are listed in Table 4. Locating these points in Fig. 1 shows that for each estimate of filtering impact, the model predicts severe impacts on large phytoplankton and zooplankton. For both estimates of local impact, zebra mussel filtering drives

Table 4. Estimates of filtering impact (*bM*) for the western basin of Lake Erie.

	Filtering impact (day^{-1})	
Filtering rate	Local	Whole basin
Low	2.93	0.44
High	13.3	2.0

Note: See Appendix B for sources.

zooplankton and large phytoplankton extinct. Using the larger of the averaged values gives the same result, whereas the smaller value results in zooplankton density increasing by an order of magnitude. These predictions are clearly inconsistent with survey data. Samples from the western basin of Lake Erie immediately following the dreissenid invasion show that zooplankton neither increased nor decreased significantly but generally remained within the bounds of pre-dreissenid seasonal variation (Wu and Culver 1991). Although inedible phytoplankton may have decreased relative to edible phytoplankton (Wu and Culver 1991), neither trophic group has been excluded from the community. Wu and Culver's (1991) data might have been collected before the system reached the predicted equilibrium values; however, more recent data (e.g., Johannsson et al. 2000) from the western basin of Lake Erie confirm that zooplankton have neither increased nor crashed.

Model behaviour before the mussel invasion also deviates significantly from observed behaviour. Predicted equilibrium phytoplankton densities in the absence of zebra mussels are roughly an order of magnitude higher than the densities observed just before the zebra mussel invasion: given $bM = 0$ and the parameter values in Table 2, predicted values for R^*, S^*, L^*, and Z^* are 0.027, 11, 21, and 0.67 µg P·L^{-1}, respectively; thus the value for $S^* + L^*$ is approximately eight times the value of 4 µg P·L^{-1} that Leach (1993) observed in the western basin of Lake Erie in 1988 (conversion from µg chlorophyll (chl)·L^{-1} to µg P·L^{-1} assuming the 1:1 P-to-chl ratio given by Reynolds 1984) and is approximately three times the value of 12 µg P·L^{-1} summer chlorophyll expected, given the input phosphorus concentration for our model (R_{in} = 33 µg P·L^{-1}) and the Dillon–Rigler (Dillon and Rigler 1974) statistical relationship linking spring phosphorus concentrations to summer chlorophyll densities. This discrepancy can be easily explained. When $bM = 0$, our model is structured so that the total phosphorus concentration in the water ($R^* + S^* + L^* + Z^*$) must equal the inflow concentration (R_{in}). Although predicted R^* and Z^* values (0.027 and 0.67 µg P·L^{-1}, respectively) may be too small compared with pre-dreissenid data (e.g., zooplankton biomass on the order of 100 µg·L^{-1} dry mass (Wu and Culver 1991) or approximately 1.8 µg P·L^{-1}, using the conversion factor from Peters and Rigler (1973)), altering parameter values to redistribute phosphorus such that S^* and L^* take on smaller, more reasonable values would clearly make the values for R^* and Z^* too large. Hence, the most likely explanation for the discrepancy between model predictions and data for pre-dreissenid invasion phytoplankton densities is that in the real system, phosphorus accumulates in components (e.g., detritus) that are not explicitly represented in our well-mixed model. However, if a phosphorus diversion of this sort is introduced into our model, we find that the sensitivity of both phytoplankton and zooplankton to mussel filtering is greatly increased, thus exacerbating the discrepancy between observed and predicted behaviour already noted above.

Fig. 2. (*a*) Effect of large phytoplankton interference on equilibrium zooplankton concentration, Z^*: solid line, $a_L = 0$; broken line, $a_L = 0.5a_S$; dotted line, $a_L = a_S$. All three lines are identical for $bM > 0.75$ ($L^* = 0$). (*b*) Effect of self-shading on zooplankton equilibrium. Broken line indicates Z^* without self-shading. Predictions with and without self-shading are identical for $bM <$ 0.73 ($L^* > 0$ in the model with self-shading).

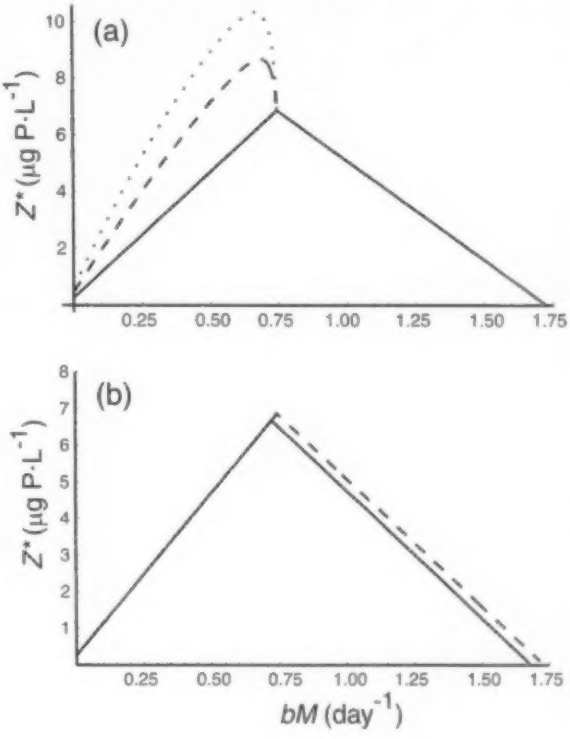

We now ask whether additional positive effects on either zooplankton feeding efficiency (i.e., reduction in feeding interference by inedible zooplankton) or phytoplankton productivity (i.e., reduction of phytoplankton self-shading) arising from declines in phytoplankton abundance could be sufficient to decrease the sensitivity of the zooplankton community to mussel filtering (i.e., expand the range of filtering impacts that zooplankton can withstand; Fig. 1).

Inedible phytoplankton interference is simply time spent by zooplankton handling inedible phytoplankton. In the basic model, this is represented by $a_LT_L > 0$. The effects of including interference in the model are displayed in Fig. 2*a*. We let $T_L = T_S$ and vary the attack rate, a_L. As a_LT_L increases, the potential for dreissenid filtering to reduce interference increases and the initial positive effect of dreissenids on zooplankton increases. However, including interference in the model does not affect the value of filtering impact at which $Z^* = 0$.

Self-shading reduces the phytoplankton population growth terms, G_S and G_L. We apply the self-shading function used by Padilla et al. (1996), which was described by Carpenter

(1992). This function reduces G_S and G_L in proportion to the total phytoplankton density, $S + L$. For small phytoplankton,

$$(9) \qquad G_S = \left(\frac{v_S SR}{k_S + R}\right)\left(1 - \frac{S + L}{z}\right)$$

where $z = 97$ µg P·L^{-1} for the western basin of Lake Erie (8 m average depth; see Carpenter 1992). The expression for G_L is also multiplied by the term $1 - (S + L)/z$.

As mussel filtering impact increases, phytoplankton density decreases, and this reduces self-shading. However, this modification of the basic model has only minor quantitative effects on the predictions for Z^* (Fig. 2*b*). Over the range of filtering impact for which $L^* > 0$, the predictions for Z^* are identical. In this region, self-shading decreases large phytoplankton density, but small phytoplankton benefit from higher concentrations of available phosphorus. This compensation for the reduction of primary production by self-shading maintains zooplankton at the same density whether the self-shading effect is present or absent in the model. Once the filtering impact exceeds the level sufficient to drive the large phytoplankton to extinction, we see a relatively small reduction in the productivity of the small phytoplankton that remain. This is reflected in a small reduction in equilibrium zooplankton abundance and, consequently, reduction in the filtering impact sufficient to drive zooplankton to extinction.

Predicted mussel ingestion rates and expected mussel food requirements

Our results suggest that the dreissenid population in the western basin of Lake Erie is capable of consuming primary production rapidly enough to drive zooplankton and even some phytoplankton taxa extinct, yet such extinctions have not been observed. A possible explanation for this discrepancy between model predictions and field observations is that gross overestimates of mussel ingestion rates are obtained when measured mussel filtering rates are simply multiplied by average water column phytoplankton densities. To examine this possibility, we compared mussel ingestion rates predicted using this approach with an estimate of the food requirements of a typical mussel, as derived from the dreissenid energy budget developed by Stoeckmann and Garton (1997). This energy budget is based on laboratory measurements of respiration plus field estimates of total growth and reproductive investment in the western basin of Lake Erie. It provides an estimated daily ration of 3.85 cal·day^{-1} for an individual mussel in the field and this converts to 0.15 µg P·day^{-1}, using the following conversion factors: 1000 cal·g^{-1} phytoplankton wet weight (Stoeckmann and Garton 1997), 0.1 g C·g wet weight^{-1} (Shuter 1978), and the C–P ratio of 48:1 in phytoplankton biomass (Reynolds 1984).

The ingestion rate estimate obtained by multiplying measured filtration rates (approximately 1.5 L·day^{-1} (Walz 1978)) and Leach's (1993) post-dreissenid invasion phytoplankton abundance measurements (monthly mean chlorophyll for 1989–1990 varies from 1 and 3 µg·L^{-1}) is 1.5–4.5 µg P·day^{-1}, an order of magnitude larger than the bioenergetics estimate of mussel food requirements. If we compare estimated consumption rates (= $b(S^* + L^*)$) from our mixed model over a range of mussel densities (Fig. 3), we obtain ingestion rates that are even higher. These unrealistically high ingestion rates could stem from overestimating the mussel filtering rate (b). However, laboratory-based estimates of b are more likely to underestimate the true value, not overestimate it, because they are derived from mussels held in an unnatural environment. Furthermore, dreissenids are more likely to filter near their maximum rate (Walz 1978; Sprung and Rose 1988) when they are exposed to low food densities. Hence, we suspect the problem lies elsewhere.

Fig. 3. Consumption rate per individual mussel at equilibrium phytoplankton density, using the lower estimate of filtering rate, $b = 1.5$ L·day^{-1} (Walz 1978).

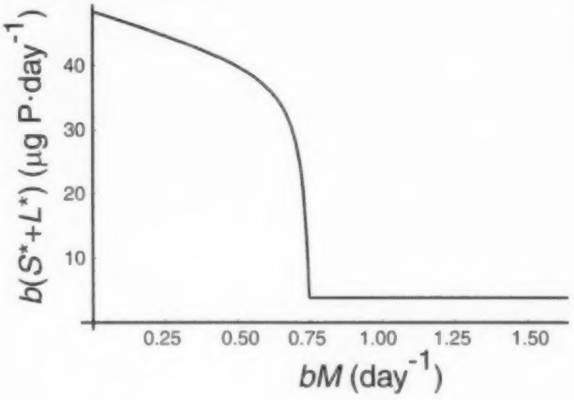

Failures of the well-mixed model: a summary

The responses of our well-mixed model to a zebra mussel invasion failed to match many of the observed responses of the western basin of Lake Erie to the mussel invasion that began there in 1989. Some of the more instructive failures are listed here. (*i*) The model predicts that zooplankton abundance will increase significantly in the early stages of the invasion, when overall filtering rate is still relatively low; this was not observed. (*ii*) The model predicts that both zooplankton and larger species of phytoplankton will be driven to extinction by mussel filtering rates that are significantly less than those currently operating in the real system; this was not observed. (*iii*) Realistic phosphorus input rates produce equilibrium phytoplankton densities in the model that are an order of magnitude greater than observed; this discrepancy can be remedied by allowing some phosphorus to accumulate in a detritus pool; however, diverting phosphorus into detritus (e.g., $f < 1$) further reduces the maximum filtering impact that large phytoplankton and zooplankton can withstand. (*iv*) Mussel consumption rates derived from observed values for both mussel filtering rate and phytoplankton density are much larger than expected mussel food requirements.

Each of these discrepancies ultimately derives from the assumption that all of the phytoplankton in the water column are equally accessible to zebra mussel predation. This assumption denies a basic fact of zebra mussel biology, namely that they are bottom dwellers, whose access to surface water is dependent on high levels of turbulence and the absence of bottom boundary layers. In the section that follows, we extend our model to explicitly recognize the spatial separation between mussels and their prey, and we show that

Table 5. Equations for the two-compartment model.

$$\frac{\mathrm{d}R_1}{\mathrm{d}t} = Q(R_{\mathrm{in}} - R_1) + l_S S_1 + l_L L_1 + l_Z Z_1 + \frac{(1-\varepsilon) a_S S_1 Z_1}{1 + a_S T_S S_1 + a_L T_L L_1} + \mu_1(R_2 - R_1) - \frac{v_S S_1 R_1}{R_1 + k_S} - \frac{v_L L_1 R_1}{R_1 + k_L}$$

$$\frac{\mathrm{d}R_2}{\mathrm{d}t} = Q(R_{\mathrm{in}} - R_2) + l_S S_2 + l_L L_2 + l_Z Z_2 + \frac{(1-\varepsilon) a_S S_2 Z_2}{1 + a_S T_S S_2 + a_L T_L L_2} + \mu_2(R_1 - R_2) - \frac{v_S S_2 R_2}{R_2 + k_S} - \frac{v_L L_2 R_2}{R_2 + k_L} + fbM(S_2 + L_2)$$

$$\frac{\mathrm{d}S_1}{\mathrm{d}t} = \frac{v_S S_1 R_1}{R_1 + k_S} - (Q + l_S) S_1 - \left(\frac{a_S S_1 Z_1}{1 + a_S T_S S_1 + a_L T_L L_1}\right) + \mu_1(S_2 - S_1)$$

$$\frac{\mathrm{d}S_2}{\mathrm{d}t} = \frac{v_S S_2 R_2}{R_2 + k_S} - (bM + Q + l_S) S_2 - \left(\frac{a_S S_2 Z_2}{1 + a_S T_S S_2 + a_L T_L L_2}\right) + \mu_2(S_1 - S_2)$$

$$\frac{\mathrm{d}L_1}{\mathrm{d}t} = \frac{v_L L_1 R_1}{R_1 + k_L} - (Q + l_L) + \mu_1(L_2 - L_1)$$

$$\frac{\mathrm{d}L_2}{\mathrm{d}t} = \frac{v_L L_2 R_2}{R_2 + k_L} - (bM + Q + l_L) + \mu_2(L_1 - L_2)$$

$$\frac{\mathrm{d}Z_1}{\mathrm{d}t} = \frac{\varepsilon a_S S_1 Z_1}{1 + a_S T_S S_1 + a_L T_L L_1} - (l_Z + Q) Z_1 + \mu_1(Z_2 - Z_1)$$

$$\frac{\mathrm{d}Z_2}{\mathrm{d}t} = \frac{\varepsilon a_S S_2 Z_2}{1 + a_S T_S S_2 + a_L T_L L_2} - (l_Z + Q) Z_2 + \mu_2(Z_1 - Z_2)$$

this extension permits a simple resolution of all of the discrepancies between predicted and observed behaviour that we identified in our well-mixed model.

Model II: partial mixing in a two-compartment model

Dreissenids are restricted to the bottom surface of the basin and potentially refilter the lowest portion of the water column more quickly than it mixes with water near the surface (Yu and Culver 1999; Ackerman et al. 2001). This hypothesis is supported by chlorophyll samples taken at multiple depths above mussel beds that show a gradient of increasing concentration with height for approximately 1–2 m above the benthos (MacIsaac et al. 1992, 1999; Ackerman et al. 2001). Although dreissenid filtering does not necessarily cause this gradient, low prey availability near the benthos implies that mussel filtering impact may be limited by the rate of vertical mixing. Furthermore, the patchy distribution of dreissenid populations within a basin suggests that mussel filtering impact may also be limited by horizontal mixing. These considerations suggest that there may be effective spatial separation between zebra mussels and their prey. We extend our well-mixed model to explicitly include such spatial separation in order to examine its role in moderating the impact of zebra mussel filtering on the pelagic food chain.

Structure

To analyze the effects of spatial structure on the predicted impact of mussels, we incorporate the simplest possible representation of spatial processes in our model. We divide the well-mixed compartment into two compartments, one occupied by dreissenids and the other unoccupied. Mussel filtering directly affects only the occupied compartment, but the two compartments are connected by mixing. In this structure, dreissenids are potentially limited by the rate of delivery of phytoplankton from the unoccupied to the occupied compartment. The two-compartment structure is not intended to represent true compartmentalization of lakes, such as thermal stratification, which severely restricts mixing. Rather, it is the simplest approximation to a continuously mixing basin in which localized mussel populations create differences in the effective filtering impact across space.

Equations for the two-compartment model are listed in Table 5. Modifications consist of splitting each food web component into populations in compartments occupied and unoccupied by zebra mussels and adding a mixing term to each equation. For simplicity, we assume that all four components have equal mixing rates between compartments and that basin inflow and outflow enter and leave the compartments in proportion to their relative volumes. The mixing rate for compartment i (μ_i) is proportional to the rate of water crossing the boundary surface shared by the two compartments, divided by the volume of the compartment:

$$\mu_i = \frac{\sigma A}{V_i} \tag{10}$$

where A is the shared surface area, V_i is the volume of compartment i, and σ is a rate coefficient (with units m·day^{-1}).

The three parameters in eq. 10 are functions of physical characteristics of the basin that are difficult to quantify. Shared surface area and volume of each compartment depend on the fraction of the bottom of the basin that is occupied by dreissenids, the patchiness of the occupied habitat, and the fraction of the water column that is included in the occupied compartment. The mixing rate coefficient σ depends on turbulence in the water column generated by forces such as wind or currents.

Fig. 4. Equilibria for the two-compartment model as functions of water mixing rate: (*a*) zooplankton; (*b*) phosphorus; (*c*) small phytoplankton; and (*d*) large phytoplankton. We arbitrarily assume that the occupied compartment includes one-half of the water column. Relative size of the two compartments is held constant by increasing the mixing rates by the same factor, maintaining the ratio $\mu_2/\mu_1 = V_1/V_2 = (1 - (0.5)(0.15)/((0.5)(0.15)) = 12.3$ for 15% occupied surface. We set $bM = 5.86$ day^{-1}, the lower value of the local filtering impact multiplied by 2 in order to maintain the same mussel abundance used in the original calculation of filtering impact. The whole-basin average filtering impact is therefore $bM = 5.86(V_2/(V_1 + V_2)) = 0.44$ day^{-1}. ○, compartment 1, mussels absent; ×, compartment 2, mussels present. Arrows and dotted lines indicate basic single-compartment model equilibria for (*x*) mussels absent, (*y*) $bM = 5.86$ day^{-1}, and (*z*) $bM = 0.44$ day^{-1}.

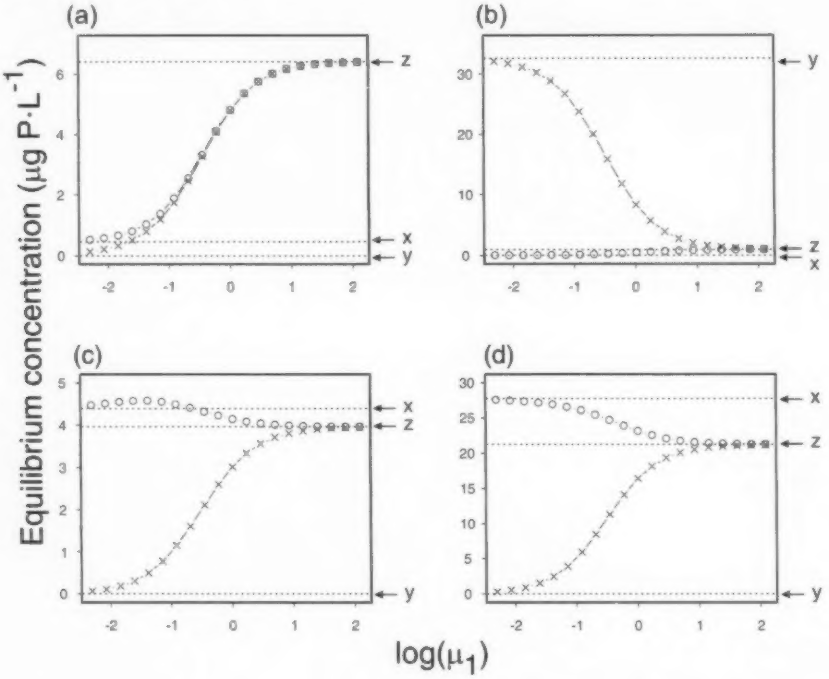

Qualitative behaviour

A thorough analysis of the effects of spatial structure on the model behavior is beyond the scope of this paper. Here, we present numerical solutions for the equilibria over a limited range of parameter values in order to show how mussel filtering can suppress phytoplankton populations, despite having a negligible effect on zooplankon abundance. In particular, we examine two abiotic features that are clearly linked to mussel filtering impact. First, increasing both μ_is by the same factor increases the rate of mixing between the two compartments caused by, for example, increasing turbulence (higher σ) or more patchily distributed mussel beds (higher A). Second, increasing $\mu_1/\mu_2 = V_2/V_1$, where $i = 1$ for the unoccupied compartment and $i = 2$ for the occupied compartment, represents increasing the fraction of the bottom that is occupied or the fraction of the water column that is included in the occupied compartment, either of which increases the volume of the occupied compartment (V_2).

Equilibria calculated over a range of mixing rates with constant μ_1/μ_2 are displayed (Fig. 4). The equilibria vary between two extremes. First, with low mixing, the two compartments act approximately like isolated basins, either with or without dreissenids. Hence, the equilibria approach values calculated from the single-compartment model. In the occupied compartment, S^*, L^*, and Z^* approach zero because the mussel filtering impact is sufficient to drive all three plankton groups extinct. In the unoccupied compartment, the equilibria approach values from the single-compartment model with $bM = 0$. As mixing increases, the two compartments act increasingly like a single well-mixed basin with mussel filtering impact diluted by the additional water volume of the unoccupied compartment.

We demonstrate the responses of the equilibria to increasing the area of the occupied compartment with filtering impact held constant (Fig. 5). Increasing the fraction of the benthos occupied by dreissenids implies that V_2 increases and V_1 decreases. If we assume that mixing increases with the proportion of benthic surface area occupied by dreissenids (i.e., vertical mixing), the ratio A/V_2, and therefore μ_2, are constant (eq. 10). Similarly, V_1 decreases and A increases, so μ_1 increases with occupied surface area. We fix μ_2 at a low value, where the equilibria approach values for isolated basins in Fig. 4, so spatial structure has a large effect. (For large μ_2, the basin is approximately well mixed, and increasing the fraction of bottom surface occupied is effectively the same as increasing bM in Fig. 4.) The results in Fig. 5 demonstrate how increasing the fraction occupied by mussels enriches the unoccupied compartment with recycled phosphorus but simultaneously increases phytoplankton losses to mussel filtering in the occupied compartment. The

Fig. 5. Equilibria for the two-compartment model with increasing fraction of surface occupied (increasing μ_1/μ_2, $\mu_2 = 0.1$ day^{-1}): (*a*) zooplankton; (*b*) phosphorus; (*c*) small phytoplankton; and (*d*) large phytoplankton. In the occupied compartment, $bM = 5.86$ day^{-1} (see Fig. 4 legend). ○, compartment 1, mussels absent; ×, compartment 2, mussels present. Equilibrium phosphorus concentration in compartment 1 multiplied by 100 for clarity.

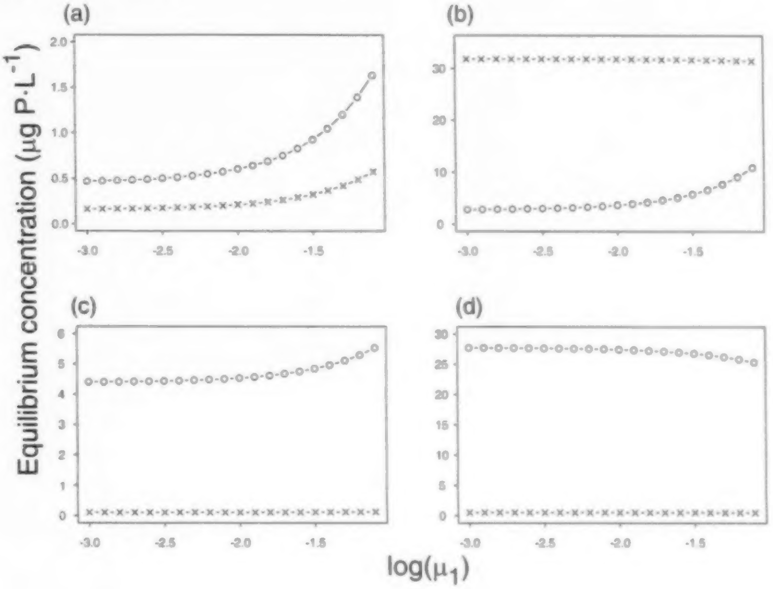

changing balance between nutrient delivery and population losses favors the faster-growing small phytoplankton, which supports higher equilibrium zooplankton density.

We show that spatial isolation of mussels allows zooplankton and phytoplankton to persist, despite high mussel density and filtering rate, by reducing the effective filtering impact (Figs. 4, 5). However, spatial isolation reduces the positive effect of mussel filtering on zooplankton only slightly and only if mixing is low enough that the two compartments act as nearly separate basins. With such slow mixing, the effect of mussel filtering on both phytoplankton groups is weak (Fig. 4). Even at this low mixing rate, the zooplankton equilibrium increases with the fraction of benthic surface that is occupied by mussels, but the effect on phytoplankton abundance is minimal (Fig. 5). Indeed, the mechanism causing the increase in zooplankton in the single-compartment model operates in the identical fashion in the two-compartment model: mussel filtering decreases the competitive effect of large phytoplankton, which allows small phytoplankton to acquire a larger share of the available phosphorus and indirectly benefits zooplankton.

The importance of nutrient competition to predicting the effect of dreissenid filtering on zooplankton suggests that sequestration and burial of phosphorus by mussels provides a key to understanding the insensitivity of zooplankton populations to the dreissenid invasion in the western basin of Lake Erie. Although reducing the fraction of phosphorus returned to the water column by mussels quickly reduces productivity such that the planktonic food web cannot persist in the single-compartment model, spatial isolation can minimize this effect of dreissenids. We demonstrate the effect of dreissenid filtering on the equilibria for low mixing and low fraction of phosphorus returned to the water column ($f = 0.01$; Fig. 6). Under these conditions, zooplankton density in the unoccupied compartment is insensitive to mussel filtering impact, whereas both phytoplankton groups decrease but persist for a broad range of plausible values. Most phosphorus consumed by mussels is lost from the system, and the competitive advantage of small phytoplankton over large phytoplankton is offset by reduced nutrient supply.

Discussion

We used a simple model to show that basic assumptions about plankton dynamics result in unrealistically extreme effects of dreissenid filtering. However, consideration of the spatial structure created when sessile benthic filter feeders invade a pelagic food web leads to radically different results, which are consistent with empirical data from the western basin of Lake Erie. Previous studies have suggested that dreissenid filtering impact is not simply related to mussel density, as in the well-mixed case, but also depends on local effects. For instance, Yu and Culver (1999) demonstrated that mussels refilter water more rapidly than seston is replenished by mixing and that refiltering increases with mussel clumping. MacIsaac et al. (1999) reproduced the observed vertical gradient in chlorophyll concentration over a mussel bed with a simulation model of mussel grazing and phytoplankton distribution in a continuous vertical cross section of the water column. Here, we simplified the spatial structure into distinct compartments occupied and unoccupied by dreissenids to analyze the indirect effects of mussel filtering on zooplankton and phytoplankton.

Fig. 6. Equilibria for the two-compartment model with increasing filtering impact, low phosphorus recycling by mussels ($f = 0.01$), and low mixing ($\mu_1 = 0.01\ \text{day}^{-1}$, $\mu_2 = 0.123\ \text{day}^{-1}$): (*a*) zooplankton; (*b*) phosphorus; (*c*) small phytoplankton; and (*d*) large phytoplankton. ○, compartment 1, mussels absent; ×, compartment 2, mussels present.

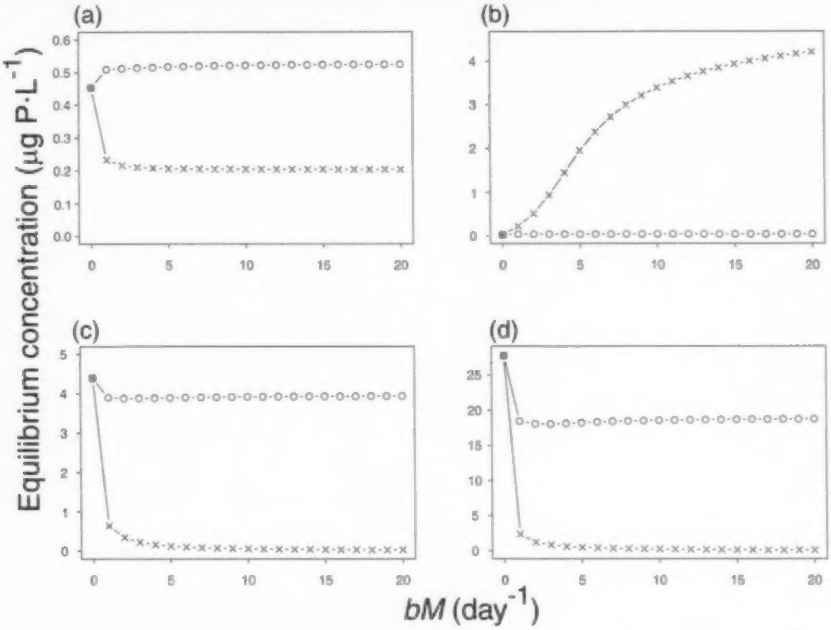

Our analysis of the single-compartment model, in which we assumed the entire water column is well mixed, demonstrated that the initial positive effect of dreissenids on zooplankton density is predicted for a broad range of conditions. This response is driven by the difference in competitive abilities of the two phytoplankton groups. Such differences have been documented in diverse taxa (reviewed in Andersen 1997). By excluding terms describing phytoplankton self-shading and inedible phytoplankton interference with zooplankton filtering, we showed that these mechanisms can contribute to the positive effect, but they are not necessary to explain it. However, the initial increase in zooplankton is not sufficient to offset high mussel filtering impact and the model predicts that zooplankton disappear from the system at filtering rates that are much lower than those that have been observed. Indeed, with a well-mixed water column, the food web cannot withstand a mussel filtering impact greater than the maximum growth rate of edible phytoplankton, and the value of this parameter (ν_S) is bounded by a large body of empirical data (e.g., Andersen 1997). We conclude that even with more careful parameterization, our well-mixed, single-compartment model can not account for the observed insensitivity of zooplankton abundance to mussel filtering.

The well-mixed model developed in this paper differs from earlier work by Padilla et al. (1996) in several ways. The most important difference is in our treatment of water flow through the system and its effect on nutrients and plankton groups. We assumed that water movement through the system imposes a density-independent loss term on each component of the food web such that nutrients and all three planktonic groups flow out of the system at a rate that is proportional to their density in the basin. This assumption is based on the expectation that the biotic and abiotic components of the model will exhibit largely passive movement with respect to water outflow from the system. In contrast, Padilla et al. (1996) assumed that biotic components remain in the system, whereas available phosphorus is flushed out at a constant rate, independent of its concentration. If the flushing rate is less than the inflow rate, the system accumulates phosphorus with time. It is difficult to see how this structure could be realized in the field; however, it is this buildup of phosphorus over the growing season that offsets phytoplankton production lost to zebra mussel filtering and thus is fundamental to the prediction of the Padilla et al. (1996) model that zooplankton will be relatively insensitive to zebra mussel filtering. In our model, the same prediction derives from the well-founded assumption that the phytoplankton community consists of edible and inedible forms of algae that compete for the same limiting nutrient. In our well-mixed model, careful accounting for phosphorus inflow and outflow leads to the prediction that the zooplankton population increases for low mussel abundance but can not withstand realistically high mussel filtering impact.

However, our model is still a highly simplified representation of the plankton community. For instance, in experiments with two zooplankton taxa with different feeding modes, Sommer et al. (2001) demonstrated an interactive effect on total phytoplankton density. Similarly, the phytoplankton community and its responses to herbivory and nutrient supply can be complex and vary spatially and temporally. Evidence from the western basin of Lake Erie suggests that, in offshore waters, the density of some phytoplankton taxa increased after dreissenid invasion, whereas others decreased (Makarewicz et al. 1999; Munawar and Munawar 1999). On the other hand, Nicholls and Hopkins (1993) found that all species decreased in nearshore samples.

Nevertheless, we suggest that the mechanisms underlying the indirect effects of mussel filtering on plankton populations, revealed by our analysis of the basic model, operate in natural systems. Indeed, the predicted increase in relative abundance of edible phytoplankton in response to mussel filtering is consistent with data from the western basin of Lake Erie (Wu and Culver 1991). Furthermore, the processes that drive the counterintuitive effect of dreissenid filtering on zooplankton in the basic model are crucial to explaining our results from the spatially structured model. The ability of zooplankton to persist despite strong mussel filtering impact depends on limited delivery of phytoplankton to the benthos and phosphorus burial by dreissenids, in addition to differences in edibility and competitive ability between phytoplankton groups. Low mixing between compartments reduces the capture rate of mussels, similar to low filtering impact in the well-mixed model; however, the positive effect of low filtering impact on zooplankton is offset by phosphorus burial in the two-compartment model. These mechanisms are not specific to the two-compartment spatial structure that we have used in our model but are applicable to a continuously mixing water column.

Results from the two-compartment model support the conclusion that water column turnover time, a frequently reported measure of filtering impact (e.g., MacIsaac et al. 1992; Bunt et al. 1993; Bailey et al. 1999) that is based on the assumption that the water column is well-mixed, generally overestimates the direct effect of mussels on plankton dynamics (Yu and Culver 1999; Ackerman et al. 2001). Instead, we suggest that the realized dreissenid filtering impact is modified by abiotic features of the basin, such as turbulent mixing, depth, and spatial arrangement of suitable benthic substrate. These characteristics determine the rate of phytoplankton delivery to mussels.

Mixing rate and phosphorus recycling are probably correlated and typically low in the western basin of Lake Erie. Turbulent mixing of the water column resuspends mussel feces and pseudofeces, in which much of the captured food is deposited (e.g., Walz (1978) found that over 60% of captured phytoplankton was rejected as pseudofeces at high food concentration). Although wind at the water surface can mix the entire water column in such a shallow basin, current velocity near the benthos is often low (MacIsaac et al. 1999; Ackerman et al. 2001). The chlorophyll gradient above mussel beds observed by MacIsaac et al. (1992, 1999) and Ackerman et al. (2001) suggests a combination of filtering at the bottom surface and relatively slow turbulent mixing with upper portions of the water column.

The two-compartment model predicts that if mixing and dreissenid recycling are low, changes in mussel abundance above a relatively low density will have little effect on phytoplankton or zooplankton populations. After the invasion has surpassed this threshold, mussels capture nearly all phytoplankton that enter the occupied compartment. This prediction implies that dreissenids can be food-limited while their food is still abundant in the upper portion of the water column, even in a shallow, unstratified basin. Alternatively, zebra mussels may obtain a substantial portion of their food from dead or sinking phytoplankton (Yu and Culver 1999) and even dissolved organic carbon (Roditi et al. 2000), which could weaken the link between mussel and phytoplankton dynamics. Knowledge of the rate at which phytoplankton are delivered to the benthos by turbulent mixing would allow estimation of the relative importance of food and suitable benthic habitat to dressenid population regulation.

Acknowledgements

We thank O. Johannsson, S. Peacor, and three anonymous reviewers for helpful comments on the manuscript. Funding was provided by the Great Lakes Fisheries Commission.

References

Ackerman, J.D., Loewen, M.R., and Hamblin, P.F. 2001. Benthic–pelagic coupling over a zebra mussel reef in western Lake Erie. Limnol. Oceanogr. **46**: 892–904.

Andersen, T. 1997. Pelagic nutrient cycles: herbivores as sources and sinks. Springer-Verlag, Berlin.

Bailey, R.C., Grapentine, L., Stewart, T.J., Schaner, T., Chase, M.E., Mitchell, J.S., and Coulas, R.A. 1999. Dreissenidae in Lake Ontario: impact assessment at the whole lake and Bay of Quinte spatial scales. J. Gt. Lakes Res. **25**: 482–491.

Bastviken, D.T.E., Caraco, N.F., and Cole, J.J. 1998. Experimental measurements of zebra mussel (*Dreissena polymorpha*) impacts on phytoplankton community composition. Freshw. Biol. **39**: 375–386.

Berg, D.J., Fisher, S.W., and Landrum, P.F. 1996. Clearance and processing of algal particles by zebra mussels (*Dreissena polymorpha*). J. Gt. Lakes Res. **22**: 779–788.

Berkman, P.A., Haltuch, M.A., Tichich, E., Garton, D.W., Kennedy, G.W., Gannon, J.E., Mackey, S.D., Fuller, J.A., and Liebenthal, D.L. 1998. Zebra mussels invade Lake Erie muds. Nature (Lond.), **393**: 27–28.

Bridgeman, T.B., Fahnenstiel, G.L., Lang, G.A., and Nalepa, T.F. 1995. Zooplankton grazing during the zebra mussel (*Dreissena polymorpha*) colonization of Saginaw Bay, Lake Huron. J. Gt. Lakes Res. **21**: 567–573.

Bunt, C.M., MacIsaac, H.J., and Sprules, W.G. 1993. Pumping rates and projected filtering impacts of juvenile zebra mussels (*Dreissena polymorpha*) in western Lake Erie. Can. J. Fish. Aquat. Sci. **50**: 1017–1022.

Carpenter, S.R. 1992. Destabilization of planktonic ecosystems and blooms of blue-green algae. *In* Food web management: a case study of Lake Mendota. *Edited by* J.F. Kitchell. Springer-Verlag, Berlin. pp. 461–481.

Coakley, J.P., Brown, G.R., Ioannou, S.E., and Charlton, M.N. 1997. Colonization patterns and densities of zebra mussel *Dreissena* in muddy offshore sediments of western Lake Erie, Canada. Water Air Soil Pollut. **99**: 623–632.

Czech, B., and Krausman, P.R. 1997. Distribution and causation of species endangerment in the United States. Science (Wash., D.C.), **277**: 1116–1117.

Dermott, R., and Munawar, M. 1993. Invasion of Lake Erie offshore sediments by *Dreissena*, and its ecological implications. Can. J. Fish. Aquat. Sci. **50**: 2298–2304.

Dillon, P.J., and Rigler, F.H. 1974. The phosphorus–chlorophyll relationship in lakes. Limnol. Oceanogr. **19**: 767–773.

Hebert, P.D.N., Muncaster, B.W., and Mackie, G.L. 1989. Ecological and genetic studies on *Dreissena polymorpha* (Pallas): a new mollusc in the Great Lakes. Can. J. Fish. Aquat. Sci. **46**: 1587–1591.

Horgan, M.J., and Mills, E.L. 1997. Clearance rates and filtering activity of zebra mussel *Dreissena polymorpha*: implications for freshwater lakes. Can. J. Fish. Aquat. Sci. **54**: 249–255.

Idrisi, N., Mills, E.L., Rudstam, L.G., and Stewart, D.J. 2001. Impact of zebra mussels (*Dreissena polymorpha*) on the pelagic lower trophic levels of Oneida Lake, New York. Can. J. Fish. Aquat. Sci. **58**: 1430–1441.

Johannsson, O.E., Dermott, R., Graham, D.M., Dahl, J.A., Millard, E.S., Myles, D.D., and LeBlanc, J. 2000. Benthic and pelagic secondary production in Lake Erie after the invasion of *Dreissena* spp. with implications for fish production. J. Gt. Lakes Res. **26**: 31–54.

Johnson, L.E., and Carlton, J.T. 1996. Post-establishment spread in large-scale invasions: dispersal mechanisms of the zebra mussel *Dreissena polymorpha*. Ecology, **77**: 1686–1690.

Kryger, J., and Riisgård, H.U. 1988. Filtration rate capacities in 6 species of European freshwater bivalves. Oecologia, **77**: 34–38.

Leach, J.H. 1993. Impacts of the zebra mussel (*Dreissena polymorpha*) on water quality and fish spawning reefs in western Lake Erie. *In* Zebra mussels: biology, impacts: and control. *Edited by* T.F. Nalepa and D.W. Schloesser. Lewis Publishers, Boca Raton, Fla. pp. 381–397.

MacIsaac, H.J., Johannsson, O.E., Ye, J., Sprules, W.G., Leach, J.H., McCorquodale, J.A., and Grigorovich, I.A. 1999. Filtering impacts of an introduced bivalve (*Dreissena polymorpha*) in a shallow lake: application of a hydrodynamic model. Ecosystems, **2**: 338–350.

MacIsaac, H.J., Sprules, W.G., Johannsson, O.E., and Leach, J.H. 1992. Filtering impacts of larval and sessile zebra mussels (*Dreissena polymorpha*) in western Lake Erie. Oecologia, **92**: 30–39.

Mack, R.N., Simberloff, D., Lonsdale, W.M., Evans, H., Clout, M., and Bazzaz, F.A. 2000. Biological invasions: causes, epidemiology, global consequences, and control. Ecol. Appl. **10**: 689–710.

Makarewicz, J.C., Lewis, T.W., and Bertram, P. 1999. Phytoplankton composition and biomass in the offshore waters of Lake Erie: pre- and post-*Dreissena* introduction (1983–1993). J. Gt. Lakes Res. **25**: 135–148.

McCauley, E., Nisbet, R.M., De Roos, A.M., Murdoch, W.W., and Gurney, W.S.C. 1996. Structured population models of herbivorous zooplankton. Ecol. Monogr. **66**: 479–501.

Mellina, E., and Rasmussen, J.B. 1994. Patterns in the distribution and abundance of zebra mussel (*Dreissena polymorpha*) in rivers and lakes in relation to substrate and other physicochemical factors. Can. J. Fish. Aquat. Sci. **51**: 1024–1036.

Mellina, E., Rasmussen, J.B., and Mills, E.L. 1995. Impact of zebra mussel (*Dreissena polymorpha*) on phosphorus cycling and chlorophyll in lakes. Can. J. Fish. Aquat. Sci. **52**: 2553–2573.

Munawar, M., and Munawar, I.F. 1999. The changing phytoplankton biomass and its composition in Lake Erie: a lakewide comparative analysis. *In* State of Lake Erie (SOLE): past, present and future. *Edited by* M. Munawar, T. Edsall, and I.F. Munawar. Backhuys Publishers, Leiden. pp. 125–154.

Nalepa, T.F., and Schloesser, D.W. (*Editors*). 1993. Zebra mussels: biology, impacts, and control. Lewis Publishers, Boca Raton, Fla.

Nalepa, T.F., Wojcik, J.A., Fanslow, D.L., and Lang, G.A. 1995. Initial colonization of the zebra mussel (*Dreissena polymorpha*) in Saginaw Bay, Lake Huron: population recruitment, density, and size strucutre. J. Gt. Lakes Res. **21**: 417–434.

Nalepa, T.F., Fahnenstiel, G.L., and Johengen, T.H. 1999. Impacts of the zebra mussel (*Dreissena polymorpha*) on water quality: a case study in Saginaw Bay, Lake Huron. *In* Nonindigenous freshwater organisms: vectors, biology, and impacts. *Edited by* R. Claudi and J.H. Leach. Lewis Publishers, Boca Raton, Fla. pp. 255–271.

Nicholls, K.H., and Hopkins, G.J. 1993. Recent changes in Lake Erie (North Shore) phytoplankton: cumulative impacts of phosphorus loadings and the zebra mussel introduction. J. Gt. Lakes Res. **19**: 637–647.

Olsen, Y., and Østgaard, K. 1985. Estimating release rates of phosphorus from zooplankton: model and experimental verification. Limnol. Oceanogr. **30**: 844–852.

Padilla, D.K., Adolph, S.C., Cottingham, K.L., and Schneider, D.W. 1996. Predicting the consequences of dreissenid mussels on a pelagic food web. Ecol. Model. **85**: 129–144.

Parker, I.M., Simberloff, D., Lonsdale, W.M., Goodell, K., Wonham, M., Kareiva, P.M., Williamson, M.H., VonHolle, B., Moyle, P.B., Byers, J.E., and Goldwasser, L. 1999. Impact: toward a framework for understanding the ecological effects of invaders. Biol. Invas. **1**: 3–19.

Peters, R.H., and Rigler, F.H. 1973. Phosphorus release by *Daphnia*. Limnol. Oceanogr. **18**: 821–839.

Pimentel, D., Lach, L., Zuniga, R., and Morrison, D. 2000. Environmental and economic costs of nonindigenous species in the United States. BioScience, **50**: 53–65.

Reeders, H.H., bij de Vaate, A., and Noordhuis, R. 1993. Potential of the zebra mussel (*Dreissena polymorpha*) for water quality management. *In* Zebra mussels: biology, impacts, and control. *Edited by* T.F. Nalepa and D.W. Schloesser. Lewis Publishers, Boca Raton, Fla. pp. 439–451.

Reynolds, C.S. 1984. The ecology of freshwater phytoplankton. Cambridge University Press, Cambridge.

Roditi, H.A., Fisher, N.S., and Sanudo-Wilhelmy, S.A. 2000. Uptake of dissolved organic carbon and trace elements by zebra mussels. Nature (Lond.), **407**: 78–80.

Scavia, D., Lang, G.A., and Kitchell, J.F. 1988. Dynamics of Lake Michigan plankton: a model evaluation of nutrient loading, competition, and predation. Can. J. Fish. Aquat. Sci. **45**: 165–177.

Shuter, B.J. 1978. Size dependence of phosphorus and nitrogen subsistence quotas in unicellular microorganisms. Limnol. Oceanogr. **23**: 1248–1255.

Sommer, U., Sommer, F., Santer, B., Jamieson, C., Boersma, M., Becker, C., and Hansen, T. 2001. Complementary impact of copepods and cladocerans on phytoplankton. Ecol. Lett. **4**: 545–550.

Sprung, M., and Rose, U. 1988. Influence of food size and food quality on the feeding of the mussel *Dreissena polymorpha*. Oecologia, **77**: 526–532.

Stoeckmann, A.M., and Garton, D.W. 1997. A seasonal energy budget for zebra mussels (*Dreissena polymorpha*) in western Lake Erie. Can. J. Fish. Aquat. Sci. **54**: 2743–2751.

Strayer, D.L., Caraco, N.F., Cole, J.J., Findlay, S., and Pace, M.L. 1999. Transformation of freshwater ecosystems by bivalves. BioScience, **49**: 19–27.

Ten Winkel, E.H., and Davids, C. 1982. Food selection by *Dreissena polymorpha* Pallas (Mollusca: Bivalvia). Freshw. Biol. **12**: 553–558.

Vanderploeg, H.A., Liebig, J.R., Carmichael, W.W., Agy, M.A., Johengen, T.H., Fahnenstiel, G.L., and Nalepa, T.F. 2001. Zebra mussel (*Dreissena polymorpha*) selective filtration promoted toxic *Microcystis* blooms in Saginaw Bay (Lake Huron) and Lake Erie. Can. J. Fish. Aquat. Sci. **58**: 1208–1221.

Walz, N. 1978. The energy balance of the freshwater mussel *Dreissena polymorpha* Pallas in laboratory experiments and

Lake Constance. I. Pattern of activity, feeding and assimilation efficiency. Arch. Hydrobiol. **55**: 83–105.

Wu, L., and Culver, D.A. 1991. Zooplankton grazing and phytoplankton abundance: an assessment before and after invasion of *Dreissena polymorpha*. J. Gt. Lakes Res. **17**: 425–436.

Yu, N., and Culver, D.A. 1999. Estimating the effective clearance rate and refiltration by zebra mussels, *Dreissena polymorpha*, in a stratified reservoir. Freshw. Biol. **41**: 481–492.

Appendix A: response of equilibria to dreissenid invasion

First, we differentiate R^* with respect to M:

$$\text{(A1)}\quad \frac{\mathrm{d}R^*}{\mathrm{d}M} = \frac{k_L b v_L}{(v_L - (l_L + bM + Q))^2}$$

This expression is positive for all $M \geq 0$, so mussel invasion increases the equilibrium concentration of available phosphorus. Similarly,

$$\text{(A2)}\quad \frac{\mathrm{d}S^*}{\mathrm{d}M} = \frac{(l_Z + Q)a_L T_L}{a_S(\varepsilon - T_S(l_Z + Q))}\frac{\mathrm{d}L^*}{\mathrm{d}M}$$

Because $\varepsilon - T_S(l_Z + Q) > 0$ for $S^* > 0$ (Table 3), the change in the two phytoplankton groups must have the same sign.

Differentiating Z^* with respect to M and setting $M = 0$ gives

$$\text{(A3)}\quad \left.\frac{\mathrm{d}Z^*}{\mathrm{d}M}\right|_{M=0} = \left(\frac{v_S k_S \dfrac{\mathrm{d}R^*}{\mathrm{d}M}}{(k_S + R^*)^2} - b\right)\left(\frac{1 + a_S T_S L^* + a_L T_L L^*}{a_S}\right) + \left(\frac{v_S R^*}{k_S + R^*} - (l_S + Q)\right)\left(\frac{a_S T_S \dfrac{\mathrm{d}S^*}{\mathrm{d}M} + a_L T_L \dfrac{\mathrm{d}L^*}{\mathrm{d}M}}{a_S}\right)$$

where the derivatives on the right-hand side are evaluated at $M = 0$. For the case in which large phytoplankton do not interfere with zooplankton filtering ($a_L T_L = 0$), $\mathrm{d}S^*/\mathrm{d}M = 0$ (eq. A2) and the second term in eq. A3 disappears. With $a_L T_L = 0$, we can insert eq. A1 into eq. A3 and simplify to obtain

$$\text{(A4)}\quad \left.\frac{\mathrm{d}Z^*}{\mathrm{d}M}\right|_{M=0} = \left(\frac{v_S k_S v_L k_L}{((k_L - k_S)(l_L + Q) + v_L k_S)^2} - 1\right) \times \left(\frac{1 + a_S T_S S^*}{a_S}\right) b$$

The second term in parentheses is positive if $S^* \geq 0$. If $(k_L - k_S)(l_L + Q)$ is small relative to $v_L k_S$, the first term is positive if

$$\text{(A5)}\quad \frac{v_S k_L}{v_L k_S} > 1$$

This condition is eq. 8 in the text.

Phytoplankton density ($S^* + L^*$) must decrease with M during the initial invasion because R^* and Z^* increase, and total phosphorus in the system remains the same or decreases (if $f < 1$) with M.

Appendix B: parameterization

Water inflow and phosphorus concentration

Mellina et al. (1995, their table 1) summarize hydrological parameters for the western basin of Lake Erie. To calculate the water inflow rate, we divide average daily water inflow (0.518 $\mathrm{km^3 \cdot day^{-1}}$) by basin volume (28 $\mathrm{km^3}$) to obtain Q = 0.02 $\mathrm{day^{-1}}$. For the phosphorus concentration of water inflow, we divide the average phosphorus load for 1987–1990 (Nicholls and Hopkins 1993, their table 1) by the average annual water inflow from Mellina et al. (1995). The result is R_{in} = 33 $\mathrm{\mu g\ P \cdot L^{-1}}$.

Phytoplankton

The Monod model of phosphorus uptake by phytoplankton depends on two parameters: the maximum uptake rate (v_S, v_L) and the half-saturation concentration (k_S, k_L). Based on a literature survey of parameter estimates for individual phytoplankton species, Andersen (1997) suggested that the upper and lower quartiles of the distribution are reasonable approximations for two species groups with a trade-off between competitive ability and grazer resistance. Scavia et al. (1988) and Padilla et al. (1996) present values for phytoplankton groups distinguished by their edibility to zooplankton in Saginaw Bay (Lake Huron) and Green Bay (Lake Michigan), respectively. Estimates of maximum uptake rates for edible and inedible phytoplankton in both bays are roughly equal to the upper and lower quartiles in Andersen's (1997) survey distribution. We use the upper quartile for small phytoplankton (v_S = 1.8 $\mathrm{day^{-1}}$) and the lower quartile for large phytoplankton (v_L = 0.8 $\mathrm{day^{-1}}$).

The difference between the two phytoplankton groups in their half-saturation constants reported by Scavia et al. (1988) and Padilla et al. (1996) was small relative to the difference between quartiles in Andersen (1997), which suggests that the primary competitive difference between small and large phytoplankton is in their maximum uptake rates. Although estimates of the half-saturation concentrations from Scavia et al. (1988) are consistent with Andersen's (1997) survey, the values used by Padilla et al. (1996) are an order of magnitude larger than the upper quartile of the survey distribution. This seems surprising, because the parameter represents a composite of several species and should take a typical value. Hence, we let $k_S = k_L$ = 0.7 $\mathrm{\mu g\ P \cdot L^{-1}}$, the median of the distribution from Andersen (1997).

Phytoplankton loss to sinking and other density-independent mortality is difficult to measure. Values listed by Scavia et al. (1988) and Padilla et al. (1996) suggest the range 0–0.05 $\mathrm{day^{-1}}$. Because the western basin of Lake Erie does not stratify, phytoplankton cannot be trapped beneath the thermocline and may be resuspended by turbulence. Hence, we use a value at the low end of the range and let $l_S = l_L$ = 0.01 $\mathrm{day^{-1}}$.

Zooplankton

Zooplankton require six parameters: capture rates (a_S, a_L) and handling times (T_S, T_L) for the two phytoplankton groups, excretion rate (l_Z), and assimilation efficiency (ε). Our estimates for these parameters are based on measurements of adult *D. galeata*. We use data from McCauley et al. (1996), who report carbon ingestion and loss rates. We convert their estimates to units of phosphorus.

We assume that the ratio of phosphorus and carbon in *Daphnia* tissue is approximately constant. Hence, we use the mass-specific maintenance rate, 0.176 day^{-1}, reported by McCauley et al. (1996) for the loss parameter l_Z. This value falls within the range of phosphorus excretion rates measured directly in *D. pulex* by Olsen and Østgaard (1985).

Zooplankton capture rate and handling time for edible phytoplankton can be calculated from maximum ingestion rate ($I_{\max}$) and half-saturation food concentration (F_{H}) as $a_S = I_{\max}/F_{\mathrm{H}}$ and $T_S = 1/I_{\max}$. Using the ratio P:C = 0.02 for phytoplankton (Reynolds 1984), P:C = 0.038 for *Daphnia* (Peters and Rigler 1973), and $I_{\max} = 0.025$ mg C·day^{-1} and $F_{\mathrm{H}} = 0.98$ mg C·L^{-1} for *D. galeata* (McCauley et al. 1996), we obtain $a_S = 0.16$ L·(μg P·day)$^{-1}$ and $T_S = 0.32$ days. We assume $T_L = T_S$ and $a_L = a_S$ to study the effects of inedible phytoplankton interference.

We let $\varepsilon = 0.54$, based on measurements of phosphorus assimilation efficiency by Peters and Rigler (1973).

Dreissenid filtering impact

MacIsaac et al. (1992) estimate the whole basin filtering impact per unit benthic area to be $bM = 13.9\ \text{m}^3\cdot\text{m}^{-2}\cdot\text{day}^{-1}$. This value is based on their measurements of mussel density and size structure and on size-specific filtering rate measurements from Kryger and Riisgård (1988). We divide the estimate from MacIsaac et al. (1992) by the average depth of the western basin of Lake Erie (7 m) to obtain the volume-specific filtering impact, 2.0 day^{-1}. If 15% of the benthic surface is occupied by mussels, the local impact is 13.3 day^{-1}.

We take our lower estimate of dreissenid filtering rate from Walz (1978). Walz's estimate of b is 0.22 times Kryger and Riisgård's (1988) value. Hence, the local and whole-basin filtering impacts are 2.93 day^{-1} and 0.44 day^{-1}, respectively.

Partitioning of dissolved thallium by seston in Lakes Erie and Ontario

Michael R. Twiss, Benjamin S. Twining, and Nicholas S. Fisher

Abstract: The fate of thallium (Tl) was traced in the epipelagic and coastal waters of Lake Erie (in 2000) and Lake Ontario (in 2001) sampled during the summer period of thermal stratification. Fractionation of ^{204}Tl bound to particulate matter was conducted to trace the scavenging potential of various seston size ranges (0.2–2 µm, 2–20 µm, and 20–210 µm). Added [^{204}Tl]-Tl(I) scavenged by seston over 1–3 days was 0.34–4.05% in Lake Erie and 0.09–0.21% in Lake Ontario, where scavenging was correlated with suspended particulate matter content and chlorophyll *a* concentration. There was no consistent trend with respect to Tl scavenging by a particular size fraction, except at coastal sites in Lake Erie where most Tl was scavenged by the 2–20 µm seston. Partition coefficients (K_d) of Tl scavenging by seston in Lake Ontario were 938–1483 L·kg^{-1}. At the same pelagic site in Lake Ontario, [^{204}Tl]-dimethylthallium partitioned into seston ($K_d = 807 \pm 258$) to a lesser degree than added Tl(I) ($K_d = 998 \pm 297$), a finding consistent with laboratory assays of these two Tl species. These results suggest that the plankton food web plays a role in the geochemical cycle of this toxic metal in the water column of the lower Great Lakes.

Résumé : Nous avons suivi le sort du thallium (Tl) dans les eaux épipélagiques et côtières des lacs Érié (2000) et Ontario (2001) lors d'échantillonnages durant la période estivale de stratification thermique. Nous avons étudié la fractionation du ^{204}Tl lié à la matière particulaire pour évaluer le potentiel de récupération par le seston de différentes tailles (0,2–2 µm, 2–20 µm et 20–210 µm). La quantité de [^{204}Tl]-Tl(I) ajouté récupérée par le seston au bout de 1–3 jours varie de 0,34 à 4,05 % au lac Érié et de 0,09 à 0,21 % au lac Ontario où la récupération est en corrélation avec le contenu en matière particulaire en suspension et la concentration de chlorophylle *a*. Il n'y a pas de tendance stable dans la récupération de Tl par une fraction particulière du seston, excepté à des sites côtiers du lac Érié où la majorité du Tl est récupérée par le seston de 2–20 µm. Le coefficient de partition (K_d) de la récupération de Tl par le seston au lac Ontario varie de 938–1483 L·kg^{-1}. Au même site pélagique du lac Ontario, le [^{204}Tl]-diméthylthallium se répartit dans le seston ($K_d = 807 \pm 258$) moins fortement que le Tl(I) ajouté ($K_d = 998 \pm 297$), ce qui est en accord avec des tests de laboratoires faits avec ces deux formes de Tl. Nos résultats montrent que le réseau alimentaire planctonique joue un rôle dans le cycle géochimique de ce métal toxique dans la colonne d'eau dans les Grands Lacs inférieurs.

[Traduit par la Rédaction]

Introduction

Thallium is a highly toxic metal that has only recently been measured reliably in Great Lakes waters. Concentrations of this metal are elevated in industrially impacted aquatic environments, such as the lower Great Lakes, where Tl enters open waters primarily as Tl_2O, a combustion product resulting from the smelting of sulfide ores, cement manufacturing, and fossil fuel combustion (World Health Organization 1996). Average total dissolved thallium concentrations range in the Great Lakes from 5.9 pmol·L^{-1} in Lake Superior to 28 pmol·L^{-1} in Lake Ontario, 42 pmol·L^{-1} in Lake Erie, 49 pmol·L^{-1} in Lake Huron, and 70 pmol·L^{-1} in Lake Michigan, with levels as high as 176 pmol·L^{-1} measured in the industrially impacted Hamilton Harbour, Lake Ontario (Cheam 2001).

The chemical speciation of Tl in the Great Lakes has been surveyed by Lin and Nriagu (1999*a*). Constant depth profiles of dissolved Tl concentrations suggest that Tl is relatively nonreactive. Approximately 5% of Tl in the water column of Great Lakes water is particulate Tl (>0.4 µm; Lin and Nriagu 1999*a*). Of the dissolved Tl in the water column, approximately 70% is Tl(III) (Lin and Nriagu 1999*a*), despite the fact that Tl(I) is the stable redox form of Tl in surface waters. Although Tl^{3+} is predicted to be a very particle-reactive ion on the basis of its high first hydrolysis constant ($K_{\mathrm{TlOH}^{2+}} = 10^{11.3}$; Lin and Nriagu 1998) and thus accumulated to a high degree by phytoplankton (sensu Fisher 1986), Tl(III) speciation is dominated by the inert $Tl(OH)_3$ complex (Table 1). As a result, the highly soluble, weakly reactive Tl^{+} ion is the more bioactive inorganic Tl species, despite it being much less toxic than the Tl^{3+} ion (Ralph and Twiss 2002).

Little is known about the aquatic biogeochemistry of this potentially hazardous trace metal in freshwaters, including an understanding of the routes of Tl uptake from the dis-

Received 10 September 2002. Accepted 16 May 2003. Published on the NRC Research Press Web site at http://cjfas.nrc.ca on 24 November 2003.
J17090

M.R. Twiss.[1,2] Department of Chemistry, Biology and Chemical Engineering, Ryerson Polytechnic University, 350 Victoria Street, Toronto, ON M5B 2K3, Canada.
B.S. Twining and N.S. Fisher. Marine Sciences Research Center, Stony Brook University, Stony Brook, NY 11794-5000, U.S.A.

[1] Corresponding author (e-mail: mtwiss@clarkson.edu).

[2] Present address: Department of Biology, Clarkson University, Potsdam, NY 13699-5805, U.S.A.

Can. J. Fish. Aquat. Sci. **60**: 1369–1375 (2003) doi: 10.1139/F03-119

Table 1. Thermodynamic estimation of inorganic thallium (Tl) speciation in Great Lakes surface waters, pH 8, total Tl = 1.2 nM.

Thallium species	Concentration ($mol \cdot L^{-1}$)	Proportion of total Tl (%)
Tl^3+	1.7×10^{-17}	1×10^{-6}
$TlOH^2+$	3.5×10^{-12}	0.3
$Tl(OH)_2+$	1.5×10^{-10}	13
$Tl(OH)_3$	5.9×10^{-10}	49
$Tl(OH)_4^-$	9.7×10^{-11}	8
Tl+	3.6×10^{-10}	30
TlOH	7.2×10^{-14}	0.006

Note: Inorganic chemical speciation of redox states of Tl was calculated using MINEQL+ (ver. 4.5) with Tl hydrolysis constants reported by Lin and Nriagu (1998) and assuming a 7:3 ratio of Tl(III) to Tl(I) (Lin and Nriau 1999*a*). The speciation of dimethylthallium, $(CH_3)_2Tl^+$, with respect to hydrolysis is predicted to be 100% $(CH_3)_2Tl^+$ at pH 8 ($K_{DMT\text{-}OH} = 10^{-12.95}$; Martell et al. 1998).

solved phase into the microbial food web and subsequently into higher organisms such as fish. The bioconcentration factor of Tl in lake trout from Lake Michigan is calculated to be 10 000 (Lin et al. 2001), a level that may place fish consumers at risk of chronic Tl poisoning. Modeling the fate and transport of Tl in the water column of the Great Lakes requires knowledge of accumulation of this element by seston, including the plankton. The plankton community can greatly influence the fate of bioactive trace metals in the water column of the Great Lakes (Twiss and Campbell 1998*b*), and it is the principal link between the dissolved phase and higher organisms. The objective of the present study is to examine Tl accumulation within the planktonic food web of Lakes Erie and Ontario. We hypothesized that the picoplankton (0.2–2 μm) size fraction, comprised of rapidly growing bacteria and cyanobacteria, will accumulate the most Tl and transfer this metal, through protozoan grazing activity, to the larger plankton size fractions (nanoplankton, 2–20 μm; microplankton, 20–210 μm), as observed for the transfer of Cd and Zn in epipelagic Lake Erie (Twiss et al. 1996).

In this study, we used radioactive ^{204}Tl, a β- and γ-emitting radioisotope (half-life = 3.8 years), to follow the fate of Tl(I) added to lake water. Although Tl(I) is the stable redox form of Tl in oxic freshwaters, we have shown that partitioning between the Tl(III) redox form rapidly (within 30 h) occurs towards an approximate 7:3 ratio of Tl(III) to Tl(I) (Twining et al. 2003), the ratio reported by Lin and Nriagu (1999*a*, 1999*b*) for stable Tl measured in Great Lakes surface waters and rivers. Thus, the experimental design used here follows the incorporation of both redox forms of Tl, although no attempt was made to differentiate between redox forms partitioning into the particulate phase.

New evidence suggests that Tl may be found as both inorganic and organometallic forms in the dissolved phase in the Great Lakes. The organometallic compound dimethylthallium, $Tl(CH_3)_2^+$, has been reported to comprise from 3 to 48% of the total dissolved Tl in 20% of samples analyzed from pristine Atlantic ocean sites, and the presence of this Tl species is associated with biotic activity (Shedlbauer and Heumann 1999). Therefore, we also examined the partitioning of dimethylthallium and compared it with the accumulation of inorganic Tl.

Materials and methods

All experiments were conducted on the CCGS *Limnos* using the onboard Environment Canada Portable Clean Room facility. Pelagic and coastal Lake Erie and Lake Ontario stations were examined in 2000 and 2001, respectively (Fig. 1). At each station, a temperature and turbidity depth profile was determined using an electronic probe (Sea-Bird Electronics, Bellevue, Wash.). Turbidity was measured as light transmittance (%*T*) through a 25-cm path length operating at a 670-nm wavelength. Materials used for water sampling and experimental treatments were acid-cleaned, as described elsewhere (Twiss and Campbell 1998*a*).

Lake Erie

Surface water was collected in the eastern (station 23) and central (station 84) basins from a depth of 10 m using an acid-cleaned, Teflon®-coated Go-Flo® bottle (General Oceanics, Miami, Fla.) suspended on a Kevlar® line. Water was collected in the western basin (3 m, station 969; 5 m, station 357) using a Niskin bottle. Water was screened through a 210-μm nylon mesh and added to 2-L polycarbonate bottles using the technique described in Twiss and Campbell (1998*a*). Water (2 L) was injected with 111 kBq of $^{204}Tl(I)$ in a 2 $mol \cdot L^{-1}$ HCl solution and received an equimolar amount of NaOH added immediately after to neutralize the addition of the acid. The form of ^{204}Tl was confirmed to be Tl(I) using an ion-exchange speciation technique (Twining et al. 2003). An addition of 1.2 $nmol \cdot L^{-1}$ Tl resulted from the ^{204}Tl addition (about 30–40 times greater than the ambient level; Cheam 2001). Treatments were conducted in triplicate. Bottles were sealed and placed in a ship-deck incubator that provided 10% ambient sunlight attenuated with neutral density screening and a constant temperature (22–23 °C, Lake Erie experiments; 19–22 °C, Lake Ontario experiments) maintained by pumping surface lake water constantly through the incubator.

Water used to begin the experiments was characterized for size-fractionated chlorophyll *a* (chl *a*) content using a parallel filtration technique. Chlorophyll *a* was determined onboard by fluorometric analysis (Welschemeyer 1994) following extraction in 90% acetone.

At timed intervals, the bottles were sampled for size-fractionated scavenging of ^{204}Tl as determined by parallel filtration: 200 mL was filtered onto a 20-μm filter (nylon screen; Millipore), 100 mL was filtered onto a 2-μm filter (polycarbonate membrane; Millipore), and 50 mL was filtered onto a 0.2-μm filter (polycarbonate membrane; Millipore). All filters were 47 mm in diameter and were rinsed with 10 mL of ultrafiltered (<30 kDa) lake water to remove any ^{204}Tl loosely adhered to particle surfaces or retained on the filter in the dissolved phase. Two 1-mL samples were removed from each bottle at each sampling time to ensure that no change in total aqueous radioactivity in the bottles occurred. Beta radioactivity in the samples was measured with a liquid scintillation counter after the addition of EcoLume® scintillation fluid.

Filter blanks were prepared by filtering prefiltered (0.2 μm) radioactive water and rinsing as above. Radioactivity on the

Fig. 1. Map of study areas in the Laurentian Great Lakes. Experiments were conducted on Lake Erie in 2000 and on Lake Ontario in 2001.

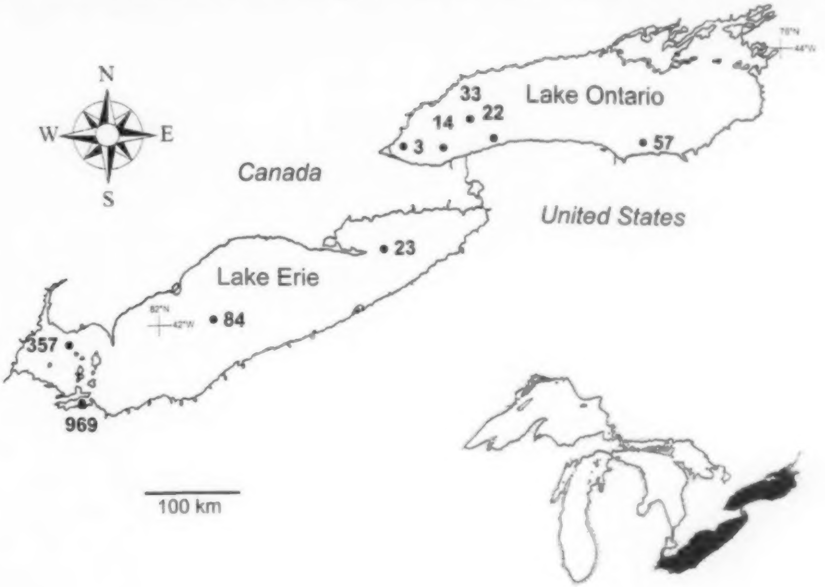

filter blanks (87 ± 12 counts per minute, cpm) was subtracted from the radioactivity measured on each filter before radioactivity was calculated by the method of difference for each size fraction. The detection limit was calculated as 3 × standard deviation (SD) of the filter blanks above the filter blanks, i.e., 123 cpm. The range in ratio of the background to sample signal was 1–21% for Lake Erie (average 7.5%) and 26–50% (average 34%) for Lake Ontario; this was calculated from the minimum observed sample radioactivity in each scavenging assay.

Lake Ontario

In 2001, water was collected at depth using a trace metal clean pumping system (polyethylene-coated Teflon® tubing suspended at depth using Kevlar® line weighted with a Teflon®-coated stainless steel weight) using a Teflon® double-diaphragm pneumatic pump (Husky model No. 307) that delivered lake water directly from depth into the clean laboratory on the ship. At each station, water was pumped from the sampling depth of 10 m for at least 30 min before taking the sample. Samples were collected after passing through a 210-µm polyethylene screen contained within a 90-mm Teflon® filter holder (Savillex Corp., Minnetonka, Minn.).

Water used to begin the experiments was characterized for size-fractionated chl *a* content, and suspended particulate matter (0.2–210 µm) was determined in triplicate at each station by filtering 400–1000 mL of lakewater (<210 µm) onto a preweighed 0.2-µm pore size membrane filter. ^{204}Tl accumulation by the plankton was determined as described above with the exception that plankton were size-fractioned into the picoplankton (0.2–2 µm) and the combined nanoplankton and microplankton (2–210 µm). At station 33, a comparative scavenging experiment was conducted using two forms of thallium, [^{204}Tl]-Tl(I) (see above) and dimethylthallium (DMT), [^{204}Tl]- $Tl(CH_3)_2^+$. The specific activity of [^{204}Tl]-$Tl(CH_3)_2^+$ (>99% pure) was 11 × 10^9 Bq ^{204}Tl·mol Tl^{-1}. Details of the DMT synthesis and verification of the purity of the product are described elsewhere (Twiss et al. 2004).

The partition coefficient of added Tl(I) and DMT at each Lake Ontario study station was determined by dividing the ^{204}Tl content of the plankton (>0.2 µm) at the end of the exposure period (45–70 h) by the dissolved ^{204}Tl concentration:

$$(1) \qquad K_d = ([^{204}\mathrm{Tl}]_{>0.2\ \mu m}/\mathrm{SPM})/[^{204}\mathrm{Tl}]_{<0.2\ \mu m}$$

where K_d is partition coefficient (L·kg^{-1}), $[^{204}\mathrm{Tl}]_{>0.2\ \mu m}$ is ^{204}Tl scavenged by suspended particulate matter (>0.2 µm; Bq·L^{-1}), SPM is suspended particulate matter (>0.2 µm; kg·L^{-1}), and $[^{204}\mathrm{Tl}]_{<0.2\ \mu m}$ is dissolved (<0.2 µm) ^{204}Tl (Bq·L^{-1}).

Results

Water column profiling demonstrated thermal stratification at all stations in Lake Ontario and Lake Erie, except station 357 (western basin) and station 969 (Sandusky Bay). Water temperature in Lake Ontario was approximately 6 °C cooler than in Lake Erie because of the greater mean depth of Lake Ontario (86 m) compared with Lake Erie (18 m).

Thallium did not strongly bind to particles. ^{204}Tl(I) added to lake water was weakly scavenged by seston in both Lake Erie (Fig. 2) and Lake Ontario (Fig. 3). Total scavenging of ^{204}Tl was greater in the pelagic Lake Erie stations (approximately 0.3–0.5% of total ^{204}Tl; Table 2) than in pelagic Lake Ontario (0.1–0.2% of total ^{204}Tl; Table 3). Nonparametric analysis (Spearman correlation) showed that Tl scavenging was significantly correlated with SPM ($P = 0.04$) and chl *a* ($P < 0.01$) in Lake Ontario. However, correlation of scavenging with chl *a* was not observed for the data from Lake Erie ($P = 0.54$), even if the shallow water stations (357 and 969) are removed from the data set ($P = 0.20$). Stations with

Fig. 2. Partitioning of added ^{204}Tl(I) by seston in surface waters of Lake Erie. Values are mean ± standard deviation, n = 3. Note the differing ordinate scales. Seston size fractions: ○, 0.2–2 µm; □, 2–20 µm; △, 20–210 µm. Stn., station.

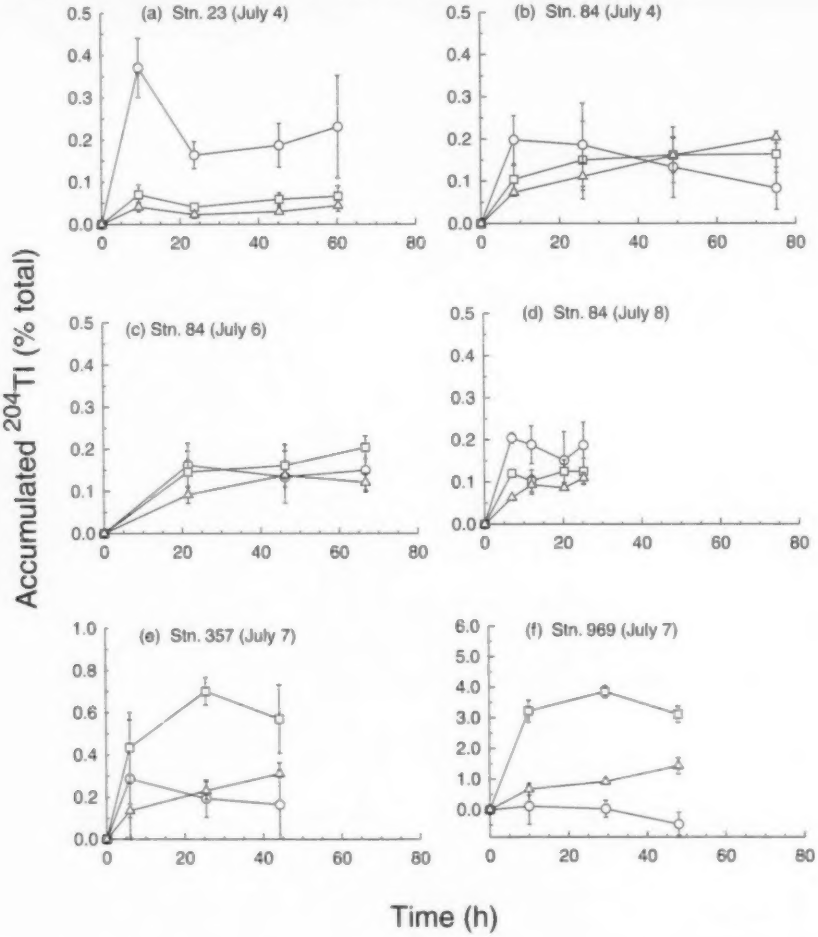

lower chl *a* biomass in Lake Erie possessed greater ^{204}Tl scavenging than observed in the Lake Ontario stations at comparable chl *a* concentrations; this suggests that non-chlorophyllous material was responsible for marked amounts of Tl scavenging at the Lake Erie stations.

The partition coefficients (K_d) for inorganic ^{204}Tl observed in Lake Ontario were relatively constant throughout the study sites (K_d = 1164 ± 241, mean ± SD). The K_d of [^{204}Tl]-DMT was slightly less than that of inorganic Tl (Table 3), similar to lower bioconcentration factors of DMT versus inorganic Tl measured in the laboratory (Twiss et al. 2004).

Most ^{204}Tl was accumulated rapidly (within 24 h) into a given size fraction. An experiment to show short-term uptake patterns showed that uptake had reached a maximum level within 12–20 h (Fig. 2*d*).

In the Lake Ontario study, the combined nanoplankton and microplankton size fraction (2–210 µm) accumulated the most ^{204}Tl. This trend was evident even at sites where the picoplanktonic chl *a* biomass exceeded that of the 2–210 µm size fraction (e.g., stations 22 and 57).

The plankton size fractions showed different accumulation patterns with respect to added inorganic ^{204}Tl (Fig. 3*e*) and [^{204}Tl]-Tl$(CH_3)_2^+$ (Fig. 3*f*). As observed at all Lake Ontario stations studied, the 0.2–2 µm size fraction consistently accumulated less inorganic ^{204}Tl, whereas the opposite was observed for the organic Tl species, dimethylthallium, at this particular station, station 33. Chemical speciation of ^{204}Tl following the exposure period of 62 h (Fig. 3*f*) using an ion-exchange technique (Twining et al. 2003) revealed that essentially all ^{204}Tl in the dissolved phase was [^{204}Tl]-Tl$(CH_3)_2^+$. On the other hand, approximately 70% of ^{204}Tl-Tl(I) added to the lake water was oxidized to Tl(III) within 60 h, as observed repeatedly in other lake water samples (Twining et al. 2003).

Discussion

The observations made in the present study serve to illustrate the initial geochemical fate of atmospherically deposited inorganic Tl following its entry into the surface waters

Fig. 3. Partitioning of added ^{204}Tl(I) (*a–e*) and [^{204}Tl]-$(CH_3)_2Tl^+$ (*f*) by seston in surface waters of Lake Ontario. Values are mean ± standard deviation, $n = 3$. Note the differing ordinate scales. Seston size fractions: ○, 0.2–2 µm; □, 2–210 µm. Stn., station.

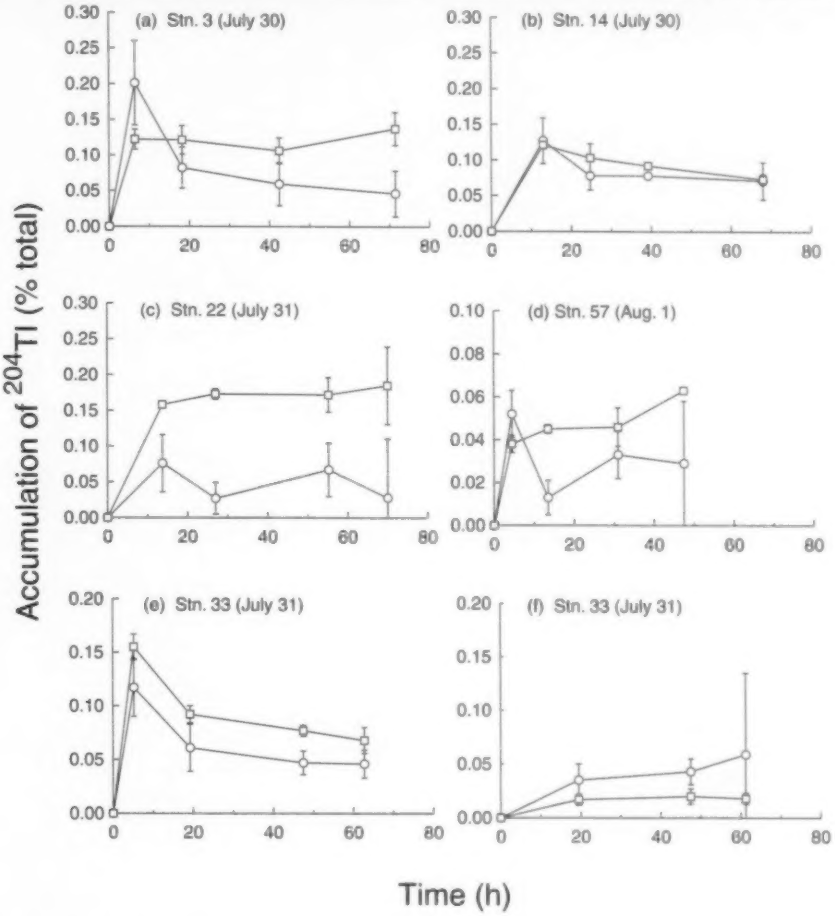

Table 2. Water quality, thallium (Tl) sorption by particles (>0.2 µm), and size-fractionated phytoplankton biomass at Lake Erie study stations in 2000.

Station	Latitude	Longitude	Date	°C	%*T*	^{204}Tl sorption (% total)[a]	Chlorophyll *a*, µg·L^{-1} (% total) 0.2–2 µm	2–20 µm	20–210 µm	0.2–210 µm
23	42°30′26″	79°53′54″	4 July 2000	16.5	72	0.34±0.12	0.20 (13)	1.03 (66)	0.33 (21)	1.56
84	41°56′25″	81°39′33″	5 July 2000	20.7	75	0.45±0.04	0.09 (3)	1.00 (38)	1.55 (59)	2.64
84	41°56′25″	81°39′33″	6 July 2000	20.9	76	0.48±0.04	0.53 (16)	1.07 (31)	1.81 (53)	3.41
84	41°56′25″	81°39′33″	8 July 2000	20.6	75	0.42±0.04	0.15 (13)	0.40 (35)	0.58 (51)	1.13
357	41°48′48″	82°58′54″	7 July 2000	22.6	62	1.05±0.11	0.13 (10)	1.04 (76)	0.19 (14)	1.36
969	41°36′30″	82°55′33″	7 July 2000	23.1	36	4.05±0.29	3.01 (31)	5.22 (54)	1.45 (15)	9.68

Note: Water sampling depth was 10 m except at stations 357 (5 m) and 969 (3 m). %*T*, percentage light transmittance (670 nm wavelength) over a path length of 25 cm.

[a] Measured at final time point (Fig. 2).

of the lower Great Lakes. Because Tl enters primarily as Tl_2O, ^{204}Tl(I) is the appropriate chemical form to use as a tracer of atmospherically deposited Tl. One issue in using a radiotracer for these types of studies is the addition of the element to the lake water at concentrations that exceed natural ambient levels. The amount of tracer added to lake water here (1.5 nmol·L^{-1}) is assumed to have caused no toxicity, as inferred from previous studies that show this level of Tl to be sublethal to a Lake Erie chlorophyte (Ralph and Twiss 2002) and a freshwater diatom (Twiss et al. 2004).

Table 3. Water quality, thallium sorption by particles (> 0.2 μm), suspended particulate matter (SPM), size-fractionated phytoplankton biomass, and observed partition coefficient of Tl at Lake Ontario study stations (10 m depth) in 2001.

Station	Latitude	Longitude	Date	°C	%*T*	^{204}Tl sorption (% total)[a]	SPM, mg·L^{-1} (0.2–210 μm)	Chlorophyll *a*, μg·L^{-1} (% total) 0.2–2 μm	2–210 μm	0.2–210 μm	K_d Tl, >0.2 μm
3	43°16′06″	79°37′12″	30 July 2001	18.4	77	0.18±0.02	1.24±0.13	0.72 (32)	1.54 (68)	2.26	1483±187
14	43°23′36″	79°29′12″	30 July 2001	14.3	76	0.14±0.03	1.38±0.05	0.72 (37)	1.24 (63)	1.97	1044±179
22	43°17′48″	79°00′18″	31 July 2001	16.1	76	0.21±0.06	1.57±0.03	1.35 (58)	0.98 (42)	2.33	1357±403
33	43°35′48″	78°48′06″	31 July 2001	19.6	80	0.11±0.01	1.14±0.03	0.45 (24)	1.42 (76)	1.86	998±51
						0.08±0.08[b]					807±255[b]
57	43°16′30″	77°35′12″	1 Aug. 2001	6.9	86	0.09±0.03	0.98±0.01	0.82 (54)	0.70 (46)	1.52	938±297

Note: %*T*, percentage light transmittance (670 nm wavelength) over a path length of 25 cm.

[a] Measured at final time point (Fig. 3).

[b] Tl added as [^{204}Tl]-Tl(CH$_3$)$_2^+$.

The redox disequilibrium observed in Great Lakes surface waters and in tributaries of these lakes is essentially 70% Tl(III) and 30% Tl(I), even though Tl(I) is the stable redox state of ionic Tl in oxic surface waters (Lin and Nriagu 1998). In a series of experiments designed to examine the rate of Tl(I) oxidation in lake water and the role of seston, we found that Tl(I) oxidizes to Tl(III) in the presence of seston (<1 μm) and the ratio of 70% Tl(III) to 30% Tl(I) is attained within 24 h (Twining et al. 2003). Thus, the patterns of Tl scavenging reported here are due to two main functions: partitioning of metal between the dissolved and solid phase and change in redox state from Tl(I) to Tl(III).

The rapid change in redox state of Tl has a direct bearing on the fate of Tl in surface waters. In living systems, Tl$^+$ can behave as a K$^+$ analogue, and although Tl$^+$ has a 2- to 10-fold greater affinity for uptake than K$^+$ in (Na,K)-ATPase membrane porters (Brismar 1998), the high ambient K$^+$ concentration in the lower Great Lakes ($\approx 10^{-4.7}$ mol·L^{-1}) (Rockwell et al. 1989) and low Tl(I) concentrations ($\approx 10^{-11}$ mol·L^{-1}) effectively inhibit a high degree of Tl$^+$ uptake, as illustrated in laboratory experimentation (Twiss et al. 2004). The oxidation of Tl(I) to Tl(III) and the high degree of Tl(III) hydrolysis reduce both the availability of Tl$^+$ for internalization by biota and the concentration of Tl^{3+}, the ionic form of Tl that should be highly surface reactive but is instead complexed by hydroxide ions to form the dominant inert controlling phase, Tl(OH)$_3$. It follows that Tl scavenging in the water column will be inhibited by competition with K$^+$ and the extent of hydrolysis of oxidized Tl. The constant concentration of Tl with depth observed in the water column of Lakes Erie and Ontario (Cheam et al. 1995) is therefore a result of the factors preventing this metal from being effectively scavenged by particles, despite the fact that Tl^{3+} should be strongly sorbed by seston. A similar observation was made in a comparative study involving the scavenging of a suite of non-redox active metals (Cs, Cd, Zn, Gd) in Lake Erie. It was hypothesized that Gd(III) would partition more readily to seston than Cd(II) and Zn(II) and, in turn, more than Cs(I), and thus, scavenging would correlate positively with the respective first hydrolysis constants of these elements (Twiss and Campbell 1998*a*). However, solution phase chemistry, namely complexation of Gd with carbonate ions, reduced Gd^{3+} availability for surface complexation reactions to such an extent that Cd and Zn were scavenged more effectively.

Our study has demonstrated the accumulation of Tl from the dissolved phase into the seston that contains organisms of the planktonic food web in Lakes Erie and Ontario. We hypothesized that the picoplankton (0.2–2 μm) size fraction would accumulate the most Tl and transfer this metal to higher plankton fractions (2–210 μm) by trophic transfer. The data collected do not support this proposed mechanism. Picoplankton were not the primary scavengers in Lake Ontario or in four of the six Lake Erie stations. At the Lake Erie stations where the seston 0.2–2 μm scavenged the most Tl, scavenging was not correlated to greater amounts of plankton biomass, as inferred from chl *a* content.

The fate of DMT appears to be distinct from that of inorganic Tl, despite the relatively similar K_d values. At station 33 (Lake Ontario), where the direct comparison between Tl(I) and DMT was made, DMT tended to be accumulated primarily by the picoplanktonic size fraction (0.2–2 μm), whereas the added inorganic Tl(I) was accumulated to a greater extent by the plankton >0.2 μm. Both forms of Tl are bioactive, as demonstrated by a reduction of uptake by phytoplankton when exposed to Tl(I) and DMT in the dark at 1 °C (Twiss et al. 2004). Based on this limited set of observations, we suggest that the fate of DMT is different from that of inorganic Tl, although these two chemical species are linked as there is no anthropogenic source of DMT.

In summary, this study of Tl fate in the surface waters of Lakes Erie and Ontario demonstrates that both inorganic Tl and dimethylthallium are weakly associated with seston in the epilimnion as demonstrated by measured K_d values of approximately 1000 for both species. Because K_d for Tl in seston is approximately 1000 yet the bioconcentration factor of Tl in lake trout in the Great Lakes is approximately 10 000 (Lin et al. 2001), it follows that this element is clearly bioaccumulated at higher trophic levels. Seston and the plankton component of this material are most likely a link in the transfer of this element from the dissolved phase into larger aquatic organisms.

Acknowledgements

This research was funded by a grant (No. R/CTP-26) from the New York Sea Grant Foundation to N.S.F. and M.R.T. and a grant from the Natural Sciences and Engineering Research Council of Canada to M.R.T. We thank Charles G. Trick (University of Western Ontario) for use of the scintillation counter and acknowledge the logistical support provided by Bob Hess and Barry Moore of Technical Operations, Environment Canada.

References

Brismar, T. 1998. Thallium transport in cellular membranes. *In* Thallium in the environment. *Edited by* J.O. Nriagu. John Wiley and Sons, New York. pp. 31–44.

Cheam, V. 2001. Thallium contamination of water in Canada. Water Qual. Res. J. Can. **36**: 851–877.

Cheam, V., Lechner, J., Desrosiers, R., Sekerka, I., Lawson, G., and Mudroch, A. 1995. Dissolved and total thallium in Great Lakes water. J. Gt. Lakes Res. **21**: 384–394.

Fisher, N.S. 1986. On the reactivity of metals for marine phytoplankton. Limnol. Oceanogr. **31**: 443–449.

Lin, T.-S., and Nriagu, J. 1998. Revised hydrolysis constants for thallium(I) and thallium(III) and the environmental implications. J. Air Waste Manag. Assoc. **48**: 151–156.

Lin, T.-S., and Nriagu, J. 1999*a*. Thallium speciation in the Great Lakes. Environ. Sci. Technol. **33**: 3394–3397.

Lin, T.-S., and Nriagu, J. 1999*b*. Thallium speciation in river waters with Chelex 100 resin. Anal. Chim. Acta, **395**: 301–307.

Lin, T.-S., Nriagu, J., and Wand, X.-Q. 2001. Thallium concentration in lake trout from Lake Michigan. Bull. Environ. Contam. Toxicol. **67**: 921–925.

Martell, A.E., Smith, R.M., and Motekaitis, R.J. 1998. NIST critical stability constants of metal complexes database. Version 5.0. U.S. Department of Commerce, Gaithersburg, Md.

Ralph, L., and Twiss, M.R. 2002. Comparative toxicity of Tl(I), Tl(III) and Cd(II) to the unicellular alga *Chlorella* isolated from Lake Erie. Bull. Environ. Contam. Toxicol. **68**: 261–268.

Rockwell, D.C., Salisbury, D.K., and Lesht, B.M. 1989. Water quality in the middle Great Lakes: results of the 1985 USEPA survey of Lakes Erie, Huron and Michigan. U.S. Environ. Protect. Assoc., Great Lakes National Program, Chicago, Ill., EPA-905/6-89-001.

Shedlbauer, O.F., and Heumann, K.G. 1999. Development of an isotope dilution mass spectrophotometric method for dimethylthallium speciation and first evidence of its existence in the ocean. Anal. Chem. **71**: 5469–5464.

Twining, B.S., Twiss, M.R., and Fisher, N.S. 2003. Oxidation of thallium by freshwater plankton communities. Environ. Sci. Technol. **37**: 2720–2726.

Twiss, M.R., and Campbell, P.G.C. 1998*a*. Scavenging of ^{137}Cs, ^{109}Cd, ^{65}Zn, and ^{153}Gd by plankton of the microbial food web in pelagic Lake Erie surface waters. J. Gt. Lakes Res. **24**: 776–790.

Twiss, M.R., and Campbell, P.G.C. 1998*b*. Trace metal cycling in the surface waters of Lake Erie: linking ecological and geochemical fates. J. Gt. Lakes Res. **24**: 791–807.

Twiss, M.R., Campbell, P.G.C, and Auclair, J.C. 1996. Regeneration, recycling and trophic transfer of trace metals by microbial food web organisms in the pelagic surface water of Lake Erie. Limnol. Oceanogr. **41**: 1425–1437.

Twiss, M.R., Twining, B.S., and Fisher, N.S. 2004. Bioconcentration of inorganic and organic thallium by freshwater phytoplankton. Environ. Toxicol. Chem. **23**. In press.

Welschemeyer, N.A. 1994. Fluorometric analysis of chlorophyll *a* in the presence of chlorophyll *b* and pheopigments. Limnol. Oceanogr. **39**: 1985–1992.

World Health Organization. 1996. Thallium. Environmental Health Criteria No. 182, World Health Organization, Geneva.

Movement patterns of the tropical shad hilsa (*Tenualosa ilisha*) inferred from transects of ^{87}Sr/^{86}Sr isotope ratios in their otoliths

David A. Milton and Simon R. Chenery

Abstract: We examine ^{87}Sr/^{86}Sr isotope ratios in transects across the otoliths of the diadromous tropical shad hilsa, *Tenualosa toli*, to assess the extent of movement of fish within the large Meghna (Ganges) River system and adjacent coastal waters. Hilsa collected from marine, estuarine, and freshwater habitats were born in all main rivers in Bangladesh. All fish moved widely, entering water of marine ^{87}Sr/^{86}Sr isotope ratio by 1 year of age. Most returned to fresh water after they reached sexual maturity, but not necessarily to their natal region. Comparison of the ^{87}Sr/^{86}Sr isotope and Sr/Ca ratios of hilsa showed that in the Meghna River, ^{87}Sr/^{86}Sr isotope ratios can only distinguish fish from waters when the salinity was less than 5‰. Sr/Ca ratios were more useful for interpreting fish movements at higher salinities. To assess whether whole-otolith ^{87}Sr/^{86}Sr isotope ratios reflected the ratios of the water of natal origin, we compared the ^{87}Sr/^{86}Sr ratios of otolith cores with the mean ^{87}Sr/^{86}Sr isotope ratio of the whole transect. We found major differences between the two measurements, suggesting that ^{87}Sr/^{86}Sr isotope ratios from whole-otolith assays may not accurately reflect the natal origin of the fish.

Résumé : Nous avons examiné les rapports des isotopes ^{87}Sr/^{86}Sr dans des transects d'otolithes du poisson diadrome tropical, l'alose toli (*Tenualosa toli*), pour évaluer les déplacements des poissons dans le grand système de rivières du Meghna (Gange) et les eaux côtières adjacentes. Les aloses récoltées dans les habitats marins, les estuaires et les eaux douces sont originaires de l'ensemble des grandes rivières du Bangladesh. Tous les poissons se déplacent considérablement et ils pénètrent dans les eaux à rapport d'isotopes ^{87}Sr/^{86}Sr marin vers l'âge de 1 an. La plupart retournent en eau douce à la maturité sexuelle, mais pas nécessairement à leur région d'origine. Une comparaison des rapports d'isotopes ^{87}Sr/^{86}Sr et des rapports Sr/Ca chez l'alose indique que, dans le Meghna, les rapports d'isotopes ^{87}Sr/^{86}Sr peuvent permettre de distinguer les poissons seulement dans les eaux de salinité de moins de 5 ‰. Les rapports Sr/Ca sont plus utiles pour interpréter les déplacements des poissons aux salinités plus élevées. Pour évaluer si les rapports d'isotopes ^{87}Sr/^{86}Sr d'otolithes entiers reflètent les rapports des eaux d'origine, nous avons comparé les rapports d'isotopes ^{87}Sr/^{86}Sr de carottes d'otolithes avec le rapport d'isotopes ^{87}Sr/^{86}Sr moyen de tout le transect. Les différences importantes entre les deux mesures indiquent que les rapports d'isotopes ^{87}Sr/^{86}Sr de l'otolithe entier ne reflètent pas de façon précise l'origine du poisson.

[Traduit par la Rédaction]

Introduction

Otolith microchemistry has become a powerful tool for examining the migration patterns of fish, especially those that move between marine and fresh water (Kalish 1990; Secor 1992; Rieman et al. 1994). Analytical techniques that measure changes in the concentration of selected elements across the otolith enable you to infer changes in the environment that the fish have experienced. Strontium (Sr) is one of the elements for which concentration in water changes in relation to the salinity (Ingram and Sloane 1992; Secor et al. 1995). Ratios of strontium to calcium (Sr:Ca) in otoliths of several species have been shown to vary directly with ambient salinity (Rieman et al. 1994; Mugiya and Tanaka 1995; Secor et al. 1995). Other elements that have been shown to vary between marine and freshwater populations of fish include barium, magnesium, manganese, and zinc (Pender and Griffin 1996).

These and other studies suggest that concentrations of some trace elements in otoliths are directly related to their concentrations in the water (e.g., strontium (Secor et al. 1995), barium (Bath et al. 2000), and lithium (Milton and Chenery 2001*a*)). However, these relationships may be altered by factors such as fish physiology, growth rates, and stress (Kalish 1992; Sadovy and Severin 1992; Friedland et al. 1998). Several studies have shown that at least strontium, barium, and lead concentrations in the otoliths of several species are related to water concentrations (Farrell and Campana 1996; Geffen et al. 1998; Bath et al. 2000). However, the relationship and affinity of otoliths for each element varies.

Recently, Kennedy et al. (1997, 2000) and Ingram and Weber (1999) demonstrated a strong positive relationship

Received 21 May 2002. Accepted 31 January 2003. Published on the NRC Research Press Web site at http://cjfas.nrc.ca on 26 November 2003.
J16901

D.A. Milton.[1] CSIRO Marine Research, P.O. Box 120, Cleveland 4163 Qld., Australia.
S.R. Chenery. Analytical Geochemistry Group, British Geological Survey, Keyworth, Nottingham NG12 5GG, United Kingdom.

[1] Corresponding author (e-mail: david.milton@csiro.au).

doi: 10.1139/F03-133

between the ratio of Sr isotopes (^{87}Sr:^{86}Sr) in whole otoliths of two salmon species and the water that each species inhabits. Methods that use ratios of common isotopes have the advantage that there should be no selectivity for either isotope and so otolith ratios should mirror those in the water. Strontium has many properties that make it a good tracer for detecting movements of fish between freshwater systems that differ in their underlying geology (Peterman et al. 1970; Kistler and Peterman 1973) and the sea. Strontium isotope ratios in fresh water vary depending on the mixture of dissolved strontium derived from limestone or silicate rocks (Palmer and Edmonds 1992), whereas marine water Sr isotope ratio is stable throughout the world (0.70918: Hodell et al. 1989).

Tropical shads, *Tenualosa* species, are commercially valuable species caught on the coast and in rivers across southern Asia (Blaber et al. 2003*a*). The most widespread species, hilsa *Tenualosa ilisha*, shows a range of movement patterns that vary between locations (Rahman and Moula 1992). Some remain in fresh water, whereas others are believed to migrate to the sea and return to spawn. In Bangladesh, the largest landings of hilsa previously occurred in the freshwater reaches of the Meghna River but are now coming from the fisheries in the Bay of Bengal as the riverine catches decline (Haldar et al. 2002). It is not known where these fish were born or where they have been since birth.

Traditionally, studies of fish movement have involved tagging fish and recapturing them later. Earlier studies using tags showed that individual hilsa could move long distances (>1000 km), e.g., from the Hoogly to the Meghna River (Pillay et al. 1963). However, these studies provide no data on the timing or frequency of movements and the relative importance of marine and freshwater habitats. Hilsa are extremely delicate and mortality is very high during tagging (Pillay et al. 1963). Thus, indirect methods such as otolith chemistry offer an alternative approach to understanding the movements in these species.

The aims of this study were (1) to determine whether transects of Sr isotope ratios in hilsa otoliths can be used to infer movement of fish between different rivers and the sea at various stages during their life, (2) to compare the information obtained from Sr isotope ratios with that from the more commonly used Sr/Ca ratios, and (3) to assess the value of transects of ^{87}Sr/^{86}Sr isotope ratios as population markers relative to whole-otolith assays.

Materials and methods

Sample collection

Otoliths were removed from hilsa collected directly from fishers in coastal, estuarine, and freshwater reaches of the major rivers in Bangladesh (Fig. 1; Milton and Chenery 2001*b*). The number of fish analysed varied between sites. Hilsa were chosen from sites representing the range of conditions that the fish experience in Bangladesh. This included inland freshwater (Goalando), estuarine (Ramgoti), and marine (Cox's Bazar) habitats. Five fish from Sylhet, in remote northeast Bangladesh, were also analysed because hilsa from this site had distinctive otolith chemistry (Milton and Chenery 2001*b*) and morphology (Salini et al. 2003). At the same time as when fish were collected, a sample of water was taken mid-water and acidified to a concentration of 1% trace metal grade nitric acid and analysed by inductively coupled plasma atomic emission spectrometry (ICP-AES) for a range of elements including Sr (Milton and Chenery 2001*a*).

Otolith microchemistry analysis

Before chemical analysis, each otolith was mounted in thermoplastic cement on a labelled microscope slide and ground along the transverse axis with heavy-duty silicon carbide paper until the core region of the otolith was exposed. The otolith was then polished to the core with 1200-grade wet-and-dry sandpaper moistened with double-distilled water. Water use was kept to a minimum during otolith preparation to minimise and standardise any preparation bias (Milton and Chenery 1998; Proctor and Thresher 1998). To remove any contamination, the surface was wiped vigorously after polishing with a piece of tissue paper moistened with 0.5 mol·L^{-1} aristar nitric acid. The slides were then placed in plastic bags until analysed by laser-ablation multicollector inductively coupled plasma mass spectrometry (LA-MC-ICPMS).

MC-ICPMS measures the isotope composition of samples with high precision (Walder 1997; Halliday et al. 1998). Our analyses of Sr isotopes in otoliths were carried out on a P54 instrument (VG Instruments, U.K.) in the Natural Environment Research Council Isotope Geoscience Laboratory (NIGL), British Geological Survey. The instrument is fitted with nine Faraday cups for signal detection; in this case, the ions were arranged as follows: L2, ^{84}Sr$^+$; L1, ^{85}Rb$^+$; Axial, ^{86}Sr$^+$; H1, ^{87}Sr/Rb$^+$; H2, ^{88}Sr$^+$; H3, ^{89}Y$^+$.

Before each day's analysis, the LA-MC-ICPMS was optimised for maximum Sr and Y signals and stability with 100 μg·L^{-1} NIST SRM987 solution of Sr doped with 10 μg·L^{-1} Y and ablations of the North Sea deep-sea coral *Lophelia pertusa* that has a typical Sr concentration of 8000 μg·g^{-1}. For this optimisation, argon gas was fed through a Cetac MCN6000 desolvating nebuliser and the output was coupled through the laser ablation cell before reaching the injector of the MC-ICPMS. Typical running conditions for the P54 MC-ICPMS were as follows: plasma power, 1350 W; plasma coolant gas, 13.0 L·min^{-1}; plasma auxiliary gas, 1.10 L·min^{-1}; injector gas, 0.75 L·min^{-1}; nebuliser sweep gas, 0.53 L·min^{-1}.

The laser ablation system was a VG Microprobe 2 (VG Instruments), operating at a wavelength of 266 nm. Laser conditions such as energy and beam size were varied between sample types to give a total Sr signal of greater than 1V where possible, depending on the minimum Sr concentration in the otolith. Sr concentrations in the otolith vary by up to a factor of about 6 (500–3000 μg·g^{-1}). Typical laser parameters were 0.56 mJ pulse energy, 250-μm-wide ablation path, 3 Hz firing, and 10 μm·s^{-1} stage translation. Laser conditions for ablating *L. pertusa* were somewhat less intense because of the higher Sr concentration.

Transects of up to 250 ablations were made across the distal portion of the otolith from the rim to the core. Initially, we made multiple transects along different growth axes (distal and proximal) on three otoliths. There was little variation between ablations in the same growth zone of different

Fig. 1. Map of Bangladesh showing collection sites for hilsa *Tenualosa ilisha* and literature water samples (water sampling sites: A, Patna; B, Rajshahi, C, Chilmari, D, Gauhati; E, Bhairob Bazar; F, Bhola).

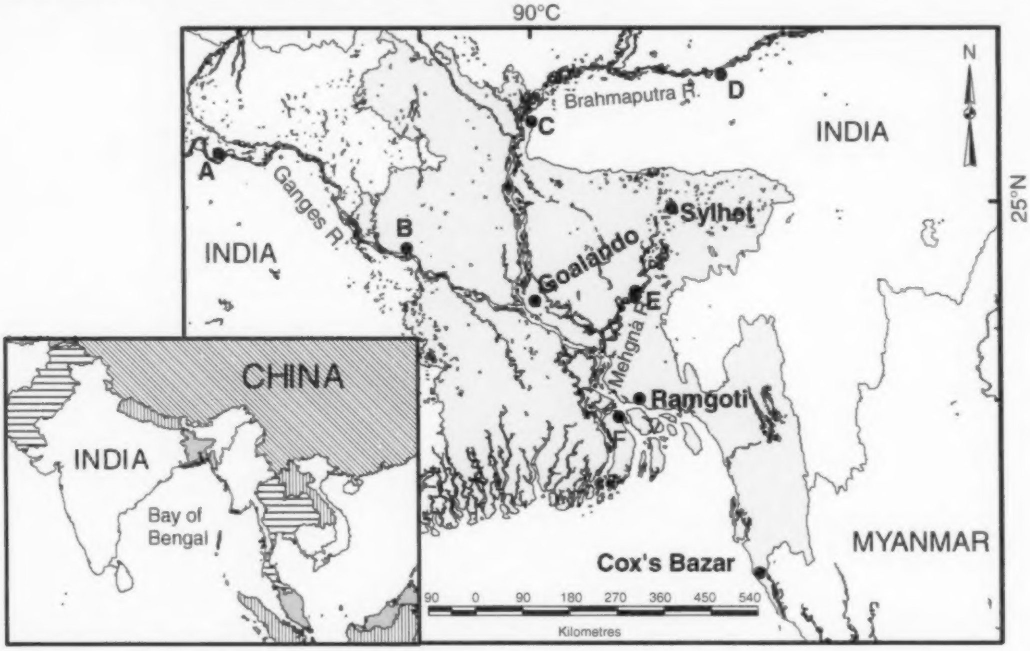

transects (<5%). Consequently, only one transect was undertaken on all other fish.

Data acquisition was as a series of signal integrations of 10 s in a single block, with exponential corrections for mass bias using measured ^{88}Sr:^{86}Sr versus the true ratio. A correction factor was derived using an exponential mass bias model within the instrument software. Correction for Rb isobaric interference was made with the natural ^{85}Rb:^{87}Rb. These corrections were normally small, as Rb was routinely measured in hilsa otoliths and was less than 1 μg·g^{-1} (Milton and Chenery 2001*a*). Each analysis was preceded by peak-centring on ^{89}Y and zero-point correction at 0.5 atomic mass units from the peak. A minimum of 50 ratios (50 × 10 s integrations) was recorded for the SRM987 standard and the coral material. All ratios were electronically logged for transfer to an Excel spreadsheet for off-line processing of the data. Once transferred to the spreadsheet, data on the SRM987 standard and coral were used to calculate both internal and external error statistics. If the data were outside the error of expected values for the SRM987 isotopic standard solution, otolith isotope ratios were further corrected for mass bias. *Lophelia pertusa* was used as a matrix-matched (calcium carbonate) reference sample for a seawater signature. This hard coral species was considered appropriate as it grows in large colonies at over 800 m in the North Sea northeast of Scotland with no freshwater input. Data from the otoliths were smoothed with a five-point rolling median to reduce high frequency noise before plotting.

All otoliths analysed by LA-MC-ICPMS in this study had previously been analysed at their core and rim by LA-ICPMS (Milton and Chenery 2001*b*). Three ablations were made at each location (core and rim). We used the Sr/Ca ratio (in mM·M^{-1}) of the mean of these ablations as a measure of the absolute Sr concentration at the rim of each fish. We then converted the voltages of the ablations in the LA-MC-ICPMS transects to Sr/Ca ratios.

After chemical analysis, otoliths were returned to the laboratory and the age at each ablation (in daily increments) was estimated. Ablations that were made at similar ages in different fish (within three increments) were assumed to be comparable. Fish ageing methods followed those used in previous studies of *Tenualosa* (Blaber et al. 1996, 1999, 2003*b*).

Data analysis

Sr isotope ratios of ablations in the otoliths of fish while they were in the sea were analysed to assess the relative importance of fish, age, and relative Sr concentration as sources of Sr isotope variation. Fish was treated as the main effect with fish age and relative Sr concentration as covariates. The assumption that the slope of the relationship of each covariate was homogeneous was tested before analysis. The period of marine residency was assumed to start when the ^{87}Sr:^{86}Sr in the otolith approached the marine water ratio (0.70918) for two or more consecutive ablations.

The Sr isotope ratios of the first four ablations at the core of each otolith were assumed to describe the ratio during the first month after birth. The mean of these were compared with the mean of the entire otolith transect by *t* test.

All water Sr isotope ratios were obtained from the scientific literature (Krishnaswami et al. 1992; Palmer and Edmonds 1992; Galy et al. 1999). The mean Sr isotope ratios were calculated where multiple measurements were available for sites on the major rivers in Bangladesh.

Mean Sr isotope ratios of the outer three ablations of transects of fish from sites in which the measured salinity

Table 1. Mean Sr concentration in water from the three major rivers that flow into Bangladesh and the Sr isotope ratio (^{87}Sr:^{86}Sr) of the deep-sea coral *Lophelia pertusa* analysed as a control.

Sample	Site	Season	Sr (μmol·L^{-1})	^{87}Sr:^{86}Sr ± 95% CI	Source
Coral 1	Deep sea	—	91.3	0.70924±0.00005	This study
Coral 2	Deep sea	—		0.70919±0.00005	This study
	Deep sea	—		0.70917±0.00004	This study
Coral 3	Deep sea	—		0.70920±0.00004	This study
Coral 4	Deep sea	—		0.70930±0.00015	This study
Coral 5	Deep sea	—		0.70909±0.00007	This study
Upper Brahmaputra	Gauhati (D)	Dry	0.67	0.7197±0.0003	Krishnaswami et al. (1992)
	—	Dry	0.93	0.7210	Palmer and Edmonds (1992)
	Chilmari (C)	Dry	—	0.7218	Galy et al. (1999)
Middle Brahmaputra	Goalando (Aricha Ghat)	Dry	—	0.7260	Galy et al. (1999)
		Wet	1.58	0.7257[a]	Palmer and Edmonds (1992)
Ganges	Patna (A)	Wet	1.017	0.7249±0.0010[b]	Krishnaswami et al. (1992)
		Wet	1.82	0.7245[a]	Palmer and Edmonds (1992)
		Dry	2.27	0.7224[a]	Palmer and Edmonds (1992)
	Rajshahi (B)	Wet	—	0.7291	Galy et al. (1999)
		Dry	—	0.7235	Galy et al. (1999)
Upper Meghna	Bhairob Bazar (E)	Wet	—	0.7160	Galy et al. (1999)
	Nangalband (E)	Wet	—	0.7162	Galy et al. (1999)
Lower Meghna	Bhola (F)	Wet	—	0.7226	Galy et al. (1999)
Rainwater	Bangladesh	Wet	22.6±0.7	0.7122±0.0024	Galy et al. (1999)

Note: Sites within each river are arranged from headwaters to the lower reaches and their site codes in Fig. 1 are enclosed in parentheses. CI, confidence interval.

[a] Samples collected in November 1983 (Wet) and March 1982 (Dry).

[b] Samples collected in peak flow in September 1982.

was greater than 0‰ (Ramgoti and Cox's Bazar) were used to calculate the salinity that the fish had experienced with the equation in Ingram and DePaolo (1993). This method requires the marine and riverine end-member Sr concentrations and Sr isotope ratios. The marine Sr isotope and Sr concentrations are known and we obtained the river Sr isotope ratio from Galy et al. (1999).

Results

The Sr isotope ratios of river water from the three major tributaries of the Meghna River (Ganges, Brahmaputra, and Meghna rivers) differ (Table 1). All data were obtained from studies that used similar analytical methods. There is evidence that the ratios can vary seasonally, or between years, but the data are sparse. Data available indicate that most variation in water Sr isotope ratios is within 0.002 of the mean (95% confidence limits). Strontium concentration also appears to vary regionally by up to three times (Table 1). Data from the repeated analyses of the deep-sea coral show that the MC-ICPMS can produce accurate and precise results. The overall mean Sr isotope ratio of the coral was 0.7092 ± 0.0001 and remarkably close to the modern marine Sr isotope ratio of 0.70918 (Hodell et al. 1989). There was no relationship between the Sr isotope ratio and the Sr/Ca ratio of any of the coral samples.

Provenance of hilsa from each area

Transects of Sr isotope ratios in the otoliths of five fish from the remote population at Sylhet showed a consistent pattern (Fig. 2). Four of the fish were born in water with Sr isotope ratios similar to that in the upper Meghna River (Sylhet). Each fish spent varying periods in water with Sr isotope ratios similar to that region before migrating to the lower estuary or the coast. All five had recently returned to the upper Meghna River. One fish spent about 3 months in water with Sr isotope ratios similar to that in the middle reaches of the Brahmaputra River before migrating to marine waters (Fig. 2*a*).

The age at which fish migrate to the sea appears to vary, three migrated at about 3 months of age, whereas one migrated after 2 months and the other at 5 months. Most spent about 3 months in the sea before migrating back to the upper Meghna River. Two fish (Fig. 2*b*) spent a short time in another river that had a lower isotopic ratio (~0.712). Most of the fish caught at Ramgoti in the lower estuary and at the marine site, Cox's Bazar, were also born in water with a similar Sr isotope ratio (Table 2; Fig. 3).

All three fish analysed from the lower estuary (Ramgoti) and the two from the sea (Cox's Bazar) had spent most of their life in water with marine Sr isotope ratios. They all remained in the sea after migrating there and showed no evidence of any movements into fresh water during their adult lives (>250 increments; Blaber et al. 2003*a*). Four migrated to the sea by 4 months of age, similar to the pattern found in the Sylhet fish. There was only one fish that showed a different migration history and this fish was born in water with a Sr isotope ratio similar to that of the upper Meghna River. This fish then moved downstream and entered the lower Meghna River for about 3 months before migrating to the sea at about 8 months of age (Fig. 3).

Hilsa from Goalando in the middle Brahmaputra River (Fig. 1) showed different patterns to those from other sites (Fig. 3*c*). One appears to have been born in the lower Ganges and made a partial migration downstream before returning for a short period and then migrating to the sea for about

Fig. 2. $^{87}Sr/^{86}Sr$ isotope ratios of five fish collected from the isolated site at Sylhet. Horizontal lines represent water $^{87}Sr/^{86}Sr$ isotope ratios from the literature. Shaded zones are the 95% confidence limits of these values. Each line represents the trace of one fish: (*a*) fish 4369, fish 4367, and fish 4368; (*b*) fish 4353 and fish 4350.

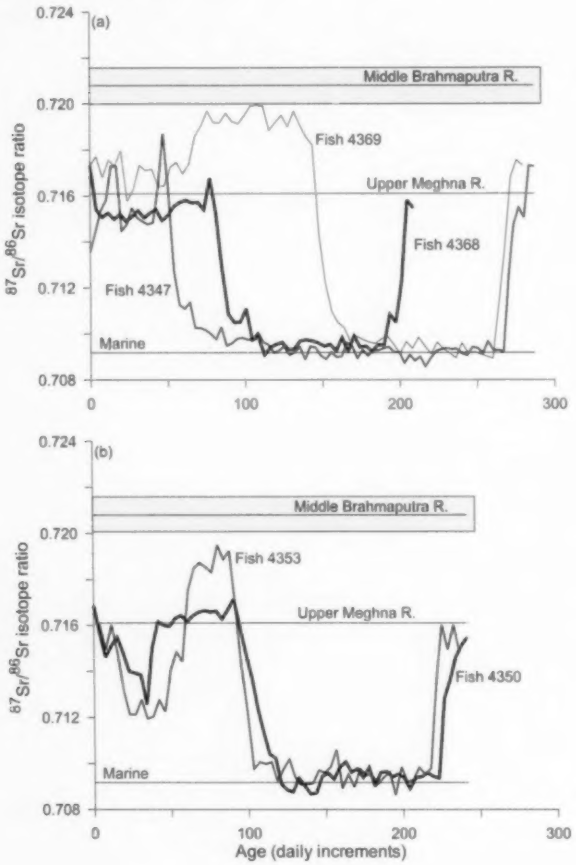

Fig. 3. Transects of $^{87}Sr/^{86}Sr$ isotope ratios of eight fish from three sites in the main Meghna River – Brahmaputra River system that vary in salinity: (*a*) marine, Cox's Bazar; (*b*) estuarine, Ramgoti; (*c*) fresh water, Goalando. Horizontal lines represent mean water $^{87}Sr/^{86}Sr$ isotope ratios from the literature. Each line represents the trace of one fish.

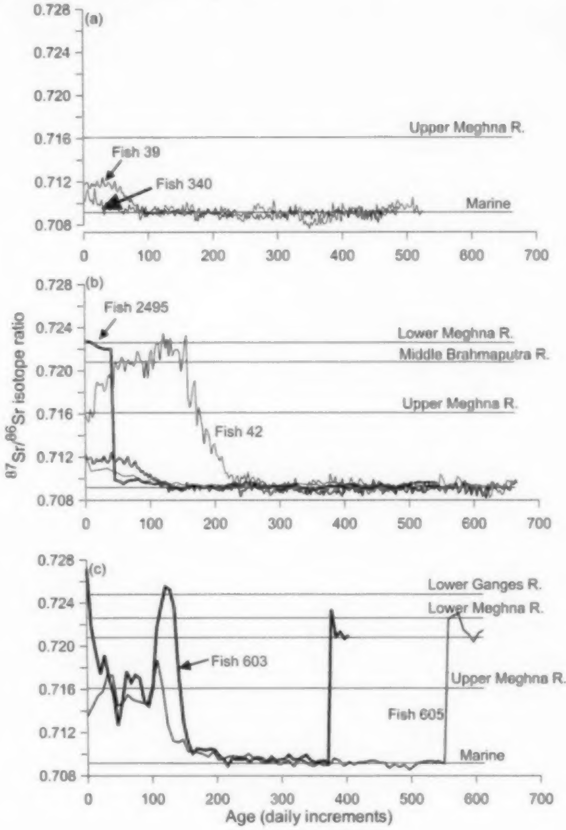

7 months and returning shortly before capture. The other fish made a seaward migration at 4 months of age and returned after more than a year at sea.

Comparison of the Sr isotope ratio of hilsa during the period when they lived in the sea showed that measurements were precise (coefficient of variation (CV) < 0.1%). Most of the variation was within fish (77.7% variation) (Table 2). Fish and Sr relative concentration accounted for a similar amount of the variation (fish, $F_{[10,632]} = 17.6$; Sr concentration, $F_{[1,632]} = 16.5$; both, $P < 0.0001$). The effect of age on Sr isotope ratios was not significant ($P > 0.21$).

The Sr isotope and Sr/Ca ratios of two fish from Sylhet show that both ratios distinguish between the marine and freshwater phases of the growth of each fish (Fig. 4). Sr/Ca ratios increased during the period when each fish was in marine waters and were low during the freshwater phase. Hilsa caught at the estuarine and freshwater sites in the main Meghna River also showed a similar pattern (Fig. 5). However, Sr/Ca ratios of the fish caught at the marine site (Fig. 5*a*) showed a downward trend during that part of the growth phase when the Sr isotope ratios were showing a marine value. This suggests a possible movement of the fish towards water of lower salinity not detectable in the Sr isotope ratios. This is not surprising as the Sr isotope mixing curve for the Meghna River shows that it would be difficult to distinguish salinities greater than 5‰ (Fig. 6).

This was also reflected in the calculated salinities of fish from sites where salinity was greater than zero (Table 3). The salinity calculated from Hilsa Sr isotope ratios at Ramgoti was only 2‰, yet the mean Sr isotope ratio was close to the marine ratio of 0.7092. These calculated values were also very similar to the measured salinity recorded at the time of fish collection (Table 3) and that calculated from the Sr isotope mixing curve (Fig. 6).

Value of Sr isotope ratio transects as population markers

There was quite a wide discrepancy between the otolith Sr isotope ratio of each fish at birth and the mean of the entire transect (Table 4). Analysis of covariance of mean Sr isotope ratio among sites showed that site was the major source of

Table 2. Strontium isotope ratios ($^{87}Sr:^{86}Sr$; mean ± standard error (SE)) and coefficient of variation (CV, %) of Sr/Ca ratios (Sr:Ca; in $mM \cdot M^{-1}$) in transects across the otoliths of hilsa from Bangladesh analysed by laser ablation MC-ICPMS.

Site	Fish	Length (mm)	Weight (g)	Age (increments)	Mean $^{87}Sr:^{86}Sr$ ± SE	CV of $^{87}Sr:^{86}Sr$ (%)	CV of Sr:Ca (%)	*N*
Sylhet	4347	200	170	288	0.70915±0.00004	0.03	12.1	30
Sylhet	4350	173	109	223	0.70936±0.00007	0.05	19.7	27
Sylhet	4353	170	119	218	0.70949±0.00008	0.06	18.2	26
Sylhet	4368	152	72	190	0.70952±0.00005	0.03	26.3	18
Sylhet	4369	190	150	260	0.70948±0.00006	0.04	17.1	20
Cox's Bazar	39	305	570	489	0.70903±0.00003	0.05	13.7	138
Cox's Bazar	340	320	642	492	0.70903±0.00005	0.08	13.4	138
Ramgoti	42	385	1050	667	0.70933±0.00004	0.06	9.0	160
Ramgoti	43	365	995	658	0.70900±0.00003	0.04	20.0	105
Ramgoti	450	360	980	638	0.70937±0.00003	0.02	12.4	62
Ramgoti	2495	330	720	531	0.70937±0.00002	0.03	2.5	111
Goalando	603	265	375	405	070950±0.00004	0.03	13.6	54
Goalando	605	360	925	613	0.70928±0.00005	0.05	13.8	75
Overall					0.70917±0.00003	0.10	9.1	964

Note: All Sr isotope ratios refer to those ablations taken when the fish was in water of presumed marine Sr isotope ratio (0.70918); *N*, the number of ablations taken between the otolith core and rim.

Fig. 4. Transects of Sr/Ca ratio (broken lines; in $mM \cdot M^{-1}$) and $^{87}Sr/^{86}Sr$ isotope ratio (solid lines) of two fish from Sylhet that had contrasting patterns in their $^{87}Sr/^{86}Sr$ isotope ratios: (*a*) fish 4369 and (*b*) fish 4347.

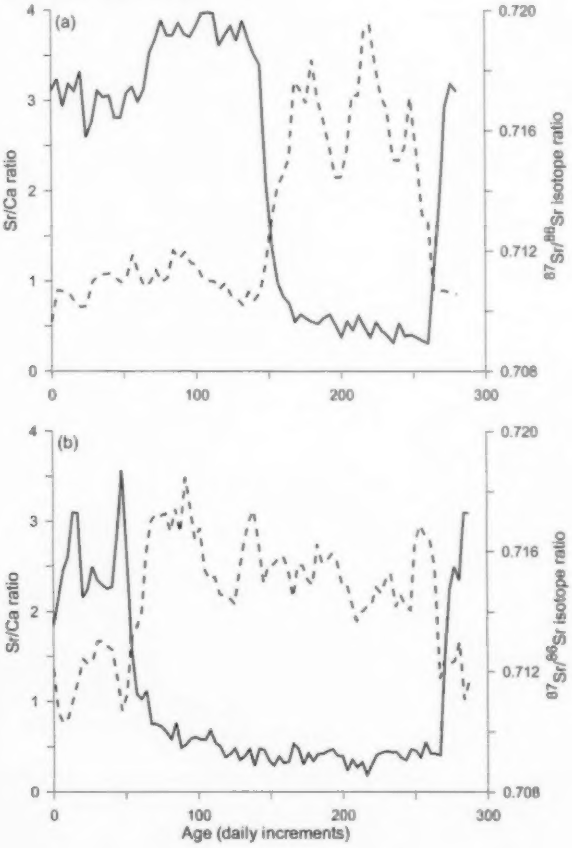

variation in otolith Sr isotope ratio ($F_{[3,1216]} = 12.87$, $P < 0.0001$) and that the effects of age and otolith Sr concentration were insignificant ($P > 0.05$). The model only explained 8% of the variation in otolith Sr isotope ratios. Comparison of the least squares means at each site revealed that the significance of the site effect was due largely to fish from Sylhet. No significant difference could be detected among the mean Sr isotope ratios of fish from the three other sites (Cox's Bazar, Ramgoti, and Goalando) ($P > 0.19$ in all comparisons). This means that the natal origin of these fish could not be separated by their mean ratio even though the ratio at birth could be assigned to identifiable rivers (Table 4).

Discussion

We have been able to construct an accurate history of the movement of each hilsa between different water bodies. Our results show that there is great potential for methods such as laser ablation MC-ICPMS in the study of fish movement. Otoliths do not differentiate between isotopes of Sr and so more directly reflect the concentration of the isotopes in the water or diet (Kennedy et al. 2000). Our data indicate that hilsa from the three major rivers in Bangladesh can be distinguished by the Sr isotope ratio in their otoliths.

Like the recent studies of Sr isotope ratios in whole otoliths (Ingram and Weber 1999; Kennedy et al. 2000), we found that otolith Sr isotope ratios vary more than those of the water. Uptake of ambient water Sr isotope ratios is rapid and our data suggest that otolith Sr isotope ratios reflect those in the water within a week. For movement into estuarine or marine waters, this appears to be due to the steep gradient in the Sr isotope ratios and the swamping effect of the high concentration of Sr in seawater. The rate of incorporation by hilsa was similar to that found for Sr and other trace elements in otoliths of juvenile barramundi (Milton and Chenery 2001*a*).

There have been numerous studies using changes in otolith Sr concentration to infer movements between freshwater and

Fig. 5. Transects of Sr/Ca ratio (broken lines; in $mM \cdot M^{-1}$) and $^{87}Sr/^{86}Sr$ isotope ratio (solid lines) of three fish from the main Meghna River – Brahmaputra River system that were caught at sites with varying salinities: (*a*) fish 39 from the marine site (Cox's Bazar); (*b*) fish 42 from the estuarine site (Ramgoti); (*c*) fish 605 from the freshwater site (Goalando).

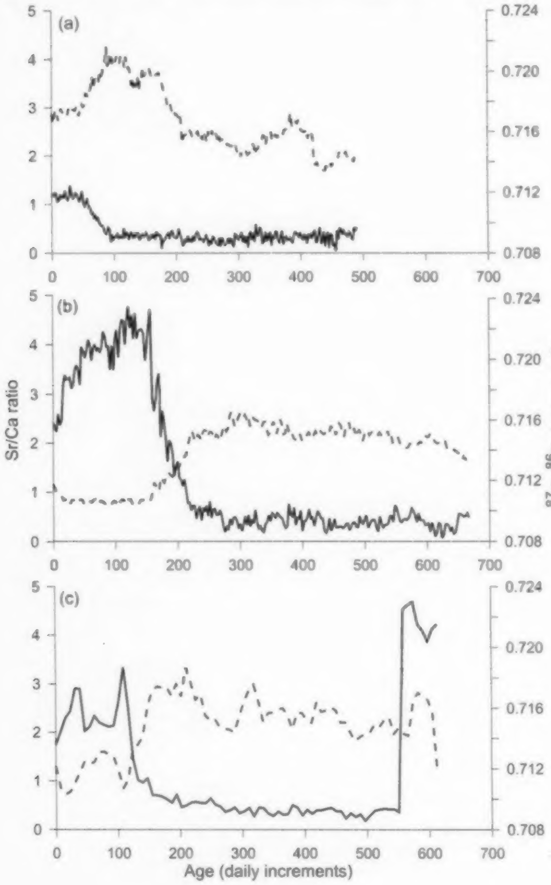

Fig. 6. The estimated Sr mixing curve for the lower Meghna River with the mean salinities calculated from measured water Sr concentrations and the Sr isotope ratios in the rim of otoliths of hilsa from the est uarine (Ramgoti) and marine (Cox's Bazar) sites.

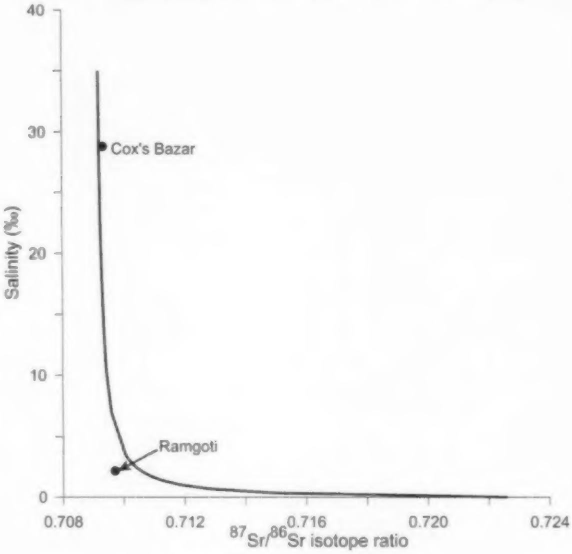

marine environments. However, as Secor and Rooker (2000) have pointed out, otolith Sr concentration has been correlated with several factors besides salinity, including growth rate, temperature, and physiology. The use of Sr isotope ratios removes much of these confounding effects and makes the interpretation of fish movements more straightforward. This will particularly be the case in environments in which the Sr isotope ratios differ greatly from the marine ratio, such as in the Ganges–Brahmaputra system examined here.

Comparison between Sr isotope and Sr/Ca ratios in our fish suggest that both approaches distinguish hilsa movements between fresh and marine waters. Where measurements of the Sr concentration in otoliths may be more helpful is in distinguishing fish movements between waters with salinity greater than 5‰, as the Sr isotopic ratio may not be resolvable at higher salinities (Holmden et al. 1997). This appears to be the case in measurements of hilsa caught in the upper Bay of Bengal. We recorded salinities as low as 17‰ as far as 200 km from the mouth of the Meghna River (D.A. Milton, unpublished data). Yet, the Sr isotope ratios were indistinguishable from measurement variation in marine ratios.

Despite the difficulty in analytically resolving the Sr isotope ratios of hilsa living in waters with salinities >5‰, our estimates of the salinity from otolith Sr isotope ratios were surprisingly accurate for the few data we have. This suggests that if additional samples were taken across a greater range of salinities, the method could be used to develop an accurate salinity history of an individual. This could lead to the detection of finer-scale fish movements within upper estuaries than is currently possible even with a Sr–salinity relationship like that produced by Secor et al. (1995) for striped bass (*Morone saxatilis*). It is often difficult to interpret Sr/Ca ratios from fish collected in estuarine waters. Hilsa Sr/Ca ratios of fish in estuarine waters (>5‰) varied more widely than Sr isotope ratios during the same period. Sr/Ca ratios of fish in estuarine and marine waters vary quite widely between species (Secor and Rooker 2000). However, there appears to be little differential incorporation of Sr isotopes, which makes interpreting data less ambiguous.

Unlike traditional approaches such as tagging that require large sample sizes, the use of Sr isotope ratios in otoliths holds great promise as it can potentially provide a much more accurate history of the environment that each fish has experienced. It has greatest application in species that move across strong salinity gradients or between tributaries of rivers that have sediments of different geology. Sr isotope ratios are stable in marine waters, and so this approach will have limited application in studies of wholly marine fishes or species that live in mainly lower estuarine waters.

Besides studies of fish movements, Sr isotope ratios can be used as natural population markers in a similar way to

Table 3. The mean calculated salinity at Cox's Bazar, Ramgoti, and Goalando (based on otolith Sr isotope ratios (^{87}Sr:^{86}Sr) and water Sr concentration) and the measured salinity when the fish were collected.

Site	Mean ^{87}Sr:^{86}Sr in hilsa otoliths	Salinity calculated from otolith Sr isotope ratios	Water salinity measured at collection site	Water Sr concentration (µmol·L^{-1})
Seawater	0.7092*	—	35	91.3
Cox's Bazar	0.7093	28.8	29	75.3
Ramgoti	0.7096	2.2	2–4	5.3
Goalando	0.7210	0.0	0	2.1
Lower Meghna River	0.7226*	—	0	0.7

Note: Known Sr isotope ratios of river and marine water end members are also shown; asterisk (*) indicates that water ^{87}Sr/^{86}Sr ratios are from the literature).

Table 4. The Sr isotope ratio (^{87}Sr:^{86}Sr) at the core (birth), overall mean Sr isotope ratio, and Sr/Ca ratios (Sr:Ca; in mM·M^{-1}) of hilsa in Bangladesh measured by the MC-ICPMS.

Habitat	Site	Fish	^{87}Sr:^{86}Sr at birth	Mean ^{87}Sr:^{86}Sr ± SE	Mean Sr:Ca ± SE	*N*
Freshwater	Sylhet	4347	0.71655	0.71105±0.00030	2.18±0.07	86
Freshwater	Sylhet	4350	0.71686	0.71238±0.00004	1.35±0.03	60
Freshwater	Sylhet	4353	0.71648	0.71223±0.00045	1.89±0.08	58
Freshwater	Sylhet	4368	0.71731	0.71230±0.00041	1.70±0.06	50
Freshwater	Sylhet	4369	0.71733	0.71454±0.00054	1.65±0.11	66
Marine	Cox's Bazar	39	0.71180	0.70945±0.00006	2.74±0.04	234
Marine	Cox's Bazar	340	0.71024	0.70923±0.00004	2.71±0.04	232
Estuarine	Ramgoti	42	0.71587	0.71240±0.00003	1.79±0.04	248
Estuarine	Ramgoti	43	0.71180	0.70944±0.00006	2.74±0.04	232
Estuarine	Ramgoti	450	0.71236	0.70958±0.00006	2.03±0.05	80
Estuarine	Ramgoti	2495	0.72263	0.71044±0.00032	2.54±0.04	121
Freshwater	Goalando	603	0.72714	0.71306±0.00006	0.96±0.05	61
Freshwater	Goalando	605	0.71356	0.70928±0.00003	2.14±0.07	80

Note: SE, standard error; *N*, the number of ablations in each transect between otolith core and rim.

trace elements. The trace element composition, morphology, and parasite fauna of hilsa from Sylhet have previously been shown as distinctive (Milton and Chenery 2001*b*; Alam 2002; Salini et al. 2003). These studies suggested that the population might be more isolated than hilsa from elsewhere in Bangladesh. Our results suggest that the fish from this region appear to be undertaking a return migration from the upper Meghna River to the sea. Four of the five fish migrated at a similar age and were in spawning condition by the time they returned (Blaber et al. 2003*a*). Local fishers in Sylhet claim that hilsa are only available during the monsoonal wet season when the river levels are high and the habitat is suitable. Our data suggest that they spend the dry season in coastal or marine habitats.

The movement pattern of hilsa from other areas differed from that found in Sylhet. We found limited evidence that hilsa from the main river systems (lower Meghna, Brahmaputra, and Ganges rivers) were undertaking similar migrations. All fish were born in fresh water and spent variable amounts of time in the rivers before migrating to the lower estuary or the sea. We could not distinguish between the otolith Sr isotope ratios of hilsa caught in estuarine and marine waters. It is not clear at what salinity the water Sr isotope ratio becomes identical to marine ratios. Four of the six fish caught in the estuary and sea that we analysed had otolith Sr isotope ratios between those in the adjacent fresh water and that of marine waters. These fish may have been born in the major spawning ground of hilsa in the lower estuary around Ramgoti where salinities vary between 0‰ and 5‰ (Blaber et al. 2003*b*).

Our data clearly show that there are benefits in the use of laser-ablation MC-ICPMS to more accurately measure natal Sr isotope ratios if the data are to be used as population markers. Mean values obtained from whole-otolith assays (Ingram and Weber 1999; Kennedy et al. 2000) provided good discrimination among salmon species that have strong homing instincts. However, for species such as hilsa that appear to disperse more randomly, Sr isotope ratios of whole otoliths would inaccurately assign fish among populations and rivers.

In conclusion, we have shown that transects of ^{87}Sr/^{86}Sr isotope ratios in otoliths of hilsa with laser-ablation MC-ICPMS can provide precise and accurate chronologies of movements of a fish through water bodies with differing Sr isotope ratios. Hilsa from four regions in Bangladesh showed widespread movement among regions, and all fish examined had spent several months in water with marine Sr isotope ratios. The data supported previous findings (Milton and Chenery 2001*b*; Alam 2002) that hilsa from the remote population in Sylhet were distinct and showed that fish from that region had a common homing strategy. This differs from our analyses of hilsa from elsewhere in Bangladesh showing that fish moved freely among rivers with different Sr isotope ratios.

Comparison between the mean Sr isotope ratio of each fish (equivalent to whole-otolith assay) and the ratio at the otolith core (birth) showed wide variation. Mean Sr isotope ratios of hilsa from marine, estuarine, and riverine sites in the main Meghna River could not be distinguished, suggesting that studies using whole-otolith Sr isotope ratios as a population marker may be inaccurate, depending on the life history of the species.

Acknowledgements

We thank Bronwyn Gillanders, Mick Haywood, and two anonymous referees for constructive comments on an earlier draft of the manuscript. This work was partly funded by the Australian Centre for International Agricultural Research (PN 9430) and the British Geological Survey.

References

Alam, A. 2002. Comparison of the parasite fauna of *Tenualosa ilisha* from different locations in Bangladesh. *In* International Terubok Conference Proceedings. *Edited by* S.J.M. Blaber, D.J. Brewer, D.A. Milton, and C. Biano. Sarawak Development Corporation, Kuching, Malaysia. pp. 133–148.

Bath, G.E., Thorrold, S.R., Jones, C.M., Campana, S.E., McLaren, J.W., and Lam, J.W.H. 2000. Strontium and barium uptake in aragonitic otoliths of marine fish. Geochim. Cosmochim. Acta, **64**: 1705–1714.

Blaber, S.J.M., Milton, D.A., Pang, J., Wong, P., Boon-Teck, O., Nyigo, L., and Lubim, D. 1996. The life history of the tropical shad *Tenualosa toli* from Sarawak: first evidence of protandry in the Clupeiformes? Environ. Biol. Fishes, **46**: 225–242.

Blaber, S.J.M., Brewer, D.T., Milton, D.A., Merta, G.S., Efizon, D., Fry, G., and van der Velde, T. 1999. The life history of the protandrous tropical shad *Tenualosa macrura* (Alosinae: Clupeidae): fishery implications. Estuar. Coast. Shelf Sci. **49**: 689–701.

Blaber, S.J.M., Milton, D.A., Chenery, S.R., and Fry, G. 2003*a*. New insights into the life history of *Tenualosa ilisha* and fishery implications. *In* Biodiversity, status, and conservation of the world's shads. *Edited by* K.E. Limburg and J.R. Waldman. Am. Fish. Soc. Symp. **35**: 223–240.

Blaber, S.J.M., Milton, D.A., Brewer, D.T., and Salini, J.P. 2003*b*. Biology, fisheries and status of tropical shads (*Tenualosa*) in south and south east Asia. *In* Biodiversity, status, and conservation of the world's shads. *Edited by* K.E. Limburg and J.R. Waldman. Am. Fish. Soc. Symp. **35**: 49–58.

Galy, A., France-Lanord, C., and Derry, L.A. 1999. The strontium isotopic budget of Himalayan rivers in Nepal and Bangladesh. Geochim. Cosmochim. Acta, **63**: 1905–1925.

Geffen, A.J., Pearce, N.J., and Perkins, W.T. 1998. Metal concentrations in fish otoliths in relation to body composition after laboratory exposure to mercury and lead. Mar. Ecol. Prog. Ser. **165**: 235–245.

Farrell, J., and Campana, S.E. 1996. Regulation of calcium and strontium deposition on the otoliths of juvenile tilapia, *Oreochromis niloticus*. Comp. Biochem. Physiol. A, Comp. Physiol. **115**: 103–109.

Friedland, K.D., Reddin, D.G., Shimizu, N., Haas, R.E., and Youngson, A.F. 1998. Strontium:calcium ratios in Atlantic salmon (*Salmo salar*) otoliths and observations on growth and maturation. Can. J. Fish. Aquat. Sci. **55**: 1158–1168.

Haldar, G.C., Mazid, M.A., Rahman, M.A., and Amin, S.M.N. 2002. The present status of the Hilsa (*Tenualosa ilisha*) fishery in Bangladesh. *In* International Terubok Conference Proceedings. *Edited by* S.J.M. Blaber, D.J. Brewer, D.A. Milton, and C. Biano. Sarawak Development Corporation, Kuching, Malaysia. pp. 57–66.

Halliday, A.N., Lee, D-C., Christensen, J.N., Rehkamper, M., Yi, W., Luo, X., Hall, C.M., Ballentine, C.J., Pettke, T., and Stirling, C. 1998. Application of multiple collector ICPMS to cosmochemistry, geochemistry, and paleoceanography. Geochim. Cosmochim. Acta, **62**: 919–940.

Hodell, D.A., Mueller, P.A., McKenzie, J.A., and Mead, G.A. 1989. Strontium isotope stratigraphy and geochemistry of the late neocene ocean. Earth Planet. Sci. Lett. **92**: 165–178.

Holmden, C., Creaser, R.A., and Muehlenbachs, K. 1997. Paleosalinities in ancient barckish water systems determined by ^{87}Sr/^{86}Sr ratios in carbonate fossils: a case study from the western Canada sedimentary basin. Geochim. Cosmochim. Acta, **61**: 2105–2118.

Ingram, B.L., and DePaolo, D.J. 1993. A 4300 year strontium isotope record of estuarine paleosalinity in San Francisco Bay, California. Earth Planet. Sci. Lett. **119**: 103–119.

Ingram, B.L., and Sloane, D. 1992. Strontium isotopic composition of estuarine sediments as paleosalinity–paleoclimate indicator. Science (Wash. D.C.), **255**: 68–72.

Ingram, B.L., and Weber, P.K. 1999. Salmon origin in California's Sacramento – San Joaquin river system as determined by otolith strontium isotopic composition. Geology, **27**: 851–854.

Kalish, J.M. 1990. Use of otolith microchemistry to distinguish the progeny of sympatric anadromous and non-anadromous salmonids. Fish. Bull. U.S. **88**: 657–666.

Kalish, J.M. 1992. Stress induced changes in the concentration of elements in the otoliths of Australian salmon. J. Exp. Mar. Biol. Ecol. **162**: 265–277.

Kennedy, B.P., Folt, C.L., Blum, J.D., and Chamberlain, C.P. 1997. Natural isotope markers in salmon. Nature (Lond.), **387**: 766–767.

Kennedy, B.P., Blum, J.D., Folt, C.L., and Nislow, K.H. 2000. Using natural strontium isotopic signatures as fish markers: methodology and application. Can. J. Fish. Aquat. Sci. **57**: 2280–2292.

Kistler, R.W., and Peterman, Z.E. 1973. Variations in Sr, Rb, K, Na, and initial ^{87}Sr/^{86}Sr in Mesozoic granitic rocks and intruded wall rocks in central California. Geol. Soc. Am. Bull. **84**: 3489–3512.

Krishnaswami, S., Trivedi, J.R., Sarin, M.M., Ramesh, R., and Sharma, K.K. 1992. Strontium isotopes and rubidium in the Ganga–Brahmaputra river system: weathering in the Himalayas, fluxes to the Bay of Bengal and contributions to the evolution of oceanic ^{87}Sr/^{86}Sr. Earth Planet. Sci. Lett. **109**: 243–253.

Milton, D.A., and Chenery, S.R. 1998. The effect of otolith storage methods on the concentrations of elements detected by laser-ablation ICPMS. J. Fish Biol. **53**: 785–794.

Milton, D.A., and Chenery, S.R. 2001*a*. Sources and uptake of trace metals in otoliths of juvenile barramundi (*Lates calcarifer*). J. Exp. Mar. Biol. Ecol. **264**: 47–65.

Milton, D.A., and Chenery, S.R. 2001*b*. Can otolith chemistry detect the population structure of the shad hilsa *Tenualosa ilisha*? Comparison with the results of genetic and morphological studies. Mar. Ecol. Prog. Ser. **222**: 239–251.

Mugiya, Y., and Tanaka, S. 1995. Incorporation of water-borne strontium into otoliths and its turnover in the goldfish *Carassius auratus*: effects of strontium concentrations, temperature and 17 β-estradiol. Fish. Sci. **61**: 29–35.

Palmer, M.R., and Edmonds, J.M. 1992. Control over the strontium composition of river water. Geochim. Cosmochim. Acta, **56**: 2099–2111.

Pender, P.J., and Griffin, R.K. 1996. Habitat history of Barramundi *Lates calcarifer* in a north Australian river system based on barium and strontium levels in scales. Trans. Am. Fish. Soc. **125**: 679–689.

Peterman, Z.E., Carmichael, I.S.E., and Smith, L.A. 1970. ^{87}Sr/^{86}Sr ratios of Quaternary lavas of the Cascade Range, northern California. Geol. Soc. Am. Bull. **81**: 311–318.

Pillay, S.R., Rao, K.V., and Mathur, P.K. 1963. Preliminary report on the tagging of the hilsa *Hilsa ilisha*. Proc. Indo-Pacific Fish. Council, **10**: 28–36.

Proctor, C.H., and Thresher, R.E. 1998. Effects of specimen handling and otolith preparation on concentration of elements in fish otoliths. Mar. Biol. **131**: 681–694.

Rahman, M.J., and Moula, G. 1992. Management-orientated research on the hilsa fisheries of Bangladesh. Naga, **15**: 34–35.

Rieman, B.E., Myers, D.L., and Nielsen, R.L. 1994. Use of otolith microchemistry to discriminate *Oncorhynchus nerka* of resident and anadromous origin. Can. J. Fish. Aquat. Sci. **51**: 68–77.

Salini, J.P., Milton, D.A., Rahman, M.J., and Hussain, M.G. 2003. Allozyme and morphological variation throughout the geographic range of the tropical shad, hilsa *Tenualosa ilisha*. Fish. Res. **64**. In press.

Sadovy, Y., and Severin, K.P. 1992. Trace elements in biogenic aragonite: correlation of body growth rate and strontium levels in the otoliths of the white grunt, *Haemulon plumeri* (Pisces: Haemulidae). Bull. Mar. Sci. **50**: 237–257.

Secor, D.H. 1992. Application of otolith microchemistry analysis to investigate anadromy in Chesapeake Bay striped bass *Morone saxatilis*. Fish. Bull. U.S. **90**: 798–806.

Secor, D.H., and Rooker, J.R. 2000. Is otolith strontium a useful scalar of life cycles in estuarine fishes? Fish. Res. **46**: 359–371.

Secor, D.H., Henderson-Arzapalo, A., and Piccoli, P.M. 1995. Can otolith microchemistry chart patterns of migration and habitat utilisation in anadromous fishes? J. Exp. Mar. Biol. Ecol. **192**: 15–33.

Walder, A.J. 1997. Advanced isotope ratio mass spectrometry II: isotope ratio measurement by multiple collector inductively coupled plasma mass spectrometry. *In* Modern isotope ratio mass spectrometry. *Edited by* I.T. Platzner. John Wiley and Sons, London. pp. 83–108.

The effect of cloud cover on the development of habitat quality indices for juvenile Atlantic salmon (*Salmo salar*)[1]

Philippe Girard, Daniel Boisclair, and Michel Leclerc

Abstract: We tested the validity of the predictions made by a habitat probabilistic index (HPI) developed using a description of the physical conditions (depth, flow velocity, grain size) used and avoided by parrs during days of different cloudiness. Thirteen surveys were designed to estimate the number and the distribution of parrs actively foraging within a 300-m reach of a river. During these surveys, the number of parrs actively foraging ranged from 12 to 118, cloud cover ranged from 5% to 100%, and water temperature ranged from 16.5 °C to 21.7 °C. The number of parrs actively foraging was negatively related to cloud cover ($r^2 = 0.44$ to 0.88) but was independent of water temperature. HPI models developed under low (<33%) and intermediate (34–67%) cloud cover explained 82% to 98% of the local variations of fish density. The HPI model developed under high cloud cover (67–100%) was unable to predict fish distribution observed during cloudy days. Our results suggest that HPI models developed when cloudiness is >67% may have a limited predictive power.

Résumé : Nous avons testé la validité des prédictions faites par un indice probabiliste d'habitat (IPH) développé à l'aide d'une description des conditions physiques (profondeur, vélocité du courant, taille du substrat) utilisées et évitées par des tacons durant des jours de différents couverts nuageux. Nous avons effectué treize survols visant à estimer le nombre total, la distribution et les conditions utilisées et évitées par les tacons qui s'alimentent activement dans une section de 300 m de rivière. Durant ces survols, le nombre de tacons s'alimentant de façon active a varié entre 12 et 118, le couvert nuageux a varié entre 5 % et 100 % et la température de l'eau a varié entre 16,5 °C et 21,7 °C. Le nombre de tacons s'alimentant de façon active a été négativement relié au couvert nuageux ($r^2 = 0,44$ à 0,88) mais a été indépendant de la température de l'eau. Les modèles IPH développés sous un couvert nuageux faible (<33 %) et intermédiaire (34–67 %) ont expliqué 82 % à 98 % des variations locales de la densité des tacons. Le modèle IPH développé sous un couvert nuageux important (67–100 %) a été incapable de prédire la distribution des poissons lors de jours nuageux. Nos résultats suggèrent que les modèles IPH développés lorsque le couvert nuageux >67 % peuvent avoir un pouvoir prédictif limité.

Introduction

Numerical habitat models (NHM) have been developed to estimate fish habitat quality in rivers and to predict the effect of natural and anthropogenic perturbations on the quantity, quality, and distribution of habitats for fish (Bovee 1978, 1982). Biological models imbedded within NHM are intended to estimate fish habitat quality using the environmental conditions used or avoided by fish and the conditions available to fish (deGraaf and Bain 1986; Morantz et al. 1987; Guay et al. 2000). Conditions used or avoided by fish are defined by recording physical variables at locations where fish are present or at locations where fish are absent. These data are often obtained by performing visual surveys of fish distribution. Hence, factors that determine the adoption by fish of an actively foraging or a cryptic behaviour may affect fish visibility to observers, the environmental conditions defined as used or avoided by fish, and consequently the predictions made by biological models.

The diurnal foraging behaviour of juvenile Atlantic salmon (*Salmo salar*) in the summer consists of holding a position on or above the substrate (most often a rock referred to as "home-rock") and performing frequent movements in the water column or towards the surface to capture invertebrates that drift in the flow (Kalleberg 1958; Fausch 1984). Numerous studies indicate that in the fall and winter,

---

Received 9 May 2002. Accepted 6 June 2003. Published on the NRC Research Press Web site at http://cjfas.nrc.ca on 26 November 2003.
J16890

P. Girard and D. Boisclair.[2] Université de Montréal, Département de sciences biologiques, C.P. 6128 Succursale Centre-ville, Montréal, QC H3C 3J7, Canada.
M. Leclerc. INRS-Eau, Université du Québec, CP 7500, Sainte-Foy, QC G1V 4C7, Canada.

[1] Contribution to the program of CIRSA (Centre Interuniversitaire de Recherche sur le Saumon Atlantique).

[2] Corresponding author (e-mail: Daniel.Boisclair@Umontreal.ca).

doi: 10.1139/F03-118

juvenile Atlantic salmon (herein referred to as parrs) exhibit a cryptic behaviour during the day and emerge from the interstices of the substrate during the night (Rimmer et al. 1983; Cunjak 1988; Bremset 2000). However, the diurnal cryptic behaviour of parrs may not occur only during the fall–winter period. Fraser et al. (1995) observed that parrs that lived in a river draining a glacial catchment (water temperature of 7.7–8.4 °C) displayed a cryptic behaviour during the day and emerged from the substrate during the night even in the summer. Manipulations of water temperature under laboratory conditions showed that parrs could be induced to adopt a diurnal cryptic behaviour when temperature is decreased below 15 °C while they continued to express a diurnal foraging behaviour at temperatures above 16 °C (Fraser et al. 1995). Adoption of a diurnal cryptic behaviour at water temperatures below 10–15 °C has been hypothesised to be a consequence of a reduced swimming performance at low temperatures (Webb 1978; Rimmer et al. 1984). The lower swimming capability has been argued to impede on the ability of fish to escape endothermic predators (Heggenes et al. 1993; Fraser et al. 1995). In situ observations performed by Gries et al. (1997) and Gries and Juanes (1998) during mid- and late summer suggest that parrs may display a cryptic behaviour during daylight hours even at temperatures above 16 °C. The effect of light intensity on the reactive distance (Benfield and Minello 1996) and the foraging efficiency (Fraser and Metcalfe 1997) of fish preying on drifting invertebrates may be invoked to explain the adoption by fish of a cryptic behaviour even during daylight hours of the summer period. Yet, the effect of light intensity on fish behaviour and on the predictions made by habitat models is not known.

The objectives of our work were (1) to assess the relative importance of water temperature and light intensity on the diurnal foraging activity of Atlantic salmon parrs during the summer and (2) to evaluate the effects of the potential interaction between water temperature, light intensity, and parr behaviour on the quality, quantity, and distribution of summer habitats predicted by biological models imbedded within NHM.

Material and methods

The approach used to attain our objective combined four operations: (1) the assessment of the number and location of parrs actively foraging under different light conditions and water temperatures; (2) the development of a hydrodynamic model to define the physical conditions used and avoided by parrs; (3) the development of biological models for different light conditions and water temperatures; and (4) the comparison between real fish distribution and habitat distribution predicted using NHM implemented with biological models developed under different conditions.

Study site and species

Sampling was conducted in the Escoumins River in the Haute-Côte-Nord Region of Quebec at ~600 km northeast of Montreal (Fig. 1). The watershed of the Escoumins River covers an area of 979.7 km^2. The flow of this river is controlled by dams constructed at the head of the river and on its main tributaries. The study site was a 300-m reach located 20 km from the junction of the Escoumins and St. Lawrence rivers. The width of the reach studied ranged from 21.7 m to 47.5 m. This reach consisted of a series of pools (maximum depth of 1.4 m) and riffles. The average slope of the reach was 0.2%. The substrate ranged from gravel (diameter of 4×10^{-5} to 0.032 m) to metric boulders (over 1 m in diameter). The reach did not contain areas covered by wood debris and the canopy was absent.

We studied age-1+ and age-2+ juvenile Atlantic salmon (*Salmo salar*), hereafter referred to 1+ and 2+. In our study, 1+ (7.5- to 10-cm fork length (FL)) and 2+ (9- to 11.5-cm FL) fish were treated indistinguishably because they could not be discriminated by visual observations. Parrs represented 97% of the fish observed over the reach. Other fish species observed were brook charr (*Salvelinus fontinalis*), American eel (*Anguilla rostrata*), longnose sucker (*Catostomus catostomus*), and sea lamprey (*Petromyzon marinus*).

Numerical habitat modelling

NHM consists of a hydrodynamic model and a biological model. The NHM used is a two-dimensional hydrodynamic model that predicts the variation of water depth and flow velocity over the surface area of a reach at a given flow (Leclerc et al. 1990, 1995). This model was inputted with the topographic description of the riverbed, the mapping of substrate grain size over the reach modeled, a series of physical coefficients (water viscosity and friction), and assumptions about fluid dynamics (conservation of water, mass, and momentum; Secretan et al. 2001; Secretan and Leclerc 1998). The biological model used is the habitat probabilistic index (HPI; Guay et al. 2000). This model is a multivariate logistic regression designed to distinguish the physical conditions used and avoided by fish. HPI models use depth (m), flow velocity ($m \cdot s^{-1}$), and substrate grain size (m) as independent variables. HPI values range from 0 (poor habitats) to 1 (best habitats) and have been argued to represent the probability of finding a fish under given physical variables (Guay et al. 2000). NHM combines the predictions of the hydrodynamic model (water depth, flow velocity), the map of substrate grain size, and the biological model to produce a map of the spatial heterogeneity of habitat quality.

Sampling

Fish activity, light intensity, and water temperature

We assessed the number and the location of parrs actively foraging over the complete surface area of the reach studied, under different water temperature and light intensity conditions. Parrs were considered to be actively foraging when they held a position on or above the substrate or when they fed. The number and location of parrs actively foraging was estimated by snorkelling the complete surface area of our study site during a total of 13 surveys (from 29 June to 5 August 2001). Each survey began at noon and was completed within 2 to 4 h. Observers snorkelled following a zigzag trajectory extending from one shore to the other while swimming always in an upstream direction to avoid fish disturbance (Cunjak et al. 1988). Each parr that was actively foraging was recorded by marking its home-rock with a coloured stone. The observers used a gentle movement of their

Fig. 1. Location of the study site in the province of Quebec, Canada.

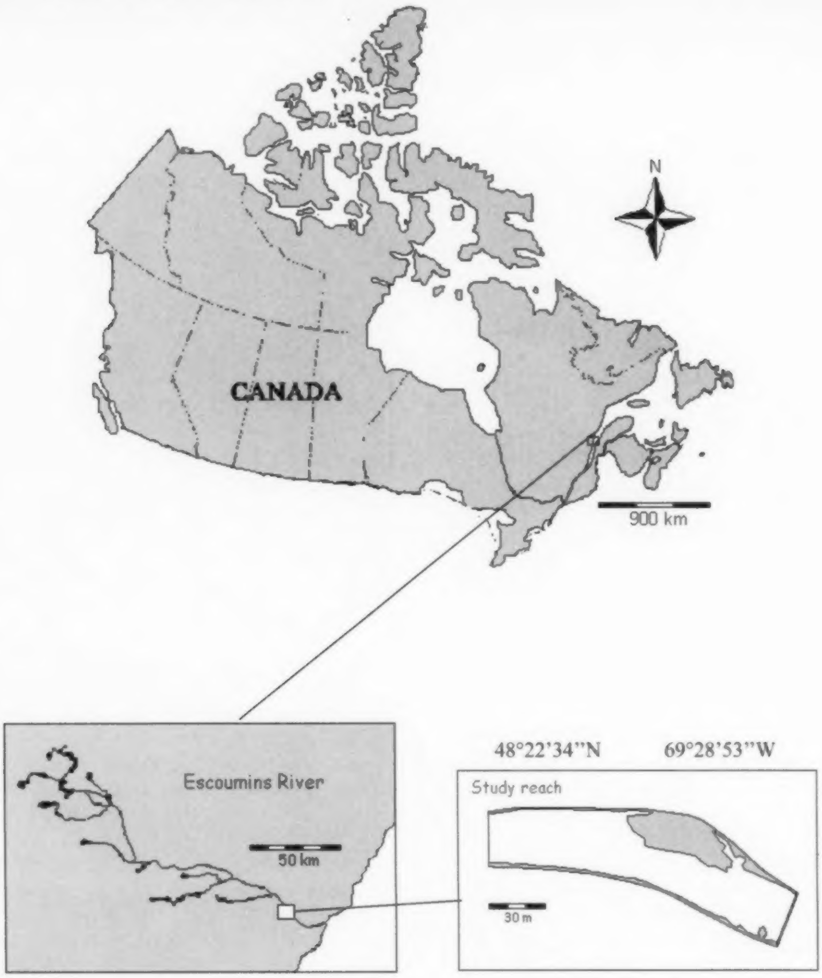

arms to direct the fish downstream and thereby avoid the recording of a second data point for a same fish. The coloured stones were georeferenced with a total station (electronic theodolite combined with an electronic distance measurement system, Sokkia SET3B; Sokkia Corp., Mississauga, Ont.) and an electronic data logger (Sokkia SDR33). Light intensity was assessed indirectly using a visual estimation of the percent cloudiness. The cloudiness and water temperature in the thalweg (measured with a hand thermometer) were noted at the beginning, middle, and end of each survey. Our surveys allowed us to count parrs and obtain precise maps of the distribution of actively foraging fish under contrasting light and water temperature conditions. Flow was noted at the beginning and end of each sampling day from the gauging station of the Ministère de l'Environnement du Québec 9 km from the river mouth. No tributaries entered the Escoumins River between the study reach and the gauging station. Flow was estimated to ensure that (*i*) each survey would be performed under a similar flow and (*ii*) the hydrodynamic simulations would be performed under the flow prevailing during the mappings of fish distribution.

Development of a hydrodynamic model

The development of the biological model (HPI) requires the description of the depth, flow velocity, and substrate grain size used and avoided by fish. These data were obtained using the hydrodynamic model and the map of substrate composition over the surface area of the reach. The hydrodynamic model was developed using the topography and the map of substrate composition of the reach. We quantified the latitude, longitude, and altitude of 2589 sampling points distributed over the riverbed and shores and above the high-water level of the reach. These points represented the complete range of morphological, topographic, and granulometric variations in the study reach. Each point was georeferenced with the total station. For each point, substrate grain size was estimated visually using the concept of *D*50 (Wolman 1954). Given that the volume of a stone is deter-

Table 1. Cloud cover (%) measured before, in the middle of, and after underwater fish surveys. Average cloud cover and water temperature (°C) for each survey are also shown.

	Cloud cover (%)				
Surveys	Before	Middle	After	Average	Average water temperature (°C)
29 June	100	100	100	100	16
30 June	90	90	100	93.3	18
1 July	100	100	100	100	16
5 July	10	5	0	5.0	20
7 July	70	50	100	73.3	19
8 July	75	70	60	68.3	18
9 July	20	30	40	30.0	20
10 July	70	85	100	85.0	19
1 August	15	70	15	33.3	20
2 August	50	100	100	83.3	21
3 August	5	10	20	11.7	21
4 August	50	20	0	23.3	21
5 August	10	20	40	23.3	20

mined by three axes (A being the longest axis, and C the shortest), $D50$ is defined as the length (in metres) of the B axis of the median stone within an area of 1 m^2. We evaluated the quality of the predictions of the hydrodynamic model by measuring depth and flow velocity (averaged over 30 s using a Price or Pygmy current meter (Gurley Precision Instruments, Troy, N.Y.) installed at 40% of the height of the water column) at 30 locations distributed over our reach. These locations represented the widest range of physical conditions available in the reach. Flow was noted at the gauging station before and after these measurements. Field measurements of depth and flow velocity were compared with predictions made by the hydrodynamic model at the 30 locations under the corresponding flow.

Calculations

Development of biological models

The 13 surveys were classified in three categories of cloud cover: low (0–33.3%), intermediate (33.4–66.7%), and high (66.8–100%). Six surveys were performed under low cloud cover, one under intermediate cloud cover, and six under high cloud cover. HPI models were developed using three of the 13 surveys (one for each category of cloud cover). The surveys used to develop HPI models under low and high cloud were selected at random within our data set. A HPI model for each of these surveys was developed by overlaying the map of fish distribution and the maps of the physical variables (i.e., depth, flow velocity, and substrate grain size). The conditions used by parrs during a survey were obtained by noting depth, flow velocity, and substrate grain size at each location where a fish was observed. The conditions avoided by parrs were taken as depth, flow velocity, and substrate grain size at points of the reach where no fish were observed within a radius of 2 m. For each survey, the number of points used to describe the conditions avoided by fish was equal to the number of fish observed during this survey. The data of the conditions used and avoided by fish were used to develop one matrix per survey. Each matrix had four columns. The first column described the presence (1) or the absence (0) of fish. The three other columns contained water depth, current velocity, and substrate size at sites used or avoided by fish. Each matrix was subjected to a Gaussian multivariate logistic regression (Guay et al. 2000). This procedure allowed us to predict HPI with depth, flow velocity, and substrate grain size under three levels of cloud cover (0%, 50%, and 100%).

NHM partitions the surface area of the reach modelled into a mosaic of triangular tiles. NHM assigns a value of depth, flow velocity, and substrate grain size to six points that delimit each triangular tile (at the three summits and in the middle of each side of a triangle). NHM further calculates a habitat quality index for each of these points by inputting the HPI model with point-specific values of depth, flow velocity, and substrate grain size. Maps of areas of the reach having similar habitat quality indices (further referred to as habitat patches) were drawn using these points. The habitat quality predictions were grouped in 10 classes (0–1 with steps of 0.1). Three habitat maps were created, one for each HPI model developed for different cloud cover.

Statistical analyses

Fish activity, light intensity, and water temperature

The relationship between the number of parrs actively foraging, cloud cover, and water temperature was evaluated with a multiple regression. This analysis was performed using the average cloud cover and the average water temperature noted at the beginning, in the middle, and at the end of our surveys as independent variables. Average cloud cover was always within 10% of the cloud cover observed in the middle of our surveys except on 7 July and 1 August (Table 1). On these dates, average cloud differed by 25–40% from cloud cover in the middle of the surveys. The relationship between the number of parrs actively foraging, water temperature, and cloud cover was evaluated using either the average cloud cover or, for 7 July and 1 August, the cloud cover observed in the middle of the survey. Average water temperature varied by less than 1 °C during any given survey. The partial regression coefficients were quantified with

Fig. 2. Variations of the number of actively foraging fish (shaded bars) with (*a*) cloud cover (black line) and (*b*) water temperature (black line).

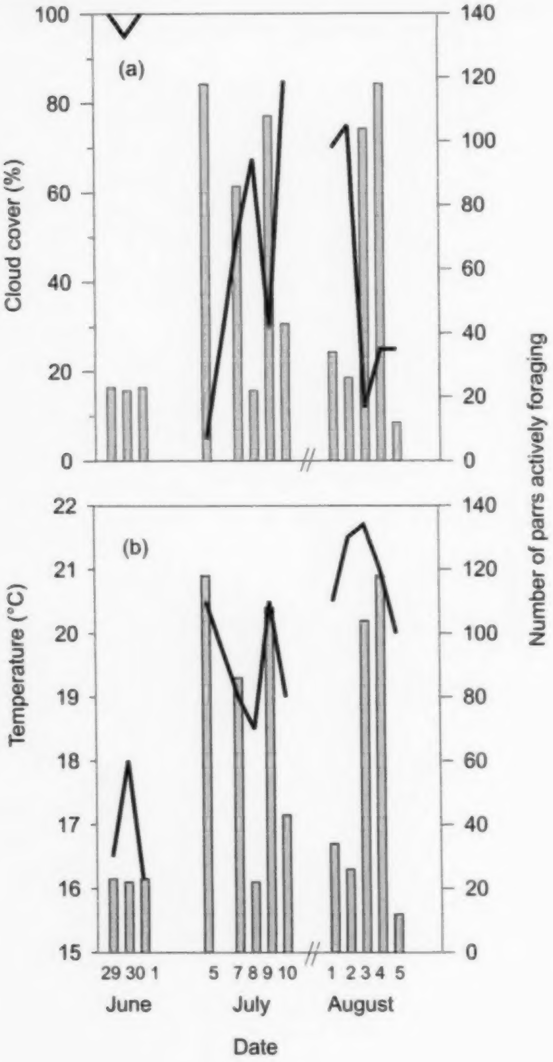

Fig. 3. Relationship between the number of parrs actively foraging and (*a*) cloud cover ($r^2 = 0.88$) or (*b*) water temperature ($r^2 = 0.37$). The sampling performed on 5 August is represented by a diamond. The regression lines were estimated without the sample of 5 August.

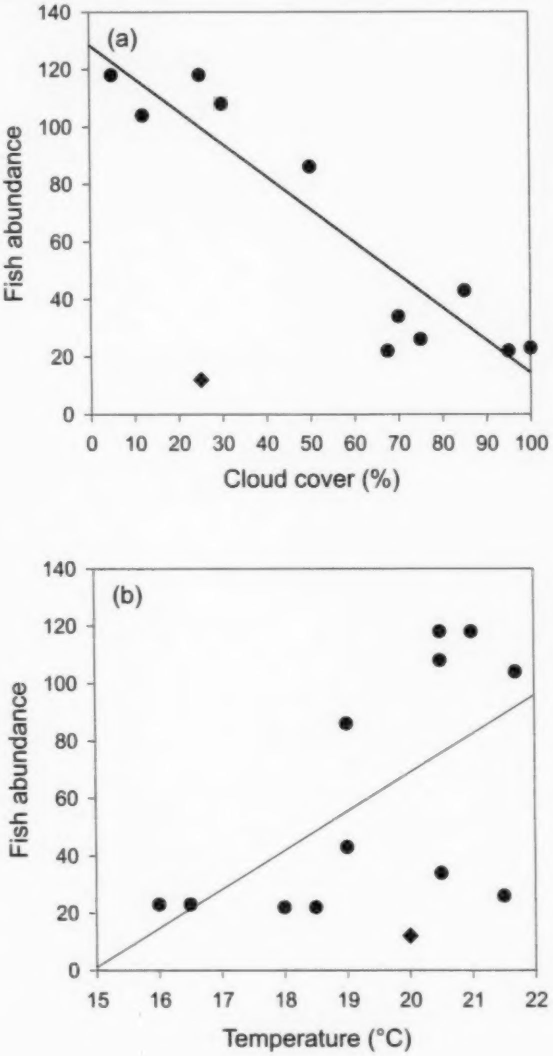

a multiple linear regression and permutation tests (Anderson and Legendre 1999).

Validity of the predictions made by the hydrodynamic model

We evaluated the predictive power of our hydrodynamic model by comparing the values of depth and flow velocity predicted by the hydrodynamic model to 30 real measures taken under the same flow. Predicted and measured values of depth and velocity were compared using a type II regression model (Mesplé et al. 1996). The predictions of the hydrodynamic model were considered valid if the 95% confidence intervals (CI) of slope and the intercept of the relationships between predicted and measured values included unity and zero, respectively. Mean and variance of predicted and measured values were compared with *t* and *F* statistics.

Comparison between fish distribution and predicted distribution pattern of habitats

We compared real fish distribution with the distribution of habitats predicted by NHM implemented with the three HPI models using two surveys (one low and one high cloud cover) selected at random from the 10 remaining surveys. A polynomial regression was used to assess the positive relationship between fish density and predicted HPI values assigned to habitat patches. This was done six times (combinations of three HPI models and two surveys). Because predictions of

Table 2. The mean and the variance of the two physical variables predicted by the hydrodynamic model (depth and flow velocity) and corresponding values measured in the field (n = 30).

	Depth (m)		Flow velocity ($m \cdot s^{-1}$)	
	Predicted	Field	Predicted	Field
Mean	0.434	0.366	0.440	0.434
Variance	0.038	0.031	0.033	0.036

HPI models were tested with a fish distribution taken from the same reach and, potentially, with the same fish used to develop HPI models, it can be expected, because of an autocorrelation between our dependent and independent variables, that HPI models will be adequate to predict fish distribution in the reach in which HPI models were developed. Hence, our procedure should not be interpreted as an attempt to validate HPI models, but as an attempt to identify invalid HPI models.

Results

Fish activity, light intensity, and water temperature

The number of fish observed over the complete reach during the different surveys ranged from 12 to 118 (average = 57 fish; Fig. 2). Cloud cover ranged from 5% to 100% and water temperature ranged from 16.5 °C to 21.7 °C among the surveys (Table 1). Multiple regression analysis showed that average cloud cover explained 44% of the variability of the number of fish actively foraging during our surveys (p = 0.001). Water temperature had no statistically significant effect on the number of fish observed (p = 0.48). A similar analysis using cloud cover in the middle of our surveys on 7 July and 1 August (for which the average was not within 10% of the cloud cover observed in the middle of the survey) suggested that cloud cover explained 58% of the variability of the number of fish observed (p = 0.001). Hence, the number of fish actively foraging decreased with cloud cover (Fig. 3*a*) but was unaffected by water temperature (Fig. 3*b*) in the range of conditions observed among the surveys. The last sampling point of the summer (5 August) was characterized by a very low number of fish observed (n = 12), despite the low cloud cover (25%; Fig. 3*a*) and the warm water temperature (20 °C; Fig. 3*b*). Elimination of the last sampling point of the summer from our analysis had no effect on our interpretation other than increasing the percentage of the variance of the number of fish observed explained by average cloud cover to 88% (using cloud cover in the middle of the surveys for 7 July and 1 August). We found a statistically significant relationship between average cloud cover (middle of survey values used for 7 July and 1 August) and water temperature (p < 0.05 tested by permutations). Water temperature tended to increase as cloud cover decreased (r = –0.64).

Validity of the predictions made by the hydrodynamic model

The mean (depth, t = –1.22, p = 0.15; flow velocity, t = 0.28, p = 0.90) and the variance (depth, F = 1.18, p = 0.59; flow velocity, F = 1.59, p = 0.83) of the predictions made by the hydrodynamic model were not significantly different from the mean and the variance of the measures taken in the field at a comparable flow (Table 2). Furthermore, predicted and measured values were correlated (r^2 = 0.84 for depth; r^2 = 0.62 for flow velocity). The slope of both major axes calculated between measured and predicted depth or velocities was not significantly different from 1 (Table 3). In addition, the intercept of these axes was not significantly different from 0 (Table 3). Our results, together with arguments provided by Guay et al. (2001), suggest that the precision of the hydrodynamic model was sufficient for our purposes.

Table 3. Lower and upper limits of the 95% confidences intervals of slope and intercept of the relationship (major axis) between predicted and measured depths and flow velocities for a discharge of 4.5 $m^3 \cdot s^{-1}$.

	Depth (m)		Flow velocity ($m \cdot s^{-1}$)	
Limits	Slope	Intercept	Slope	Intercept
Lower	0.821	–0.00052	0.712	–0.088
Upper	1.176	0.14392	1.217	0.131

The average discharge measured at the gauging station during sampling days of summer 2001 was 6.8 $m^3 \cdot s^{-1}$ (range = 5.0 to 8.1 $m^3 \cdot s^{-1}$). The hydrodynamic simulation used in this work was implemented at this average flow. According to this simulation, the maximum water depth for a discharge of 6.8 $m^3 \cdot s^{-1}$ was 1.40 m and the maximum flow velocity was 1.09 $m \cdot s^{-1}$. A complete description of the depths, flow velocities, and substrate grain size available to fish over the study reach according to the NHM are presented in Table 4.

Biological models

The surveys selected for the development of HPI were 5 July (flow of 6.1 $m^3 \cdot s^{-1}$, 5% cloud cover, number of fish observed = 141), 7 July (flow of 6.3 $m^3 \cdot s^{-1}$, 50% cloud cover, number of fish observed = 105), and 29 June (flow of 8 $m^3 \cdot s^{-1}$, 100% cloud cover, number of fish observed = 32). The following multivariate logistic regression model (Guay et al. 2000) was used to predict HPI values under different combinations of depth, flow velocity, and substrate grain size:

$$(1) \qquad \text{HPI} = 1/(1 + e^{-\lambda})$$

The three λ equations obtained using data collected under low (λ_L), intermediate (λ_I), and high cloud cover (λ_H) were

$$(2) \qquad \lambda_L = -2.39 + 5.73D + 3.03V + 0.52S - 6.29D^2$$

$$(3) \qquad \lambda_I = -3.06 + 9.88D + 3.31V - 4.13S - 9.68D^2$$

$$(4) \qquad \lambda_H = -11.25 + 27.65D + 4.21V + 61.34S - 31.43D^2$$

where D is the depth (m), V is the flow velocity ($m \cdot s^{-1}$), and S is the substrate grain size (m). The maps of habitat quality obtained using the three different HPI models always predicted relatively low habitat quality indices near the shores (HPI values from 0 to 0.1; Fig. 4). Furthermore, the maps of habitat quality indices predicted by HPI models developed under different cloud cover shared a common feature for rel-

Table 4. Depth (m), flow velocities ($m \cdot s^{-1}$), and substrate grain size (m) available over the study reach at a discharge of 6.8 $m^{-3} \cdot s^{-1}$. The availability of each physical condition is expressed as a percentage of the wetted surface of the reach.

Depth (m)	Percent available	Velocities ($m \cdot s^{-1}$)	Percent available	Substrate (m)	Percent available
0.0–0.3	31.4	0.0–0.2	7.1	Gravel (4×10^{-5}–0.032)	5.2
0.3–0.6	54.6	0.2–0.4	28.7	Pebble (0.032–0.064)	40.4
0.6–0.9	10.4	0.4–0.6	43.7	Cobble (0.064–0.25)	51.8
0.9–1.2	3.3	0.6–0.8	14.5	Boulder (0.25–1)	2.5
>1.2	0.3	>0.8	6.0	Metric boulder (>1)	0.1

atively high HPI values (0.6–0.7 or 0.9–1.0 depending of the model). The three HPI models predicted high HPI values just upstream of an island in the middle of the reach and relatively low HPI values near the upstream limit of this reach. Differences in HPI values predicted by these models were most obvious between HPI models developed with cloud cover <67% (low and intermediate cloud cover) and the HPI model developed with cloud cover >67% (high cloud cover). According to the models developed with <67% cloudiness, the study reach did not contain any habitat with a HPI index higher than 0.8. The surface area of habitat patches assigned the HPI values ranging from 0.9 to 1.0 represented 15% of the reach when using the HPI model developed with >67% cloudiness (near the left bank of the midsection of the reach; Fig. 4). The HPI values predicted by the models developed with <67% cloudiness in this same area were relatively low (0–0.1 or 0.4–0.5). Despite these differences, the HPI values averaged over the complete reach were very similar regardless of the model used (0.51, 0.54, and 0.51 for HPI models developed under low, intermediate, and high cloud cover, respectively).

Comparison between fish distribution and predicted distribution pattern of habitats

The maps of habitat quality predicted using NHM implemented with our three HPI models (Fig. 4) were compared with the real fish distribution during two surveys selected at random among days of low (9 July, 30% cloud cover, flow = 8.1 $m^3 \cdot s^{-1}$; Fig. 5*a*) and high (1 July, 100% cloud cover, flow = 5.5 $m^3 \cdot s^{-1}$; Fig. 5*b*) cloud cover. We found statistically significant and positive relationships ($p < 0.005$) between real fish densities in habitat patches under low cloud cover and HPI predictions for all HPI models (Fig. 6). However, the HPI models developed under low and intermediate cloud cover explained a larger fraction of the local variations of fish density at low cloud cover (94% and 98%, respectively) than the model developed under high cloud cover (82%). Relationships between fish densities under high cloud cover and predicted habitat quality were positive and statistically significant only for the HPI models developed under low and intermediate cloud cover ($p < 0.005$, $r^2 = 0.88$ and 0.79, respectively). The HPI model developed under high cloud cover was unable to predict fish distribution during the day of high cloud cover ($p > 0.1$; Fig. 6).

Discussion

Our results indicate that the number of fish adopting an actively foraging behaviour during the day may vary 5- to 10-fold among consecutive days of a summer. Our analyses further suggest that under the range of physical conditions found in our study, this variation is mostly related to the percent cloud cover ($0.44 < r^2 < 0.88$) and, by extension, to light intensity. Variations of water temperature did not explain a significant fraction of the among-day variations of the number of parrs adopting a diurnal foraging behaviour. Because increases in water temperature positively influence chemical and physiological processes in fish such as digestion rates and, thus, potential consumption rates (Elliott 1972; He and Wurtsbaugh 1993), it is possible that fish could increase their foraging activities during days when digestion rate and consumption rates are less limited by water temperature. This possibility is consistent with the studies of Fraser et al. (1995) and Bremset (2000), who found a clear positive relationship between the number of actively foraging parrs and water temperature. The lack of relationship between the foraging activity of parrs and water temperature in our study may be related to the small range of water temperature that we observed (16.5–21.7 °C) relative to Fraser et al. (1995; 2–18.5 °C) and Bremset (2000; 0–18 °C). The effect of the temperature range on the interpretation of our results is confirmed by the observation of Jonsson et al. (2001), who found that consumption rates of parrs in the lab at 16 °C did not differ from those estimated at 21 °C. Although fish foraging behaviour may be affected by water temperature in the range of 0 –18 °C, our results suggest that this effect is not statistically significant in the temperature range observed during our study.

One approach that can be used to interpret the relationship found between the number of actively foraging fish and cloud cover is to hypothesize that foraging strategies, like many other traits, have evolved to maximize fitness (Metcalfe and Steele 2001). It has been suggested that foraging strategies are chosen by fish on the basis of selective pressures defined by food availability or feeding rate (Lampert 1987; Reiriz et al. 1998; Metcalfe et al. 1999) and predation risk (Sih 1987; Eklöv 1997; Warburton and Brown 1997). In this context, fish may be hypothesized to select a foraging strategy that maximizes the ratio of food intake to predation risk. Our results are consistent with the hypothesis that factors decreasing the food intake – predation risk ratio may induce a larger proportion of a population of parrs to adopt a cryptic behaviour. Food intake is directly related to conditions that affect the capture efficiency of fish (Metcalfe and Steele 2001). Mechanistic models suggest that the capture efficiency of fish that hold a sit-and-wait position on or above the substrate partly depends on their ability to detect a food item and react sufficiently quickly to capture a prey before it is

Fig. 4. Maps of habitat quality indices predicted by habitat probabilistic index (HPI) models developed under (*a*) low, (*b*) intermediate, and (*c*) high cloud cover in the reach studied. HPI values ranging from 0 to 1 by intervals of 0.1 are represented using 10 shades of colour. Shores and islands are represented in grey. Simulations were performed for a flow of 6.8 $m^3 \cdot s^{-1}$.

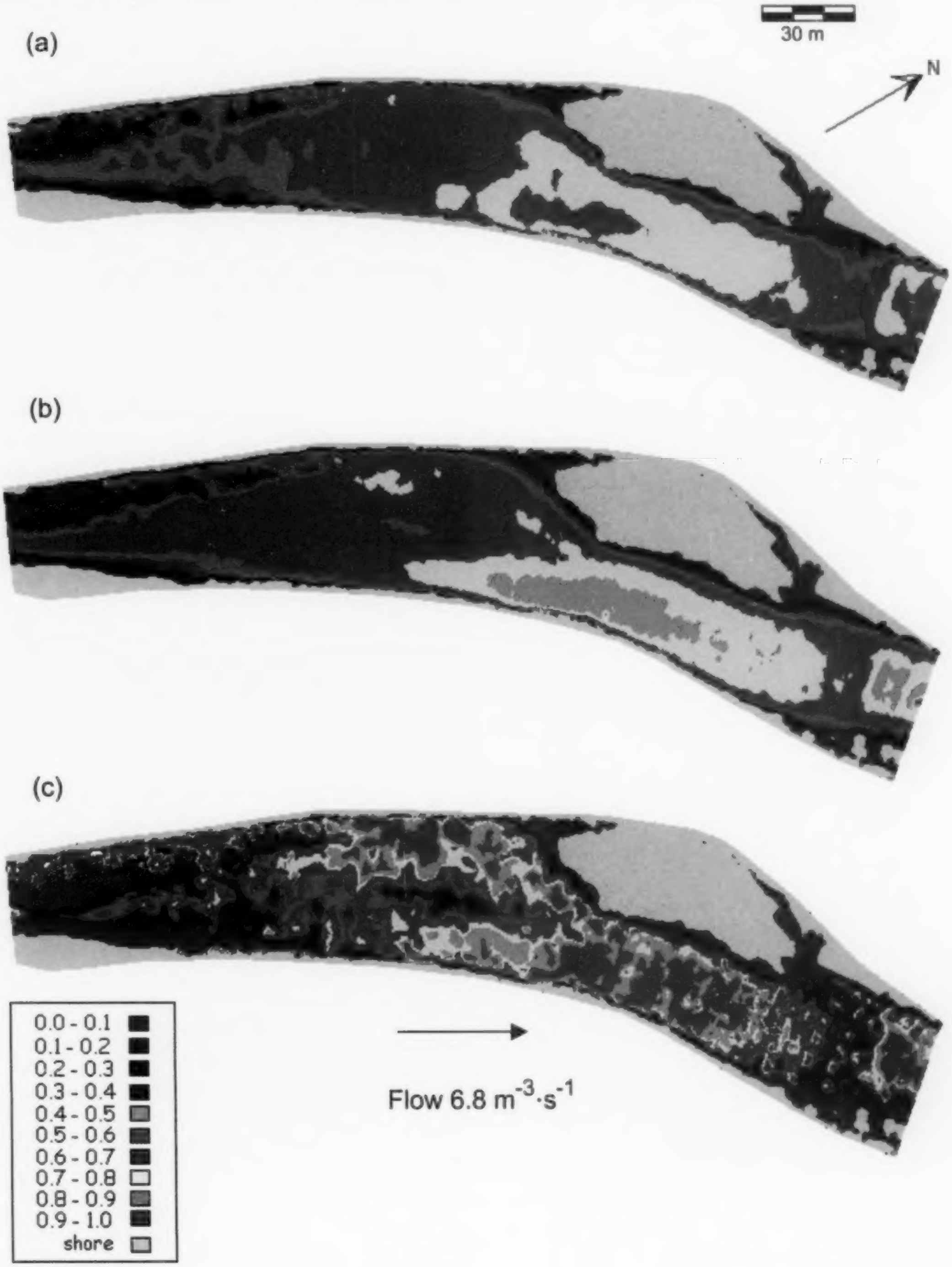
30 m
N
(a)
(b)
(c)
0.0 - 0.1
0.1 - 0.2
0.2 - 0.3
0.3 - 0.4
0.4 - 0.5
0.5 - 0.6
0.6 - 0.7
0.7 - 0.8
0.8 - 0.9
0.9 - 1.0
shore
Flow 6.8 m^-3·s^-1

Fig. 5. Observed fish distribution under (*a*) low and (*b*) high cloud cover in the reach studied. Each point represents the location of a single fish. The scale is in metres.

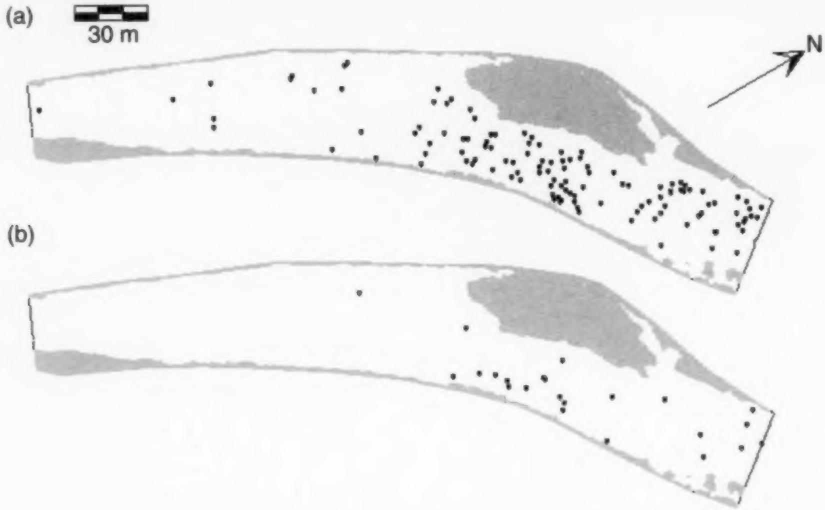

carried downstream (Hughes and Dill 1990; Metcalfe et al. 1997). Hence, any condition that will influence the reactive distance of the fish will also influence the time available to capture a prey and, therefore, the capture efficiency and food intake. It has been demonstrated that in low turbidity conditions, such as those encountered in Escoumins River, light intensity positively influences the reactive distance of parrs to preys and, consequently, their food intake (Benfield and Minello 1996). Light intensity may also affect the predation risk of parrs. The common merganser (*Mergus merganser*), the most important predator of parrs in Escoumins River, is a visual feeder. The efficiency of this predator is highest during daylight hours (Cramp and Simmons 1977). However, there are indications that light intensity may decrease predation risks affecting parrs. To detect fish, the common merganser submerges its head and visually scans areas underneath the water surface (Alvo 1995). This strategy is useful where depth is relatively important (<4 m) and flow velocity is moderate. In the Escoumins River, where mean depth is nearly 0.4 m and mean flow velocity is >0.8 $m \cdot s^{-1}$, prey detection directly from the surface is more common (as used by the juvenile mergansers; Foreman 1976). Hence, cloud cover, which directly influences light reflection on water surface, may improve the efficiency of mergansers to detect parrs. One interpretation of our results is that the negative relationship found between the abundance of actively foraging parrs and cloud cover may be driven simultaneously by the two selective pressures that determine fish foraging strategies. Under low cloud cover, higher light intensity may improve the ability of parrs to capture their prey and may diminish the risk of predation of parrs by mergansers. As cloud cover increases, the food intake – predation risk ratio may decrease (food intake decreases and predation risk increases), and consequently, as exemplified by our results, fewer fish adopt an actively foraging behaviour. The number of fish adopting an actively foraging behaviour was more strongly related to estimates of cloud cover in the middle of the surveys (when these were >20% different from estimates at the beginning or end of surveys) than to average cloud cover (including estimates noted at the beginning and end of surveys). This may suggest that the evaluation by fish of the benefits and costs associated with a certain level of cloud cover is done within minutes of a sudden change of cloud cover. Although our observations are consistent with the hypothesis that fish may select a foraging strategy (active or cryptic behaviour) that maximizes the food intake – predation risk ratio, we do not have any data (consumption or predation rates) allowing us to directly test this hypothesis.

Our analyses show that the quality of the predictions made by a habitat quality model such as HPI depends on the cloud cover prevailing during the collection of the data used to develop this biological model. HPI models developed under low to intermediate cloud cover could adequately predict habitat quality and fish distribution under any cloud cover. This is expected as HPI models were applied to the reach in which it was developed. Furthermore, many of the fish georeferenced to produce the map of fish distribution against which NHM predictions were tested may have been the same fish used to develop the HPI models. As such, our work cannot be interpreted as a statistically appropriate validation of HPI models. However, it is our contention that the inability of the HPI model developed under high cloud cover to predict fish distribution under these cloud conditions, despite the autocorrelation that exists within our data, is an indication that HPI models developed under high cover may be flawed. One alternate hypothesis that could explain the difficulty of a HPI model developed under high cloud cover to predict fish distribution is that this model was also developed using fewer fish (n = 64) than models under low and intermediate cloud cover (n = 210–282). We tested this hypothesis by assessing the performance of HPI models developed under low and intermediate cloud cover with a sample size identical to that used under high cloud cover conditions.

Fig. 6. Relationship between fish densities in habitat patches assigned different habitat probabilistic index (HPI) values during (*a*, *c*, *e*) low or (*b*, *d*, *f*) high cloud cover, and HPI values predicted by HPI models developed under (*a*, *b*) low, (*c*, *d*) intermediate, or (*e*, *f*) high cloud cover.

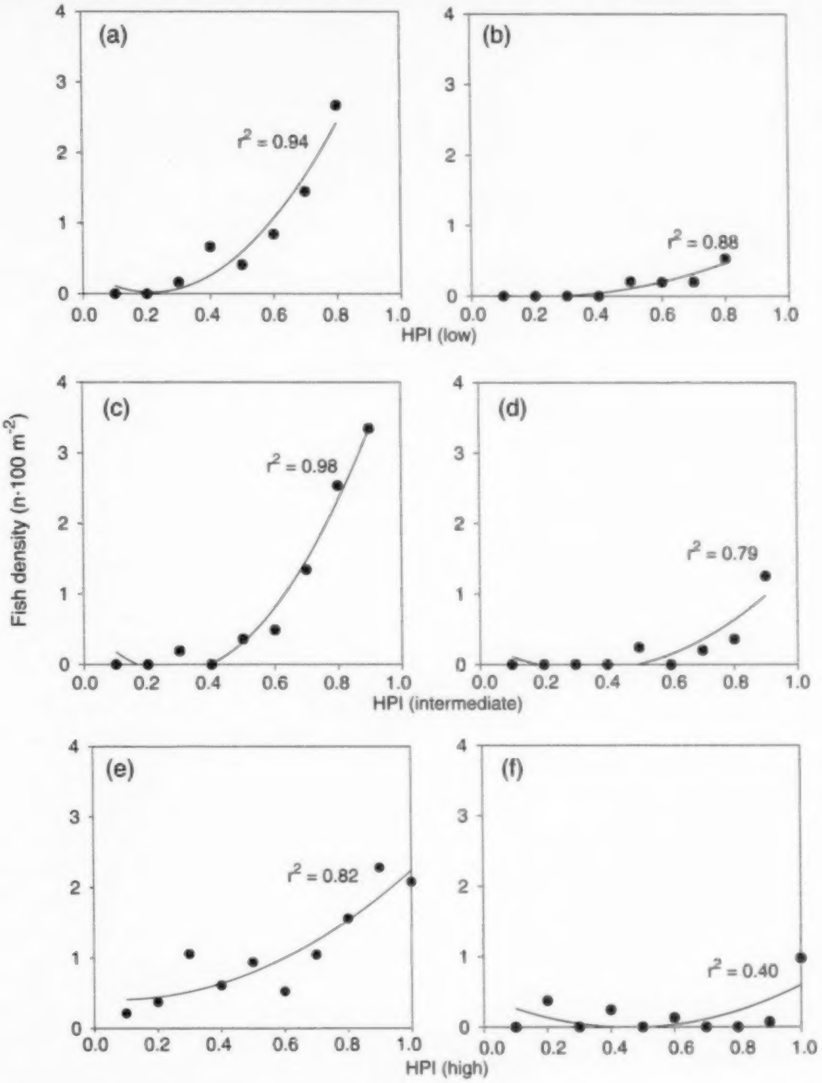

During this process, locations where fish were present or absent were selected at random within our data sets. These analyses showed that despite the lower sample size ($n = 64$), HPI models developed under low and intermediate cloud cover could adequately predict local variations of habitat quality and fish density within habitat patches ($r^2 = 0.85$–0.95), regardless of cloud cover. These simulations confirm that biologically meaningful and robust HPI models of parrs of Atlantic salmon may be developed only when cloud cover is <67%.

Acknowledgments

We thank Jean-François Bertrand, Sébastien Dupuis, and Patrick Gervais for their help in the field. We also thank the team of the Centre Interuniversitaire de Recherche sur le Saumon de l'Atlantique (CIRSA), Explo-Nature, and Jean-Marie Belisle from the Escoumins ZEC for logistic support. Funding for this research was provided by the Natural Sciences and Engineering Research Council of Canada (Collaborative Special Project), the Fondation de la Faune du Québec, the Government of Québec (Ministère de l'Environnement et de la Faune), the Governement of Canada (Economic Development), and the financial partners of CIRSA Inc. (Corporation de soutien aux initiatives de recherches sur le saumons atlantique): ALCAN, Association de la rivière Ste-Marguerite, Atlantic Salmon Federation, Boisaco, Bureau fédéral de développement régional (Québec), CRSNG, Conseil régional de développement de la Côte-Nord, Corporation municipale de Sacré-Cœur-sur-le-fjord-du-Saguenay, Corporation de pêche Sainte-Marguerite, Fédération Québécoise pour le Saumon de l'Atlantique, Fond décentralisé de création d'emploi de la Côte-Nord, and Hydro-Québec. Philippe Girard was supported by a postgraduate scholarship from Natural Sciences and Engineering Research Council of Canada.

References

Alvo, R. 1995. Grand Bec-Scie. *In* Les oiseaux nicheurs du Québec: atlas des oiseaux nicheurs du Québec méridional. *Edited by* J. Gauthier and Y. Aubry. Association québécoises des groupes d'ornithologues, Société québécoise de protection des oiseaux, Service canadien de la faune, Environnement Canada, région du Québec, Montréal. pp. 344–347.

Anderson, M.J., and Legendre, P. 1999. An empirical comparison of permutation methods for tests of partial regression coefficients in a linear model. J. Stat. Comput. Simul. **62**: 271–303.

Benfield, M.C., and Minello, T.J. 1996. Relative effects of turbidity and light intensity on reactive distance and feeding of an estuarine fish. Environ. Biol. Fishes, **46**: 211–216.

Bovee, K.D. 1978. The incremental method of assessing habitat potential for coolwater species, with management implications. Am. Fish. Soc. Spec. Publ. No. 11. pp. 340–346.

Bovee, K.D. 1982. A guide to stream habitat analysis using instream flow incremental methodology. Instream Flow Inf. Pap. 12. U.S. Fish. Wildl. Serv. FWS-OBS 82/26.

Bremset, G. 2000. Seasonal and diel changes in behaviour, microhabitat use and preferences by young pool-dwelling Atlantic salmon, *Salmo salar*, and brown trout, *Salmo trutta*. Environ. Biol. Fishes, **59**: 163–179.

Cramp, S., and Simmons, K.E.L. 1977. The birds of the western Palearctic. Vol. 1. Oxford University Press, Oxford.

Cunjak, R.A. 1988. Behaviour and microhabitat of young Atlantic salmon (*Salmo salar*) during winter. Can. J. Fish. Aquat. Sci. **45**: 2156–2160.

Cunjak, R.A., Randall, R.G., and Chadwick, E.M.P. 1988. Snorkelling versus electrofishing: a comparison of census techniques in Atlantic salmon rivers. Nat. Can. (Rev. Ecol. Syst.), **115**: 89–93.

deGraaf, D.A., and Bain, L.H. 1986. Habitat use and preferences of juveniles of Atlantic salmon in two Newfoundland rivers. Trans. Am. Fish. Soc. **115**: 671–681.

Eklöv, P. 1997. Effects of habitat complexity and prey abundance on the spatial and temporal distributions of perch (*Perca fluviatilis*) and pike (*Esox lucius*). Can. J. Fish. Aquat. Sci. **54**: 1520–1531.

Elliott, J.M. 1972. Rates of gastric evacuation in brown trout *Salmo trutta* L. Freshw. Biol. **2**: 1–18.

Fausch, K.D. 1984. Profitable stream positions for salmonids: relating specific growth rate to net energy gain. Can. J. Zool. **62**: 441–451.

Foreman, L.D. 1976. Observations of common Merganser broods in northwestern California. Calif. Fish Game, **62**: 207–212.

Fraser, N.H.C., and Metcalfe, N.B. 1997. The costs of becoming nocturnal: feeding efficiency in relation to light intensity in juvenile Atlantic salmon. Funct. Ecol. **11**: 385–391.

Fraser, N.H.C., Heggenes, J., Matcalfe, N.B., and Thorpe, J.E. 1995. Low summer temperatures cause juvenile Atlantic salmon to become nocturnal. Can. J. Zool. **73**: 446–451.

Gries, G., and Juanes, F. 1998. Microhabitat use by juvenile Atlantic salmon (*Salmo salar*) sheltering during the day in summer. Can. J. Zool. **76**: 1441–1449.

Gries, G., Whalen, K.G., Juanes F., and Parrish, D.L. 1997. Nocturnal activity of juvenile Atlantic salmon (*Salmo salar*) in late summer: evidence of diel activity partitioning. Can. J. Fish. Aquat. Sci. **54**: 1408–1413.

Guay, J.C., Boisclair, D., Rioux, D., Leclerc, M., Lapointe, M., and Legendre, P. 2000. Development and validation of numerical habitat models for juveniles of Atlantic salmon (*Salmo salar*). Can. J. Fish. Aquat. Sci. **57**: 2065–2075.

Guay, J.C., Boisclair, D., Leclerc, M., Lapointe, M., and Legendre, P. 2001. Science on the edge of spatial scales: a reply to the comments of Williams (2001). Can. J. Fish. Aquat. Sci. **58**: 2108–2111.

He, E., and Wurtsbaugh, W.A. 1993. An empirical model of gastric evacuation rates for fish and an analysis of digestion in piscivorous brown trout. Trans. Am. Fish. Soc. **122**(5): 717–730.

Heggenes, J., Krog, O.M.W., Lindas, O.R., Dokk, J.G., and Bremnes, T. 1993. Homeostatic behavioural responses in a changing environment: brown trout (*Salmo trutta*) become nocturnal during winter. J. Anim. Ecol. **62**: 295–308.

Hughes, N.F., and Dill, L.M. 1990. Position choice by drift-feeding salmonids: model and test for Arctic grayling (*Thymallus arcticus*) in subarctic mountain streams, interior Alaska. Can. J. Fish. Aquat. Sci. **47**: 2039–2048.

Jonsson, B., Forseth, T., Jensen, A.J., and Naesje, T.F. 2001. Thermal performance in juvenile Atlantic salmon, *Salmo salar* L. Funct. Ecol. **15**: 701–711.

Kalleberg, H. 1958. Observations in a stream tank of territoriality and competition in juvenile salmon and trout (*Salmo salar* L. and *S. trutta* L.). Rep. Inst. Freshw. Res. Drottningholm, **39**: 55–98.

Lampert, W. 1987. Vertical migration of freshwater zooplancton: indirect effects of vertebrate predators on algal communities. *In* Predation: direct and indirect impacts on aquatic communities. *Edited by* W.C. Kerfoot and A. Sih. University Press of New England, Hanover, N.H. pp. 291–300.

Leclerc, M., Bellemare, J.F., Dumas, G., and Dhatt, G. 1990. A finite element model of estuarian and river flows with moving boundaries. Adv. Water Res. **4**: 158–168.

Leclerc, M., Boudreault, J., Bechara, J., and Corfa, G. 1995. Two dimensional hydrodynamic modelling: a neglected tool in the instream incremental methodology. Trans. Am. Fish. Soc. **124**(5): 645–662.

Mesplé, F., Troussellier, M., Casellas, C., and Legendre, P. 1996. Evaluation of simple statistical criteria to quantify a simulation. Ecol. Model. **88**: 9–18.

Metcalfe, N.B., and Steele, G.I. 2001. Changing nutritional status causes a shift in the balance of nocturnal to diurnal activity in European minnows. Funct. Ecol. **15**: 304–309.

Metcalfe, N.B., Valdimarsson, S.K., and Fraser, N.H. 1997. Habitat profitability and choice in a sit-and-wait predator: juvenile salmon prefer slower currents on darker nights. J. Anim. Ecol. **66**: 866–875.

Metcalfe, N.B., Fraser, N.H.C., and Burns, M.D. 1999. Food availability and the nocturnal vs. diurnal foraging trade-off in juvenile salmon. J. Anim. Ecol. **68**: 371–381.

Morantz, D.L., Sweeney, R.K., Shirvell, C.S., and Longard, D.A. 1987. Selection of microhabitat in summer by juvenile Atlantic salmon (*Salmo salar*). Can. J. Fish. Aquat. Sci. **44**: 120–129.

Reiriz, L., Nicieza, A.G., and Brana, F. 1998. Prey selection by experienced and naive juvenile of Atlantic salmon. J. Fish Biol. **53**: 100–114.

Rimmer, D.M., Paim, U., and Saunders, R.L. 1983. Autumnal habitat shift of juvenile Atlantic salmon (*Salmo salar*) in a small river. Can. J. Fish. Aquat. Sci. **40**: 671–680.

Rimmer, D.M., Paim, U., and Saunders, R.L. 1984. Changes in the selection of microhabitat by juvenile of Atlantic salmon (*Salmo* *salar*) at the summer–autumn transition in a small river. Can. J. Fish. Aquat. Sci. **41**: 469–475.

Secretan, Y., and Leclerc, M. 1998. MODELEUR: a 2D hydrodynamic GIS and simulation software. *In* Proceeding of the Hydroinformatics '98 International Conference, Copenhagen. A.A. Balkema, Rotterdam.

Secretan, Y., Leclerc, M., Duchesne, S., and Heniche, M. 2001. Une méthodologie de modélisation numérique de terrain pour la simulation hydrodynamique bidimensionnelle. Rev. Sci. Eau, **14**(2): 187–212.

Sih, A. 1987. Predators and prey lifestyle: an evolutionary and ecological overview. *In* Predation: direct and indirect impacts on aquatic communities. *Edited by* W.C. Kerfoot and A. Sih. University Press of New England, Hanover, N.H. pp. 203–224.

Warburton, K., and Brown, C. 1997. Predator recognition and anti-predator responses of the rainbow fish *Melanotaenia eachamensis*. Behav. Ecol. Sociobiol. **41**: 61–68.

Webb, P.W. 1978. Temperature effects on acceleration in rainbow trout (*Salmo gairdneri*). J. Fish. Res. Board Can. **35**: 1417–1422.

Wolman, M.G. 1954. A method of sampling coarse river bed material. Trans. Am. Geophys. Union, **35**: 951–956.

Assessment of the transferability of biological habitat models for Atlantic salmon parr (*Salmo salar*)[1]

J.C. Guay, D. Boisclair, M. Leclerc, and M. Lapointe

Abstract: We assessed the transferability of the habitat suitability index (HSI) and the habitat probabilistic index (HPI) between two rivers. Transferability was measured by the ability of HSI and HPI models developed in the Sainte-Marguerite River to predict the distribution of Atlantic salmon parr (*Salmo salar*) in the Escoumins River. HSI and HPI were based on the pattern of utilization by fish of water depth, current velocity, and substrate size. HSI was developed using the preference curve approach, and HPI was developed using a multiple logistic regression. Predicted values of HSI and HPI in Escoumins River ranged from 0 (poor habitat) to 1 (excellent habitat). Fish density in habitat patches assigned different HSI or HPI values ranged from 0 to 1 fish·100 m^{-2}. Only HPI adequately predicted local variations in parr density ($r^2 = 0.84$) in habitat patches of Escoumins River. Our results suggest that HSI is less transferable between rivers than HPI. Differences in substrate size between the two rivers is suspected to impede the transferability of the HSI model. We also argue that the mathematical structure of HPI provides a larger degree of flexibility that facilitates its transferability and its potential generalization.

Résumé : Nous avons évalué la transférabilité d'un indice de qualité d'habitat (IQH) et d'un indice probabiliste d'habitat (IPH) entre deux rivières. Nous avons mesuré la transférabilité de ces deux modèles biologiques développés dans la rivière Sainte-Marguerite par leur habileté à prédire la distribution des tacons de saumon atlantique (*Salmo salar*) dans la rivière Escoumins. Le développement de l'IQH et de l'IPH repose sur les patrons d'utilisation par les tacons de la profondeur de l'eau, de la vitesse du courant et de la taille du substrat. L'IQH a été établi selon l'approche des courbes de préférence tandis que l'IPH a été construit en utilisant la régression logistique multiple. Les valeurs prédites d'IQH et d'IPH dans la rivière Escoumins ont varié entre 0 (mauvais habitat) à 1 (excellent habitat). Les densités de tacons dans les parcelles d'habitat auxquelles ont été attribuées différentes valeurs d'IQH ou d'IPH ont varié entre 0 et 1 tacon·100 m^{-2}. Le modèle numérique d'habitat utilisant l'IPH a été le seul qui a permis de prédire la distribution des tacons ($r^2 = 0{,}84$) dans les parcelles d'habitat de la rivière Escoumins. Nos résultats suggèrent que l'IQH est plus sensible au processus de transférabilité que peut l'être l'IPH. La différence de la taille du substrat entre les deux rivières semble empêcher la transférabilité de l'IQH. Nous avançons que la structure mathématique de l'IPH fournit un degré de flexibilité plus grand, ce qui facilite sa transférabilité et sa généralisation potentielle.

Introduction

Numerical habitat models (NHM) are used to evaluate the effect of variations of flow on the quantity and quality of fish habitats in rivers (Thomas and Bovee 1993; Leclerc et al. 1996; Guay et al. 2000). Numerical habitat models are divided into two parts: first, a hydrodynamic model predicting local variations of depth, current velocity, and substrate size within a reach for any given flow (Bovee 1982; Leclerc et al. 1990); and second, a biological model providing a quantitative estimate of the propensity of fish to use given environmental conditions (Bovee 1982; Leclerc et al. 1995). The propensity of fish to use a specific depth, current velocity, or substrate size is quantified with a habitat suitability criteria (HSC; ranging from 0 to 1). HSC may also express the utilisation ratio of a given environmental condition to its availability within a reach (Heggenes 1991). Variations in HSC over the complete range of an environmental condition define the preference curve of fish for this environmental condition (deGraaf and Bain 1986; Morantz et al. 1987;

Received 24 May 2002. Accepted 31 August 2003. Published on the NRC Research Press Web site at http://cjfas.nrc.ca on 5 December 2003.
J16908

J.C. Guay and D. Boisclair.[2] Université de Montréal, Département de sciences biologiques, C.P. 6128, succursale Centre-ville, Montréal, QC H3C 3J7, Canada.
M. Leclerc. INRS-Eau, C.P. 7500, Sainte-Foy, QC G1V 4C7, Canada.
M. Lapointe. McGill University, Department of Geography, 805 Sherbrooke W, Montréal, QC H3A 2K6, Canada.

[1] Contribution to the program of CIRSA (Centre Interuniversitaire de Recherche sur le Saumon Atlantique).

[2] Corresponding author (e-mail: Daniel.Boisclair@UMontreal.ca).

doi: 10.1139/F03-120

Heggenes 1996). Knowledge of HSC values for depth, current velocity, and substrate size permit estimates of the propensity of fish to use given combinations of environmental conditions. The habitat suitability index (HSI) is a commonly used joint-suitability criteria, which is calculated as the weighted geometric product of HSC for water depth, current velocity, and substrate size (Leclerc et al. 1996; Bovee et al. 1998; Guay et al. 2000). Values of HSI generally range from 0 (poor habitat) to 1 (excellent habitat). The surface area of habitat patches assigned a given HSI value (e.g., from 0.5 to 0.6) usually range from 10^1 to 10^3 m^2 (Guay et al. 2000). Estimation of HSI values for a complete series of habitats of a reach is used to evaluate the quantity, quality, and distribution of habitats within that reach. Comparison of HSI values obtained for different flows is expected to measure the effect of flow variation on fish habitat.

The existence of a relationship ($0.63 < r^2 < 0.76$; see Guay et al. 2000) between HSI values assigned to different areas of a reach and fish density observed in these areas is supported by few studies (Boudreau et al. 1996; Guay et al. 2000). This suggests that NHM provides a biologically meaningful representation of fish habitat quantity, quality, and distribution. Although the possibility of using a HSI model developed in one river to predict attributes of fish habitat in another river would greatly facilitate the routine use of NHM, attempts to assess the validity and transferability of HSI provided mixed results (Scott and Shirvell 1987; Freeman et al. 1997; Mäki-Petäys et al. 2002). Consequently, it has been suggested that the concept of transferable models should be abandoned for a more laborious river-by-river approach in which a HSI model is developed for each river modelled (Bozek and Rahel 1992; Thomas and Bovee 1993).

The study of Guay et al. (2000) showed that a new biological model, referred to as a habitat probabilistic index (HPI), was more strongly related to fish density ($0.81 < r^2 < 0.98$) than HSI ($0.63 < r^2 < 0.71$). HPI is derived from a multivariate nonlinear logistic regression (Legendre and Legendre 1998) based on a matrix of presence–absence of fish for abiotic variables such as water depth, current velocity, and substrate size. Because of its mathematical structure, HPI has been argued to more closely represent the probability of finding fish under a given set of environmental conditions than HSI or any other model currently available (Guay et al. 2000). Interestingly, the fact that HSC such as HSI do not represent the probability of finding fish in a given habitat has been identified as a key element precluding the transferability of this kind of biological model (Scott and Shirvell 1987). The objective of our study was to assess the relative transferability of HSI and HPI by predicting the spatial distribution of fish habitat and local variations in fish density in one river using HSI and HPI developed in another river.

Material and methods

Study sites and species

The rivers covered by our study are the Sainte-Marguerite (70°26′E, 48°25′N) and the Escoumins (69°28′E, 48°21′N) rivers. These rivers are located in two adjacent watersheds on the northern shore of the St. Lawrence River, approximately 600 km north–northeast of Montreal (Quebec, Canada; Fig. 1). Summer low water flow in the Sainte-Marguerite and Escoumins rivers range from 2.0 to 3.0 $m^3 \cdot s^{-1}$ and from 5.5 to 7.5 $m^3 \cdot s^{-1}$, respectively. HSI and HPI were developed in a 750-m reach of the Sainte-Marguerite River located 80 km from its discharge into the Saguenay River (Guay et al. 2000). These two models were used to predict fish distribution in a 350-m reach of the Escoumins River 25 km from its discharge at the St. Lawrence River. Our work focussed exclusively on juveniles (ages 1+ and 2+) of Atlantic salmon (*Salmo salar*). Both rivers were dominated by Atlantic salmon (>95% of observations) but shared five other fish species: brook charr (*Salvelinus fontinalis*), American eel (*Anguilla rostrata*), longnose dace (*Rhinichthys cataractae*), longnose sucker (*Catostomus catostomus*), and sea lamprey (*Petromyzon marinus*).

Numerical habitat model

NHM consist of a hydrodynamic model and a biological model (Leclerc et al. 1996; Bovee et al. 1998). The methods and computations that we used to develop the hydrodynamic and biological models have been described in detail by Guay et al. (2000). Briefly, the hydrodynamic model used is a two-dimensional model designed to predict water depth and current velocity for any combination of longitudinal (upstream–downstream axis) and transversal coordinates (left bank – right bank axis) of a river (Leclerc et al. 1994, 1996). This hydrodynamic model requires a topographic and granulometric representation of a riverbed. Coordinates of the locations used to assess river topography are used to construct a grid of triangular elements that serve as a spatial framework on which to perform the numerical habitat simulations. The hydrodynamic model is inputted with a user-defined flow and combines topographic measurements, substrate information, and a series of physical coefficients and assumptions (water viscosity and friction, equations of energy conservation and momentum). This procedure allows the hydrodynamic model to assign a value of average water depth, current velocity, and substrate size to the points located at the summit and in the middle of the sides of each of the triangular elements of the grid extending over the complete surface area of the reach modelled. Hydraulic conditions in the Escoumins River were modelled at a flow of 6.0 $m^3 \cdot s^{-1}$ because it corresponded to the average flow prevailing during the mapping of fish distribution in this river (range = 5.5–6.5 $m^3 \cdot s^{-1}$). The hydrodynamic model that we used is not appropriate to predict current velocity at very small spatial scales (i.e., point measures of current velocity as taken in the field). The hydrodynamic model that we used predicts a single current velocity in a patch of 10^1–10^3 m^2, whereas in reality, current velocity may vary 10- or 100-fold from one point to another within this patch (e.g., from 1 m upstream of a large rock to a few centimetres downstream of the same rock). Although the hydrodynamic model that we used is not able to predict current velocity variations at fine spatial scales, the current velocity value predicted in a patch corresponds to the average current velocity value within this patch (Guay et al. 2000, 2001). Hence, the hydrodynamic model used is capable of expressing variations of current velocity and, consequently, of habitat quality between patches of 10^1–10^3 m^2. We therefore limited interpretation of the predictions of NHM to this spatial scale. The ability of hydro-

Fig. 1. Location of the Sainte-Marguerite and Escoumins rivers in Québec, Canada.

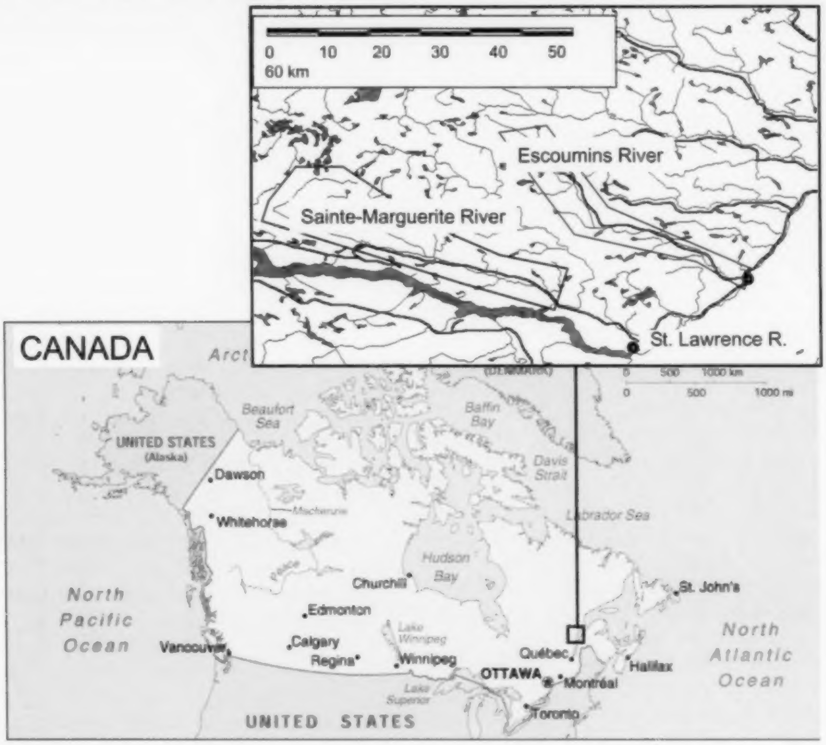
0 10 20 30 40 50
60 km
Escoumins River
Sainte-Marguerite River
St. Lawrence R.
CANADA
Arct
(DENMARK)
0 500 1000 km
0 500 1000 mi
Beaufort Sea
UNITED STATES (Alaska)
Dawson
Whitehorse
Mackenzie
Baffin Bay
Davis Strait
Labrador Sea
Hudson Bay
Churchill
Edmonton
North Pacific Ocean
Vancouver
Calgary
Regina
Lake Winnipeg
Winnipeg
Lake Superior
Québec
OTTAWA
Montréal
Toronto
Halifax
St. John's
North Atlantic Ocean
UNITED STATES

dynamic models to predict current velocity at different spatial scales has been discussed by Williams (2001) and Guay et al. (2001).

Water depth, current velocity, and substrate size obtained from the hydrodynamic model are used as inputs to the biological models to assign HSI or HPI values to the summit and the middle of the sides of each of the triangular elements. The results of the modelling exercise are maps of local variations in HSI or HPI values over the reach modelled. These maps are expected to represent patches of habitats with different ecological values and, consequently, patches of habitats potentially characterized by different fish densities. These maps are drawn using colours representing 10 classes of presumed habitat quality values (0–1 by increments of 0.1).

Sampling

Hydrodynamic model

The topographic map of the Escoumins River required to perform the hydrodynamic simulation was developed by measuring the *X*, *Y*, and *Z* coordinates (longitude, latitude, and altitude) of the riverbed at 2116 locations distributed throughout the reach studied. These coordinates were obtained using an electronic theodolite coupled with an electronic distance measurement system (Sokkia SET3B; Sokkia Corp., Mississauga, Ont.). The granulometric representation of the riverbed was obtained by estimating the mean size of the substrate (*D*50) at every location. Given that the volume of a stone is determined by three axes (*A* being the longest, *B* the intermediate, and *C* the shortest axis), *D*50 is defined as the length (in cm) of the *B* axis of the median stone within the 1-m^2 area centred on each location. *D*50 was estimated visually by observers trained during 2 days of calibration (Latulippe and Lapointe 2001).

Biological models

The two biological models used in our study were developed in the Sainte-Marguerite River using a description of the prevalent environmental conditions in a series of 1-m^2 areas used by fish (where fish were found), available to fish (selected at random regardless of the presence or absence of fish), and avoided by fish (where no fish were observed). The HSI model used requires a description of the environmental conditions used by fish and the availability of these conditions in a river. The HPI model requires data on the environmental conditions used and avoided (instead of available to fish) by fish in a river. The environmental conditions used by fish were assessed by snorkelling a 750-m reach of the Sainte-Marguerite River during two periods of the summer (16–24 July and 1–10 August 1997). Sampling was performed during mid-day (between 10:00 and 16:00) and only during days when the cloudiness was lower than 25%. Flow rate ($m^3 \cdot s^{-1}$) was recorded for every sampling day from a continuous flow station located 500 m upstream from the reach under study. Flow ranged from 1.9 $m^3 \cdot s^{-1}$ to 4.1 $m^3 \cdot s^{-1}$ in July and from 2.3 $m^3 \cdot s^{-1}$ to 5.5 $m^3 \cdot s^{-1}$ in August (both months averaged 3.7 $m^3 \cdot s^{-1}$). Water temperature during our surveys ranged from 15 °C to 23 °C in July and from 14 °C to 21 °C in August.

The snorkelling diver could cover all of the surface area of a 50- to 100-m reach (further referred to as sections) in one day. The diver swam upstream to minimise fish disturbance (Cunjak 1988). Each fish encountered was observed for 1–2 min to confirm that it displayed site fidelity. The position of each fish that displayed site fidelity was then marked with a stone coloured with fluorescent paint and was later georeferenced. The fish was then chased downstream to avoid recording two series of data for the same fish. For each fish location, water depth, mean current velocity of the water column, and substrate size ($D50$) were noted. A total of 308 fish were used to assess the environmental conditions used by parr of Atlantic salmon. Our visual observations indicated that fish behaviour was qualitatively comparable between the sampling surveys of July and August. Furthermore, overall parr abundance in the reach used to develop our biological models was relatively stable between both months (159 parrs in July, 149 parrs in August) for an average density of 0.75 parr·100 m^{-2}. These observations suggest that parr do not perform important behaviour or habitat shifts during this period of the summer.

Water depth and current velocity available to fish during a specific sampling day were predicted using the hydrodynamic model implemented with the flow rate observed in the section surveyed that day. Hence, the hydrodynamic model was used to predict water depth and current velocity at the summit and in the middle of the sides of each of the triangular elements making up the hydrodynamic grid during a given sampling day (total of 1500–2500 points). Substrate size at these points was taken directly from a mapping of substrate composition performed over the complete study reach. This procedure was used to minimize the sampling effort deployed in the field and to maximize the proportion of the reach for which physical conditions were obtained. A frequency distribution of water depth, current velocity, and substrate size over the complete length of the section surveyed for fish during a day was taken as an adequate representation of the environmental conditions available to fish during that day.

Environmental conditions avoided by fish during a sampling day were described using the hydrodynamic model, the flow rate, and the map of fish distribution observed in the section surveyed that day. The map of fish distribution during one day was overlaid on the maps of predicted water depth and current velocity and on the map of substrate size for the section surveyed that day at the proper flow. This allowed us to randomly select a total of 308 points (sum across all sampling days) in which no fish were observed (at least 2 m from the closest georeferenced parr). Water depth, current velocity, and substrate size at these 308 locations where no fish have been observed were taken as an adequate description of the environmental conditions avoided by fish.

Mapping of the spatial distribution of fish

Mapping of fish spatial distribution in the Escoumins River was performed by snorkelling the 350-m reach between 10:00 and 16:00 on two consecutive days during which cloud cover was <25% (14–15 July 1999). Flow during these days ranged from 5.5 $m^3 \cdot s^{-1}$ to 6.5 $m^3 \cdot s^{-1}$. Water temperature during the mapping of parr ranged from 14 °C to 21 °C. Fish were observed and georeferenced following an approach identical to that used to develop HSI and HPI models. However, no additional physical data were collected during the mapping of fish in the Escoumins River. Hence, fish mapping was performed during a period of the summer that was within 1 month of the sampling done to develop the biological models that we used. Furthermore, both samplings were performed under almost identical meteorological and water temperature conditions except for flow, which was 1.6 times greater in the Escoumins River than in the Sainte-Marguerite River. This situation had relatively little effect on the difference in water depth and current velocities available to fish in these rivers (see Results, Predictions of NHM).

Computations

Habitat suitability model

The habitat suitability model was developed using the environmental conditions used by fish and those available to fish in the Sainte-Marguerite River. This model requires the calculation of the propensity of fish to select given intervals of water depth, current velocity, and substrate size (see Guay et al. (2000) for a complete description of the computations). The propensity of fish to select an environmental condition, c, was estimated using a preference index I_c (ranging from 0 to 1). We used weighted preference indices for water depth (I_D), current velocity (I_V), and substrate size (I_S) to develop our HSI model (Guay et al. 2000):

$$(1) \qquad \mathrm{HSI} = I_D^{0.30} \cdot I_V^{0.38} \cdot I_S^{0.32}$$

The weight of each preference index is represented by their respective exponent and is estimated using a multiple regression analysis (Guay et al. 2000).

Habitat probabilistic model (HPI)

The model of HPI was calculated by fitting a multivariate Gaussian logistic regression model to the presence–absence fish data set of the Sainte-Marguerite River. This data set was organised as a matrix containing four columns. The first column identified if the associated environmental conditions were observed for the presence (1) or absence of a fish (0). The three other columns contained the water depth, current velocity, and substrate size at sites characterized by the presence or absence of fish. The logistic equation derived using these data produced our HPI model (Guay et al. 2000):

$$(2) \qquad \mathrm{HPI} = 1/(1 + e^{-\lambda})$$

where

$$(3) \qquad \lambda = -3.067 + 8.461D + 2.86V + 0.093S - 6.203D^2$$

and where D, V, and S are water depth (m), current velocity ($m \cdot s^{-1}$), and substrate size ($D50$; cm), respectively.

The models of HSI and HPI allowed us to produce predictions of habitat quality for parr at any point of a reach for which water depth, current velocity, and substrate size can be estimated. In our study, water depth and current velocity were estimated using the hydrodynamic simulation of the study reach of Escoumins River, and substrate composition was extracted from the field-derived map of riverbed substrate size.

Data analysis

We tested the ability of HSI or HPI models developed in the Sainte-Marguerite River to predict the distribution of parr habitat and density in the Escoumins River by comparing the strength of the relationship between real fish density and predicted HSI or HPI values. This was performed in five steps. First, we overlaid the map of expected habitat quality according to HSI or HPI and the map of observed fish distribution in the reach. Water depth and current velocity required to calculate HSI and HPI in the Escoumins River were obtained using a hydrodynamic model. The procedure by which the hydrodynamic model was used to predict water depth and current velocity (and to obtain substrate composition) within the reach studied in the Escoumins River was identical to that used to obtain these predictions in the Sainte-Marguerite River. Second, we calculated the total surface area of the reach associated with each of the 10 classes of HSI or HPI (increments of 0.1 from 0 to 1). Third, we counted the total number of fish observed in the areas associated with each of the 10 classes of HSI or HPI. Fourth, we calculated the average fish density in each of these areas (number of fish·100 m^{-2}). Finally, we tested the existence of a significant relationship between HSI or HPI and real fish density using regression analysis.

Results

Predictions of NHM

The depth and velocity values observed in the Sainte-Marguerite River during the development of our biological models covered a range similar to that found in the Escoumins River when these models were applied (Fig. 2). However, substrate grain size in the Sainte-Marguerite River never exceeded *D*50 values of 25 cm, whereas the maximum *D*50 values observed in Escoumins River attained 106 cm. The frequency distributions of water depth, current velocity, and substrate size in the reach used in the Sainte-Marguerite River to develop our biological models were statistically different from the study reach in the Escoumins River (Kolmogorov–Smirnov two-sample test, $p < 0.001$; Fig. 2). Despite the statistical significance of these findings, average water depth and average current velocity varied only 13–16% between the two reaches (Table 1). The key difference between our sites was the average substrate size that varied threefold between reaches (average *D*50 of 4.0 cm in the Sainte-Marguerite River and 11.5 cm in the Escoumins River). Hence, in general, the Sainte-Marguerite River was characterized by slightly shallower depths and slower current velocities but threefold smaller average substrate grain size than the Escoumins River.

The surface area of the 350-m reach studied in the Escoumins River was 13 320 m^2 with a flow of 6.0 $m^3 \cdot s^{-1}$. NHM predictions of both biological models differed in the relative proportions of the reach surface area covered by specific intervals of habitat quality values. The map produced using HSI indicated that 7.5% (1004 m^2) of the reach could be assigned habitat quality values ranging from 0.7 to 1.0 (Fig. 3*a*). The maps that resulted from the use of HPI showed that 69% (9193 m^2) of the surface area of the reach could be given a habitat quality value ranging from 0.7 to 1.0 (Fig. 3*b*). Conversely, NHM implemented with HSI predicted that 82% (10 902 m^2) of the reach should be assigned habitat quality values <0.3 compared with only 4.5% (602 m^2) with HPI.

Fig. 2. Frequency distribution of (*a*) water depth, (*b*) current velocity, and (*c*) substrate size predicted by the hydraulic model for the Sainte-Marguerite River (solid bars) and the Escoumins River (hatched bars) at 6 $m^3 \cdot s^{-1}$.

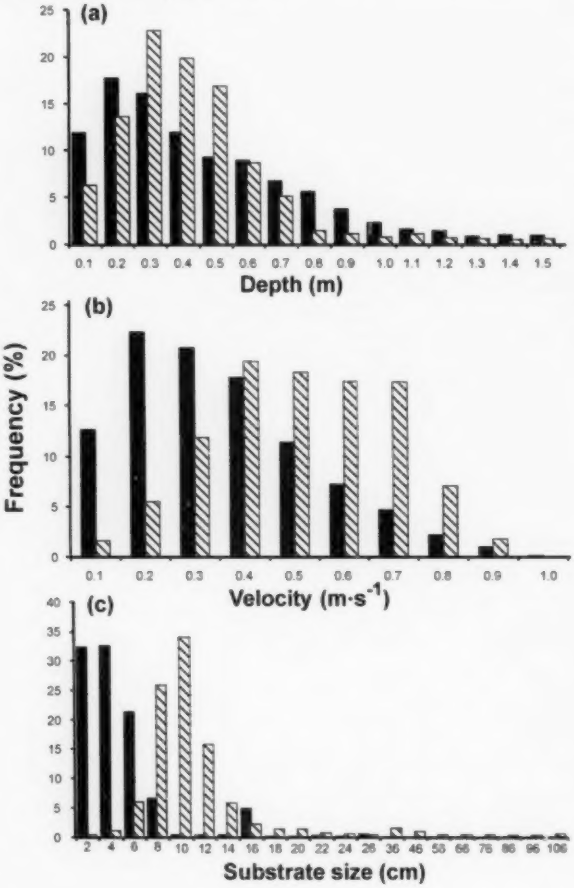

Fish distribution

We georeferenced and mapped 82 Atlantic salmon parr in the 350-m reach of the Escoumins River (Fig. 3). The average density of parr within the total wetted area of the reach was 0.63 parr·100 m^{-2} (standard deviation = 0.67). However, parr density was spatially heterogeneous. Fish density in 16 adjacent areas of relatively similar sizes (22- to 25-m sections; 560–933 m^2) indicated that parr density ranged from 0 to 2 parr·100 m^{-2}.

Table 1. Mean, standard deviation (SD), and maximum values (max.) of water depth (m), current velocity ($m \cdot s^{-1}$), and substrate size (*D*50; cm; minimum (min.) size included) for the reaches sampled in the Sainte-Marguerite River (hydraulic conditions predicted at a flow of 3 $m^3 \cdot s^{-1}$) and the Escoumins River (hydraulic conditions predicted at a flow of 6 $m^3 \cdot s^{-1}$).

	Depth			Velocity			Substrate size			
River	Mean	SD	Max.	Mean	SD	Max.	Mean	SD	Min.	Max.
Sainte-Marguerite	0.44	0.36	2.37	0.30	0.18	0.87	4.0	3.88	0.3	25
Escoumins	0.39	0.27	2.00	0.46	0.18	0.95	11.5	11.89	0.2	>50

Fig. 3. Maps of (*a*) habitat suitability index (HSI) and (*b*) habitat probabilistic index (HPI) for a flow of 6 $m^3 \cdot s^{-1}$. The colour scale is used to identify HSI and HPI values. Fish distribution is overlaid on the maps. Each black dot represents a single fish.

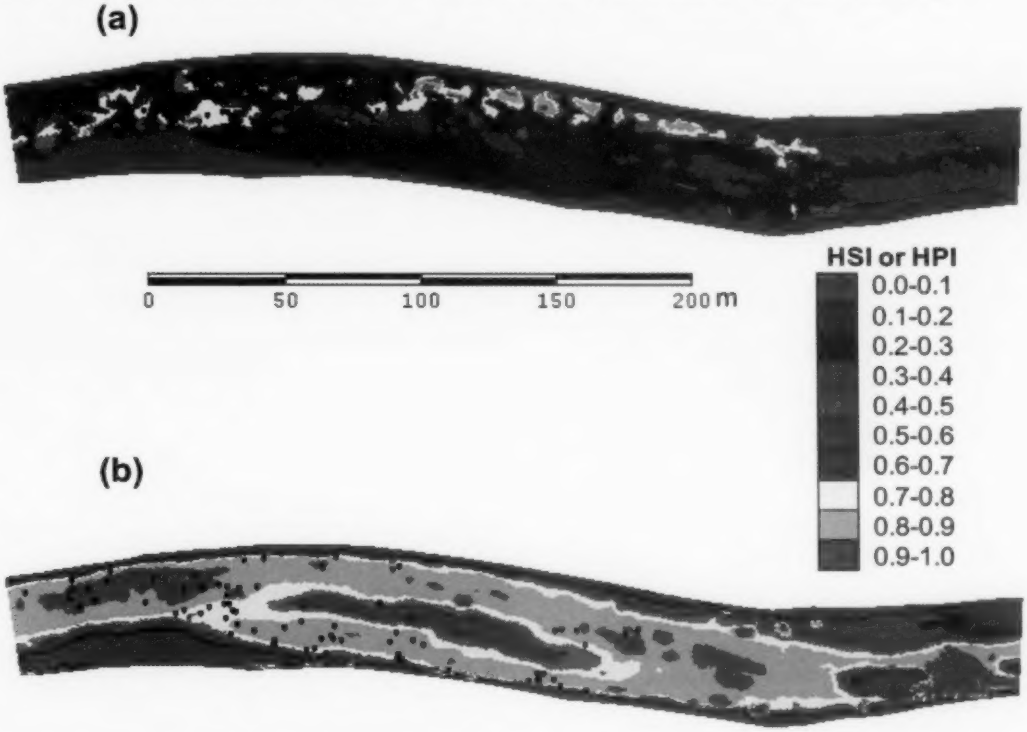

Comparison between the predictions by NHM and fish distribution

There was a poor correspondence between the prediction of the distribution of fish habitats obtained by NHM implemented with HSI and the distribution of fish within the reach of the Escoumins River. Only seven of the 82 fish mapped occurred in habitats assigned values >0.5 (presumably the best habitats according to HSI). However, 68 of the fish were found in habitats given HSI values ranging from 0.2 to 0.4. Hence, 83.9% of the parr observed in the field were located in areas representing some of the worst habitats predicted by NHM inputted with HSI. In contrast, 81 of the 82 fish were found in areas allotted HPI values >0.5. Furthermore, 89% of the fish observed were located in areas assigned HPI values ranging from 0.7 to 1.0.

Fish densities in each of the 10 classes of habitat quality values (0 to 1 by increments of 0.1) predicted by either HSI or HPI ranged from 0 to 1 fish·100 m^{-2}. We found no statistically significant relationship between the fish densities observed in the patches of habitats assigned different values of HSI ($r^2 = 0.25$; Fig. 4*a*). However, fish densities estimated at the level of patches were strongly correlated to HPI ($r^2 = 0.84$; Fig. 4*b*).

Discussion

Our results indicate that it may be possible to use a biological model developed in one river to assess fish habitat quality and to predict fish distribution pattern in another river. The possibility of using a biological model developed in one river to predict habitat quality in another river defines the term "transferability". Many authors (Thomas and Bovee 1993; Freeman et al. 1997; Leftwich et al. 1997) have used this definition of transferability. In this context, our work supports the hypothesis that biological models may be transferable from one river to another. Our analyses suggest that

Fig. 4. Relationship between fish densities and values of (*a*) habitat suitability index (HSI) and (*b*) habitat probabilistic index (HPI). For HSI, $r^2 = 0.12$, $p > 0.1$; for HPI, $y = 0.68x^2 + 0.49x - 0.21$, $r^2 = 0.84$, $p < 0.001$.

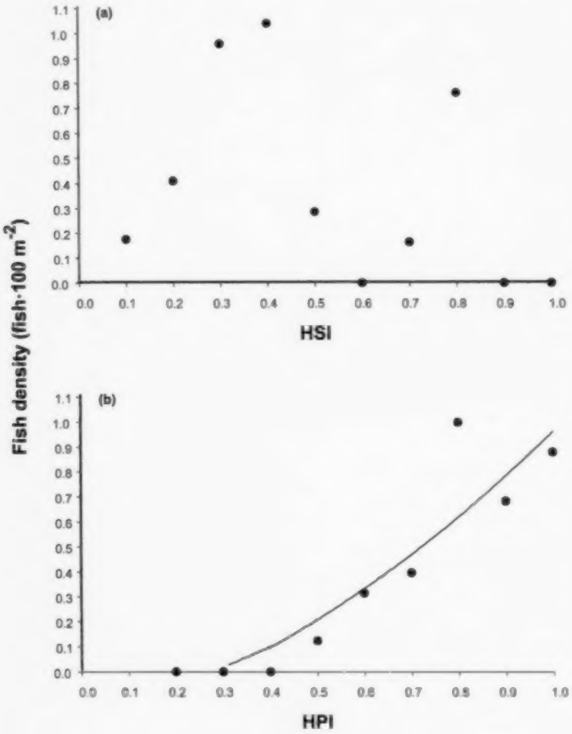

transferability may not be achievable for all biological models. The HPI model developed in the Sainte-Marguerite River was able to explain 86% of the local variation in Atlantic salmon parr density in this river (Guay et al. 2000). This same model explained 84% of local variation in fish density in the Escoumins River. Hence, the HPI model developed in the Sainte-Marguerite River could adequately rank habitat quality in the Escoumins River. The HSI model developed in the Sainte-Marguerite River was able to explain 39% of local variation in fish density in this river (Guay et al. 2000). However, HSI from the Sainte-Marguerite River could not explain a significant proportion of fish density variation in the Escoumins River. Our results suggest that HSI models may not be as transferable as HPI models. We recognise that the low fish density of the Escoumins (0.63 parr·100 m^{-2}) and Sainte-Marguerite (0.76 parr·100 m^{-2}) rivers may affect the applicability of our findings to more densely populated rivers. As such, the transferability of HPI models developed in rivers characterized by low fish densities to densely populated rivers remains to be tested. However, the low fish densities that we observed do not explain the difference between the transferability of HSI and HPI models in our study (both rivers had low fish densities).

Three hypotheses can be invoked to explain the relative transferability of the HSI and HPI models. First, for a similar number of observations about the environmental conditions used by fish, a HPI model contains more specific information than a HSI model. HSI contains information about the environmental conditions used by and available to fish. The conditions used by fish are necessarily, and completely, included within those available to fish, which creates an overlap in the information contained in both variables. The availability of the environmental conditions is, to some extent, implicitly included in HPI. However, HPI explicitly refers to conditions that are fundamentally more contrasting (those that define the presence or the absence of fish) than HSI (conditions available to fish and those used by fish). Although the conditions used and avoided by fish do overlap, the fact that both variables are potentially more contrasted may contribute to the better performance of HPI models (Guay et al. 2000). For instance, mean water depth, mean current velocity, and mean substrate size used by fish in the Sainte-Marguerite River differed from conditions available in this river by 2.3, 5.9 and 1.5%, respectively. Corresponding differences between conditions used and avoided by fish were 4.0, 18.6, and 0.97%. We performed a series of Kolmogorov–Smirnov tests to assess the difference between environmental conditions used by fish and available to fish and between conditions used and avoided by fish in the Sainte-Marguerite River. These tests indicated that the frequency distributions of water depth and current velocity used by fish did not differ significantly from those of water depth and current velocity available to fish ($p > 0.1$). The frequency distribution of substrate size used by fish was statistically different from that available to fish ($p < 0.01$). In contrast, the frequency distribution of water depth, current velocity, and substrate size used by fish were all significantly different from those avoided by fish ($p < 0.05$). Consequently, these result confirm our contention that the difference between habitat variables used by fish and those avoided by fish is larger than the difference between habitat variables used by fish and available to fish. Hence, HPI is effectively based on more contrasting variables which, we argue, allows HPI models to better differentiate good from poor habitats.

Second, the structure of HSI models may not allow one to represent the interactions among physical variables used to estimate habitat quality as well as HPI. HSI models are based on preference curves (in our study, on three preference curves or three HSC) that are developed separately and independently. For instance, a specific range of substrate size is given a high or low preference index independently of water depth or current velocity. However, it is realistic to believe that the preference of fish for one substrate size may vary with water depth and current velocity. The HSI does not allow modifying the preference index for one environmental condition with the two other conditions. In contrast, because of their structure, HPI models do not allow one to estimate a preference index for a single environmental condition, the two other conditions must be specified. Because of the statistical characteristics of multivariable logistic regressions, HPI models are developed using physical variables and the interactions that may exist among them. Explicit and structural inclusion of the interaction between environmental conditions may explain the better performance of HPI relative to HSI models in rivers for which both models are developed

(Guay et al. 2001). Our study suggests that this attribute may also provide HPI models a larger degree of flexibility, which facilitates their transferability.

Third, our HSI model may be more sensitive than our HPI model to physical variables that differ between the rivers for which transferability was attempted. Indeed, the transferability of any biological model depends on the magnitude of the difference between the rivers for which transferability is performed or assessed. Summer flows (3 $m^3 \cdot s^{-1}$ for the Sainte-Marguerite River and 5.5 $m^3 \cdot s^{-1}$ for the Escoumins River) and maximum width (15–40 m) varied, respectively, 1.8- and 2.7-fold between the reaches studied. These variables are probably meaningless in the context of among-river transferability because they may not explain among-river differences in the conditions affecting fish. Fish may experience the same conditions of depth and current velocity in two rivers that vary 10-fold in flow if the width of the high-flow river is much larger than that of the low-flow river. More importantly, frequency distributions of water depth, current velocity, and substrate size in the reach that we used in the Sainte-Marguerite River to develop our biological models were statistically different from those of the study reach in the Escoumins River. Because the range of water depth and current velocity was identical between these reaches and average values for these variables differed only 13–16% between the two reaches, the key difference between our sites may be substrate size, which differed threefold. This threefold variation in substrate size may indicate the among-river or among-site differences for which HSI is not transferable and for which HPI remains transferable. We have no field data to evaluate the degree of variability of physical variables required to impede the transferability of HPI. However, we performed a sensitivity analysis to assess the relative effect of modifying water depth, current velocity, or substrate composition by 20% on predictions made by HSI and HPI models (Table 2). This sensitivity analysis was performed in five steps. First, we calculated 1000 HSI values and 1000 HPI values with combinations of water depth, current velocity, and substrate size covering the complete range observed in the Sainte-Marguerite River. These are defined as nominal HSI or HPI values. Second, we alternatively increased water depth, current velocity, or substrate size by 20% and calculated the percent change in HSI or HPI values relative to the nominal values. Third, we decreased the value of each physical condition by 20% and calculated the percent change in HSI or HPI values relative to the nominal values. Fourth, we noted the maximum (largest increase) and the minimum (largest decrease) percent change in HSI or HPI value relative to the nominal values. Fifth, we calculated the mean of the absolute percent change in HSI or HPI values caused by a 20% increase or decrease in the physical conditions. This analysis indicated that HSI is 1.7- to 5.2-fold more sensitive than HPI to a ±20% change in depth, flow velocity, or substrate size. For instance, the absolute value of the average variation resulting from a 20% decrease in water depth was 21% for HSI compared with 10.2% for HPI. Similarly, a 20% increase in water velocity produced a 19.5% variation in HSI and a 5% variation in HPI. Furthermore, a 20% decrease in substrate size caused a 11.8% variation in HSI and only a 2.3% variation in HPI. Our analyses also showed that with one exception (20% decrease in water depth), the range of variation (increase or decrease) caused by a 20% change in any of the physical variables is smaller for HPI than for HSI. Hence, the sensitivity of HPI to 20% changes in depth, water velocity, and substrate size is not only generally smaller than for HSI (i.e., in mean absolute percent changes), its direction (increase or decrease of HPI) is also more stable and predictable than that of HSI. We can only speculate that the mathematical structure of HPI, which allows a better representation of the interaction between environmental conditions, may act as a buffer against frequently large and unstable predictions. Regardless of the ultimate cause of the apparent sensitivity of the HSI model, the greater sensitivity of HSI to substrate size than HPI, together with the fact that the study reaches of the Sainte-Marguerite and the Escoumins rivers differed mostly in substrate size, contribute to explain the difficulty of transferring the HSI model.

Table 2. Minimum, mean of absolute values, and maximum percent change in habitat suitability index (HSI) and habitat probabilistic index (HPI) resulting from a 20% increase (+20%) or decrease (–20%) in water depth (m), current velocity ($m \cdot s^{-1}$), and substrate size (D50; cm).

	HSI		HPI	
	+20%	–20%	+20%	–20%
Depth				
Minimum	–118.8	–119.4	–19.3	–133.6
|Mean|	25.7	21.0	15.3	10.2
Maximum	45.4	17.7	82.4	19.8
Velocity				
Minimum	–76.1	–69.8	–22.9	1.2
|Mean|	19.5	12.4	5.7	6.8
Maximum	47.7	7.3	–0.6	22.3
Substrate size				
Minimum	–11.4	–34.4	–16.5	0.01
|Mean|	8.0	11.8	2.2	2.3
Maximum	19.9	11.6	–0.01	15.0

It is conceptually reasonable to expect that developing HSI or HPI models based on data obtained using a wide range of environmental conditions from one or many rivers may allow one to obtain more general and more transferable models. This expectation was tested by Mäki-Petäys et al. (2002) using data on habitat use by Atlantic salmon parr and habitat availability in four Finnish rivers. They developed a general HSI model (HSI_M; geometric mean of HSC for water depth, current velocity, and substrate size) based on HSC for water depth, current velocity, and substrate size combining data from the four rivers that they studied. They also compared their HSC and the predictions of their HSI_M with similar models developed by Heggenes and Saltveit (1990; HSI_{HS}). Mäki-Petäys et al. (2002) used a two-sided χ^2 test to compare the observed proportions of fish encountered in given ranges of habitat quality predicted by their HSI_M with those expected if fish selected habitats according to their availability. HSI_M and HSI_{HS} were declared successful and transferable when these models demonstrated the nonrandom selection of habitats by fish (significant difference between observed and expected habitat use). They achieved this goal for nine of the 11 comparisons performed with HSI_M and

Fig. 5. Frequency distribution of predicted habitat values in the Escoumins River using the habitat suitability index of Mäki-Petäys et al. (2002; HSI_M). Opened bars are for habitats available ($n = 2116$); solid bars are for habitats used ($n = 82$).

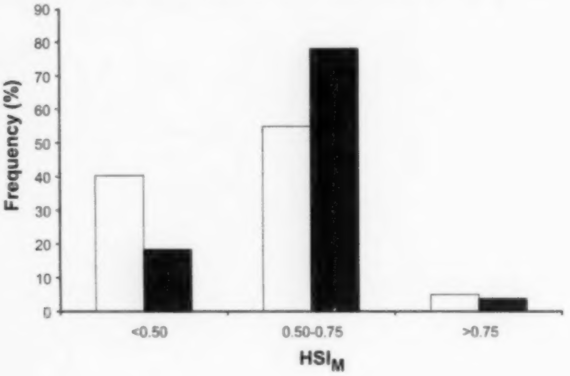

Fig. 6. Relationship between fish density and the habitat suitability index of Mäki-Petäys et al. (2002; HSI_M).

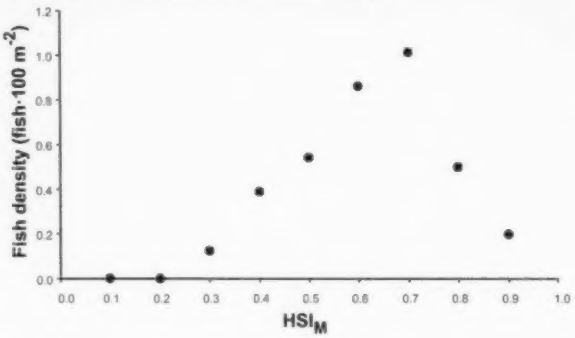

HSI_{HS}. Two points are worth noting about the work of Mäki-Petäys et al. (2002). First, technically speaking, the confirmation by these authors that HSI_M adequately determines the nonrandom habitat selection by fish is not a true test of transferability among rivers because the HSI_M was tested in the same rivers that were used to develop this model. The procedure that they adopted is closer to a test of the generality of a model (conceptually different but equally, if not more, interesting). The test that they performed with HSI_{HS} conforms to the definition of transferability generally used (Thomas and Bovee 1993; Freeman et al. 1997; Leftwich et al. 1997). Second, their study illustrates that whether or not a model is declared successful or transferable may depend on the statistical approach used to test the transferability. We calculated that for two of the nine successful comparisons performed with HSI_M and for two of the nine successful comparisons performed with HSI_{HS}, fish showed a preference for intermediate ($0.5 < HSI < 0.75$) rather than high ($HSI > 0.75$) quality habitats. Their approach was, however, capable of differentiating poor ($HSI < 0.5$) from good ($HSI > 0.5$) habitats. The procedure that we used to test the transferability requires that fish density increases continuously with habitat quality indices. The presence of peaks of fish density at intermediate habitat quality values would cause the acceptance of the null hypothesis (no significant relationship between fish density and habitat quality values) and the rejection of the hypothesis of the transferability of our models. Our statistical approach may therefore be more stringent than that used by Mäki-Petäys et al. (2002). This point can be illustrated by testing the transferability of HSI_M to the Escoumins River. For this purpose, we extracted the data from the HSC curves presented by these authors and adjusted a polynomial regression to each of their HSC. HSI_M was estimated as described by Mäki-Petäys et al. (2002). A two-sided χ^2 test confirmed that HSI_M was able to determine nonrandom habitat selection by fish (Fig. 5). However, we found no statistically significant relationship between fish density and HSI_M (Fig. 6), again because of the tendency of this model to underestimate the frequency of fish in excellent habitats. It must be recognised, however, that although HSI_M underestimated fish density for $HSI_M > 0.7$, it performed remarkably well otherwise. Water depth (mean ± standard deviation; 0.27 m ± 0.17 to 0.47 m ± 0.22 depending on the rivers) and current velocity ($0.28\ m \cdot s^{-1} \pm 0.28$ to $0.39\ m \cdot s^{-1} \pm 0.31$) in the Finnish rivers did not differ significantly from those conditions in the Escoumins River. However, the mean substrate size in three of the Finnish rivers was larger than 18 cm in diameter and, hence, larger than that found in either of our rivers. Whether the difficulty of HSI_M to predict fish density in excellent habitat is caused by the mathematical structure of this sort of biological model or by the difference that appears to exist between the substrate size of Escoumins River and the Finnish rivers studied by Mäki-Petäys et al. (2002) is difficult to establish. Interestingly, the reasons that explain why HSI from Sainte-Marguerite River could not be transferred to Escoumins River may be the same as those explaining the difficulty of transferring HSI_M to the Escoumins River. Our work suggests that the development of the kind of general model proposed by Mäki-Petäys et al. (2002) using HPI instead of HSI may further improve the potential for developing more transferable biological models.

In the same manner as differences that may exist between rivers limit transferability, our data suggest that there are also limitations to the predictions made by biological models. Our work indicates the existence of a strong relationship between HPI and fish density in both reaches for which transferability was attempted. It is possible that the HPI model developed in one reach of a river may allow for the prediction of fish distribution and density in another reach of the same river if both reaches are characterised by similar environmental conditions; however, this remains to be tested. In this sense, HPI may have a relative meaning among rivers (allow one to discriminate good from poor habitats) and an absolute meaning within a river (allow one to predict fish density). Both strategies are useful to assess, for instance, the effect of flow variations on the quantity and quality of habitats for fish. However, our analyses indicate that a HPI model structurally similar to that used in our study may not have an absolute meaning among rivers. It appears reasonable to expect that there may be more fish in habitats assigned HPI values of 0.8 than in habitats assigned HPI values of 0.4. This was true in the river in which our HPI model was developed and remained true in the river to which we attempted the transfer of our biological model. This characteristic allowed us to successfully transfer the HPI model from the Sainte-Marguerite River and to predict fish distribution patterns in the Escoumins River. However, it is not be realistic to predict fish density in one river using HSC developed in another river. For instance, HPI values of 0.4 and 0.8 in the Sainte-Marguerite River were associated with fish densities of 0.5 and 1.5 fish·100 m^{-2} (Guay et al. 2000). Yet, these same HPI values were associated with fish densities of 0.0 and 1 fish·100 m^{-2} in the Escoumins River. In fact, there is no relationship between fish densities assigned identical HPI values in both rivers ($r^2 = 0.26$, $p = 0.13$). Considering the existence of among-river relationships between fish biomass or abundance and phosphorus, food biomass, and the availability of winter habitats (Symons 1971; Randall et al. 1995; Cunjak 1996), we can only speculate that the inclusion of such variables in the framework of HPI models may improve the value of these models among rivers. Much remains to be done to confirm this possibility. However, the prospect of using one HPI model in many rivers may facilitate the achievement of the ultimate objective of NHM — to evaluate the potential impact of variations of flow regime on fish habitat quality and quantity within a river.

Acknowledgements

We thank Andres Finzi, Marie-Noëlle Chouinard, Philippe Girard, Guillaume Guénard, Marion L'Espérance, and Émilie Pelletier for help in the field. We thank the team from the Centre Interuniversitaire de Recherche sur le Saumon Atlantique (CIRSA) for logistic support. Funding for this research was provided by the Natural Sciences and Engineering Research Council of Canada (Collaborative Special Project), the Fondation de la Faune du Québec, the Government of Québec (Ministère de l'Environnement et de la Faune), the Government of Canada (Economic Development), and the financial partners of CIRSA Inc. (Corporation de soutien aux initiatives de recherche sur le saumon atlantique): ALCAN, Association de la rivière Sainte-Marguerite, Atlantic Salmon Federation, Boisaco, Bureau fédéral de développement régional (Québec), CRSNG, Conseil régional de développement de la Côte-Nord, Corporation municipale de Sacré-Cœur-sur-le-fjord-du-Saguenay, Corporation de pêche Sainte-Marguerite, Fédération québécoise pour le saumon atlantique, Fond décentralisé de création d'emploi de la Côte-Nord, and Hydro-Québec. Jean-Christophe Guay was supported by a postgraduate scholarship from the CIRSA, La Fondation J.A. Paulhus, and the Groupe de Recherche Interuniversitaire en Limnologie.

References

Boudreau, P., Bourgeois, G., Leclerc, M., Boudreault, A., and Belzile, L. 1996. Two-dimensional habitat model validation based on spatial fish distribution: application to juvenile Atlantic salmon of Moisie River (Québec, Canada). *In* Proceedings of the Second IAHR International Symposium on Habitat Hydraulics, Québec City, June 1996. Ecohydraulics 2000. *Edited by* Leclerc et al. INRS-Eau, Sainte-Foy, QC G1V 4C7. pp. B365–B380.

Bovee, K.D. 1982. A guide to stream habitat analysis using the Instream Flow Incremental Methodology. Instream Flow Information Paper 12. U.S. Department of the Interior, Fish and Wildlife Service, Office of Biological Services FWS/OBS-82/26.

Bovee, K.D., Lamb, B.L., Bartholow, J.M., Stalnaker, C.B., Taylor, J., and Henriksen, J. 1998. Stream habitat analysis using the instream flow incremental methodology. U.S. Geological Survey, Biological Resources Division Information and Technology Report USGS/BRD-1998-0004.

Bozek, M.A., and Rahel, F.J. 1992. Generality of microhabitat suitability models for young Colorado River cutthroat trout (*Oncorhynchus clarki pleuriticus*) across sites and among years in Wyoming streams. Can. J. Fish. Aquat. Sci. **49**: 552–564.

Cunjak, R.A. 1988. Behaviour and microhabitat of young Atlantic salmon (*Salmo salar*) during winter. Can. J. Fish. Aquat. Sci. **45**: 2156–2160.

Cunjak, R.A. 1996. Winter habitat of selected stream fishes and potential impacts from land-use activity. Can. J. Fish. Aquat. Sci. **53**(Suppl. 1): 267–282.

deGraaf, D.A., and Bain, L.H. 1986. Habitat use by and preferences of juvenile Atlantic salmon in two Newfoundland rivers. Trans. Am. Fish. Soc. **115**: 671–681.

Freeman, M.C., Bowen, Z.H., and Crance, J.H. 1997. Transferability of habitat suitability criteria for fishes in warmwater streams. N. Am. J. Fish. Manag. **17**: 20–31.

Guay, J.C., Boisclair, D., Rioux, D., Leclerc, M., Lapointe, M., and Legendre, P. 2000. Development and validation of numerical habitat models for juveniles of Atlantic salmon (*Salmo salar*). Can. J. Fish. Aquat. Sci. **57**: 2065–2075.

Guay, J.C., Boisclair, D., Leclerc, M., Lapointe, M., and Legendre, P. 2001. Science on the edge of spatial scales: a reply to the comments of Williams (2001). Can. J. Fish. Aquat. Sci. **58**: 2108–2111.

Heggenes, J. 1991. Comparisons of habitat availability and habitat use by an allopatric cohort of juvenile of Atlantic salmon (*Salmo salar*) under conditions of low competition in a Norwegian stream. Holarct. Ecol. **14**: 51–62.

Heggenes, J. 1996. Habitat selection by brown trout (*Salmo trutta*) and young Atlantic salmon (*S. salar*) in streams: static and dynamic hydraulic modelling. Regul. Rivers Res. Manag. **12**: 155–169.

Heggenes, J., and Saltveit, S.J. 1990. Seasonal and spatial microhabitat selection and segregation in young Atlantic salmon, *Salmo salar*, and brown trout, *Salmo trutta*, in a Norwegian river. J. Fish Biol. **36**: 707–720.

Latulippe, C., and Lapointe, M. 2001. Visual characterisation technique for gravel–cobble river bed surface sediment. Earth Surf. Proc. Land Forms, **26**: 307–318.

Leclerc, M., Bellemare, J.F., Dumas, G., and Dhatt, G. 1990. A finite element model of estuarian and river flows with moving boundaries. Adv. Water Res. **4**: 158–168.

Leclerc, M., Boudreau, P., Bechara, J.A., Belzile, L., and Villeneuve, D. 1994. A model of habitat dynamics applied to landlocked salmon (*Salmo salar*) juveniles of the Ashuapmushuan River (Québec, Canada). Bull. Fr. Pêche Piscic. **332**: 11–32.

Leclerc, M., Boudreau, A., Bechara, J.A., and Corfa, G. 1995. Two-dimensional hydrodynamic modelling: a neglected tool in the Instream Flow Incremental Methodology. Trans. Am. Fish. Soc. **124**: 645–662.

Leclerc, M., Bechara, J.A., Boudreau, P., and Belzile, L. 1996. Numerical method for modelling spawning habitat dynamics of landlocked salmon (*Salmo salar*). Regul. Rivers Res. Manag. **12**: 273–287.

Leftwich, K.N., Angermeier, P.L., and Dolloff, C.A. 1997. Factors influencing behavior and transferability of habitat models for a benthic stream fish. Trans. Am. Fish. Soc. **126**: 725–734.

Legendre, P., and Legendre, L. 1998. Numerical ecology. 2nd English ed. Elsevier Science B.V., Amsterdam, the Netherlands.

Mäki-Petäys, A., Huusko, A., Erkinaro, J., and Muotka, T. 2002. Transferability of habitat suitability criteria of juvenile Atlantic salmon (*Salmo salar*). Can. J. Fish. Aquat. Sci. **59**: 218–228.

Morantz, D.L., Sweeney, R.K., Shirvell, C.S., and Longard, D.A. 1987. Selection of microhabitat in summer by juvenile Atlantic salmon (*Salmo salar*). Can. J. Fish. Aquat. Sci. **44**: 120–129.

Randall, R.G., Kelso, J.R.M., and Minns, C.K. 1995. Fish production in freshwaters: are rivers more productive than lakes? Can. J. Fish. Aquat. Sci. **52**: 631–643.

Scott, D., and Shirvell, C.S. 1987. A critique of IFIM and observations on flow determination in New Zealand. *In* Regulated streams, advances in ecology. *Edited by* J.F. Craig and J.B. Kemper. Plenum Publishing, New York. pp. 27–43.

Symons, P.E.K. 1971. Behavioural adjustment of population density to available food by juvenile Atlantic salmon. J. Anim. Ecol. **40**: 569–587.

Thomas, J.A., and Bovee, K.D. 1993. Application and testing of a procedure to evaluate transferability of habitat suitability criteria. Regul. Rivers Res. Manag. **8**: 285–294.

Williams, J.G. 2001. Tripping over spatial scales: a comment on Guay et al. (2000). Can. J. Fish. Aquat. Sci. **58**: 2105–2107.

Migration patterns, ambient temperature, and growth of Icelandic cod (*Gadus morhua*): evidence from storage tag data

Ólafur K. Pálsson and Vilhjálmur Thorsteinsson

Abstract: Sixty data storage tags were analysed with respect to depth and ambient temperature and for relationships between depth, ambient temperature, and growth. The fish were tagged and released in April 1996–1999 on the spawning grounds at the southwest coast of Iceland. Profiles of depth and ambient temperature suggest that cod (*Gadus morhua* L.) that spawn in the study area select between two alternatives in foraging strategies, i.e., deep- or shallow-water migrations. The shallow-water fish appear to follow the seasonal trend in temperature characteristic for the shelf waters. The deep-water fish, however, migrate to deeper and cooler waters outside the spawning season and increase their vertical movement. A significant positive relationship between depth and ambient temperature was observed for the shallow-water fish, and a significant negative relationship was observed for the deep-water fish. Daily variation in depth and ambient temperature showed increasing trends with increase in depth, in particular for deep-water fish. Growth was negatively related to depth and positively related to ambient temperature. This indicates higher growth rate of cod that forage in shallow waters versus deeper waters. Supply of food, for which depth may be a reasonable proxy, offers a more likely explanation for this growth pattern than environmental temperature.

Résumé : Les données de profondeur et de température ambiante provenant de 60 étiquettes enregistreuses ont été analysées afin de voir s'il existe des relations entre la profondeur, la température ambiante et la croissance. Les poissons ont été étiquetés et relâchés en avril 1996–1999 sur les frayères de la côte sud-ouest de l'Islande. Les profils de profondeur et de température ambiante laissent croire que les morues franches (*Gadus morhua* L.) qui frayent dans la région d'étude utilisent l'une de deux stratégies de rechange de quête de nourriture, soit les migrations en eau profonde ou en eau superficielle. Les poissons d'eau superficielle semblent suivre les tendances saisonnières des caractéristiques thermiques des eaux du plateau continental. Les poissons d'eau profonde, en revanche, migrent vers les eaux plus profondes et plus froides en dehors de la saison de fraye et augmentent leur déplacement vertical. Il existe une relation positive significative entre la profondeur et la température ambiante chez les poissons d'eau superficielle; chez les poissons d'eau profonde, la relation est aussi significative, mais négative. Les variations journalières de profondeur et de température ambiante tendent à augmenter en fonction d'un accroissement de profondeur, particulièrement chez les poissons d'eau profonde. La croissance est en corrélation négative avec la profondeur et en corrélation positive avec la température ambiante; le taux de croissance est donc plus élevé chez les morues qui se nourrissent en eau moins profonde que chez celles qui se nourrissent plus en profondeur. La quantité de nourriture disponible, dont la profondeur semble être une variable de rechange adéquate, est sans doute une explication plus probable de ces patterns de croissance que la température du milieu.

[Traduit par la Rédaction]

Introduction

Environmental temperature has been found to be particularly relevant with respect to migration and spatial distribution of North Atlantic cod (*Gadus morhua* L.). Distribution of Georges Bank and Gulf of Maine cod has been found to change, seasonally and interannually, primarily with respect to changes in bottom water temperature (Mountain and Murawski 1992; Wigley and Serchuk 1992; Serchuk et al. 1994). Atlantic cod off Newfoundland have been shown to migrate along routes of suitable and stable temperature boundaries (Rose 1993). Similarly, Northeast Arctic cod were found to migrate along stable thermal paths until they reached a front area, or feeding grounds, where vertical activity increased (Stensholt 2001). Cod in the North Sea, on the other hand, are strongly influenced by tidal currents and may make pronounced vertical movements near sunrise or sunset (Arnold et al. 1994). Thus, migratory behaviour and distribution patterns may differ with respect to area, as well as season, depending on the strength of major environmental factors.

Temperature has also been identified as a major environmental factor with respect to growth of marine fish, in the field as well as in laboratory experiments. Sæmundsson

Received 12 June 2002. Accepted 31 July 2003. Published on the NRC Research Press Web site at http://cjfas.nrc.ca on 5 December 2003.
J16939

Ó.K. Pálsson[1] **and V. Thorsteinsson.** Marine Research Institute, Skúlagata 4, Box 1390, IS 121 Reykjavík/Iceland.

[1] Corresponding author (e-mail: okp@hafro.is).

Can. J. Fish. Aquat. Sci. **60**: 1409–1423 (2003) doi: 10.1139/F03-117

Fig. 1. Vertical temperature profiles (°C) of selected hydrographic sections around Iceland: (*a*) Krossanes, November 1998; (*b*) Stokksnes, June 1998; (*c*) Selvogsbanki, June 1998; (*d*) Látrabjarg, November 1998; (*e*) Kögur, September 1998; and (*f*) Siglunes, August 1998 (Source: Marine Research Institute, hydrographic database). See Fig. 2 for location of sections. Depth is indicated by a negative number. Distances in northerly and easterly directions are indicated by positive numbers, but distances in other directions are indicated by negative numbers. The sea bottom is indicated by a solid line.

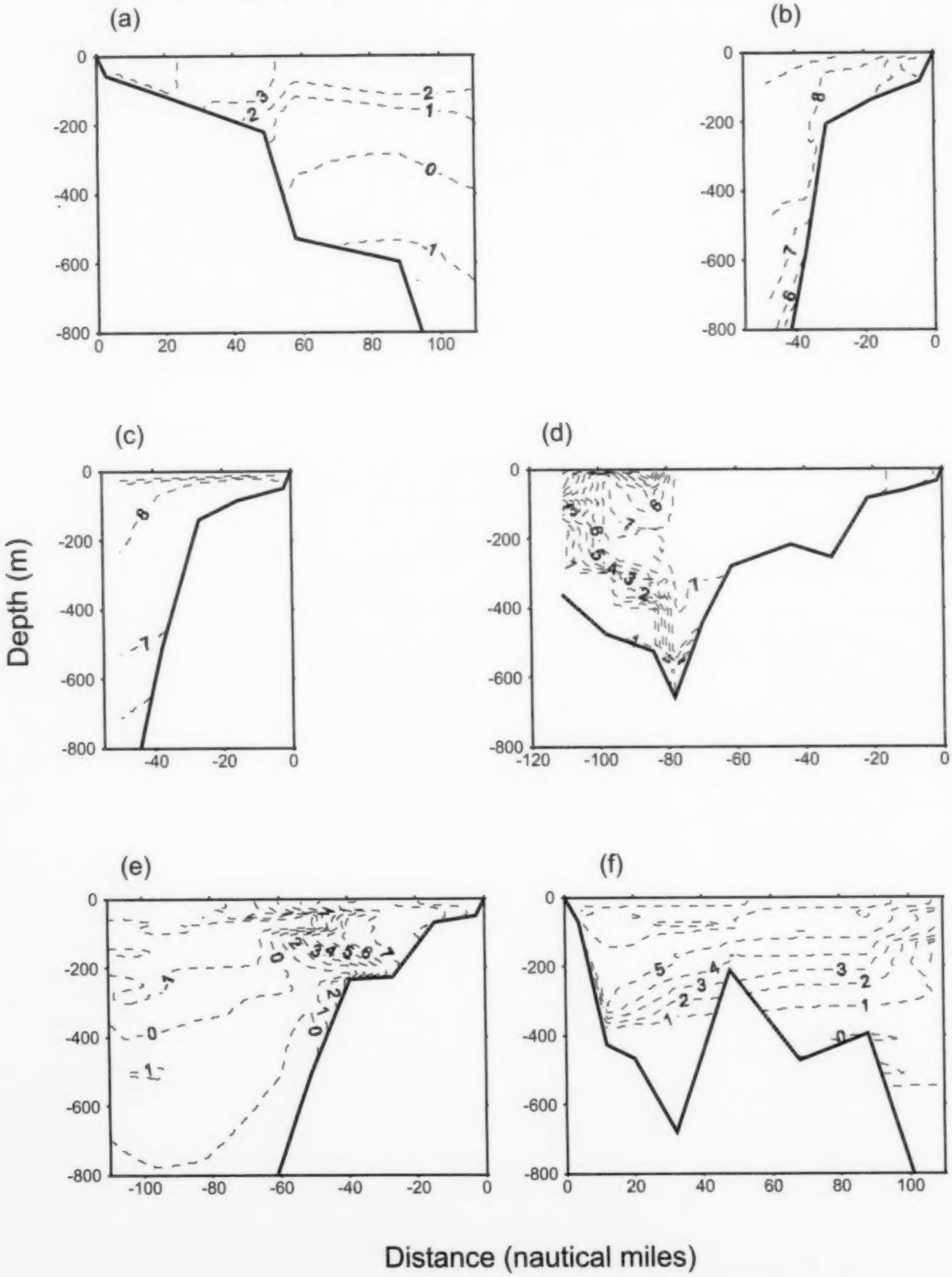

Fig. 2. (Upper panel) Icelandic and adjacent waters. (Lower panel) Icelandic waters. Area of release is indicated by lines. Position and month of recaptures are indicated by the numeral of the month of recapture of 54 data storage tags (DSTs). Six DSTs lacked information on position or month of recapture. Depth contours at 200 m and 500 m are thin lines. Locations (●) of hydrographic sections (stations) *a–f* are indicated.

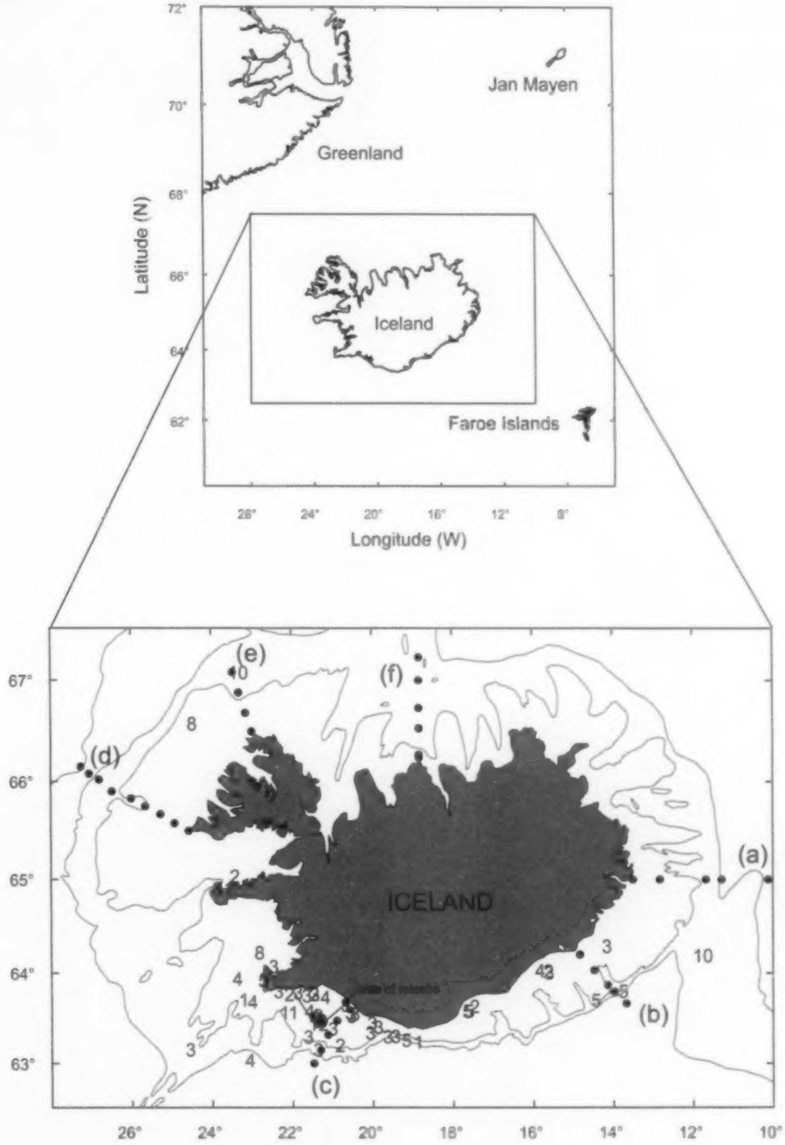

(1923) noted growth differences in Icelandic cod with respect to geographic differences in sea temperature, and Taylor (1957) found significant relations between growth parameters and environmental temperature for several North Atlantic cod stocks. Brander (1995) demonstrated that temperature, or a product of age and temperature, accounted for more than 90% of the variability in weight at age, over a wide age range, for most of 17 cod stocks in the North Atlantic. For Icelandic cod, fed ad libitum in laboratory experiments, growth rate first increased with temperature up to a maximum attained at an optimal temperature and then decreased with a further increase in temperature. Both growth rate and optimal temperature declined with fish size (Björnsson et al. 2001). Based on these laboratory studies, a model was developed to describe the food-unlimited growth rate of cod as a function of temperature and fish weight (Björnsson and Steinarsson 2002). In view of the above findings, the temperature regime of Icelandic waters would be expected to play a fundamental role in the life history of Icelandic cod.

The temperature regime of Icelandic waters is characterized by relatively warm Atlantic waters at the south and west

Fig. 3. Daily number of recordings of (*a*) 17 shallow-water fish and (*b*) 26 deep-water fish, released in 1997–1999 (set 2).

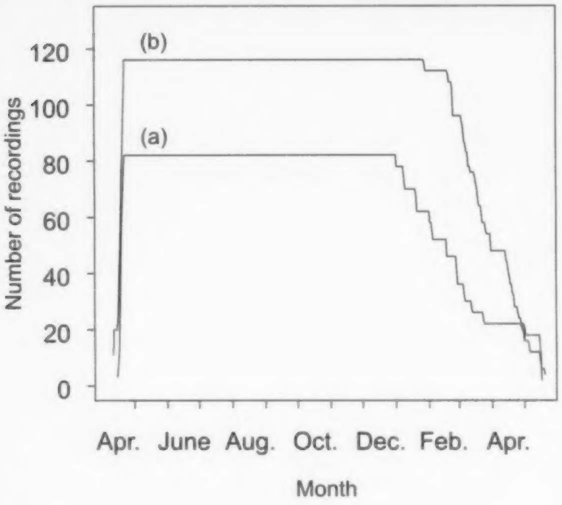

coasts and relatively cold waters of Arctic origin at the north and east coasts (Fig. 1). At the east coast, relatively low temperatures prevail and subzero temperatures are the rule below 400 m (Fig. 1*a*). Temperatures in excess of 5 °C dominate, in all seasons, in the southern regions down to depths of at least 600 m (Figs. 1*b*, 1*c*). At the northwest coast, warmer waters dominate in shallower waters, at least during summer and autumn, but lower temperatures are recorded offshore, leading to the formation of sharp, vertical temperature fronts (Figs. 1*d*, 1*e*). Off the north coast, low temperatures (<2 °C) are recorded below 400 m even during the warmest season (Fig. 1*f*). Such characteristics in temperature distribution can be used to make deductions on migrations and locations of cod, i.e., spatial structure in time, by virtue of recordings of depth and ambient temperature.

Spatial structure of Icelandic cod has been extensively documented in recent years. Mature prespawning cod appear to maintain an optimum temperature range in March in Icelandic waters, whereas spawning cod do not appear to be affected in the same fashion by higher temperatures (Begg and Marteinsdóttir 2002). Size structure of mature cod varies between spawning locations, suggesting the existence of subpopulations (Marteinsdóttir et al. 2000). Genetically based results indicate that cod spawning in southern Icelandic waters belong to different populations that display different life histories, e.g., different growth patterns (Jónsdóttir et al. 2001, 2002).

Conventional mark–recapture experiments also suggest the existence of spatial structure in Icelandic cod, such as extensive migrations of mature cod between West Greenland and Iceland, first recorded in the 1930s (Hansen et al. 1935; Hansen 1941). Spawning and postspawning migrations within Icelandic waters have also been demonstrated by extensive tagging experiments. The main spawning grounds at the southwest coast are at the centre of those migrations, which demonstrate return migrations of repeating spawners (Jónsson 1996). Furthermore, shorter migrations have been observed in localised areas at the east and northeast coasts (Thorsteinsson and Marteinsdóttir 1992). Thus, during the spawning season, mature cod seem to display a high degree of spatial structure that may be genetically or environmentally induced. The question whether or to what extent this structure remains during other periods of the year has not been addressed so far but constitutes an important issue that can be pursued using DST data.

The introduction of data storage tags (DSTs), recording depth and ambient temperature over time periods of more that a year, has provided new insight into the time period between release and recapture and can give information on vertical and horizontal migration patterns, habitat selection, and feeding strategy and possible effects of such patterns on growth, catchability, and even fishing pressure. Depth is usually interrelated with temperature, but has not, until recently, been measured as ambient temperature in biological experiments. Depth, however, can be a useful classification of the habitat in which cod live

The main objective of this analysis is to explore temporal trends in migratory patterns, behaviour, and habitat selection of mature Icelandic cod, marked and released in April 1996–1999 on relatively limited spawning grounds at the southwest coast of Iceland. Effects of depth and ambient temperature on growth are also taken into consideration. We use DST time series of depth and ambient temperature, covering time periods of up to 13 months.

Material and methods

The DSTs used for the present analysis were manufactured by Star-Oddi, Reykjavík, Iceland. The tags released in 1996–1997 were of type DST200, with a depth range of 0–400 m, a resolution of 1.6 m, and accuracy of ±2 m. The range in temperature is –2–20 °C, resolution 0.1 °C, and accuracy ±0.2 °C. The tags released in 1998–1999 were of two types: DST200, recording depth and temperature, and DST300, recording depth, temperature, and tilt. Both of these had 8-bit microprocessors with a depth range of 0–700 m, resolution in depth of 2.8 m, and accuracy of ±5.6 m. The range in temperature was set to –2–20 °C, resolution to 0.1 °C, and accuracy to ±0.2 °C.

The DST200 and DST300 have a memory and power-saving device, allowing sampling at two different rates. In the DSTs selected for this study, the recordings of depth (pressure) and temperature were stored in four different ways (types A–D, Appendix A). For tags of type A, sampling was done in intervals of 6 h during 20 days alternating with intervals of 1 h during 10 days. Of this type, 34 tags were chosen, released in 1998–1999, and recaptured in 1999–2000. For type B tags, sampling was done in intervals of 4 h during 6 days alternating with intervals of 40 min during 1 day. Fifteen tags of this type were chosen, released in 1996 and 1997, and recaptured in 1996–1998. For type C tags, sampling was done in intervals of 8 h during 7 days alternating with intervals of 40 min during 1 day. Six tags of this type were chosen, released, and recaptured in 1998. For type D tags, sampling was done in intervals of 1 h during 1 day alternating with intervals of 6 h during 6 days. Five tags of

Fig. 4. Seasonal patterns in mean daily depth of four selected data storage tags (DSTs): (*a*) DST2276, shallow-water cod (*Gadus morhua*); (*b*) DST934, "occasional" descent to deep-water phase; (*c*) DST2076, short duration of deep-water phase; (*d*) DST2233, prolonged duration of deep-water phase.

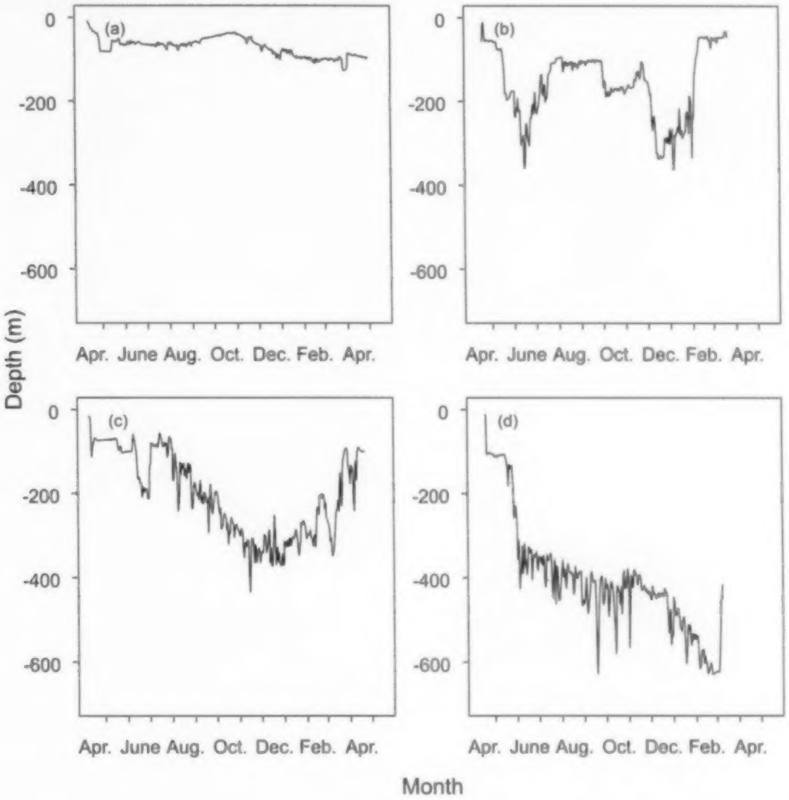

this type were chosen, released in 1997, and recaptured in 1997–1998.

A total of 60 DSTs were selected for the study (Appendix A). Tagging and release took place in April 1996–1999 on the spawning grounds at southwest Iceland (Fig. 2). Method of tagging was described in Thorsteinsson and Marteinsdóttir (1998). Days at liberty varied from 159 to 1082, but most of the fish were at liberty for 311 to 398 days. Days of recordings ranged from 159 to 395. Length of the fish at release was 63–105 cm, but most fish were larger than 80 cm. Age at recapture of 43 aged fish was 6–11 years, but the bulk of the fish were aged 7–9 years.

The data of 60 DSTs were used to gain a first overall impression of the annual cycle of the depth distributions. Of the total set, 52 tags (Appendix A, set 1) were selected to describe the frequency distributions of recordings of depth (*D*) and ambient temperature (*T*), where "ambient temperature" is defined as the sea temperature in the immediate vicinity of the fish, i.e., the in situ temperature in oceanographic terms. To cover the annual cycle to a considerable extent, only tags with a minimum of 268 days at liberty, i.e., recaptured in January of the following year or later, were selected. The first 3 days of recordings were excluded from the analysis to account for recovery period after tagging (Thorsteinsson and Marteinsdóttir 1998). Tags of all four types of recordings (A–D) were included in this set. Instead of analysing individual fish, which has been the common approach so far, we analyse the data in a population perspective by looking for overall, average trends in the parameters, as well as their range in terms of maximum and minimum values. Although a time-collapsed mean over a number of DSTs is, obviously, not a point value, it may provide a reasonable approximation to a real trend in a given variable, in this case the daily, surrounding (ambient) temperature or the depth, which is the objective of the paper. If, on the other hand, the objective were to explore more short-term (hourly) fluctuations in vertical movement, the uncollapsed series of individual DSTs would be more appropriate.

A subset of 43 DSTs recaptures (Appendix A, set 2), released in 1997–1999, was selected to further analyse seasonal patterns in depth and ambient temperature, i.e., (1) daily depth (DD) and daily ambient temperature (DT), (2) maximum values (positive or negative) of daily depth (maximum DD) and daily ambient temperature (maximum DT), and (3) variation in depth (VD = $D_t - D_{t-1}$) and variation in ambient temperature (VT = $T_t - T_{t-1}$) over a given time interval (t to $t - 1$).

In this subset, recordings of depth and temperature were selected to produce a constant time interval of 6 h (tags of

Fig. 5. Frequency distributions of recordings of depth and ambient temperature for 19 shallow-water cod (*Gadus morhua*) (*a* and *b*, respectively) and 33 deep-water cod (*c* and *d*, respectively). Depth intervals by 50 m (first interval, 0–50 m), temperature intervals by 1 °C (first interval, –1–0 °C) (set 1).

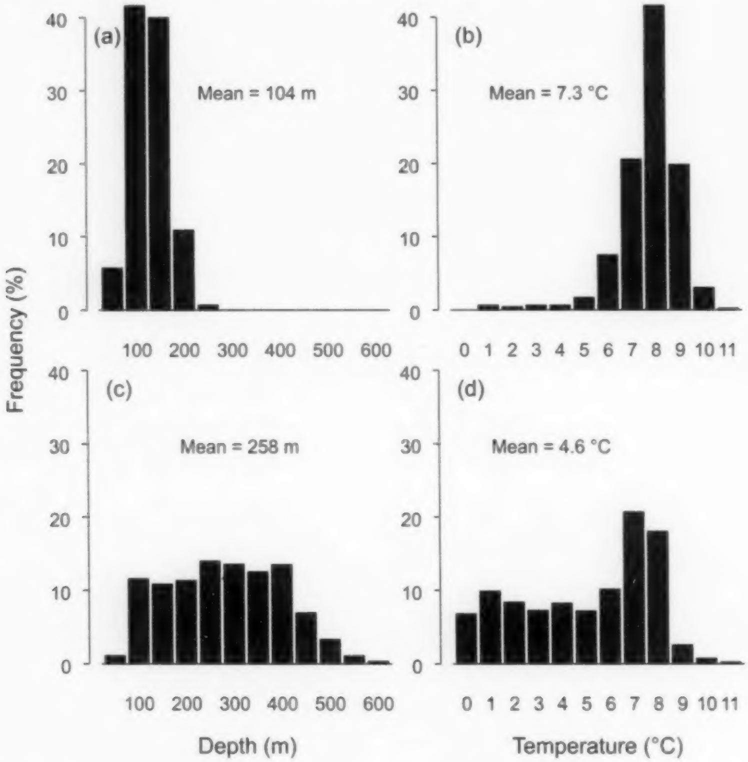

type A) or 4 h (tags of type B), hence containing four and six recordings per day, respectively. However, the exact hours (Greenwich Mean Time) of the recordings differ for individual DSTs with respect to the starting time of each DST. This set was split into a "shallow-water" group containing 17 fish (Fig. 3*a*) and a "deep-water" group containing 26 fish (Fig. 3*b*). Because tags were selected with respect to a minimum of 268 days at liberty, number of recordings remains stable until January of the following year. During the first months of the following year, recordings decrease rapidly because of recaptures, and the last tags are recaptured or stop recording in May.

A set of 32 DSTs (Appendix A, set 3) was selected to analyse relationships between mean depth, mean ambient temperature, and annual growth per fish during liberty. Annual growth (G) was calculated as

$$G = (L_{\text{recapture}} - L_{\text{release}})/d \times 365$$

where L is length (cm) at release or recapture, and d is days at liberty. This set includes tags from fish for which information on length at release and recapture is available and for which days at liberty are no more than 30 in excess of days of recordings (Appendix A). This is to ensure compatibility between time series of depth and temperature and the growth period of the fish. To minimize seasonal effects on growth, most of the fish selected for the growth analysis were at liberty for 9–13 months, or close to a year. Five fish were at liberty for 5–8 months, covering the main growth season, which is the latter half of the year (Pálsson 1980). Correcting for seasonal changes in growth of those fish may have been appropriate but was not considered meaningful because of the lack of data on growth seasonality.

Results

Frequency distributions of depth and temperature

Positions and months of recaptures are basically contained within area and season of spawning (Fig. 2). The cod were released in a relatively limited area on the spawning grounds selected for this study. Most of the recaptures were in the vicinity of the release area in January through May of the following year, i.e., around the spawning season. Thus, recapture location does not give much insight into migrations of the fish but demonstrates a return spawning migration.

Depth patterns of individual fish are found to be highly variable. An inspection of mean, daily depth of 60 individual fish suggests two main foraging strategies or depth levels selected by these cod during feeding migrations (Fig. 4): (1) shallow-water fish that spend virtually all of their time above 200 m depth (Fig. 4*a*), and (2) other fish that spend a variable part of their time in waters deeper than 200 m (Figs. 4*b*–4*d*). In view of this, the 52 DSTs of set 1 were

Fig. 6. Box-and-whisker plot of 186 173 depth recordings from 60 data storage tags by months, showing median (white middle line), upper and lower quartiles (dark bar above and below the median), and upper and lower extremes (whiskers), excluding outliers. Outliers are shown individually by horizontal lines and are defined as values 1.5 times larger than the interquartile range. Note that the large number of outliers in April–June produces a dark bar below the lower extreme.

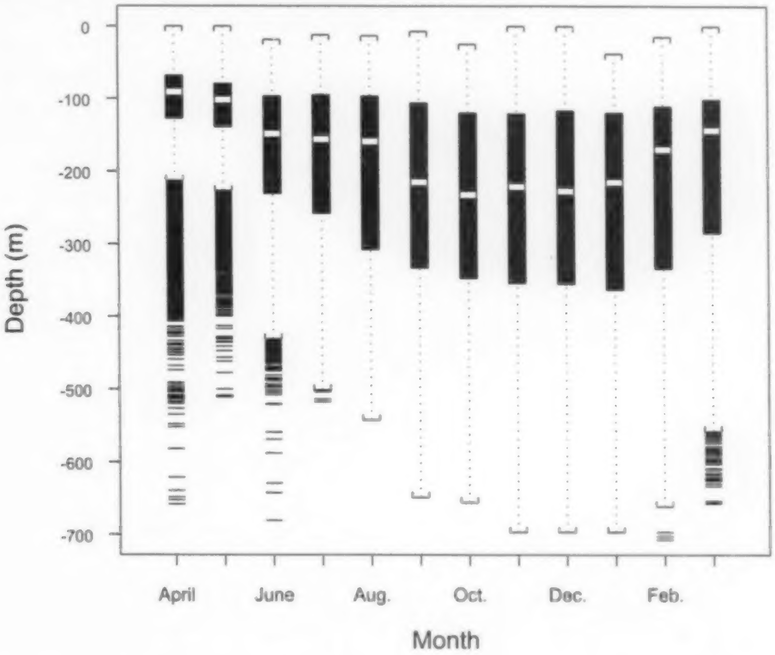

split into two groups with respect to depth distribution: (1) 19 shallow-water cod that spend most of their time (>90% of recordings) at depths less than 200 m (the fish were in the length range of 58–103 cm and had a mean length of 91.1 cm and standard deviation of 10.7 cm), and (2) 33 deep-water cod that spend more than 10% of their time (>10% of recordings) at depths greater than 200 m (this includes all other fish available meeting the criterion of more than 268 days at liberty). These fish were in the length range of 63 to 105 cm and had a mean length of 91.0 cm and standard deviation of 10.8 cm.

The frequency distributions of depth and ambient temperature of the two groups indicate their partial separation (Fig. 5). As to be expected, the depth distributions are very different, the depth profile of the shallow-water group mainly being in the depth range of 50–150 m (mean 107 m). The depth profile of the deep-water group is mainly in the depth range of 50–350 m but reaching down to 600 m (mean 259 m). The temperature profile is also quite different because the shallow-water group is mainly recorded in the temperature range of 6.0–9.0 °C (mean 7.3 °C). The deep-water group, on the other hand, is recorded in a much broader range of ambient temperatures of −1.0–7.0 °C (mean 4.6 °C), although a clear peak is observed at 6.0–8.0 °C.

Of a total of 110 984 temperature recordings of deep-water cod, 43 991 (40%) were below 4 °C, 26 881 (24%) were below 2 °C, and 5776 (5%) were below 0 °C. To find temperatures below 4 °C, within the depth range of 200–600 m, the fish would have to migrate to the waters of the east coast (Fig. 1*a*) or the northwest coast (Fig. 1*d*). Temperatures below 0 °C, within depths of 200–600 m, are only found off the northern and eastern coasts (Figs. 1*e*, 1*f*, and 1*a*). This indicates a considerably higher proportion of long-distance migration among Iceland cod than suggested by the location of recaptures.

Seasonal trends in depth and ambient temperature

Monthly distributions of depth recordings from the whole data set of 60 DSTs indicate a clear seasonal trend in the depth preference of the cod (Fig. 6). During the main spawning season, in April and May, most of the fish were recorded at a depth above 200 m, although a number of recordings were located in deeper waters. Median depth was 91 and 102 m, respectively, and the interquartile range was narrow. During June–August, median depth increased to 149 m through 159 m and upperquartile range and upper extreme expanded. In September, median depth increased to 215 m and upper quartile range and upper extreme expanded further. This situation remained fairly similar until January when an opposite trend sets in marking the beginning of a return spawning migration.

Clear seasonal trends were observed for shallow-water cod in mean daily depth and, in particular, in mean daily ambient temperature, when the data set of 52 DSTs was grouped by the preferences of deep versus shallow foraging (Figs. 7*a*, 7*b*). After release, mean daily depth increased from approximately 50 m to a level of 100–110 m in late May. In August, depth increased further and reached a maximum of 121 m in

Fig. 7. Seasonal trends in mean daily depth (*a* and *c*), and mean daily ambient temperature (*b* and *d*) of 17 shallow-water cod (*Gadus morhua*) (*a* and *b*) and 26 deep-water cod (*c* and *d*) released 1997 through 1999 (set 2). Notice different scales.

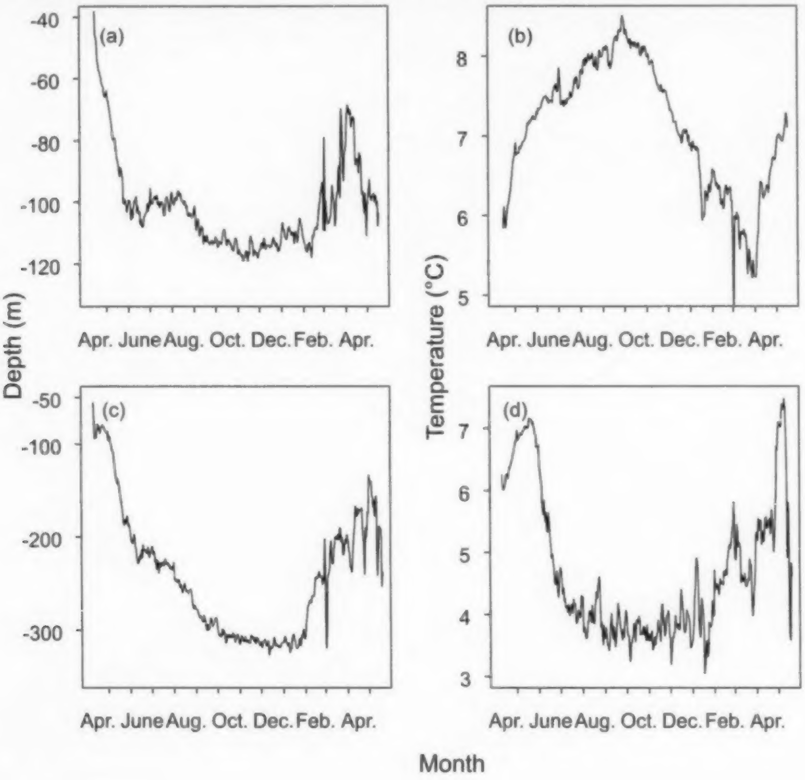

November. During the following months, a gradual decrease in depth was observed until late March, at which time mean daily depth decreased abruptly to 60–80 m during a period of 19 days and then increased swiftly again to previous level (Fig. 7*a*). After release, mean daily temperature increased initially from 5.8 °C to 6.8 °C during a period of 3 weeks. Then it rose more or less linearly to a peak of 8.5 °C in late September and declined subsequently to a low of 5.2 °C almost 1 year after release. This was followed by an increase to 6.7 °C during a period of 7 days, and the fish appeared to embark on a similar pattern as 1 year earlier (Fig. 7*b*).

Distinct seasonal trends were observed for deep-water cod in mean daily depth and mean daily ambient temperature (Figs. 7*c* and 7*d*, respectively). During the first month after release, mean daily depth remained relatively stable above 100 m. During May and early June, it increased to a depth of approximately 225 m, and in August and September, it increased again to more than 300 m and remained at that level during the following months. In February of the next year, a decreasing, although fluctuating, trend in mean daily depth set in, reaching a low of 116 m in late April (Fig. 7*c*). Mean daily ambient temperature increased at first from 6.0 °C to 6.9 °C over a period of 3 weeks and remained at that level until early June. During June, the temperature decreased rapidly to less than 5 °C and started to fluctuate increasingly over the remaining period. During July and August, a slower but fluctuating decrease was observed to a temperature of approximately 4 °C. In late April of the next year, mean daily temperature increased suddenly to more than 7.0 °C and remained at that level during 10 days and then declined abruptly towards the end of the recordings (Fig. 7*d*).

The seasonal trends in depth of the two groups of fish have some common features, although the depth levels are different. Following an initial, rapid increase in depth, the fish of both groups remain at an intermediate depth level over a couple of months during summer. Then a more gradual descent takes place until a maximum level of mean daily depth is reached during October through December, and the fish remain at this level until they start ascending for the repetition of spawning migrations.

Some parameters of depth and ambient temperature vary markedly between the two groups of fish (Table 1). The mean variation in depth (VD) is about four times higher for deep-water cod than for shallow-water cod or 18.0 m vs. 4.6 m, respectively, as overall monthly means. The mean standard deviation in ambient temperature is markedly higher for deep-water cod than for shallow-water cod, or 2.1 °C and 0.7 °C, respectively. The range in ambient temperature is also higher for deep-water cod, as indicated by minimum and maximum values (Table 1), although mean temperature is higher for shallow water cod than for deep-water cod, or 7.1 °C vs. 4.6 °C, respectively. The mean variation in ambient temperature (VT) is

Table 1. Monthly values of some parameters of depth (m) and ambient temperature (°C) for 17 shallow-water and 26 deep-water cod.

	April	May	June	July	Aug.	Sept.	Oct.	Nov.	Dec.	Jan.	Feb.	Mar.	April	May	Mean
Shallow-water cod															
Mean depth	60	85	103	100	101	110	113	116	114	110	109	97	84	99	100.1
Standard deviation	19	30	32	32	36	41	38	34	31	35	29	29	22	18	30.4
Min. depth	12	14	21	34	13	10	31	36	52	38	15	15	23	44	25.5
Max. depth	101	242	226	173	184	252	210	223	200	250	178	181	172	158	196.4
Mean absolute VD	2.5	4.8	7.0	5.2	5.4	4.7	4.5	4.5	3.9	3.8	4.2	5.9	3.9	3.4	4.6
Mean temperature	6.3	7.0	7.5	7.5	7.9	8.1	8.2	7.7	7.1	6.5	6.3	5.7	6.3	7.0	7.1
Standard deviation	0.5	0.4	0.3	1.0	0.8	1.1	0.9	0.7	0.8	1.0	0.6	0.6	0.7	0.3	0.7
Min. temperature	4.4	5.6	6.2	3.3	3.7	3.2	3.5	5.4	2.7	1.6	4.0	2.8	4.8	5.7	4.1
Max. temperature	7.2	7.7	9.7	10.9	10.4	10.7	10.4	8.8	8.3	7.9	7.4	7.1	7.4	7.9	8.7
Mean absolute VT	0.06	0.05	0.07	0.10	0.12	0.12	0.10	0.07	0.09	0.13	0.11	0.14	0.06	0.05	0.09
No. recordings	999	2545	2463	2545	2569	2521	2487	2521	2511	2182	1393	790	661	267	
Deep-water cod															
Mean depth	84	145	214	228	256	289	306	311	316	312	258	217	199	174	236.4
Standard deviation	28	75	89	101	109	106	95	98	105	121	149	125	110	48	97.1
Min. depth	6	15	54	33	29	66	75	54	78	73	36	23	49	103	49.6
Max. depth	172	500	680	514	520	631	614	610	621	616	707	633	658	417	563.8
Mean absolute VD	4.3	11.7	19.9	19.4	22.4	22.4	21.8	20.3	19.8	17.3	16.5	18.5	14.9	22.9	18.0
Mean temperature	6.5	7.0	5.3	4.1	4.0	3.8	3.7	3.8	3.8	4.0	4.7	4.8	5.4	6.6	4.8
Standard deviation	0.5	0.7	2.4	2.8	2.9	3.0	3.0	2.8	2.8	2.5	2.3	2.0	1.6	1.5	2.2
Min. temperature	4.8	0.1	–0.3	–0.4	–0.6	–0.8	–0.6	–0.7	–0.7	–0.9	–0.7	–0.5	–0.5	1.8	–0.0
Max. temperature	7.7	7.9	9.6	8.9	9.3	11.4	9.8	8.4	8.0	7.8	8.1	7.9	7.6	7.8	8.6
Mean absolute VT	0.06	0.12	0.35	0.30	0.42	0.53	0.50	0.42	0.40	0.43	0.39	0.33	0.30	0.28	0.35
No. recordings	1511	3600	3484	3600	3652	3548	3536	3548	3588	3647	3010	2088	1158	213	

Note: Min., minimum; Max., maximum; VD, variation in depth; VT, variation in ambient temperature; No., number.

Fig. 8. Relationships between depth and ambient temperature (set 2): (*a*) daily means of 17 shallow-water cod (*Gadus morhua*) released 1997 through 1999; (*b*) daily means of 26 deep-water cod released 1997 through 1999; and (*c*) means of 60 individual data storage tags released 1996 through 1999.

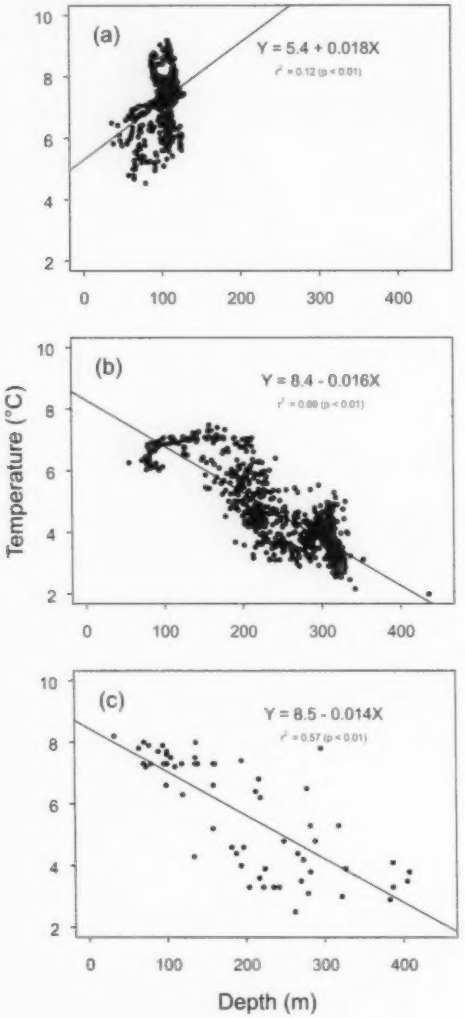

about four times higher for deep-water cod than for shallow-water cod, or 0.35 °C vs. 0.09 °C, respectively, indicating more extensive vertical movements of the deep-water fish than the shallow-water fish.

Interactions of depth, temperature, and growth

Interactions of depth and ambient temperature differ between the two groups of fish. Although there is a significant positive relationship between mean daily depth and mean daily ambient temperature for the shallow-water group of fish (Fig. 8*a*), the reverse is true for the deep-water group (Fig. 8*b*). A similar negative relationship was observed between mean depth and mean ambient temperature of the 60 individual fish of the data set (Fig. 8*c*).

Variations in depth and ambient temperature over a given time interval tend to increase with increasing depth. This is seen for deep-water fish in increased mean daily variation in depth (DVD) below approximately 150 m (Fig. 9*c*) and increased mean daily variation in ambient temperature (DVT) below approximately 170 m (Fig. 9*d*). For shallow-water fish, however, this is less clear, although increased variation is indicated below approximately 80 m (Figs. 9*a* and 9*b*). This pattern is more obvious with respect to maximum DVD and DVT, which are clearly increased at greater depth for shallow-water fish (Figs. 10*a* and 10*b*). For deep-water fish, the pattern is striking, in particular for maximum DVT (Figs. 10*c* and 10*d*). Furthermore, there is a large difference in the range of the variation between shallow-water and deep-water fish, in particular in maximum DVT. For shallow-water fish, maximum DVD rarely exceed ±50 m (Fig. 10*a*) and maximum DVT rarely exceed ±1.5 °C (Fig. 10*b*). For deep-water fish, however, maximum DVD close to ±150 m are common (Fig. 10*c*), as are maximum DVT close to ±4 °C (Fig. 10*d*). It should be noted, however, that time intervals are different (4 h in 1997 and 6 h in 1998 and 1999), which may be a source of discrepancy. A comparison of results for different time intervals indicated a negligible effect in this respect.

In view of the limited growth data available, a simple approach in data analysis was considered more adequate than a complicated modelling exercise. A simple, linear plot shows that individual growth of cod is related to depth and ambient temperature (Fig. 11). The findings are based on 32 DSTs with information on length at release and recovery available. A significant ($p < 0.05$) negative relationship is observed between depth and growth and a marginally significant ($p < 0.1$) positive relationship is observed between ambient temperature and growth. However, a relatively limited part of the variation is explained by the relationships (14.7% and 9.0%, respectively). A two-way analysis of variance (ANOVA) of growth on depth and ambient temperature shows that depth, as main effect, covers most (99%) of the explained variability, whereas ambient temperature, as main effect, covers 62% of the explained variability and depth covers the remaining 38%. A multiple linear regression of growth on depth and ambient temperature, however, falls short of being marginally significant ($p = 0.108$) but assigns markedly lower p value to depth ($p = 0.19$) than ambient temperature ($p = 0.81$). Thus, the data indicate that depth has a considerably greater explanatory power than ambient temperature with respect to growth of cod.

Individual growth of the fish at a given mean depth or ambient temperature is extremely variable. Three of the fish were particularly fast growing, with annual growth of 18.1, 20.6, and 23.0 cm·year^{-1}. The two fish of largest growth are of the shallow-water group with mean depths of 95 m and 100 m and mean ambient temperatures of 7.7 °C and 7.9 °C, whereas the third fish in this group had a mean depth of 224 m and mean ambient temperature of 3.9 °C (Appendix A). The fastest-growing fish (23.0 cm·year^{-1}) had been at liberty for 159 days only, or primarily during the period of fastest growth. The second fastest-growing fish had been at

Fig. 9. Relationships between mean daily depth and mean daily variation in depth (DVD) and mean daily variation in ambient temperature (DVT) of cod (*Gadus morhua*) released 1997 through 1999 (set 2): (*a*) depth vs. DVD of 17 shallow-water cod; (*b*) depth vs. DVT of 17 shallow-water cod; (*c*) depth vs. DVD of 26 deep-water cod; and (*d*) depth vs. DVT of 26 deep-water cod. Horizontal lines indicate zero.

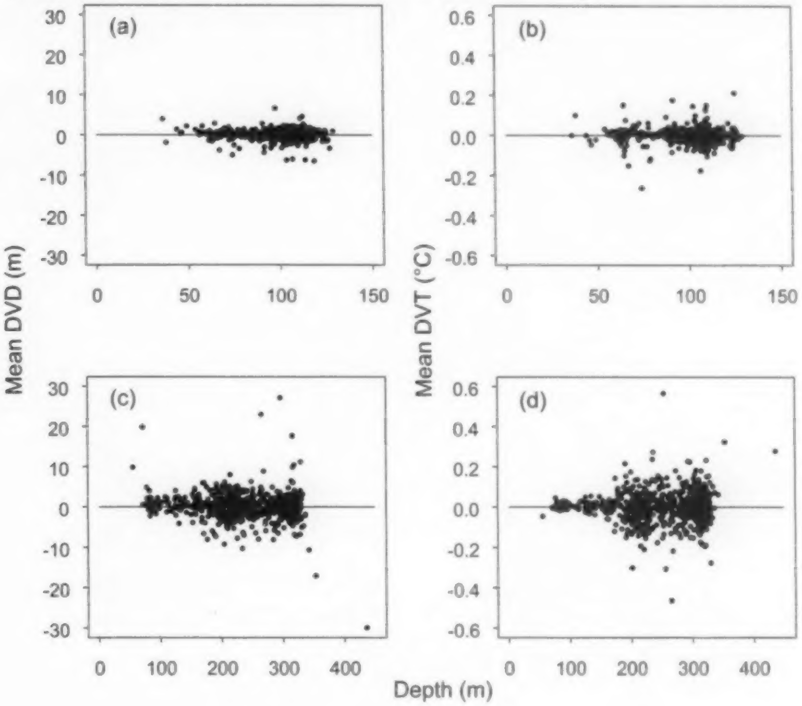

liberty for 248 days, and the third fish, 322 days. This suggests that limited coverage of the annual growth cycle may contribute to some overestimation of the annual growth of the three individual fish. In spite of this, their growth rate appears to be exceptionally high. The exclusion of those fish from the analysis has a marginal effect on the level of significance, decreasing the significance of depth (from p = 0.034 to p = 0.047) and increasing the significance of ambient temperature (from p = 0.096 to p = 0.081). Their exclusion from a multiple linear regression increases the p value of the fit from p = 0.108 to p = 0.126.

The plot of growth vs. depth indicates a fairly clear separation between 12 shallow-water fish and one deep-water fish (this fish, DST942, was recorded between 200 and 210 m during a few weeks and therefore falls into the deep-water category) at mean depth of individual fish of less than 160 m and 19 deep-water fish at mean depth greater than 180 m. The mean growth of the shallow-water fish is 8.8 cm·year^{-1} (range 0–23.0 cm·year^{-1}) at a mean depth of 104 m and mean ambient temperature of 7.6 °C. On the other hand, the mean growth of the deep-water fish is 4.8 cm·year^{-1} (range 0–18.1 cm·year^{-1}) at a mean depth of 246 m and mean ambient temperature of 4.6 °C. The mean growth of the two groups is significantly different (t test, $p < 0.05$). The plot of growth vs. ambient temperature reflects a somewhat different grouping, with 15 fish (all but three shallow-water group) at temperatures above 7 °C, 13 fish (all deep-water group) at temperature below 4.9 °C, and four deep-water fish at intermediate temperatures (5.3–6.4 °C). The mean growth of these three groups is 8.2, 5.5, and 2.8 cm·year^{-1}, respectively.

Discussion

To analyse potential differences in depth distribution and ambient temperatures, the available data set was split into two categories, i.e., shallow-water cod, which almost exclusively inhabit the continental shelf waters above 200 m, and deep-water cod, demonstrating preferences for more depth during feeding migrations. The shallow-water cod constitute a relatively well-defined group with narrow limits of depth (mostly <200 m) and ambient temperature (mostly 5.0–10.0 °C). The deep-water group, on the other hand, includes cod that inhabit the shelf waters at least during the spawning season but seek deeper waters during a variable period of the rest of the year. This suggests a selection of foraging strategies by the cod during feeding migrations, thus indicating that stock structure observed on the spawning grounds (Marteinsdóttir et al. 2000; Jónsdóttir et al. 2002) may, to some extent, be maintained outside the spawning season.

A comparison of the temperature regime of Icelandic waters and the distribution of ambient temperature of cod allows some interesting insights into migrations and locations of the fish. Some 40% of temperature recordings of deep-water cod were below 4 °C, indicating migrations to, or beyond, the waters of the east coast or the northwest coast. However, this indicates a considerably higher proportion of

Fig. 10. Relationships between mean daily depth and maximum (positive or negative) daily variation in depth (max. DVD) and maximum daily variation in ambient temperature (max. DVT) of cod (*Gadus morhua*) released 1997 through 1999 (set 2): (*a*) depth vs. max. DVD of 17 shallow-water cod; (*b*) depth vs. max. DVT of 17 shallow-water cod; (*c*) depth vs. max. DVD of 26 deep-water; and (*d*) depth vs. max. DVT of 26 deep-water cod. Horizontal lines indicate zero.

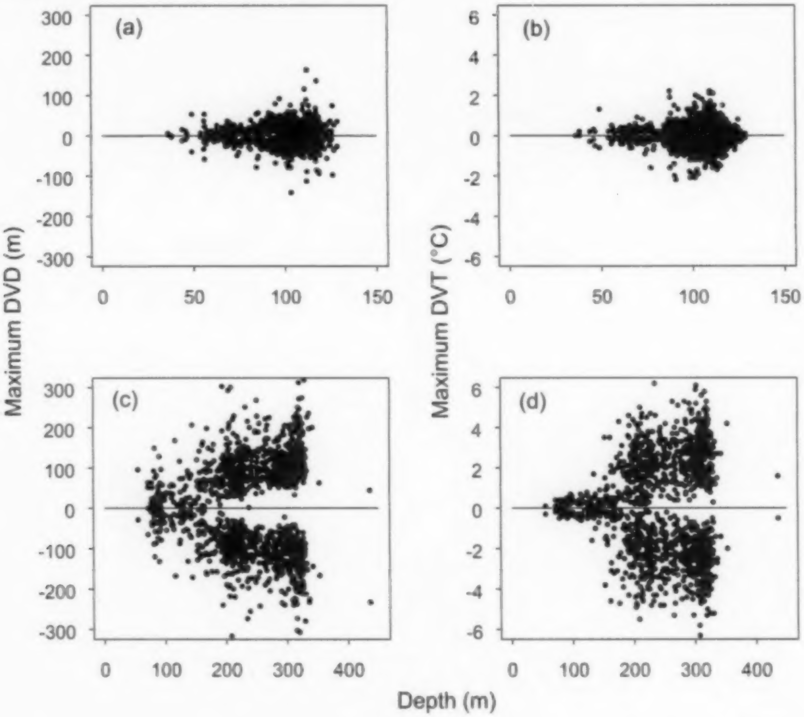

long-distance migration among Iceland cod than suggested by the location of recaptures in our data or from conventional tagging experiments, which showed that most of the recaptures (78%) were made within the main spawning grounds of the southwestern and southern coasts (Jónsson 1996).

The seasonal patterns of depth and ambient temperature are quite distinct for the two groups. It is suggested that shallow-water cod do not actively seek warmer ambient temperature at greater depths but experience the seasonal warming-up of the continental shelf waters during summer and autumn and the subsequent cooling during winter. The deep-water fish, on the other hand, seem to actively seek deeper waters, or a specific ambient temperature. At the same time, they increase their vertical activity and variability in ambient temperature to a substantially greater extent than shallow-water cod. This suggests that migratory patterns of deep-water cod in Icelandic waters may be dependent on ambient temperature, as observed for cod in other areas (Rose 1993; Stensholt 2001).

Daily variations in depth and ambient temperature indicate increased activity of the fish with increasing depth. This is most clearly indicated by maximum DVT of deep-water fish but may also be observed for shallow-water fish. There are constraints to the rate of vertical movements of fish with closed swimbladders, such as cod, that are caused by the swimbladder physiology and Boyle's law. Experimental work has shown that cod adapted to certain pressure conditions can cope with 25% reduction and 50% increase in pressure. The air in the swimbladder obeys Boyle's law, and therefore, the deeper the cod, the greater its free vertical range of activity (Blaxter and Tytler 1978; Harden Jones and Scholes 1985; Arnold and Greer Walker 1992). The increase in vertical activity observed for deep-water cod is in general agreement with the increase in the free vertical range.

Cod that go into deep waters in feeding migrations have been shown to seek polar fronts or the boundaries between the cold Arctic and the warm Atlantic waters. Feeding migrations of cod in temperature fronts is known from Barents Sea (Godø and Michalsen 2000; Stensholt et al. 2000; Stensholt 2001). In Canada, the voluntary and repetitive movements of cod across a thermocline have also been observed (Jean 1964; Clark and Green 1990). We suggest, in view of vertical activity, that the deep-water cod are more likely than shallow-water cod to seek temperature boundaries and perform periodic vertical movements at such boundaries. However, higher or lower temperature is not likely to be the ultimate objective of such movements, as higher temperature would be available in shallow water at lower cost in terms of activity. Concentrations of food are more likely to be causing such activity.

Moreover, we suggest that increased vertical migrations are likely to lead to reduced catchability of the fish, i.e., the deep-water cod, and hence decreased fishing mortality outside the spawning season. This would explain relatively few recaptures outside the spawning season and area. This is

Fig. 11. Relationships between (*a*) annual growth and mean depth and (*b*) annual growth and mean ambient temperature. Data of 32 individual cod (*Gadus morhua*): 12 shallow-water cod and 20 deep-water cod (set 3).

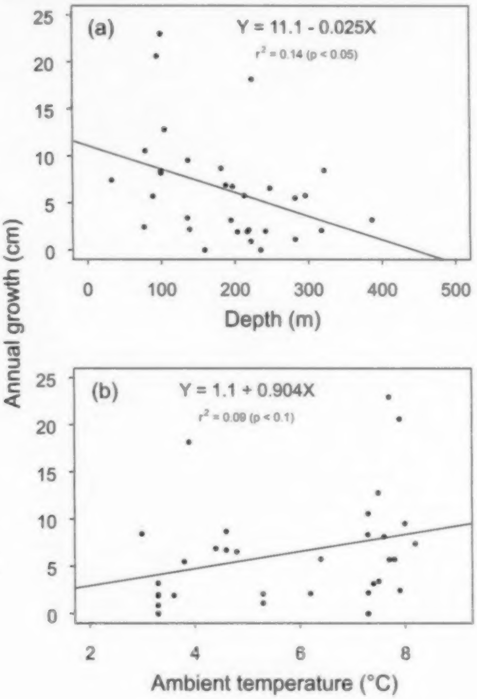

partly supported by Begg and Marteinsdóttir (2003), who recorded higher relative fishing mortality of mature cod in gill nets in inshore waters (<125 m) compared with offshore waters (>125 m). However, for demersal trawl, higher fishing mortality was recorded in most regions in offshore waters. On the other hand, Sólmundsson et al. (2003) showed that increased vertical activity of plaice (*Pleuronectes platessa*) males vs. females lead to somewhat increased catchability of spawning males west of Iceland. However, swimming activity of male plaice was interpreted mainly as movement along or near the bottom between different depth levels, within reach of towed gear. Such findings indicate that interactions between catchability and vertical movement of fish may be more complex than anticipated.

Growth of the cod was negatively related to mean depth and positively related to mean ambient temperature ranging between 3 and 8 °C. Apparently, the vertically stationary shallow-water fish inhabiting warmer waters are more productive in terms of growth than the vertically migratory deep-water fish of cooler waters. The mean ambient temperature was 7.6 °C for 13 shallow-water fish and 4.6 °C for 19 deep-water fish. In comparison, mark–recapture data with conventional tags have shown similar trends in growth in relation to temperature for cod on the Scotian Shelf. In areas with bottom temperatures around 7 °C, mean growth of 65-cm cod was approximately 9 cm and approximately 5 cm at temperatures around 4 °C (Shackell et al. 1997), corresponding to mature shallow-water and deep-water cod in Icelandic waters, respectively.

Laboratory experiments suggest 5.5 °C as optimal temperature for growth ($T_{\mathrm{opt},G}$) of cod of this size (mean length 90 cm) when fed ad libitum (Björnsson et al. 2001) and that growth rate and $T_{\mathrm{opt},G}$ decrease with reduced food ration, resulting in approximately halved growth rate, and $T_{\mathrm{opt},G}$ reduced by approximately 5 °C, with halved ration for sockeye salmon (Brett et al. 1969). Consequently, the deep-water fish appear to be closer to $T_{\mathrm{opt},G}$ than the shallow-water fish. However, it has also been shown in laboratory experiments that thermal response of cod growth is negligible within some degrees from $T_{\mathrm{opt},G}$, resulting in a flat-shaped curve of temperature vs. growth rate (Björnsson et al. 2001). Therefore, reduced growth of deep-water cod might be best explained by significantly reduced supply of food in the deeper waters. In nature, environmental temperature and depth may both be proxies for food supply. In the case of mature Icelandic cod, depth appears to be a better proxy than ambient temperature.

Thus, the deep-water cod seem to adjust to reduced ambient temperature and reduced food supply at the expense of growth. Reduced temperature means lower maintenance ration (food required to hold body weight constant) as maintenance ration increases steadily with increasing temperature and fish size (Jobling 1988). Thus, large cod may find relatively favourable conditions in deep waters, in particular, if concentrations of food are at a low level, because the fish are closer to the optimal temperature for growth and lower temperatures reduce the amount of food needed for maintenance.

In summary, profiles of depth and ambient temperature suggest that cod spawning in the area of study select between two main alternatives in foraging strategies, i.e., deep- or shallow-water migrations. It should be noted, however, that within the two strategies, there may well be further subgrouping, e.g., with respect to spawning sites or other stock characteristics. The two strategies lead to very different ambient temperatures, as well as behaviour of the cod in terms of vertical movement. This appears to significantly affect the growth of the cod, most likely because of reduced supply of food with increased depth. This may also affect catchability because of increased vertical movement of deep-water cod.

Acknowledgements

Dr. Björn Björnsson, Marine Research Institute, Reykjavik, made some valuable suggestions that improved the manuscript. Mr. Héðinn Valdimarsson, Marine Research Institute, Reykjavik, assisted in producing the vertical profiles of environmental temperature (Fig. 1). Comments from three anonymous referees markedly improved the manuscript and are greatly appreciated.

References

Arnold, G.P., and Greer Walker, M. 1992. Vertical movements of cod (*Gadus morhua* L.) and the hydrostatic function of the swimbladder. ICES J. Mar. Sci. **49**: 357–372.

Arnold, G.P., Greer Walker, M., Emerson, L.S., and Holford, B.H. 1994. Movements of cod (*Gadus morhua* L.) in relation to the tidal streams in the southern North Sea. ICES J. Mar. Sci. **51**: 207–232.

Begg, G.A., and Marteinsdóttir, G. 2002. Environmental and stock effects on spatial distribution and abundance of mature cod *Gadus morhua*. Mar. Ecol. Progr. Ser. **229**: 245–262.

Begg, G.A., and Marteinsdóttir, G. 2003. Spatial partitioning of relative fishing mortality and spawning stock biomass of Icelandic cod. Fish. Res. **59**: 343–362.

Björnsson, B., and Steinarsson, A. 2002. The food-unlimited growth rate of Atlantic cod (*Gadus morhua*). Can. J. Fish. Aquat. Sci. **59**: 494–502.

Björnsson, B., Steinarsson, A., and Oddgeirsson, M. 2001. Optimal temperature for growth and feed conversion of immature cod (*Gadus morhua* L.). ICES J. Mar. Sci. **58**: 29–38.

Blaxter, J.H.S., and Tytler, P. 1978. Physiology and function of the swimbladder. Adv. Comp. Physiol. Biochem. **7**: 311–367.

Brander, K. 1995. The effect of temperature on growth of Atlantic cod (*Gadus morhua* L.). ICES J. Mar. Sci. **52**: 1–10.

Brett, J.R., Shelbourn, J.E., and Shoop, C.T. 1969. Growth rate and body composition of fingerling sockeye salmon, *Onchorhynchus nerka*, in relation to temperature and ration size. J. Fish. Res. Board Can. **26**: 2363–2394.

Clark, D.S., and Green, J.M. 1990. Activity and movement patterns of juvenile Atlantic cod, *Gadus morhua*, in Conception Bay, Newfoundland, as determined by sonic telemetry. Can. J. Zool. **68**: 1434–1442.

Godø, O.R., and Michalsen, K. 2000. Migratory behaviour of north-east Arctic cod, studied by use of data storage tags. Fish. Res. **48**: 127–140.

Hansen, P.M. 1941. Studies on the biology of cod in Greenland waters. Rapp. P.-V. Rèun. Cons. Perm. Int. Explor. Mer, **123**: 2–77.

Hansen, P.M., Jensen, A., and Tåning, Å.V. 1935. Cod marking experiments in the waters of Greenland 1924–1933. Medd. Komm. Fisk. Havunders. Fisk. **10**: 2–119.

Harden Jones, F.R., and Scholes, P. 1985. Gas secretion and resorption in the swimbladder of the cod *Gadus morhua*. J. Comp. Physiol. B, **155**: 319–331.

Jean, Y. 1964. Seasonal distribution of cod (*Gadus morhua* L.) along the Canadian Atlantic coast in relation to water temperature. J. Fish. Res. Board Can. **21**: 429–460.

Jobling, M. 1988. A review of the physiological and nutritional energetics of cod, *Gadus morhua* L., with particular reference to growth under farmed conditions. Aquaculture, **70**: 1–19.

Jónsdóttir, Ó.D.B., Danielsdóttir, A.K., and Nævdal, G. 2001. Genetic differentiation among Atlantic cod (*Gadus morhua* L.) in Icelandic waters: temporal stability. ICES J. Mar. Sci. **58**: 114–122.

Jónsdóttir, Ó.D.B., Imsland, A.K., Danielsdóttir, A.K., and Marteinsdóttir, G. 2002. Genetic heterogeneity and growth properties of different genotypes of Atlantic cod (*Gadus morhua* L.) at two spawning sites off south Iceland. Fish. Res. **55**: 37–47.

Jónsson, J. 1996. Tagging of cod (*Gadus morhua*) in Icelandic waters 1948–1986. Rit Fiskid. **14**(1): 1–82.

Marteinsdóttir, G., Gudmundsdóttir, A., Thorsteinsson, V., and Stefánsson, G. 2000. Spatial variation in abundance, size composition and viable egg production of spawning cod (*Gadus morhua* L.) in Icelandic waters. ICES J. Mar. Sci. **57**: 824–830.

Mountain, D.G., and Murawski, S.A. 1992. Variation in the distribution of fish stocks on the northeast continental shelf in relation to their environment, 1980–1989. ICES J. Mar. Sci. **195**: 424–432.

Pálsson, Ó.K. 1980. Über die Biologie junger Gadiden der Altersgruppen 0, I und II in isländischen Gewässern. Meeresforschung, **28**(2–3): 101–145.

Rose, G.A. 1993. Cod spawning on a migration highway in the north-west Atlantic. Nature (Lond.), **366**: 458–461.

Serchuk, F.M., Grosslein, M.D., Lough, R.G., Mountain, D.G., and O'Brien, L. 1994. Fishery and environmental factors affecting trends and fluctuations in the Georges Bank and Gulf of Maine Atlantic cod stocks: an overview. ICES Mar. Sci. Symp. **198**: 77–109.

Shackell, N.L., Stobo, W.T., Frank, K.T., and Brickman, D. 1997. Growth of cod (*Gadus morhua*) estimated from mark–recapture programs on the Scotian Shelf and adjacent waters. ICES J. Mar. Sci. **54**: 383–398.

Sólmundsson, J., Karlsson, H., and Pálsson, J. 2003. Sexual differences in spawning behaviour and catchability of plaice (*Pleuronectes platessa*) west of Iceland. Fish. Res. **61**: 57–71.

Stensholt, B.K. 2001. Cod migration patterns in relation to temperature: analysis of storage tag data. ICES J. Mar. Res. **58**:770–793.

Stensholt, B.K., Michalsen, K., and Godö, G.R. 2000. Behavioural rhythm of cod during migration in the Barents Sea. ICES CM 2000/K:34.

Sæmundsson, B. 1923. On the age and the growth of the cod (*Gadus callarias* L.) in Icelandic waters. Medd. Komm. Havunders. Fisk. **VII**(3): 3–35.

Taylor, C.C. 1957. Cod growth and temperature. J. Cons. Perm. Int. Explor. Mer, **23**(1): 366–370.

Thorsteinsson, V., and Marteinsdóttir, G. 1992. Þorskmerkingar við Norðaustur- og Austurland vorið 1991 og endurheimtur sama ár [Mark–recapture experiments at the northeast and east coasts of Iceland 1991]. [In Icelandic.] Ægir, **85**: 60–64.

Thorsteinsson, V., and Marteinsdóttir, G. 1998. Size specific time and duration of spawning of cod (*Gadus morhua*) in Icelandic waters. ICES CM 1998/DD:5.

Wigley, S.W., and Serchuk, F.M. 1992. Spatial and temporal distribution of juvenile Atlantic cod *Gadus morhua* in the Georges Bank – Southern New England region. Fish. Bull. **90**: 599–606.

Appendix A

Table A1. Relevant information on the 60 data storage tags (DSTs): number (No.) and type of DST, date at release, days at liberty (d), days of recordings (d_{rec}), length (cm) at release (L_{rel}) and recapture (L_{rec}), annual growth (G), age (years) at recapture (A_{rec}), mean and range of depth (m) (D_{mean}, D_{range}, respectively) and ambient temperature (°C) (T_{mean}, T_{range}, respectively).

No.	Type	Date	d	d_{rec}	L_{rel}	L_{rec}	G	A_{rec}	D_{mean}	D_{range}	T_{mean}	T_{range}	Set
2016	200A	08/04/1998	510	322	82	NA	NA	NA	194	13–524	4.0	–0.5–7.3	D1, D2
2034	200A	08/04/1998	524	384	86	87	0.7	NA	383	9–680	2.9	–0.7–7.8	D1, D2
2047	200A	07/04/1998	375	374	72	74	1.9	7	217	8–592	3.6	–0.5–7.3	D1, D2, D3
2072	200A	07/04/1998	331	331	94	NA	NA	NA	161	9–347	7.3	5.5–10.1	D1, D2
2076	200A	07/04/1998	380	379	68	70	1.9	5	204	15–497	3.3	–0.6–8.9	D1, D2, D3

Table A1 (*concluded*).

No.	Type	Date	d	d_{rec}	L_{rel}	L_{rec}	G	A_{rec}	D_{mean}	D_{range}	T_{mean}	T_{range}	Set
2081	200A	15/04/1998	342	342	91	NA	NA	6	136	3–188	7.3	4.5–9.8	S1, S2
2115	200A	15/04/1998	348	288	92	101	9.4	NA	387	6–589	4.1	0.1–8.1	D1, D2
2119	200A	15/04/1998	320	320	95	NA	NA	NA	119	5–242	7.3	2.7–9.7	S1, S2
2127	200A	17/04/1998	491	309	95	104	6.7	7	70	9–117	7.3	2.7–11.4	D1, D2
2148	200A	17/04/1998	389	378	76	85	8.4	7	322	5–658	3.0	–0.4–10.7	D1, D2, D3
2163	200A	16/04/1998	279	279	93	NA	NA	11	64	14–216	7.8	6.1–9.7	S1, S2
2168	200A	16/04/1998	159	159	90	100	23.0	NA	100	55–134	7.7	6.7–10.1	S3
2188	200A	16/04/1998	373	373	83	NA	NA	NA	262	2–621	2.5	–0.7–7.5	D1, D2
2199	200A	16/04/1998	336	336	97	105	8.7	NA	182	6–303	4.6	0.1–8.1	D1, D2, D3
2204	200A	16/04/1998	268	268	93	100	9.5	8	137	9–235	8.0	6.3–10.7	S1, S2, S3
2222	200A	16/04/1998	311	291	87	96	10.6	7	79	18–149	7.3	1.6–10.5	S1, S2, S3
2233	200A	17/04/1998	324	324	104	NA	NA	10	405	7–631	3.5	–0.5–7.8	D1, D2
2235	200A	17/04/1998	714	278	92	108	8.2	7	71	7–250	8.0	6.0–10.4	S1, S2
2236	200A	17/04/1998	323	322	98	99	1.1	9	282	10–657	5.3	–0.2–9.6	D1, D2, D3
2266	200A	10/04/1999	349	349	101	109	8.4	7	100	25–184	7.3	4.8–8.6	S1, S2, S3
2276	200A	11/04/1999	507	384	92	103	7.9	9	73	8–130	7.2	4.4–10.1	S1, S2
2306	200A	17/04/1998	367	367	104	NA	NA	NA	327	15–707	3.9	–0.4–8.0	D1, D2
2320	200A	11/04/1999	322	322	96	112	18.1	8	224	41–450	3.9	–0.3–7.9	D1, D2, D3
2329	200A	15/04/1999	339	339	98	101	3.2	9	387	87–657	3.3	–0.4–7.6	D1, D2, D3
2399	200A	15/04/1999	343	343	101	103	2.1	9	219	10–490	6.2	–0.2–9.0	D1, D2, D3
2439	200A	13/04/1999	190	190	84	87	5.8	NA	213	19–374	6.4	–0.6–7.4	D3
2461	200A	13/04/1999	335	335	84	90	6.5	6	248	6–609	4.8	–0.3–8.4	D1, D2, D3
2463	200A	13/04/1999	367	367	102	NA	NA	NA	279	10–550	3.1	–0.8–8.2	D1, D2
2476	200A	13/04/1999	248	248	88	102	20.6	6	95	43–146	7.9	5.8–9.6	S3
2483	200A	15/04/1999	341	196	87	90	3.2	8	266	3–540	4.4	–0.4–7.8	
2508	200A	15/04/1999	268	268	84	90	8.2	7	100	5–167	7.6	2.6–9.0	S1, S2, S3
2509	200A	15/04/1999	330	330	98	100	2.2	9	139	8–232	7.3	1.9–8.5	S1, S2, S3
2510	200A	15/04/1999	404	383	68	69	0.9	7	222	10–624	3.3	–0.5–7.8	D1, D2, D3
2524	200A	15/04/1999	363	363	95	97	2.0	9	242	9–483	3.3	–0.3–7.8	D1, D2, D3
743	200B	03/05/1996	197	197	86	90	7.4	6	33	7–91	8.2	4.5–11.3	S3
754	200B	13/04/1997	574	395	69	87	11.4	7	110	11–252	7.2	4.7–10.9	S1, S2
784	200B	13/04/1997	398	395	88	94	5.5	9	282	3–399	3.8	–0.9–7.9	D1, D2, D3
807	200B	13/04/1997	1082	395	100	119	6.4	10	120	2–226	6.3	3.2–7.9	S1, S2
823	200B	14/04/1997	296	296	92	94	2.5	NA	77	32–91	7.9	5.9–10.1	S1, S2, S3
827	200B	14/04/1997	700	395	94	104	5.2	9	96	6–123	7.3	4.8–8.9	S1, S2
843	200B	15/04/1997	329	309	97	NA	NA	NA	99	17–170	6.6	4.2–9.7	S1, S2
847	200B	15/04/1997	326	326	90	96	6.7	9	197	4–401	4.6	–0.3–8.2	D1, D2, D3
851	200B	15/04/1997	315	315	63	NA	NA	NA	217	7–342	6.8	5.2–7.8	D1, D2
852	200B	15/04/1997	319	318	101	104	3.4	8	136	12–194	7.5	5.5–8.4	S1, S2, S3
857	200B	17/04/1997	402	167	91	97	5.4	8	158	16–285	5.2	0.7–7.6	
910	200B	18/04/1997	319	319	103	108	5.7	9	89	11–146	7.7	5.6–9.6	S1, S2, S3
934	200B	17/04/1997	336	336	91	NA	NA	7	159	19–413	6.6	3.5–7.7	D1, D2
935	200B	17/04/1997	698	395	101	113	6.3	11	273	3–417	4.2	–0.5–8.1	D1, D2
942	200B	17/04/1997	347	320	95	95	0.0	8	159	6–274	7.3	4.9–8.4	D1, D2, D3
2616	300C	16/04/1998	366	298	93	98	5.0	11	134	0–325	4.3	0.2–8.6	S1
2620	300C	16/04/1998	398	315	95	100	4.6	9	408	1–697	3.8	–0.5–8.0	D1
2622	300C	16/04/1998	317	316	96	101	5.8	NA	296	107–458	7.8	3.9–8.8	D1, D3
2644	300C	19/04/1998	690	381	89	96	3.7	9	288	0–610	4.8	–0.3–8.6	D1
2651	300C	19/04/1998	318	318	99	105	6.9	8	188	23–337	4.4	0–8.6	D1, D3
2657	300C	19/04/1998	340	340	90	90	0.0	9	235	0–495	3.3	–0.6–8.0	D1, D3
1481	300D	13/04/1997	314	314	88	99	12.8	8	105	20–333	7.5	5.6–9.0	S1, S3
1511	300D	17/04/1997	345	342	93	96	3.2	8	195	30–351	7.4	2.2–11.2	D1, D3
1579	300D	17/04/1997	175	175	86	87	2.1	8	318	13–520	5.3	0–7.8	D3
1582	300D	16/04/1997	376	271	95	100	4.9	8	270	110–741	3.5	–0.2–8.0	
1613	300D	18/04/1997	384	384	105	NA	NA	NA	278	3–426	6.5	4.0–7.7	D1

Note: Set refers to the subsets of the whole data used in Fig. 5 (set 1, 52 fish), Figs. 7–10 (set 2, 43 fish), and Fig. 11 (set 3, 32 fish). D, deep-water fish; S, shallow-water fish; NA, not available. Dates are given in day/month/year format.

Anthropogenic introduction of the etiological agent of withering syndrome into northern California abalone populations via conservation efforts

Carolyn S. Friedman and Carl A. Finley

Abstract: Populations of abalone have precipitously declined in California over the past several decades, largely as a result of fishing pressure and disease. Because of these declines, farmed seed abalone have been planted in an attempt to research and restore dwindling populations. Withering syndrome is a chronic disease responsible for mass mortalities of wild black abalone, *Haliotis cracherodii*, in southern and central California and is caused by the bacterium "*Candidatus* Xenohaliotis californiensis". This bacterium has been observed in wild populations of black and red (*Haliotis rufescens*) abalone south of Carmel and in farmed red abalone throughout the state. In an effort to elucidate the distribution and source of the bacterium in northern California, the presence or absence of the disease and bacterium was verified at 15 locations north of Carmel. This research revealed that both the bacterium and withering syndrome are present in abalone populations south of San Francisco. In addition, the bacterium (but not withering syndrome) is present at two locations in northern California, both associated with outplants of hatchery-reared abalone, suggesting a link between restoration efforts and the present distribution of this pathogen. These data highlight the need for careful assessment of animal health before restocking depleted populations.

Résumé : Les populations d'ormeaux ont subi un déclin rapide en Californie au cours des dernières décennies, en grande partie dû à la pression de la pêche et à la maladie. À cause de ce déclin, des ormeaux d'élevage ont été ensemencés dans le but de suivre et de restaurer les populations décroissantes. Le syndrome du dépérissement est une maladie chronique responsable des mortalités massives d'ormeaux noirs sauvages, *Haliotis cracherodii*, dans le centre et le sud de la Californie, causée par la bactérie « *Candidatus* Xenohaliotis californiensis ». La bactérie est présente dans les populations sauvages d'ormeaux noirs et rouges (*Haliotis rufescens*) au sud de Carmel et dans les élevages d'ormeaux rouges dans toute la Californie. Dans le but de déterminer la répartition et l'origine de la bactérie dans le nord de la Californie, nous avons vérifié la présence ou l'absence de la maladie et de la bactérie à 15 sites au nord de Carmel. La bactérie ainsi que le syndrome du dépérissement se retrouvent dans les populations d'ormeaux au sud de San Francisco. De plus, la bactérie, mais non le syndrome du dépérissement, existe à deux sites dans le nord de la Californie, tous deux des points d'ensemencements d'ormeaux d'élevage, ce qui semble indiquer l'existence d'un lien entre les efforts de restauration et la répartition actuelle du pathogène. Ces observations mettent en lumière l'importance de déterminer l'état de santé des animaux avant de les utiliser pour repeupler des populations en déclin.

[Traduit par la Rédaction]

Introduction

Abalone stocks have declined dramatically worldwide in the past few decades, declines that are typically associated with commercial and sport fishing and, to an unknown extent, poaching, as well as the expanding sea otter populations (in California), pollution, disease, and inadequate management (Karpov et al. 2000; Haaker et al. 2001; Shepherd et al. 2001). In addition to their commercial value, abalone are ecologically important marine invertebrates (Sloan and Breen 1988). The red abalone (*Haliotis rufescens*) is the most abundant species in California (state) and supports the only remaining recreational abalone fishery in the state. In addition, red abalone are an important herbivore in the rocky subtidal ecosystem. Dramatic declines in abalone stocks in California, Washington, Alaska, and British Columbia (B.C.;

Received 5 December 2002. Accepted 13 July 2003. Published on the NRC Research Press Web site at http://cjfas.nrc.ca on 5 December 2003.
J17222

C.S. Friedman[1,2] and C.A. Finley.[3] California Department of Fish and Game and Department of Medicine and Epidemiology, University of California, Bodega Marine Laboratory, P.O. Box 247, Bodega Bay, CA 94923, U.S.A.

[1] Corresponding author (e-mail: carolynf@u.washington.edu).
[2] Present address: School of Aquatic and Fishery Sciences, University of Washington, Box 355020, Seattle, WA 98195, U.S.A.
[3] Present address: The Cultured Abalone, 9580 Dos Pueblos Canyon Road, Goleta, CA 93117, U.S.A.

Can. J. Fish. Aquat. Sci. **60**: 1424–1431 (2003) doi: 10.1139/F03-121

Canada) have forced closures of many commercial and recreational fisheries to allow recolonization (Campbell 2000; Haaker et al. 2001; A. Bradbury, Washington Department of Fish and Wildlife, 1111 Washington St. SE, Olympia, WA 98501, personal communication). As a result of Allee effects, remaining individuals may be too spatially separated to enable successful fertilization and subsequent recruitment (Allee et al. 1949; Quinn et al. 1993; Stoner and Ray-Culp 2000). In fact, Richards and Davis (1993) found that recruitment declined when abalone population densities decreased by 50% or more. Rock reefs historically inhabited by substantial populations of abalone may undergo changes in community structure because of the absence of grazing activity by abalone, further reducing recruitment. Prime juvenile black abalone (*Haliotis cracherodii*) nursery grounds have been overgrown by *Phragmatopoma californica*, the sandcastle worm, after large-scale mortalities (>99%) of black abalone by withering syndrome in southern California (D. Richards, Channel Islands National Park Service, 1901 Spinnaker Dr., Ventura, CA 93001, personal observation). With the closure of all abalone take south of San Francisco, increased pressure on the north coast abalone populations has resulted in a reduction in abalone catch limits from 4 to 3 per day and an annual limit reduction from 100 to 24 (K. Karpov, California Department of Fish and Game (CDFG), 19160 S. Harbor Dr., Fort Bragg, CA 95437, personal communication). Despite these measures, careful management of northern California red abalone populations is needed to sustain both ecological and economic benefits.

As a direct result of concern over the sustainability of abalone populations in California (and globally), efforts to understand, conserve, and restore abalone populations have been undertaken. Abalone restoration methods are being developed in many countries and typically include the planting of large numbers of hatchery-reared seed, broodstock aggregation, and the creation of marine protected areas, or a combination of one or more of these practices (Saito 1984; Tegner 1993, 2000). Some of these efforts have shown great promise. However, the presence of a devastating disease agent causing withering syndrome in abalone populations of southern California, including abalone farms, has raised concerns that outplants before the identification of the causative agent of this disease may have introduced the pathogen into previously unaffected abalone populations. A lack of baseline data on abalone health in California made identification of the causative agent difficult (Haaker et al. 1992; Friedman et al. 1997). Such information, which is crucial for epidemiological studies, disease control via zoning of infected and uninfected areas (zones; Office International des Epizooties (OIE) 2001), and conservation efforts, was lacking before this study.

Withering syndrome (WS), a chronic wasting disease, was found in association with massive mortalities of black abalone in the waters off southern and central California. The disease was first observed in the mid-1980s along the Channel Islands, where cumulative mortality in some populations of black abalone reached 99% (Haaker et al. 1992; Lafferty and Kuris 1993; VanBlaricom et al. 1993). California's abalone aquaculture industry also sustained substantial economic losses as a result of the reduced growth rates and increased mortalities attributable to WS. The impact of the disease was especially severe during the 1997–1998 El Niño year (Moore et al. 2000).

Abalone with clinical signs of WS display a pronounced atrophy of the foot muscle and cease feeding, which is followed by rapid death (Haaker et al. 1992). A *Rickettsia*-like prokaryote (RLP), "*Candidatus* Xenohaliotis californiensis", has been identified as the etiological agent of the disease (Friedman et al. 2000, 2002; Moore et al. 2001). The range of the RLP and WS in California is not known, although such knowledge is crucial for management of abalone populations throughout the state. The possible spread of the RLP and WS into northern California, where the last remaining healthy abalone populations are found (K. Karpov, CDFG, 19160 S. Harbor Dr., Fort Bragg, CA 95437, personal communication), is reason for great concern and was the stimulus for this study.

Materials and methods

Site selection

To evaluate the geographic range of the RLP and WS in California, a stratified random sampling design was employed that included two strata: (1) near recognized human activity that could have introduced the WS bacterium (point-source location, PSL), and (2) well removed from recognized anthropogenic sources (reference location, RL). The coast was partitioned into 2-mile (3.704 km) sections north and south of each PSL site to set strata boundaries. Each 2-mile section was numbered and delineated along a smoothed 30-foot (9.14 m; 5 fathom) contour line as our pool of potential sampling sites within strata (PSL or RL). Random numbers were drawn until one number within each stratum was selected. We attempted to have one to two RL between each PSL. The sampling protocol allowed a shift in location if abalone habitat did not exist at that location. That is, we moved from that location to the closest location that had reasonable indicators of abalone habitat, such as the presence of a kelp bed, for actual in-water collection efforts. Because low abalone abundance was recognized in many locations, the protocol allowed further shifting as required to obtain the necessary sample size. In addition, we took advantage of the California Department of Fish and Game's (CDFG) biannual abalone creel survey, during which sport-caught abalone were sampled at eight of the sample locations.

Sample and data collection

We identified PSLs, defined by their proximity to a known abalone outplant location, commercial abalone facility, aquarium, or research laboratory, and RLs having no geographic proximity to any of the aforementioned PSLs (Fig. 1; Table 1). An attempt was made to collect 60 abalones (red and (or) black) per geographic location to provide a 95% confidence level of detecting the RLP in populations of animals with a prevalence of infection ≥5% (Thoesen 1994). Total length, total weight, shell weight, and visual signs of atrophy (weight loss) were recorded. Although rickettsial bacteria are found in many marine animals, few exist in abalone. Thus, the etiological agent of WS is easily identified as it produces homogeneous, basophilic, oblong, intracytoplasmic inclusions in infected digestive epithelial cells, which can be

Fig. 1. Distribution of reference locations (RL) and point source locations (PSL) along the northern and central California coast.

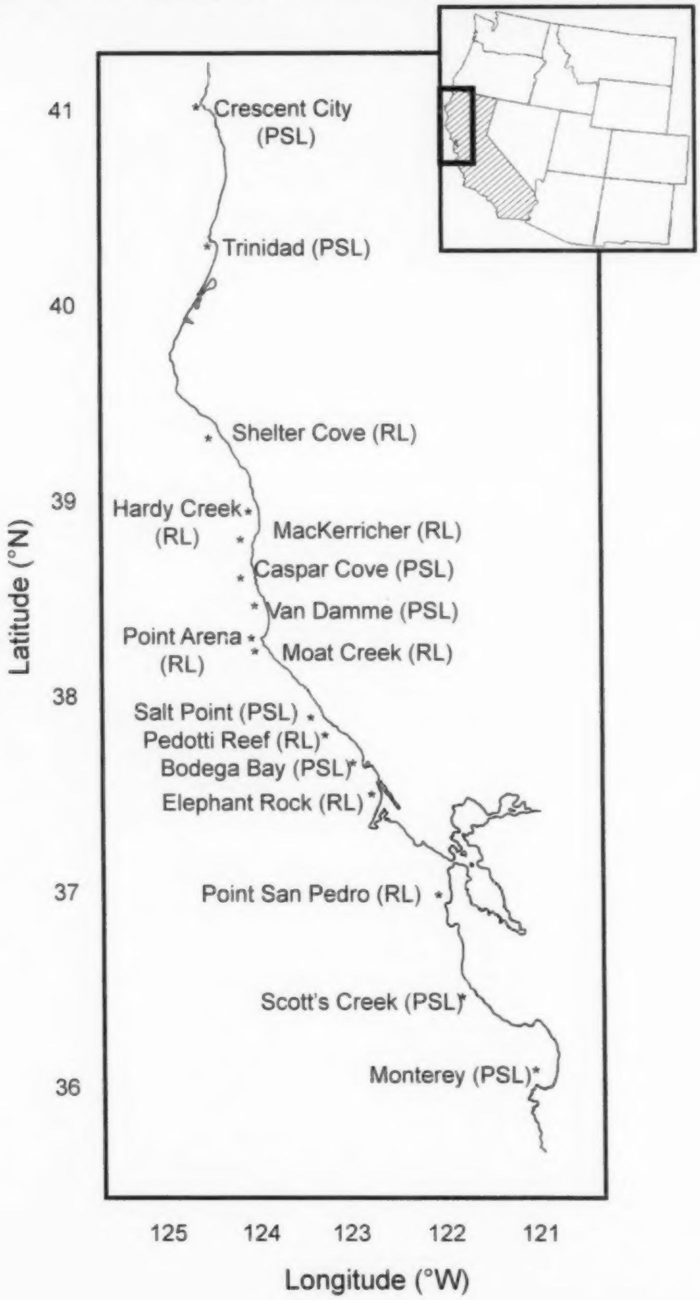
Crescent City (PSL)
Trinidad (PSL)
Shelter Cove (RL)
Hardy Creek (RL)
MacKerricher (RL)
Caspar Cove (PSL)
Van Damme (PSL)
Point Arena (RL)
Moat Creek (RL)
Salt Point (PSL)
Pedotti Reef (RL)
Bodega Bay (PSL)
Elephant Rock (RL)
Point San Pedro (RL)
Scott's Creek (PSL)
Monterey (PSL)
41
40
39
38
37
36
Latitude (°N)
125
124
123
122
121
Longitude (°W)

observed by light microscopic examination of stained tissue sections (Gardner et al. 1995; Friedman et al. 1997, 2000). In addition, 3- to 5-mm tissue cross sections containing posterior esophagus (post-esophagus), digestive gland, and foot muscle (when possible) were excised, placed in Invertebrate Davidson's solution (Shaw and Battle 1957) for 24 h, and then processed for routine paraffin histology. Deparaffinized 5-µm sections were stained with hematoxylin and eosin and viewed by bright-field microscopy for RLP inclusions (Luna 1968). When possible, digestive gland samples (~50 mg) were also removed and archived for subsequent polymerase chain reaction (PCR) analysis to further confirm the presence of the WS bacterium in histology-positive samples outside the range of WS using the methods of Andree et al. (2000).

Table 1. Sampling schedule and data collected from abalone inhabiting point source and reference (in italics) locations between December 1998 and August 2001.

Location	*Haliotis rufescens*	*Haliotis cracherodii*	RLP-positive animals	Visible atrophy	Creel (Y/N)	Date
Shelter Cove	61	0	0	0	N	December 1, 1998
Monterey	2	56	55	0	N	December 1, 1998
Scott's Creek	2	58	43	3	N	January 30, 1999
Point San Pedro	4	0	3	2	N	February 17, 1999
Bodega Bay	60	0	0	0	N	March 1, 1999
Crescent City	29	0	5	0	N	August 1, 1999
Van Damme	60	0	1	0	N	September 30, 1999
Trinidad	38	0	0	0	N	October 22, 1999
Caspar Cove	61	0	0	0	N	October 1, 1999
Salt Pt.	61	0	0	0	N	March 25, 2000
Van Damme	63	0	0	0	N	April 7, 2000
Van Damme (North/South)	74	0	1	0	N	April 24, 2000
Moat Creek	62	0	0	0	Y	April 7, 2000
Pedotti Reef	62	0	0	3	Y	April 7, 2000
MacKerricher	60	0	0	0	Y	May 7, 2000
Van Damme	70	0	0	0	N	January 1, 2001
Hardy Creek	61	0	0	0	Y	April 28, 2001
MacKerricher	61	0	0	0	Y	April 27, 2001
Van Damme	63	0	0	0	Y	April 1, 2001
Mote Creek	63	0	0	1	Y	April 1, 2001
Pedotti Reef	60	0	0	1	Y	April 27, 2001
Salt Point	61	0	0	3	Y	April–May 2001
Point Arena	61	0	0	0	Y	May 25, 2001
Elephant Rock	62	0	0	0	N	May 23, 2001
Shelter Cove	62	0	0	0	Y	May–June 2001
Van Damme	61	0	0	0	Y	June 22, 2001
Bodega Bay	60	0	0	4	N	July–August 2001

Results

Over 70% of the abalone from all geographic locations south of San Francisco were infected with the RLP, with an overall prevalence in all study sites of 7% (Table 1). In addition to the histological identification of RLP inclusions in both the post-esophagus and digestive gland, the pedal muscle of several of the animals at Point San Pedro and Scott's Creek were visibly atrophied. None of the animals from the RLs north of San Francisco showed evidence of RLP infection or clinical signs of disease. However, microscopic examination of stained tissue sections revealed that several animals at two of the eight PSLs north of San Francisco (Crescent City and Van Damme) harbored the RLP (Fig. 2) but displayed no external or microscopic signs of withering syndrome (Table 1). Identification of the intracellular bacterium as the etiological agent of withering syndrome was further confirmed using PCR; only visibly infected animals produced a 160 basepair (bp) amplicon of the 16S rDNA specific to "*Candidatus* Xenohaliotis californiensis" (Fig. 3; Andree et al. 2000). Interestingly, the PSL near Bodega Bay (Horseshoe Cove), where outplantings also occurred, is adjacent to the University of California, Davis, Bodega Marine Laboratory and is relatively close to a historic abalone farm, tested RLP-free on the first and subsequent examinations.

The log-linear relationship between the total length and total weight of adult abalone indicated that none of the RLP-positive animals found at the Van Damme (92.5 and 127.5 mm) and Crescent City (174, 175, 235, 203, and 212 mm) PSLs weighed less than other individuals within the population from which it originated (Fig. 4). In contrast, previous clinical studies on black abalone with withering syndrome indicated that the weight-to-length relationship of individuals with clinical signs of withering syndrome differs from those without clinical signs of the disease (Fig. 5).

Discussion

Presence of RLP and withering syndrome in specific zones in California

This research documents for the first time the presence of the etiological agent of withering syndrome, "*Candidatus* Xenohaliotis californiensis", in two northern California locations (Crescent City and Van Damme State Park), in addition to its presence at all locations examined south of San Francisco. A lack of baseline data made determination of the source of the RLP (i.e., natural spread of an endemic pathogen vs. an exotic pathogen) difficult. However, the large geographic distance between the RLP-infected central California sites combined with limited historical data suggest that the RLP may have been introduced into northern California via the outplanting of hatchery-reared abalone before the identification of the bacterium as the causative agent of withering syndrome. In addition, these data suggest that dis-

Fig. 2. Post-esophagus of rickettsiales-like (*a*) procaryote-infected and (*b*) uninfected red abalone, *Haliotis rufescens*, from Crescent City. Note basophilic bacterial inclusions in cytoplasm of gastrointestinal epithelial cells (arrows). Bars = 50 μm.

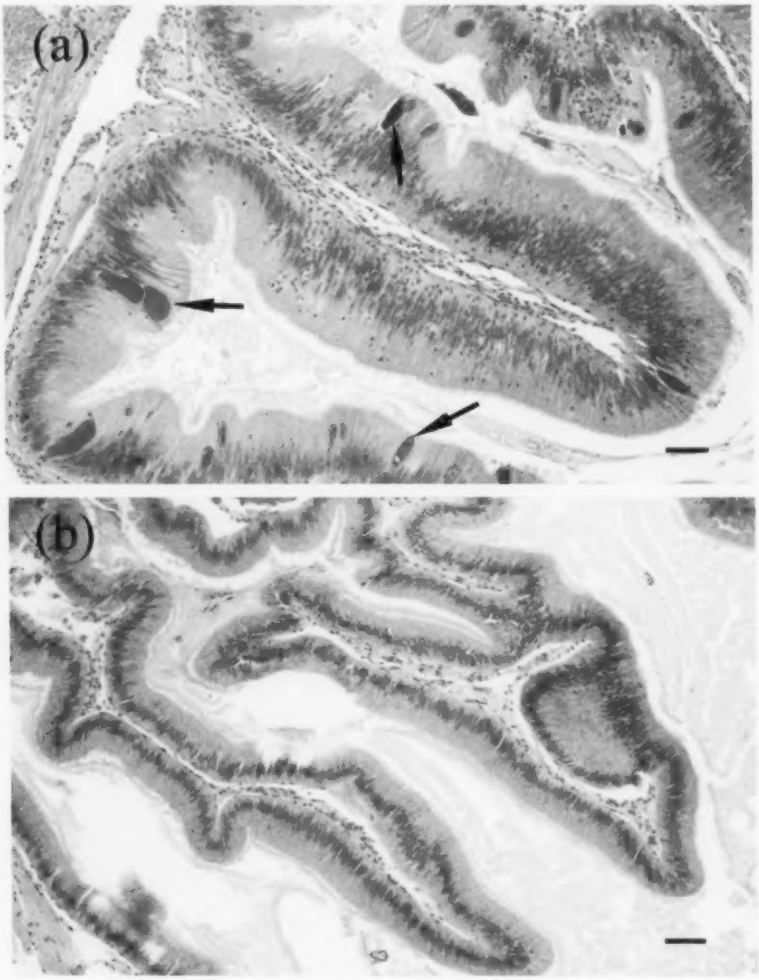

ease management zones as outlined by the OIE (2001) may be used to monitor and, hopefully, control the spread of this important pathogen in California. Based on the information gleaned from this study, central and southern California would be considered within the RLP- and WS-infected (or endemic) zone, and Van Damme State Park and Crescent City would be in additional RLP-infected zones. Areas adjacent to these areas or adjacent to point-source locations should be considered within surveillance zones in which careful assessment of a range expansion of the RLP and or WS is monitored. Northern California areas distant from the above two zones from which no infected abalone have been observed could be considered disease-free zones (OIE 2001). However, periodic assessment of the health status of abalones in disease-free zones is also warranted.

Historical spread of withering syndrome

Before January 1994, abalone at Point Arguello (south-central California) did not exhibit signs of withering syndrome (C.S. Friedman, personal observation) but have now sustained mortalities exceeding 76% (Altstatt et al. 1996; P.L. Haaker, CDFG, 4665 Lampson Ave, Suite C, Los Alimitos, CA 90720, personal observation). In addition, black abalone collected from Carmel Point were known to be RLP-negative as recently as September 1997 (C.S. Friedman and J.D. Moore, personal observation), and Año Nuevo Island was RLP-negative in the mid-1990s (Gardner et al. 1995). This evidence, in addition to the disease's progressive spread throughout the Channel Islands (Lafferty and Kuris 1993) and along the mainland coast of central California (Steinbeck et al. 1992; Altstatt et al. 1996), suggests that the RLP and withering syndrome have been moving north up the California coast and have now been observed at all of the locations that we investigated south of San Francisco.

Anthropogenic introduction of RLP into northern California

The two RLP-positive locations north of San Francisco are both PSL. The Crescent City location received five outplantings of hatchery-reared red abalone (n = 2000 – 10 500

Fig. 3. Agarose gel depicting the 160 basepair (bp) amplicon of rickettsiales-like procaryote (RLP) rDNA (arrow). Lanes 1–3 represent tissues from an uninfected (1) and infected (2, 3) red abalone, *Haliotis rufescens*, from Crescent City. Lanes 4–9 represent tissues from uninfected (4, 6, 7) and infected (5, 8) abalone from Van Damme State Park. Lane 9 contained positive control tissues from an abalone with the RLP and withering syndrome. Lane 10 contains a 1 Kb marker.

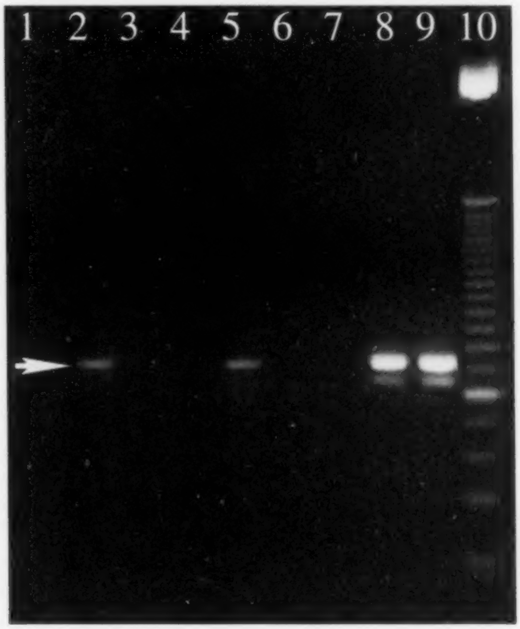

Fig. 4. Log-linear relationship of uninfected (triangles) and infected (circles) red abalone, *Haliotis rufescens*, from Van Damme State Park. Note that both groups fall into the same regression line.

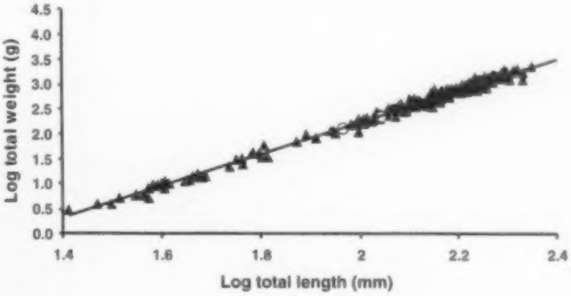

Fig. 5. Log-linear relationship between uninfected (triangles) and infected (circles) black abalone, *Haliotis cracherodii*, from historical samples. Note that the regression lines of infected and uninfected abalones differ.

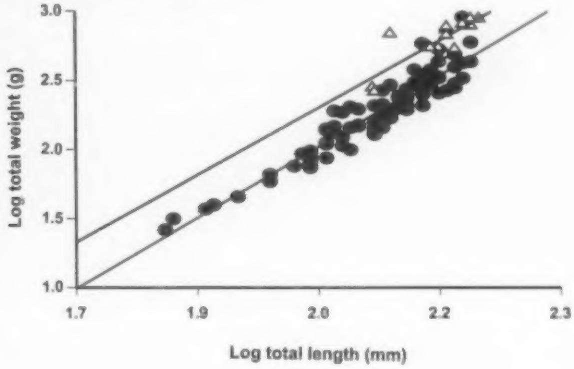

each) between 1988 and 1995, before the identification of the etiological agent of withering syndrome. This location was also in close proximity to a historic aquaculture facility in Crescent City Harbor with a long history of importing commercially reared red abalone seed from farms within what is now considered to be withering syndrome endemic areas of central and southern California. Whether the RLP infections originated from the outplants, the farm, or a combination of sources was not clear. However, in 1999, newly acquired RLP-free seed, maintained in a land-based portion of the Crescent City abalone farm, remained RLP-free after 1 year of culture (C.S. Friedman, unpublished data). The intake of this portion of the facility was in closer proximity to the water-based cages in which RLP-infected abalone were held than were the local wild red abalone population, suggesting that the source of infections in the local wild red abalone population was the outplanted animals (via survival of planted abalone or transmission of the RLP from planted to wild abalone). As abalone growth is not linear throughout its life, particularly after 4–5 years in age (or ~127 mm), it is difficult to determine if the infected Crescent City abalone were wild or from the outplants. However, the infected abalone measured 174–235 mm in size, suggesting that they far exceeded 15 years in age and that transmission occurred between planted and wild abalone (Haaker et al. 2001).

The second RLP-positive PSL in northern California, Van Damme State Park, received commercially reared outplants in 1995, again before the identification of the RLP as the etiologically agent of withering syndrome (Rogers-Bennett and Pearse 1998). Rogers-Bennett and Pearse (1998) planted 50 000 seed abalone measuring 8 ± 1.08 mm at five sites, one along the central and four along the northern California coast. Each of the following four locations north of San Francisco received 10 000 abalone in 1995: Horseshoe Cove, Salt Point, Van Damme State Park, and Caspar Cove. Although abalone were sampled from the outplant sites using geographic information from the authors, only abalone from a single location (Van Damme State Park) were found to harbor RLPs. Before the outplanting in October of 1995, 60 seed abalone, measuring 5.5–9.5 mm and originating from the same farm source population as was planted, were examined visually for sabellids and by histology for parasites. No animals were infested with sabellids and none of the seed showed evidence of RLP infection. However, a proportion of larger juvenile abalone in the same hatchery seawater system as the outplanted abalone were infected with RLP (C.S. Friedman, unpublished data). These observations suggest that the smaller abalone used by Rogers-Bennett and Pearse (1998) were likely to have been infected by the RLP at prevalence below the level of detection (5%). Given the rapid decrease in recovery and low estimated survivorship

(<1%) of the planted abalone (Rogers-Bennett and Pearse 1998) combined with the information above indicating a lack, or low level, of detection of RLP infections in abalone planted from the hatchery used by Rogers-Bennett and Pearse (1998), the probability of transmission of RLP from the hatchery seed to wild abalone in this instance is low.

Epidemiological research on the transmission dynamics of both aquatic and terrestrial animal parasites suggests that successful transmission of a parasite between hosts depends on a variety of factors, including a threshold density of the host below which transmission is unsuccessful because of death or recovery of hosts (Sato and Lotz 2001). This density is unknown for the RLP. In addition, parasite density and temperature are also important for transmission (Hoffman et al. 1995; Sato and Lotz 2001). The intensity of RLP infections and bacterial transmission in red abalones is directly temperature-dependent, particularly at temperatures exceeding 15 °C and approaching 18–19 °C (Moore et al. 2000). Thus, the low water temperatures typically encountered along the northern coast of California (8–15 °C) may be below the threshold temperature for significant bacterial replication and transmission, particularly with a single introduction event as occurred at Van Damme State Park.

The sizes of the two infected individuals found at Van Damme State Park (92.5 mm in 1999 and 127.5 mm in 2000) were within the upper size range expected if these animals were survivors of the outplants. At an average annual growth rate of 12–24 mm·year^{-1} (Trevelyan et al. 1998), the 8-mm abalones would range in size from an average of 56–104 mm in 1999 to an average of 68–128 mm in 2000. Our subsequent samplings in 2000 and 2001, which used creel-sampled abalone and did not target the specific outplant site of this cove, failed to detect any RLPs. Thus, RLP-infected individuals may be limited to the specific outplant location at Van Damme State Park or may be more widespread but below the detection limit of our sampling protocol at this site. These data suggest that the 1995 outplant is the likely source of the RLP infections in abalone at Van Damme State Park.

A lack of detection of the RLP in abalone from Horseshoe Cove near Bodega Bay, Salt Point, and Caspar Cove, three locations that received the same number of seed abalone from the same commercial facility as Van Damme State Park (RLP-positive), suggests either that the RLP was unable to become established in these locations or that the RLP is present at prevalence of <5%. These data suggest that the present distribution of "*Candidatus* Xenohaliotis californiensis" in northern California was anthropogenically influenced and that specific disease zones should be established and monitored.

It should be pointed out that we sampled only 38 abalone at the Trinidad location because of a limited population, its remote location, and consistently poor diving conditions. Any conclusions that can be drawn from a sample size of less than 60, in which all animals sampled are negative, is consequently limited.

In conclusion, our study suggests that careful attention must be paid to the health status of outplanted abalone before planting for restoration or experimental efforts and that some inherent risk will always be present when embarking on such endeavors. Similarly, knowledge of the health of animals in the waters receiving hatchery-reared outplants is important to understanding the impact of endemic diseases on the planted abalone and to documenting the introduction of previously undetected diseases from planted animals to the wild animals, as occurred in red abalone at Van Damme State Park and Crescent City, California. Such information is necessary for an effective evaluation of the health of aquatic animals associated with conservation efforts, research, aquaculture, and other anthropogenic sources of pathogens. We will continue to monitor the impact, if any, of the presence of the RLP at Van Damme State Park and Crescent City and hope that the thermal regime in the northern part of the state will reduce the spread of the RLP and development of clinical withering syndrome.

Acknowledgements

We thank Fred Wendell for his dedication to sampling abalone in this study and James D. Moore and Thea T. Robbins for editorial comments and assistance in sampling. We appreciate the editorial comments of Lorenz Hauser and Loveday Conquest. We are indebted to John Geibel, Phil Law, Konstantine Karpov, Peter L. Haaker, Catherine Greenup, Jacqueline L. Mitchell, Eva P. Mulder, Beverly Braid, Laura Rogers-Bennett, Jerry Kashiwada, Kellie O'Reilly, Jennifer O'Leary, Eric Larson, Pete Kalvass, Tom Moore, Chris VanHook, Humboldt State University dive team, Karl Menard, Will Borgeson, Henry Fasteneau, and countless other volunteers for diving and abalone-collection assistance. We thank Yuichi E. Saito for his technical assistance. This research was funded, in part, by a grant from the National Sea Grant College Program, National Oceanic and Atmospheric Administration, U.S. Department of Commerce, under project number R/F-43PD through the California Sea Grant College and the California Department of Fish, Marine Region. The views expressed herein are those of the authors and do not necessarily reflect the views of NOAA or any of its subagencies. The U.S. government is authorized to reproduce and distribute this paper for governmental purposes.

References

Allee, W.C., Emerson, A.E., Park, O., Park, T., and Schmidt, K.P. 1949. Principles of animal ecology. W.B. Saunders Company, Philadelphia, Pa.

Altstatt, J.M., Ambrose, R.F., Engle, J.M., Haaker, P.L., Lafferty, K.D., and Raimondi, P.T. 1996. Recent declines of black abalone *Haliotis cracherodii* on the mainland coast of central California. Mar. Ecol. Prog. Ser. **142**: 185–192.

Andree, K.B., Friedman, C.S., Moore, J.D., and Hedrick, R.P. 2000. A polymerase chain reaction for detection of genomic DNA of a Rickettsiales-like prokaryote associated with withering syndrome in black abalone (*Haliotis cracherodii*). J. Shellfish Res. **19**(1): 213–218.

Campbell, A. (*Editor*). 2000. Workshop on rebuilding abalone stocks in British Columbia. Can. Spec. Publ. Fish. Aquat. Sci. No. 130.

Friedman, C.S., Thomson, M., Chun, C., Haaker, P.L., and Hedrick, R.P. 1997. Withering syndrome of the black abalone, *Haliotis cracherodii* (Leach): water temperature, food availability, and parasites as possible causes. J. Shellfish Res. **16**(2): 403–411.

Friedman, C.S., Andree, K.B., Beauchamp, K.A., Moore, J.D., Robbins, T.T., Shields, J.D., and Hedrick, R.P. 2000. '*Candidatus* Xenohaliotis californiensis', a newly described pathogen of abalone, *Haliotis* spp., along the west coast of North America. Int. J. Syst. Bacteriol. **50**: 847–855.

Friedman, C.S., Haaker, P.L., and Taniguchi, I. 2002. Density dependent recruitment and resistance to withering syndrome in a population of black abalone, *Haliotis cracherodii*, at the Vandenberg Ecological Reserve. *In* Marine Ecological Reserves Research Program Research Results 1996–2001. Chapt. 5. California Sea Grant College, Marine Ecological Reserves Research Program, La Jolla, Calif.

Gardner, G.R., Harshbarger, J.C., Lake, J., Sawyer, T.K., Price, K.L., Stephenson, M.D., Haaker, P.L., and Togstad, H.A. 1995. Association of prokaryotes with symptomatic appearance of withering syndrome in black abalone *Haliotis cracherodii*. J. Invertebr. Pathol. **66**: 111–120.

Haaker, P.L., Parker, D.O., Togstad, H., Richards, D.V., Davis, G.E., and Friedman, C.S. 1992. Mass mortality and withering syndrome in black abalone *Haliotis cracherodii*, in California. *In* Abalone of the world. *Edited by* S.A. Shepard, M.J. Tegner, and S.A. Guzman del Proo. Blackwell Scientific, Oxford, England. pp. 214–224.

Haaker, P.L., Karpov, K., Rogers-Bennett, L., Taniguchi, I., Friedman, C.S., and Tegner, M.J. 2001. Abalone. *In* California's living marine resources: a status report. *Edited by* W.S. Leet, C.M. Dewees, R. Klingbeil, and E.J. Larson. University of California, Agric. Nat. Res. Publ. SG01-11. pp. 89–97.

Hoffman, E.E., Powell, E.N., Klinck, J.M., and Saunders, G. 1995. Modeling diseased oyster populations 1: modeling *Perkinsus marinus* infections in oysters. J. Shellfish Res. **14**(1): 121–151.

Karpov, K., Haaker, P., Taniguchi, I., and Rogers-Bennett, L. 2000. Serial depletion and collapse of the California abalone (*Haliotis* spp.) fishery. *In* Workshop on rebuilding abalone stocks in British Columbia. *Edited by* A. Campbell. Can. Spec. Publ. Fish. Aquat. Sci. No. 130. pp. 11–24.

Lafferty, K.D., and Kuris, A.M. 1993. Mass mortality of abalone *Haliotis cracherodii* on the California Channel Islands: tests of epidemiological hypotheses. Mar. Ecol. Prog. Ser. **96**: 239–248.

Luna, L.G. (*Editor*). 1968. Manual of histologic staining methods of the Armed Forces Institute of Pathology. 3rd ed. McGraw-Hill, New York. pp. 38–39.

Moore, J.D., Robbins, T.T., and Friedman, C.S. 2000. Withering syndrome in farmed red abalone *Haliotis rufescens*: thermal induction and association with a gastrointestinal *Rickettsia*-like prokaryote. J. Aquat. Anim. Health, **12**: 26–34.

Moore, J.D., Cherr, G.N., and Friedman, C.S. 2001. Detection of '*Candidatus* Xenohaliotis californiensis' (Rickettsiales-like prokaryote) inclusions in tissue squashes of abalone (*Haliotis* spp.) gastrointestinal epithelium using a nucleic acid fluorochrome. Dis. Aquat. Org. **46**(2): 147–152.

Office International des Epizooties. 2001. Zoning. *In* International Aquatic Animal Health Code. Chapt. 1.4.4. 4th ed. Office International des Epizooties, Paris, France. pp. 35–37.

Quinn, T., Wing, S.R., and Botsford, L.W. 1993. Harvest refugia in marine invertebrate fisheries: models and applications to the red sea urchin, *Strongylocentrotus franciscanus*. Am. Zool. **33**(6): 537–550.

Richards, D.V., and Davis, G.E. 1993. Early warnings of a modern population collapse of black abalone, *Haliotis cracherodii* Leach 1814, on the California Channel Islands. J. Shellfish Res. **12**: 189–194.

Rogers-Bennett, L., and Pearse, J.S. 1998. Experimental seeding of hatchery-reared juvenile red abalone in northern California. J. Shellfish Res. **17**(3): 877–880.

Saito, K. 1984. Ocean ranching of abalones and scallops in northern Japan. Aqua, **39**: 361–373.

Sato, M.A., and Lotz, J.M. 2001. Epidemiological parameters of white spot syndrome virus infections in *Litopenaeus vannamei* and *L. setiferus*. J. Invertebr. Pathol. **78**(1): 9–15.

Shaw, B.L., and Battle, H.I. 1957. The gross and microscopic anatomy of the digestive tract of the oyster, *Crassostrea virginica* (Gmelin). Can. J. Zool. **35**: 325–347.

Shepherd, S.A., Rodda, K.R., and Vargas, K.M. 2001. Chronicle of collapse in two abalone stocks with proposals for precautionary management. J. Shellfish Res. **20**(2): 843–856.

Sloan, N.A., and Breen, P.A. 1988. Northern abalone, *Haliotis kamtschatkana*, in British Columbia: fisheries and synopsis of life history information. Can. Spec. Publ. Fish. Aquat. Sci. No. 103.

Steinbeck, J.R., Groff, J.M., Friedman, C.S., McDowell, T., and Hedrick, R.P. 1992. Investigations into mortality among populations of the California black abalone, *Haliotis cracherodii*, on the central coast of California, U.S.A. *In* Abalone of the world. *Edited by* S.A. Shepard, M.J. Tegner, and S.A. Guzman del Proo. Blackwell Scientific, Oxford, England. pp. 203–213.

Stoner, A.W., and Ray-Culp, M. 2000. Evidence for Allee effects in an over-harvested marine gastropod: density-dependent mating and egg production. Mar. Ecol. Prog. Ser. **202**: 297–302.

Tegner, M.J. 1993. Southern California abalones: can stocks be rebuilt using marine harvest refugia? Can. Spec. Publ. Fish. Aquat. Sci. No. 50. pp. 2010–2018.

Tegner, M.J. 2000. Abalone (*Haliotis* spp.) enhancement in California: what we've learned and where we go from here. *In* Workshop on rebuilding abalone stocks in British Columbia. *Edited by* A. Campbell. Can. Spec. Publ. Fish. Aquat. Sci. No. 130. pp. 61–71.

Thoesen, J.C. (*Editor*). 1994. Bluebook, suggested procedures for the detection and identification of certain finfish and shellfish pathogens. 4th ed. Vers. 1. Fish Health Section, American Fisheries Society, Bethesda, Md.

Trevelyan, G.A., Mendoza, J.L., and Buckley, B. 1998. Increasing the yield of red abalone with the alga *Microcladia coulteri*. J. Shellfish Res. **17**(3): 631–633.

VanBlaricom, G.R., Ruediger, J.L., Friedman, C.S., Woodard, D.D., and Hedrick, R.P. 1993. Discovery of withering syndrome among black abalone *Haliotis cracherodii* Leach 1814 populations at San Nicola Island, California. J. Shellfish Res. **12**: 185–188

ERRATUM / ERRATUM

Erratum: Comparative growth and feeding in zebra and quagga mussels (*Dreissena polymorpha* and *Dreissena bugensis*): implications for North American lakes

Brad S. Baldwin, Marilyn S. Mayer, Jeffrey Dayton, Nancy Pau, Johanna Mendillo, Maura Sullivan, Aaron Moore, Aye Ma, and Edward L. Mills

Ref.: Can. J. Fish. Aquat. Sci. **59**: 680–694 (2002).

The name of the fifth author of this paper was incorrectly spelled. The correct spelling is "Johanna Mendillo". We apologize for any inconvenience this may have caused.

Received 18 November 2003. Accepted 20 November 2003. Published on the NRC Research Press Web site at http://cjfas.nrc.ca on 5 December 2003.
J16454E

B.S. Baldwin,[1] M.S. Mayer, M. Sullivan, A. Moore, and A. Ma. Biology Department, St. Lawrence University, Canton, NY 13617, U.S.A.
J. Dayton, N. Pau, J. Mendillo, and E.L. Mills. Department of Natural Resources, Cornell Biological Field Station, 900 Shackelton Point Road, Bridgeport, NY 13030, U.S.A.

[1] Corresponding author (e-mail: bbal@stlawu.edu).

doi: 10.1139/F03-150

Culinary Herbs for Short-Season Gardeners

By/par Ernest Small and /et Grace Deutsch

Co-Published with/Co-édité par Ismant Peony Press

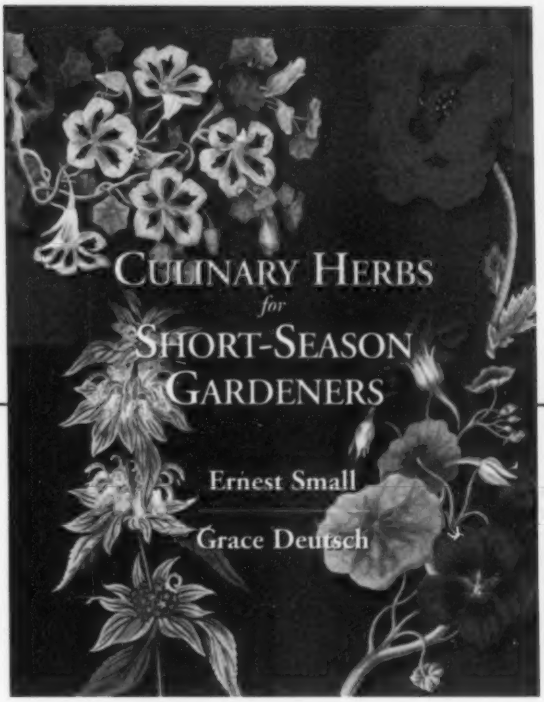

$24.95/24,95 $

Other countries $24.95 US
À l'étranger 24,95 $US

Softcover / Edition brochée
181 pages
ISBN 0-660-17785-4
NRC No./Nº du CNRC 42737

Orders may be submitted by mail or fax to: Les commandes peuvent être soumises par courrier ou par télécopieur à :

Order Office/Bureau des commandes
NRC Research Press/Presses scientifique du CNRC
National Research Council/Conseil national de recherches
Ottawa, ON K1A 0R6, Canada
Telephone/Téléphone : (613) 990-2254
Fax/Télécopieur : (613) 952-7656
E-mail: research.press@nrc.ca
Courriel : presses.scientifiques@cnrc.ca
Website: http://researchpress.nrc.ca
Site web : http://pressesscientifiques.cnrc.ca

PLEASE PRINT/LETTRES MOULÉES

☐ Payment enclosed / Paiement inclus   Charge to/ Imputer à ☐ Visa ☐ MasterCard ☐ AMEX

Account no./Nº de compte ☐☐☐☐☐☐☐☐☐☐☐☐☐☐☐☐   Expiry date/Date d'expiration ☐☐☐☐

Name/Nom

Signature

Address/Adresse

City/Ville   Province

Postal code/Code postal   Country/Pays

Telephone/Téléphone   Fax/Télécopieur

E-mail/courriel

Prepayment required unless order is accompanied by a purchase order number. Cheques or money orders should be made payable to : "Receiver General for Canada, Credit NRC". For all orders outside Canada, rates are in U.S. Dollars. All sales are final.
Les commandes doivent être payées d'avance à moins qu'elles ne soient accompagnées d'un numéro de bon de commande. Les chèques ou mandats doivent être libellés au « Receveur général du Canada, crédit du CNRC ». Toutes les ventes sont finales.

Gerhard Herzberg An Illustrious Life in Science

by/par Boris Stoicheff

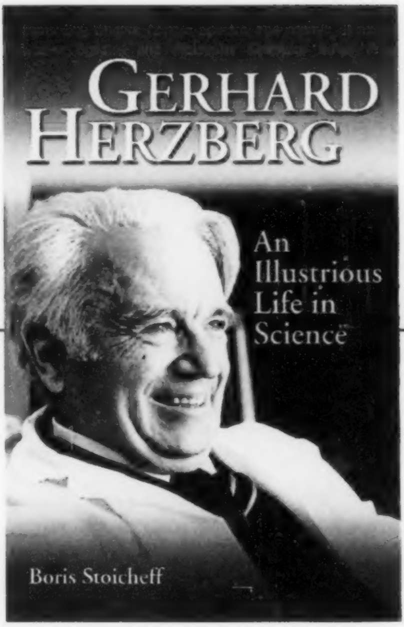

$49.95 CAN. Other countries $49.95 US
49,95 $CAN. À l'étranger 49,95 $US

Hardcover / Edition reliée
ISBN 0-660-18757-4
ISSN 1701-1833
NRC No./N° du CNRC 44462

An NRC Press Publication co-published with McGill-Queen's University Press/Une coédition des Presses du CNRC et McGill-Queen's University Press

Orders may be submitted by mail or fax to:
Les commandes peuvent être soumises par courrier ou par télécopieur à :

Order Office/Bureau des commandes

NRC Research Press/Presses scientifique du CNRC
National Research Council/Conseil national de recherches
Ottawa, ON K1A 0R6, Canada
Telephone/Téléphone : (613) 990-2254
Fax/Télécopieur : (613) 952-7656
E-mail: research.press@nrc.ca
Courriel : presses.scientifiques@cnrc.ca
Website: http://researchpress.nrc.ca
Site web : http://pressesscientifiques.cnrc.ca

PLEASE PRINT/LETTRES MOULÉES

☐ Payment enclosed Paiement inclus ☐ Charge to/ Imputer à ☐ Visa ☐ MasterCard

Account no./N° de compte ☐☐☐☐☐☐☐☐☐☐☐☐☐☐☐☐

Expiry date/Date d'expiration ☐☐☐☐

Name/Nom

Signature

Address/Adresse

City/Ville Province

Postal code/Code postal Country/Pays

Telephone/Téléphone Fax/Télécopieur

E-mail/Courriel

Prepayment required unless order is accompanied by a purchase order number. Cheques or money orders should be made payable to: "Receiver General for Canada, Credit NRC". For all orders outside Canada, rates are in U.S. Dollars. All sales are final.
Les commandes doivent être payées d'avance à moins qu'elles ne soient accompagnées d'un numéro de bon de commandes. Les chèques ou mandats doivent être libellés au « Receveur générale du Canada, crédit du CNRC ». Toutes les vent sont finales.

Marine Protected Areas and Fisheries Closures in British Columbia

By/par Glen S. Jamieson and/et Joanne Lessard

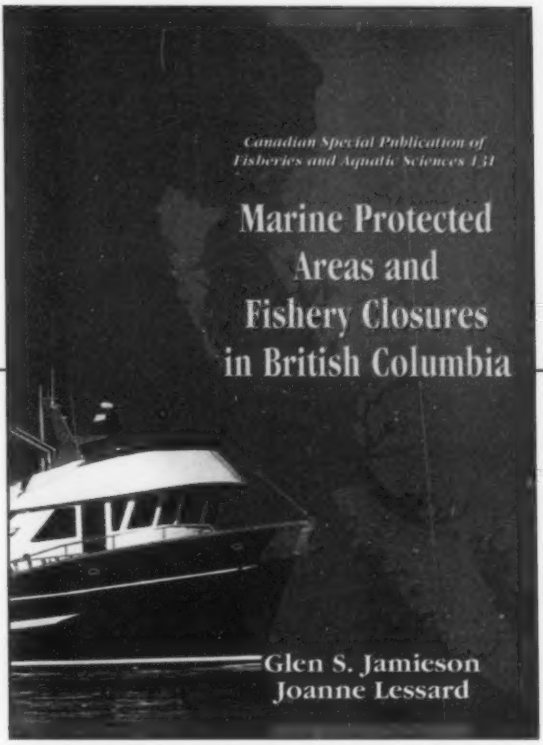

Canadian Special Publication of Fisheries and Aquatic Sciences 131
Marine Protected Areas and Fishery Closures in British Columbia
Glen S. Jamieson
Joanne Lessard

$69.95/69,95 $

Other countries $69.95 US
À l'étranger 69,95 $US

Softcover / Edition brochée
414 pages
ISBN 0-660-17788-9 ISSN 0706-6481
NRC No./Nº du CNRC 42846
(Can. Spec. Publ. Fish. Aquat. Sci. No. 131)

Orders may be submitted by mail or fax to: Les commandes peuvent être soumises par courrier ou par télécopieur à :

Order Office/Bureau des commandes

NRC Research Press/Presses scientifique du CNRC
National Research Council/Conseil national de recherches
Ottawa, ON K1A 0R6, Canada
Telephone/Téléphone : (613) 990-2254
Fax/Télécopieur : (613) 952-7656
E-mail: research.press@nrc.ca
Courriel : presses.scientifiques@cnrc.ca
Website: http://researchpress.nrc.ca
Site web : http://pressesscientifiques.cnrc.ca

PLEASE PRINT/LETTRES MOULÉES

☐ Payment enclosed Paiement inclus   Charge to/ Imputer à ☐ Visa ☐ MasterCard ☐ AMEX

Account no./Nº de compte   Expiry date/Date d'expiration

☐☐☐☐☐☐☐☐☐☐☐☐☐☐☐☐   ☐☐☐☐

Name/Nom

Signature

Address/Adresse

City/Ville   Province

Postal code/Code postal   Country/Pays

Telephone/Téléphone   Fax/Télécopieur

E-mail/courriel

Prepayment required unless order is accompanied by a purchase order number. Cheques or money orders should be made payable to : "Receiver General for Canada, Credit NRC". For all orders outside Canada, rates are in U.S. Dollars. All sales are final.
Les commandes doivent être payées d'avance à moins qu'elles ne soient accompagnées d'un numéro de bon de commande. Les chèques ou mandats doivent être libellés au « Receveur général du Canada, crédit du CNRC ». Toutes les ventes sont finales.

NRC · CNRC

The Canada Institute for Scientific and Technical Information (CISTI) requires a Director, Publishing (NRC Research Press)

The Director is responsible for setting the strategic direction for CISTI Publishing (NRC Research Press) and for its overall management. The Director manages the Research Journals, Monographs, Conference Proceedings, and Publishing Services Programs in a business like fashion to ensure that the Publishing Directorate operates on a full cost recovery basis. The Director networks with the scholarly publishing, research and library communities to ensure adequate information for the setting of the strategic direction. The Director is called to support the scholarly publishing community in Canada by sharing knowledge and encouraging dialogue between authors, publishers and libraries. The incumbent participates as an active member of the CISTI Steering Committee, and in the development and implementation of overall strategic directions for the Institute.

Education
Graduation from a recognized university, preferably in science, engineering or life sciences.

Experience
Experience in STM information dissemination management in a publishing or an R&D context. Experience in working with the academic community. Experience in developing and sustaining client relations for strategic outcomes. Experience in managing human resources in a participative, team-oriented, matrix environment.

Closing Date: 16 January 2004. Applications must be received or post-marked no later than the closing date.

TO APPLY:
APPLICATIONS MUST QUOTE COMPETITION NUMBER: 16-03-99

CONTACT PERSON: Jennifer Laidlaw, Human Resources Systems Coordinator, Montreal Road, M-20, Room 107, Ottawa, Ontario K1A 0R6, (613) 993-2024, jennifer.laidlaw@nrc-cnrc.gc.ca

Online Application is preferred method by which to apply: http://careers-carrieres.nrc-cnrcc.gc.ca/Careers/career_main.nsf/pagee/home

L'Institut canadien de l'information scientifique et technique (ICIST) offre un poste de Directeur, Édition (Presses scientifiques du CNRC)

Le (la) directeur(trice) est responsable d'établir l'orientation stratégique de la Direction de l'édition de l'ICIST (Presses scientifiques du CNRC) et de sa gestion générale. Il (elle) gère les programmes des revues scientifiques, des monographies, des comptes rendus de conférences et des services d'édition comme une entreprise afin de s'assurer que la direction procède selon un mode de recouvrement complet de ses coûts. Le (la) titulaire établit des rapports avec les collectivités d'édition savante, de recherche et de bibliothéconomie de manière à disposer de l'information nécessaire pour orienter judicieusement la stratégie d'exploitation de la Direction. Il (elle) doit également appuyer la communauté canadienne d'édition savante en partageant ses connaissances et en encourageant les échanges entre les auteurs, les éditeurs et les bibliothèques. Le (la) titulaire est membre actif du Comité de direction de l'ICIST et participe à l'élaboration et à la mise en œuvre des orientations stratégiques générales de l'Institut.

Éducation
Diplôme d'une université reconnue, de préférence en science, en ingénierie ou en sciences de la vie.

Expérience
Expérience de gestion de la dissémination de l'information STM dans le contexte de l'édition ou de la recherche et du développement. Expérience de travail avec la communauté universitaire. Expérience de l'établissement et du maintien de saines relations avec la clientèle en vue d'atteindre des objectifs stratégiques. Expérience de gestion participative, coopérative et matricielle des ressources humaines.

Date limite de réception des demandes : Le 16 janvier 2004. Les demandes seront acceptées jusqu'à la date de fermeture du concours, le sceau de la poste fera foi de cette date.

POUR FAIRE DEMANDE :
LES DEMANDES DOIVENT MENTIONNER LE NUMÉRO DE RÉFÉRENCE : 16-03-99

PERSONNE RESSOURCE : Jennifer Laidlaw, Coordonnatrice de systèmes en en ressources humaines, chemin de Montréal, édifice M-20, pièce 107, Ottawa, Ontario K1A 0R6 (613) 993-2024, jennifer.laidlaw@nrc-cnrc.gc.ca

L'application électronique est la methode recommandée pour postuler : http://careers-carrieres.nrc-nrc.gc.ca/Careers/career_main.nsf/pagef/home

Canada

ERRATUM ERRATUM

Brad S. Baldwin, Marilyn S. Mayer, Jeffrey Dayton, Nancy Pau, Johanna Mendillo, Maura Sullivan, Aaron Moore, Aye Ma, and Edward L. Mills **1432** Erratum: Comparative growth and feeding in zebra and quagga mussels (*Dreissena polymorpha* and *Dreissena bugensis*): implications for North American lakes

National Research Council Canada
Ottawa, Canada
K1A 0R6

Conseil national de recherches Canada
Ottawa, Canada
K1A 0R6

Postage paid at Ottawa
Publications mail
Registration No. 40062591

Port payé à Ottawa
Poste-publication
Enregistrement n° 40062591

USPS periodical postage paid at Champlain, N.Y.

Canadian Journal of Fisheries and Aquatic Sciences

Volume 60, Number 11, November 2003

Journal canadien des sciences halieutiques et aquatiques

Volume 60, numéro 11, novembre 2003

	ARTICLES	ARTICLES
Stephanie A. Boudreau and Norman D. Yan	**1307–1313**	The differing crustacean zooplankton communities of Canadian Shield lakes with and without the nonindigenous zooplanktivore *Bythotrephes longimanus*
David B. Bunnell, María J. González, and Roy A. Stein	**1314–1323**	Zooplankton biomass enhances growth, but not survival, of first-feeding *Pomoxis* spp. larvae
Roderick Nigel Finn and Ivar Rønnestad	**1324–1331**	The effect of acute changes in temperature and light on the aerobic metabolism of embryos and yolk-sac larvae of turbot (*Scophthalmus maximus*)
Adrian M.H. deBruyn, David J. Marcogliese, and Joseph B. Rasmussen	**1332–1344**	The role of sewage in a large river food web
Bryan A. Henderson, Nicholas Collins, George E. Morgan, and Andre Vaillancourt	**1345–1352**	Sexual size dimorphism of walleye (*Stizostedion vitreum vitreum*)
Erik G. Noonburg, Brian J. Shuter, and Peter A. Abrams	**1353–1368**	Indirect effects of zebra mussels (*Dreissena polymorpha*) on the planktonic food web
Michael R. Twiss, Benjamin S. Twining, and Nicholas S. Fisher	**1369–1375**	Partitioning of dissolved thallium by seston in Lakes Erie and Ontario
David A. Milton and Simon R. Chenery	**1376–1385**	Movement patterns of the tropical shad hilsa (*Tenualosa ilisha*) inferred from transects of ^{87}Sr/^{86}Sr isotope ratios in their otoliths
Philippe Girard, Daniel Boisclair, and Michel Leclerc	**1386–1397**	The effect of cloud cover on the development of habitat quality indices for juvenile Atlantic salmon (*Salmo salar*)
J.C. Guay, D. Boisclair, M. Leclerc, and M. Lapointe	**1398–1408**	Assessment of the transferability of biological habitat models for Atlantic salmon parr (*Salmo salar*)
Ólafur K. Pálsson and Vilhjálmur Thorsteinsson	**1409–1423**	Migration patterns, ambient temperature, and growth of Icelandic cod (*Gadus morhua*): evidence from storage tag data
Carolyn S. Friedman and Carl A. Finley	**1424–1431**	Anthropogenic introduction of the etiological agent of withering syndrome into northern California abalone populations via conservation efforts

Continued on inside back cover / Suite au verso

Canadä

Printed in Canada by / Imprimé au Canada par
University of Toronto Press Inc.
Page production by / Mise en page par
NRC Research Press / Presses scientifiques du CNRC

0706-652X(200311)60:11;1-3